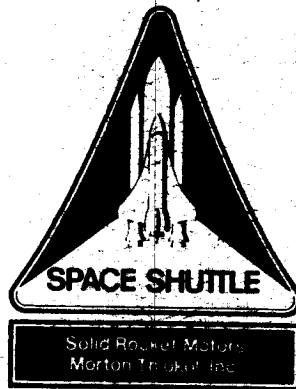


Roy Mitchell TASI
4.7844

TWR-17927



Transient Pressure Test Article (TPTA) 1.1 and 1.1A Final Test Report

Volume I

January 1988

Prepared for

**National Aeronautics and Space Administration
George C. Marshall Space Flight Center
Marshall Flight Center, Alabama 35812**

Contract No. NAS8-30490
DR No. 5-3
WBS No. HQ301-10-07
ECS No. SS602

MORTON THIOKOL, INC.

Aerospace Group

Space Operations

P.O. Box 707, Brigham City, Utah 84302-0707 (801) 863-3511

Publications No. 88842

**(NASA-CR-179322-Vol-1) TRANSIENT PRESSURE
TEST ARTICLE (TPTA) 1.1 AND 1.1A, VOLUME 1
Final Report (Morton Thiokol) 279 p**

N88-19588

CSCL 21H

G3/20

**Unclas
0133312**



TPTA 1.1 Test Article at Marshall Space Flight Center
Test Stand, Huntsville, Alabama

Transient Pressure Test Article (TPTA) 1.1 and 1.1A
Final Test Report

Prepared by:

Clarence A. Rebell 7 Feb 88.
Test Planning and Reports

Approved by:

Michael W. Wain
Test Planning and Reports
Supervisor

J. Z. Sawaga
Space Systems Engineering
Manager

J. Z. Sawaga
Systems Test and Support
Manager

Jack R. Kopp
Space Engineering Design
Manager

Mark Allison
Project Engineer

Myron Hoshino
Program Manager

Sam Njoku 2-11-88
Terrell R. Rader 2-11-88
Design Engineering

Design Engineering
Supervisor

Charles W. Johnson
Certification Planning

P. T. McKing 2-11-88
System Safety

Richard Alamo
Reliability

P. C. Lydeck 2-17-88
Data Management

MORTON THIOKOL, INC.

Space Operations

Sections of this final test report were written and reviewed by:

V. Steineck	Instrumentation
M. Lee	Ballistics
J. Burn	Structures
K. Albrechtsen	Insulation
D. Blevins	Insulation
T. Pottorff	Insulation
S. Hicken	Insulation
S. Manz	Insulation
A. Freed	Dynamics
L. Abrahamson	Grain Structures
J. Morgan	Seal Leak Check

REVISION _____

88842-8.2

DOC NO.	TWR-17927	VOL
SEC	PAGE	ii

ABSTRACT

The final test report presents the results obtained during the static hot-firing and cold-gas high Q tests of the first Transient Pressure Test Article (TPTA) 1.1. The TPTA consisted of field test Joints A and B, which were the original RSRM J-insulation configuration, with a metal capture feature. It also consisted of a flight configuration nozzle-to-case test joint (Joint D) with shorter vent slots. Fluorocarbon O-rings were used in all the test joints. The purpose of the TPTA tests is to evaluate and characterize the RSRM field and nozzle-to-case joints under the influence of ignition and strut loads during liftoff and high Q.

All objectives of the cold-gas high Q (TPTA 1.1A) test were met and all measurements were close to the predicted values. During the static hot-firing test (TPTA 1.1), the motor was inadvertently plugged by the quench injector plug, making it a more severe test, although no strut loads were applied. The motor was depressurized after approximately 11 min using an auxiliary system, and no anomalies were noted. In the static hot-firing test, pressure was incident on the insulation and the test joint gaps were within the predicted range. ➤During the static hot-firing test, no strut loads were applied because the loading system malfunctioned. For this test, all measurements were within range of similar tests performed without strut loads.

CONTENTS

Volume I

<u>Section</u>		<u>Page</u>
1	INTRODUCTION.	1
	1.1 TEST ARTICLE	1
2	OBJECTIVES.	12
3	APPLICABLE DOCUMENTS.	14
4	SUMMARY AND CONCLUSIONS	17
	4.1 SUMMARY	17
	4.1.1 Static Hot-Firing Test (TPTA 1.1).	17
	4.1.2 Cold-Gas High Q Test (TPTA 1.1A)	21
	4.2 CONCLUSIONS BY OBJECTIVES	25
	4.3 CORRELATION OF RESULTS BY CEI REQUIREMENTS	29
5	INSTRUMENTATION	31
	5.1 INTRODUCTION	31
	5.2 OBJECTIVES	31
	5.3 INSTRUMENTATION DISCUSSION	31
	5.4 CONCLUSIONS AND RECOMMENDATIONS.	40
6	PHOTOGRAPHY	41
7	TEST RESULTS AND DISCUSSION	43
	7.1 BALLISTICS	43
	7.1.1 Ballistics Introduction.	43
	7.1.2 Ballistics Objectives.	43
	7.1.3 Ballistics Results and Discussion.	43
	7.1.4 Ballistics Conclusions and Recommendations	45
	7.2 STRUCTURES EVALUATION	47
	7.2.1 Structures Introduction and Objectives	47
	7.2.2 Structures Conclusions and Recommendations	48
	7.2.3 Structures Results	50

CONTENTS (Cont)

Volume I

<u>Section</u>	<u>Page</u>
7.3 INSULATION EVALUATION.	168
7.3.1 Insulation Objectives	168
7.3.2 Insulation Conclusions	168
7.3.3 Insulation Results	169
7.4 GLOBAL FINITE ELEMENT ANALYSIS	216
7.4.1 Introduction	216
7.4.2 Model Description.	216
7.4.3 Correlations of Predictions With Test Data . . .	219
7.4.4 Conclusions.	253
7.5 GRAIN STRUCTURES	256
7.5.1 Introduction	256
7.5.2 Objectives	256
7.5.3 Results/Discussion	256
7.5.4 Conclusions/Recommendations.	256
7.6 SEAL LEAK CHECK.	259

APPENDIXES

Volume II

<u>Appendix</u>	<u>Page</u>
A DRAWING TREES	A-1
B INSTRUMENTATION LIST.	B-1
C TPTA 1.1 STATIC HOT-FIRING TEST DATA.	C-1
D TPTA 1.1A COLD-GAS HIGH Q TEST DATA	D-1

FIGURES

<u>Figure</u>		<u>Page</u>
1.1-1	TPTA 1.1 Configuration.	2
1.1-2	TPTA 1.1 Dome Joints.	5
1.1-3	Field Joint DM-8 Baseline Design.	6
1.1-4	Nozzle-to-Case Field Joint Assembly	8
1.1-5	TPTA 1.1 Finned Propellant Configuration.	9
1.1-6	TPTA Slot Propellant Configuration.	10
5.2-1	Joint A Instrumentation	32
5.2-2	Joint B Instrumentation	33
5.2-3	Joint D Instrumentation	34
5.2-4	TPTA Case Measurements.	35
5.2-5	Joint C Instrumentation	36
5.2-6	Joint E Instrumentation	37
5.2-7	Joint F Instrumentation	38
6-1	Camera Coverage	42
7.1-1	TPTA 1.1 Pressure Versus Time (1 sec)	44
7.1-2	TPTA 1.1 Pressure Versus Time	46
7.2-1	TPTA 1.1 Lift-Off Strut Loads Profile	56
7.2-2	TPTA 1.1A High Q Strut Load Profile	58
7.2-3	TPTA 1.1 Joint A Gap Deflection at Primary O-ring (0-1 sec)	74
7.2-4	TPTA 1.1 Joint A Gap Deflection at Primary O-ring (0-30 sec).	75
7.2-5	TPTA 1.1 Joint A Deflection at Primary/Secondary O-rings (0-1 sec)	77
7.2-6	TPTA 1.1 Joint A Gap Deflection at Primary/Secondary O-rings (0-30 sec).	78
7.2-7	TPTA 1.1 Joint A Gap Deflection at CF O-ring (0-1 sec).	79
7.2-8	TPTA 1.1 Joint A Gap Deflection at CF O-ring (0-30 sec).	80

FIGURES (Cont)

<u>Figure</u>		<u>Page</u>
7.2-9	TPTA 1.1 Joint B Gap Deflection at Primary O-ring (0-1 sec)	83
7.2-10	TPTA Joint B Gap Deflection at Primary O-ring (0-30 sec).	84
7.2-11	TPTA 1.1 Joint B Gap Deflection at Primary/Secondary O-rings (0-1 sec)	85
7.2-12	TPTA 1.1 Joint B Gap Deflection at Primary/Secondary O-rings (0-30 sec).	87
7.2-13	TPTA 1.1 Joint B Gap Deflection at CF O-ring (0-1 sec).	88
7.2-14	TPTA 1.1 Joint B Gap Deflection at CF O-ring (0-30 sec).	89
7.2-15	TPTA 1.1A Joint A Gap Deflection at Primary O-ring (8-20 sec).	95
7.2-16	TPTA 1.1A Joint A Gap Deflection at Primary/ Secondary O-rings (8-20 sec).	96
7.2-17	TPTA 1.1A Joint A Gap Deflection at CF O-ring (8-20 sec).	97
7.2-18	TPTA 1.1A Joint B Gap Deflection at Primary O-ring (8-20 sec).	99
7.2-19	TPTA 1.1A Joint B Gap Deflection at Primary/Secondary O-rings (8-20 sec).	100
7.2-20	TPTA 1.1A Joint B Gap Deflection at CF O-ring (8-20 sec).	101
7.2-21	TPTA 1.1 Joint A Girth Gages (0-1 sec).	109
7.2-22	TPTA 1.1 Joint A Girth Gages (0-30 sec)	110
7.2-23	TPTA 1.1 Joint B Girth Gages (0-1 sec).	114
7.2-24	TPTA 1.1 Joint B Girth Gages (0-30 sec)	115
7.2-25	TPTA 1.1A Joint A Radial Growth (8-20 sec).	121
7.2-26	TPTA 1.1A Joint B Radial Growth (8-20 sec).	122
7.2-27	TPTA 1.1 Case Girth Gages (0-1 sec)	143
7.2-28	TPTA 1.1 Case Girth Gages (0-30 sec).	144
7.3-1	HPM Configuration - Dome Joints	170
7.3-2	DM-8 J-insulation Tang Configuration - Insulated Level.	172

FIGURES (Cont)

<u>Figure</u>		<u>Page</u>
7.3-3	DM-8 J-insulation Clevis Configuration.	173
7.3-4	Joint A Clevis Insulation	174
7.3-5	Test Joint Unbonds, Joint Layout	176
7.3-6	TPTA 1.1 Insulation, Baseline Configuration	178
7.3-7	J-insulation Gap Locations.	180
7.3-8	J-insulation Transfer Medium Application.	183
7.3-9	Gap Locations	187
7.3-10	Assembled DM-8 Baseline J-insulation Joint Configuration	190
7.3-11	Test Joint A Instrumentation Locations and Summary. . .	191
7.3-12	Joint A, Bondline Normal Stress - Inboard 0 deg	194
7.3-13	Joint A Bondline Normal Stress - Inboard 240 deg. . . .	195
7.3-14	Joint A Normal Stress - Outboard 0 deg.	196
7.3-15	Joint A Normal Stress - Outboard 240 deg.	197
7.3-16	Joint A Capture Hook Seal Pressure - 135 deg.	198
7.3-17	Test Joint B Instrumentation Locations and Summary. . .	199
7.3-18	Joint B Capture Hook Seal Pressure - 135 deg.	201
7.3-19	Typical J-insulation Clevis Bondline Heat Effects . . .	202
7.3-20	Joint A J-insulation Bondline Heat Effects.	204
7.3-21	Pressure-Sensitive Adhesive Failure Locations	205
7.3-22	Joint Bondline Summary.	206
7.3-23	Joint B J-insulation Clevis Soot Path	209
7.3-24	Joint B J-insulation Clevis Soot Path	210
7.3-25	Test Joint Clevis Unbond Inspection Locations	212
7.3-26	Nozzle-to-Case Joint (Joint D) Gas Path to Wiper O-ring.	213
7.4-1	TPTA Finite Element Model	217
7.4-2	ETA Ring Model.	218
7.4-3	TPTA Field Joint Model.	220
7.4-4	Axial Stations of Predicted Strain Gages.	221

FIGURES (Cont)

<u>Figure</u>		<u>Page</u>
7.4-5	TPTA 1.1 Ignition Pressure Time Trace	222
7.4-6	TPTA Post-Test Correlation, Predicted Versus Measured Hoop Strain at Sta 1511.0 due to Maximum Ignition Pressure (876 psig)	223
7.4-7	TPTA Post-Test Correlation, Predicted Versus Measured Axial Strain at Sta 1511.0 Due to Maximum Ignition Pressure (876 psig)	225
7.4-8	TPTA Post-Test Correlation, Predicted Versus Measured Hoop Strain at Sta 1498.0 Due to Maximum Ignition Pressure (876 psig)	226
7.4-9	TPTA Post-Test Correlation, Predicted Versus Measured Axial Strain at Sta 1498.0 Due to Maximum Ignition Pressure (876 psig)	227
7.4-10	TPTA Post-Test Correlation, Predicted Versus Measured Hoop Strain at Sta 1501.0 Due to Maximum Ignition Pressure (876 psig)	228
7.4-11	TPTA Post-Test Correlation, Predicted Versus Measured Axial Strain at Sta 1501.0 Due to Maximum Ignition Pressure (876 psig)	229
7.4-12	TPTA Post-Test Correlation, Predicted Versus Measured Hoop Strain at Sta 1797.6 Due to Maximum Ignition Pressure (876 psig)	230
7.4-13	TPTA Post-Test Correlation, Predicted Versus Measured Axial Strain at Sta 1797.6 Due to Maximum Ignition Pressure (876 psig)	231
7.4-14	TPTA 1.1A Applied Maximum Q Strut Loads	233
7.4-15	TPTA Post-Test Correlation, Predicted Versus Measured Hoop Strain at Sta 556.5 Due to Maximum Q Strut Loads (No Pressure)	234
7.4-16	TPTA Post-Test Correlation, Predicted Versus Measured Axial Strain at Sta 556.5 Due to Maximum Q Strut Loads (No Pressure)	235
7.4-17	TPTA Post-Test Correlation, Predicted Versus Measured Hoop Strain at Sta 1411.5 Due to Maximum Q Strut Loads (No Pressure)	236
7.4-18	TPTA Post-Test Correlation, Predicted Versus Measured Axial Strain at Sta 1411.5 Due to Maximum Q Strut Loads (No Pressure)	237

FIGURES (Cont)

<u>Figure</u>		<u>Page</u>
7.4-19	TPTA Post-Test Correlation, Predicted Versus Measured Hoop Strain at Sta 1466.5 Due to Maximum Q Strut Loads (No Pressure)	238
7.4-20	TPTA Post-Test Correlation, Predicted Versus Measured Axial Strain at Sta 1466.5 Due to Maximum Q Strut Loads (No Pressure)	239
7.4-21	TPTA Post-Test Correlation, Predicted Versus Measured Hoop Strain at Sta 1498.0 Due to Maximum Q Strut Loads (No Pressure)	240
7.4-22	TPTA Post-Test Correlation, Predicted Versus Measured Axial Strain at Sta 1498.0 Due to Maximum Q Strut Loads (No Pressure)	241
7.4-23	TPTA Post-Test Correlation, Predicted Versus Measured Hoop Strain at Sta 1501.0 Due to Maximum Q Strut Loads (No Pressure)	242
7.4-24	TPTA Post-Test Correlation, Predicted Versus Measured Axial Strain at Sta 1501.0 Due to Maximum Q Strut Loads (No Pressure)	243
7.4-25	TPTA Post-Test Correlation, Predicted Versus Measured Hoop Strain at Sta 1511.0 Due to Maximum Q Strut Loads (No Pressure)	244
7.4-26	TPTA Post-Test Correlation, Predicted Versus Measured Axial Strain at Sta 1511.0 Due to Maximum Q Strut Loads (No Pressure)	245
7.4-27	TPTA Post-Test Correlation, Predicted Versus Measured Hoop Strain at Sta 1797.6 Due to Maximum Q Strut Loads (No Pressure)	246
7.4-28	TPTA Post-Test Correlation, Predicted Versus Measured Axial Strain at Sta 1797.6 Due to Maximum Q Strut Loads (No Pressure)	247
7.4-29	Joint B Gap Opening Prediction Locations.	250
7.4-30	TPTA Post-Test Correlation, Predicted Versus Measured Gap Opening at Aft Field Joint Inner Clevis Leg Midland Due to Maximum Q Pressure (610 psig).	251
7.4-31	TPTA Post-Test Correlation, Predicted Versus Measured Gap Opening at Aft Field Joint Inner Clevis Leg Tip Due to Maximum Q Pressure (610 psig).	252

FIGURES (Cont)

<u>Figure</u>		<u>Page</u>
7.4-32	TPTA Post-Test Correlation, Predicted Versus Measured Gap Opening at Aft Field Joint Inner Clevis Leg Midland Due to Maximum Q Pressure (No Pressure)	254
7.4-33	TPTA Post-Test Correlation, Predicted Versus Measured Gap Opening at Aft Field Joint Inner Clevis Leg Tip Due to Maximum Q Pressure (No Pressure)	255

TABLES

<u>Table</u>		<u>Page</u>
1.1-1	Major Test Components	4
4.1-1	TPTA Test Summary	19
4.1-2	TPTA Static Hot-Firing Test Summary	22
5.3-1	Inoperable Instruments.	39
7.2-1	TPTA 1.1 Joint A Temperatures at T=0 Sec.	60
7.2-2	TPTA 1.1 Joint A Temperatures at Maximum Chamber. . . .	61
7.2-3	TPTA 1.1 Joint B Temperatures at T=0 sec.	62
7.2-4	TPTA 1.1 Joint B Temperatures at Maximum Chamber Pressure.	63
7.2-5	TPTA 1.1 Joint D Temperatures at T=0 sec.	64
7.2-6	TPTA 1.1 Joint D Temperatures at Maximum Chamber Pressure.	65
7.2-7	TPTA 1.1 Joint A Pressures at Maximum Chamber Pressure.	67
7.2-8	TPTA 1.1 Joint B Pressures at Maximum Chamber Pressure.	68
7.2-9	TPTA 1.1 Joint D Pressures at Maximum Chamber Pressure.	69
7.2-10	TPTA 1.1A Joint A Pressures at Maximum Load	70
7.2-11	TPTA 1.1A Joint B Pressures at Maximum Load	71
7.2-12	TPTA 1.1A Joint D Pressures at Maximum Load	72
7.2-13	TPTA 1.1 Joint A Maximum Gap Summary.	81
7.2-14	Comparison of TPTA 1.1 Joint A Gaps With JES-3A	82
7.2-15	TPTA 1.1 Joint B Maximum Gap Summary.	90
7.2-16	Comparison of TPTA 1.1 Joint B Gaps With JES-3A	91
7.2-17	Comparison of TPTA 1.1 Joint D Gaps With NJES-2B. . . .	92
7.2-18	TPTA 1.1 Joint D Maximum Gap Summary.	93
7.2-19	TPTA 1.1 Joint A Maximum Gap Summary.	98
7.2-20	TPTA 1.1 Joint B Maximum Gap Summary.	102
7.2-21	TPTA 1.1 Joint D Maximum Gap Summary.	104
7.2-22	TPTA 1.1 Maximum Axial Growth in Joints A and B	105
7.2-23	TPTA 1.1A Maximum Axial Growth in Joints A and B. . . .	106

TABLES (Cont)

<u>Table</u>		<u>Page</u>
7.2-24	Comparison of Maximum Axial Growth in Joints A and B of TPTA 1.1 Test with JES-3A Test.	107
7.2-25	TPTA 1.1 Joint A Radial Growth.	108
7.2-26	TPTA 1.1 Joint B Radial Growth.	112
7.2-27	Comparison of Joints A and B Radial Growth in TPTA 1.1 Test With JES-3A Test	113
7.2-28	TPTA 1.1 Joint D Radial Growth.	116
7.2-29	Comparison of Joint D Radial Growth in TPTA 1.1 Test With NJES-2B Test	117
7.2-30	TPTA 1.1A Joint A Radial Growth	118
7.2-31	TPTA 1.1A Joint B Radial Growth	119
7.2-32	TPTA 1.1A Joint D Radial Growth	120
7.2-33	TPTA 1.1 Joint A Tang Area Stresses	123
7.2-34	TPTA 1.1A Joint A Tang Area Stresses.	124
7.2-35	TPTA 1.1 Joint A Outer Clevis Leg Stresses.	125
7.2-36	TPTA 1.1A Joint A Outer Clevis Leg Stresses	126
7.2-37	TPTA 1.1 Joint A in Hole Stresses	128
7.2-38	TPTA 1.1A Joint A in Hole Stresses.	129
7.2-39	TPTA 1.1 Joint B Hoop and Axial Stresses (Inner Clevis Leg, Tang Area, and Alignment Holes).	130
7.2-40	TPTA 1.1A Joint B Hoop and Axial Stresses (Inner Clevis Leg, Tang Area, and Alignment Holes).	131
7.2-41	TPTA 1.1 Joint B Pinhole Stresses	132
7.2-42	TPTA 1.1A Joint B Pinhole Stresses.	137
7.2-43	TPTA 1.1 Joint D Stresses	140
7.2-44	TPTA 1.1A Joint D Stresses.	141
7.2-45	TPTA 1.1 Case Membrane Girth Gage Data.	142
7.2-46	TPTA 1.1A Case Membrane Girth Gage Data	146
7.2-47	TPTA 1.1 Case Membrane Strain Gage Data	147

TABLES (Cont)

<u>Table</u>		<u>Page</u>
7.2-48	TPTA 1.1A Case Membrane Strain Gage Data.	148
7.2-49	TPTA 1.1 Joint E Maximum Deflections.	149
7.2-50	TPTA 1.1 Joint E Radial Growth.	150
7.2-51	TPTA 1.1 Joint E Stress	151
7.2-52	TPTA 1.1A Joint E Maximum Deflections	152
7.2-53	TPTA 1.1A Joint E Radial Growth	153
7.2-54	TPTA 1.1A Joint E Stress.	154
7.2-55	TPTA 1.1 Joint C Maximum Deflections.	156
7.2-56	TPTA 1.1 Joint C Radial Growth.	157
7.2-57	TPTA 1.1 Joint C Stresses	158
7.2-58	TPTA 1.1A Joint C Maximum Deflection.	159
7.2-59	TPTA 1.1A Joint C Radial Growth	160
7.2-60	TPTA 1.1A Joint C Stresses.	161
7.2-61	TPTA 1.1 Joint F Maximum Deflections.	162
7.2-62	TPTA 1.1 Joint F Radial Growth.	163
7.2-63	TPTA 1.1 Joint F Stress	164
7.2-64	TPTA 1.1A Joint F Maximum Deflections	165
7.2-65	TPTA 1.1A Joint F Radial Growth	166
7.2-66	TPTA 1.1A Joint F Stress.	167
7.3-1	J-insulation Joint Gap Analysis Summary	181
7.3-2	Joint A Transfer at J-Insulation ID Tip	184
7.3-3	Joint B Transfer at J-Insulation ID Tip	186
7.3-4	Nozzle-to-Case Gap Summary.	188
7.5-1	TPTA 1.1 Firing, Insulation Shear Stress Gages - Comparison and Analysis	257
7.6-1	Joint A Leak Check Results.	260
7.6-2	Joint B Leak Check Results.	261
7.6-3	Joint D Leak Check Results.	262

LIST OF ACRONYMS

CEI	contract end item
CF	capture feature
D&V	development and verification
ETA	external tank attach
HPM	high performance motor
ICD	interface control drawing
JES	Joint Environment Simulator
LVDT	linear variable differential transformer
MEOP	maximum expected operating pressure
MSFC	Marshall Space Flight Center
NBR	nitrile butadiene rubber
NJES	Nozzle Joint Environment Simulator
RSRM	redesigned solid rocket motor
SRB	solid rocket booster
SSME	Space Shuttle main engines
TPTA	transient pressure test article
USBI	United Space Boosters, Incorporated

LIST OF TECHNICAL WORDS AND PHRASES

Max Q loads	ETA strut loads at time of maximum dynamic pressure
High Q boost	SRB maximum dynamic pressure event time
Lift-off	maximum internal pressure event time during SRB ignition of RSRM

INTRODUCTION

This report presents the results obtained during the first transient pressure test article (TPTA) 1.1 test. The static hot-firing test (TPTA 1.1) was conducted on 19 Nov 1987 and the cold-gas high Q (sometimes referred to as max Q) test (TPTA 1.1A) was performed on 24 Nov 1987. Both tests were conducted at Marshall Space Flight Center (MSFC) in accordance with NASA document SE-019-019-2H, which was derived from CTP-0006, Transient Pressure Test Article (TPTA) 1.1 Test Plan. The TPTA tests were designed to evaluate and characterize the RSRM joint performance under ignition and strut-induced loads. The igniter propellant, propellant slabs, and nozzle were designed to simulate +3 sigma solid rocket motor (SRM) pressure and burn rate ignition transient. Max Q signifies maximum aerodynamic loading that occurs in flight.

TPTA 1.1 and 1.1A consisted of field test Joints A and B, which were the original J-insulation configuration; and the flight configuration of the nozzle-to-case joint designated as test Joint D. The test article was in a vertical position for the test, simulating the flight setup configuration. Fluorocarbon O-rings were used in all test joints, and these joints were required to be within $70 \pm 5^\circ\text{F}$ prior to both tests. Combined pressure and other representative axial loads were applied during the static hot-firing test. During the high Q test the chamber was pressurized to 612 psia and strut loads were applied. The chamber and primary O-rings on the field joints were pressurized to 612 psia by using nitrogen during the high Q test. Joint displacement, axial and radial growth, stresses, strain, temperature, and pressures were measured.

1.1 TEST ARTICLE

Hardware for the first TPTA 1.1 and 1.1A tests featured the redesigned joint configuration at each of the two field joints and at the nozzle joint as illustrated in Figure 1.1-1. This test article basically combined the Joint Environment Simulator (JES) and Nozzle Joint Environment Simulator (NJES)

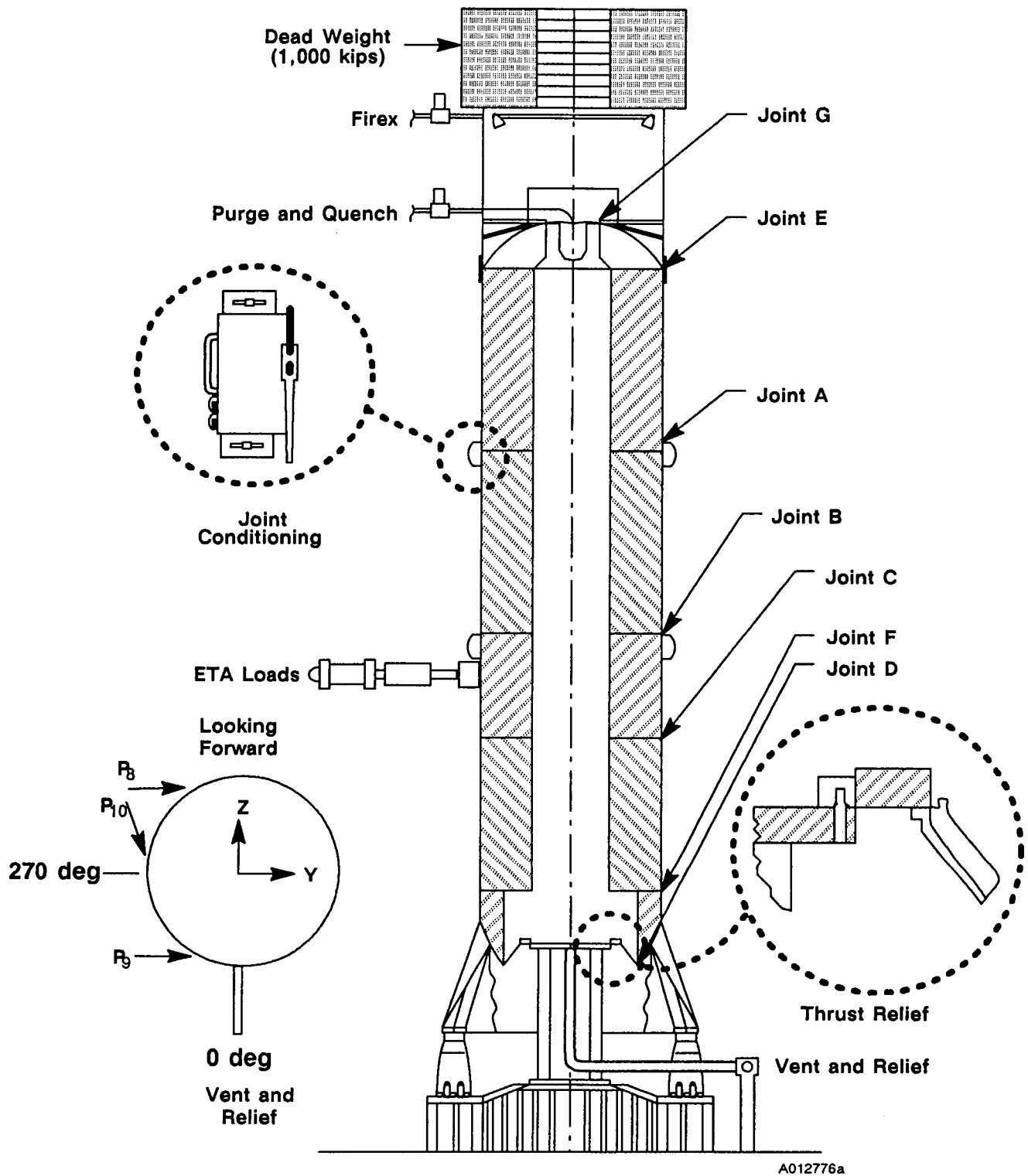


Figure 1.1-1. TPTA 1.1 Configuration

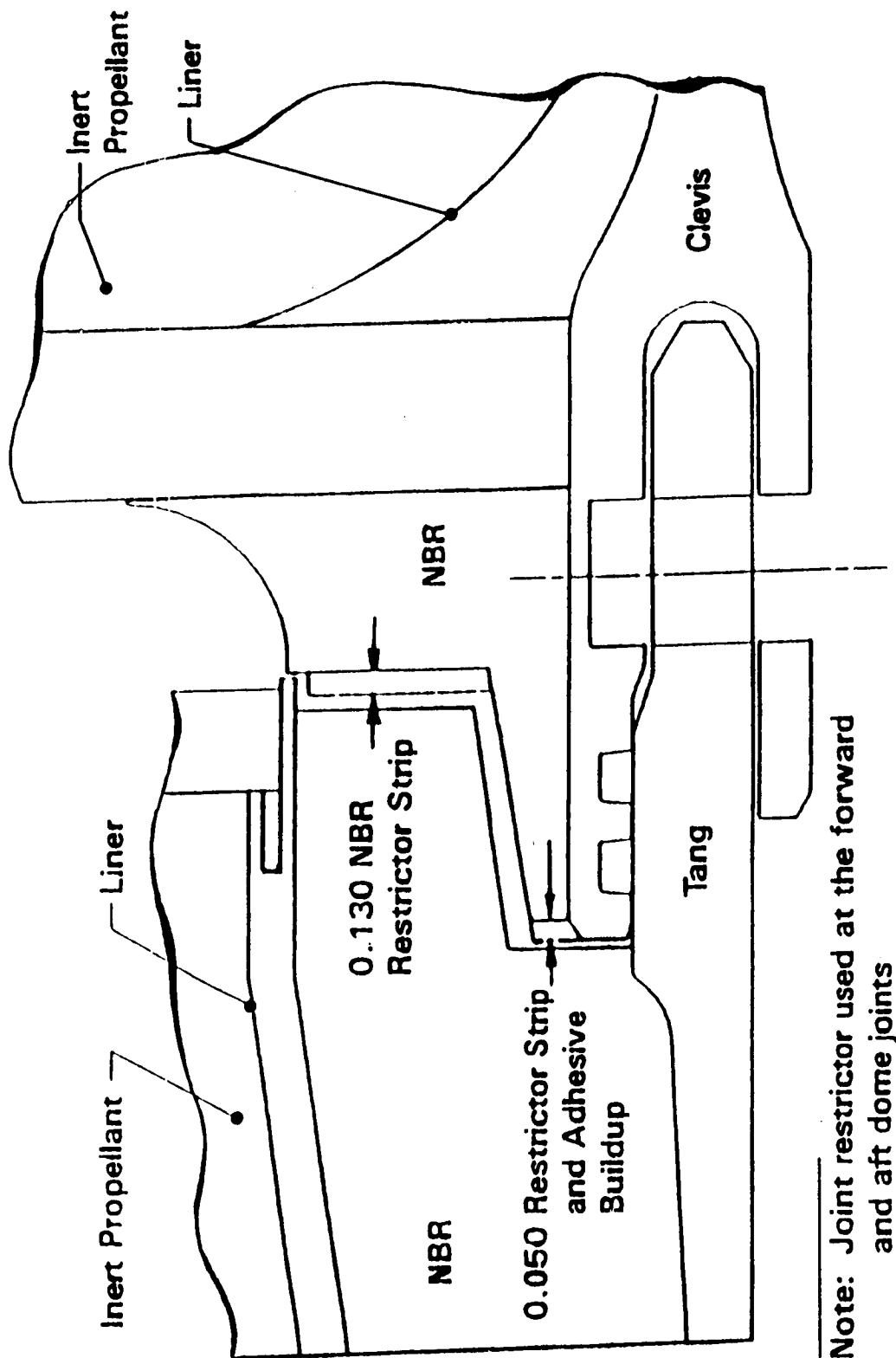
test articles into one. The JES test series simulated a 3 sigma pressure transient in the field joints without strut loads, while the NJES test series did the same in the nozzle-to-case joint. The test article was stacked in a subscale configuration. This test article had a dead weight of 1,000 \pm 20 kips to simulate weight of a complete solid rocket booster (SRB) including ET (external tank)/orbiter loads. Part numbers and serial numbers of the major test components are listed in Table 1.1-1. Appendix A contains the drawing tree.

Part numbers and serial numbers of the major test components are listed in Table 1.1-1. Figure 1.1-1 illustrates the test setup. Details of the joints are as follows:

- a. The forward dome/forward cylinder joint (Joint E) was a nontest vented modified HPM joint, containing a fluorocarbon (V747) O-ring in the primary groove and a saturated polysiloxane O-ring in the secondary groove (Figure 1.1-2). This joint was conditioned to an average of 83°F prior to the static hot-firing test and to an average of 89°F during the cold-gas high Q test.
- b. The forward cylinder/aft cylinder joint (Joint A) had an unvented DM-8 J-insulation configuration with three fluorocarbon O-rings (Figure 1.1-3). Fluorocarbon filler was used in the region between the capture feature (CF) and primary O-rings. This region is referred to as the V_2 volume. Pressure-sensitive adhesive was used on the tang and clevis 360 deg. No intentional defects were configured in the joint, which was conditioned to an average of 76°F prior to the static hot-firing test and at 80°F during the cold-gas high Q test.
- c. The aft cylinder/ETA joint (Joint B) had an unvented DM-8 J-insulation configuration (Figure 1.1-3) with three fluorocarbon O-rings. Polysiloxane V_2 filler was used in the V_2 volume. Pressure-sensitive adhesive was used on the tang and clevis 360 deg. No intentional defects were configured in the joint, which was conditioned to an average of 75°F prior to the static firing test and at 79°F during the cold-gas high Q test.

Table 1.1-1. Major Test Components

<u>Component</u>	<u>Part No.</u>	<u>Serial No.</u>
Forward Dome	1U51473-02	23
Forward Cylinder	1U52982-02	09
Aft Cylinder	1U52982-02	10
ETA Segment	1U50716-06	23
Stiffener Segment	1U50715-02	11
Aft Dome	1U50129-11	13
Fixed Housing	1U52945-101	1
Propellant Cartridge (45 fins)	7U52933	NA
Igniter Assembly	1U50776	NA
<u>CF O-rings</u>		
Forward Cylinder/Aft Cylinder	7U75204-13	60
Aft Cylinder/ETA	7U75204-13	31
Wiper O-ring	7U75204-47	6
<u>Primary O-rings</u>		
Forward Dome/Forward Cylinder	7U75204-22	5
Forward Cylinder/Aft Cylinder	7U75204-22	63
Aft Cylinder/ETA	7U75204-22	57
ETA/Stiffener Segment	7U75204-21	44
Stiffener Segment/Aft Dome	7U75204-22	62
<u>Secondary O-rings</u>		
Forward Dome/Forward Cylinder	7U75397-07	3
Forward Cylinder/Aft Cylinder	7U75204-22	65
Aft Cylinder/ETA	7U75204-22	58
ETA/Stiffener Segment	7U75204-21	51
Stiffener Segment/Aft Dome	7U75397-07	10



Note: Joint restrictor used at the forward and aft dome joints

Figure 1.1-2. TPTA 1.1 Dome Joints

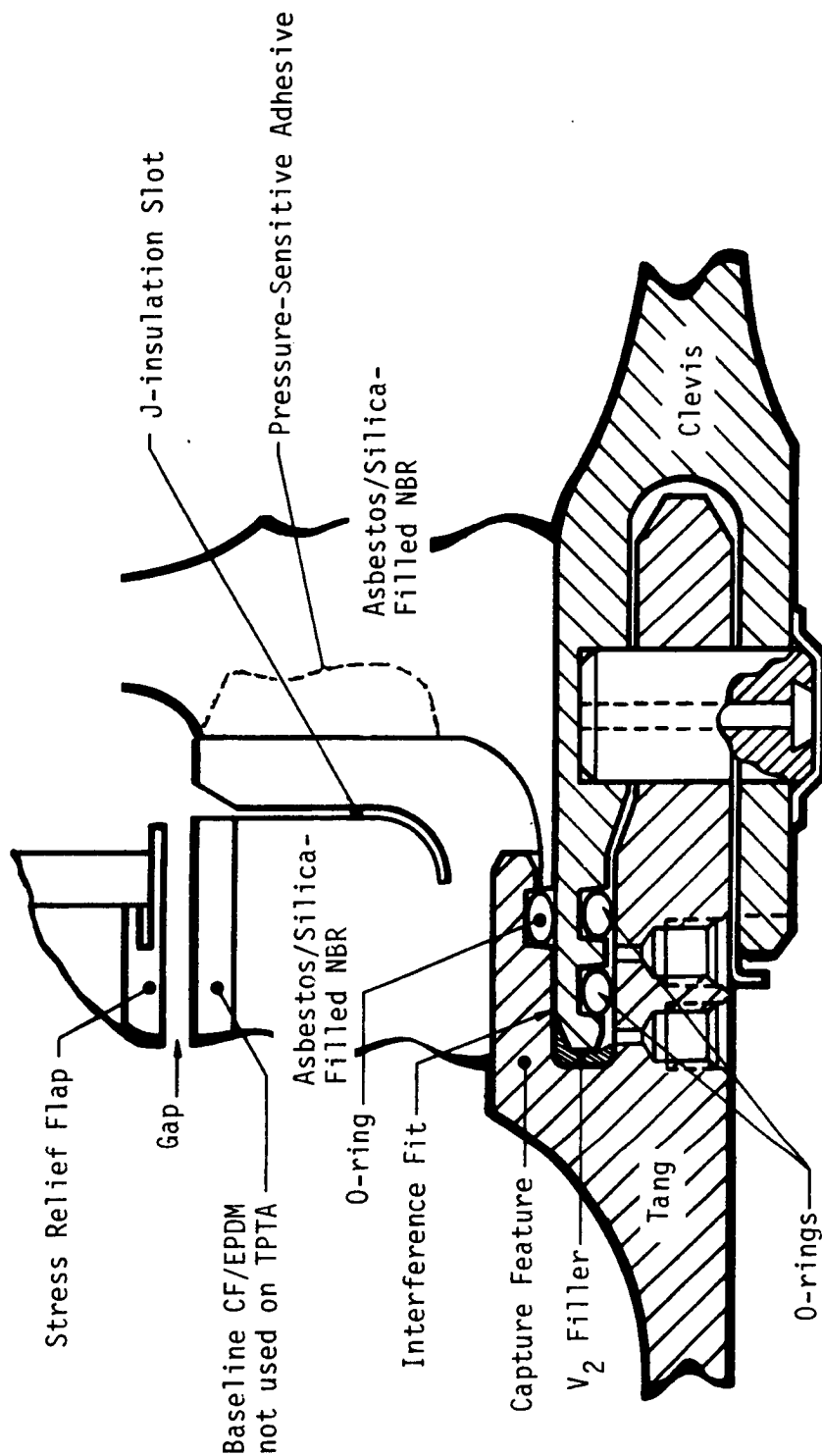


Figure 1.1-3. Field Joint DM-8 Baseline Design

- d. The ETA segment/stiffener segment joint (Joint C) was a nontest RSRM factory joint with a fluorocarbon primary O-ring and fluorocarbon secondary O-ring. This joint was not temperature conditioned for either of the tests. The joint temperature was 50°F prior to the static hot-firing test and 64°F during the cold-gas high Q test.
- e. The stiffener segment/aft dome joint (Joint F) was a nontest vented HPM joint (Figure 1.1-2). It had a fluorocarbon primary O-ring and an unsaturated polysiloxane secondary O-ring. This joint was conditioned to an average of 83°F prior to the static hot-firing test and to an average of 89°F during the cold-gas high Q test.
- f. The aft dome/fixed housing joint (Joint D) was the baseline RSRM configuration test joint with three fluorocarbon O-rings and radial bolts. The aft dome had shorter vent slots than the RSRM configuration. The joint configuration is illustrated in Figure 1.1-4. This joint was conditioned to an average of 82°F prior to the static hot-firing test and 83°F during the cold-gas high Q test.

Components used in the TPTA configuration include an aft skirt, a re-designed 360-deg ETA ring, a forward adapter assembly (dummy forward skirt), with an approximately 1,000-kips axial load weight. Internal insulation and inert propellant simulated flight motor internal geometry. The propellant cartridge (45 fins) consisted of an insulated insert containing sheets of TP-H1214 propellant, which were bonded to insulated fins. Figures 1.1-5 and 1.1-6 illustrate the propellant configuration. Slot propellant was used to simulate slot burning in the motor and contribute to maximum chamber pressure. The TPTA ignition system is comprised of two SRM initiators, an electromechanical safety and arming (S&A) device, and a standard flight igniter. The igniter adapter was equipped with a gaseous nitrogen quench port. Total propellant weight was 413.9 lb. All joint pins and pin retainers were flight configuration hardware.

Hot gases did not get past the J-insulation in the static hot-firing test and the CF primary O-rings sealed in the cold-gas high Q test. Joint D has pressure to the wiper O-ring, which sealed. All measurements were

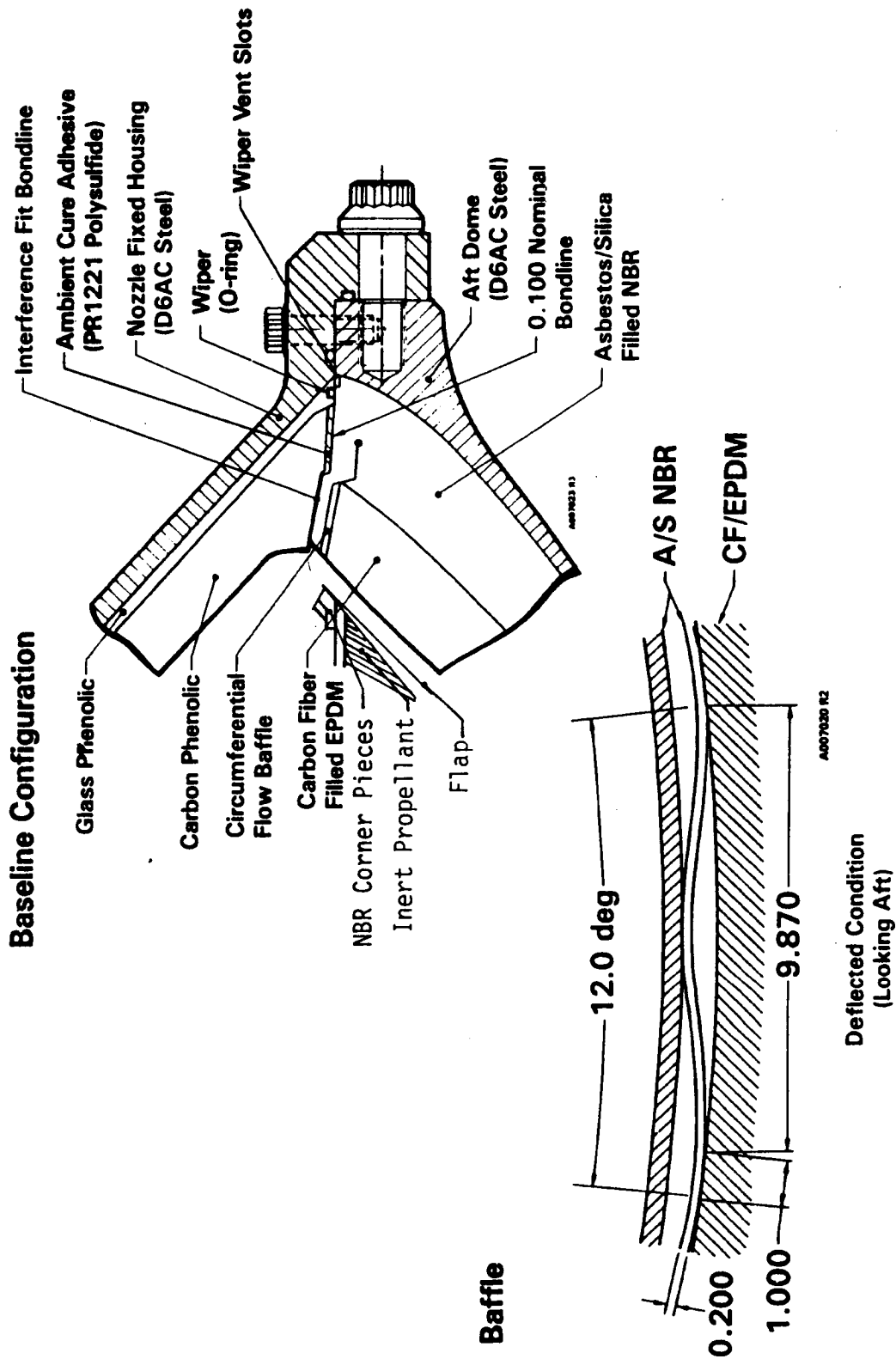


Figure 1.1-4. Nozzle-to-Case Joint Assembly

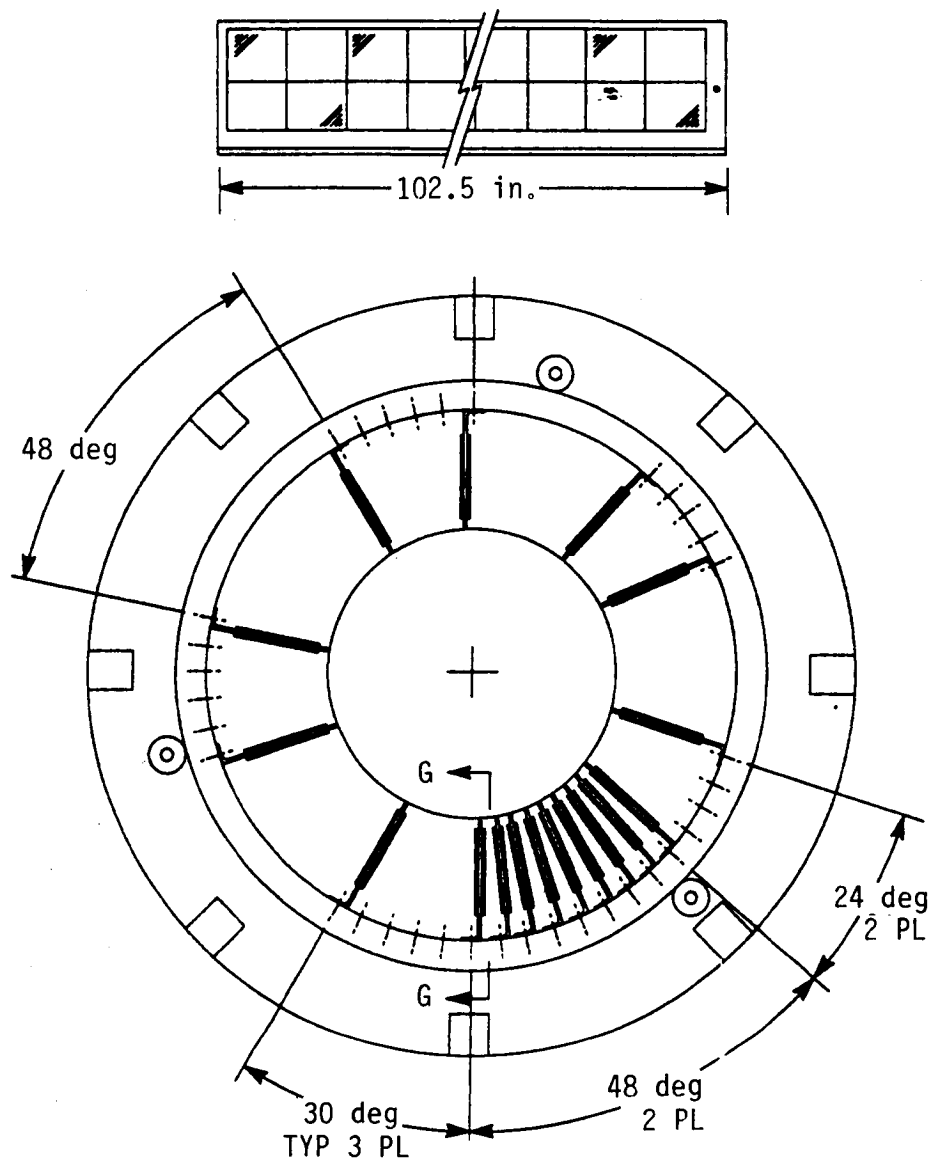


Figure 1.1-5. TPTA 1.1 Finned Propellant Configuration

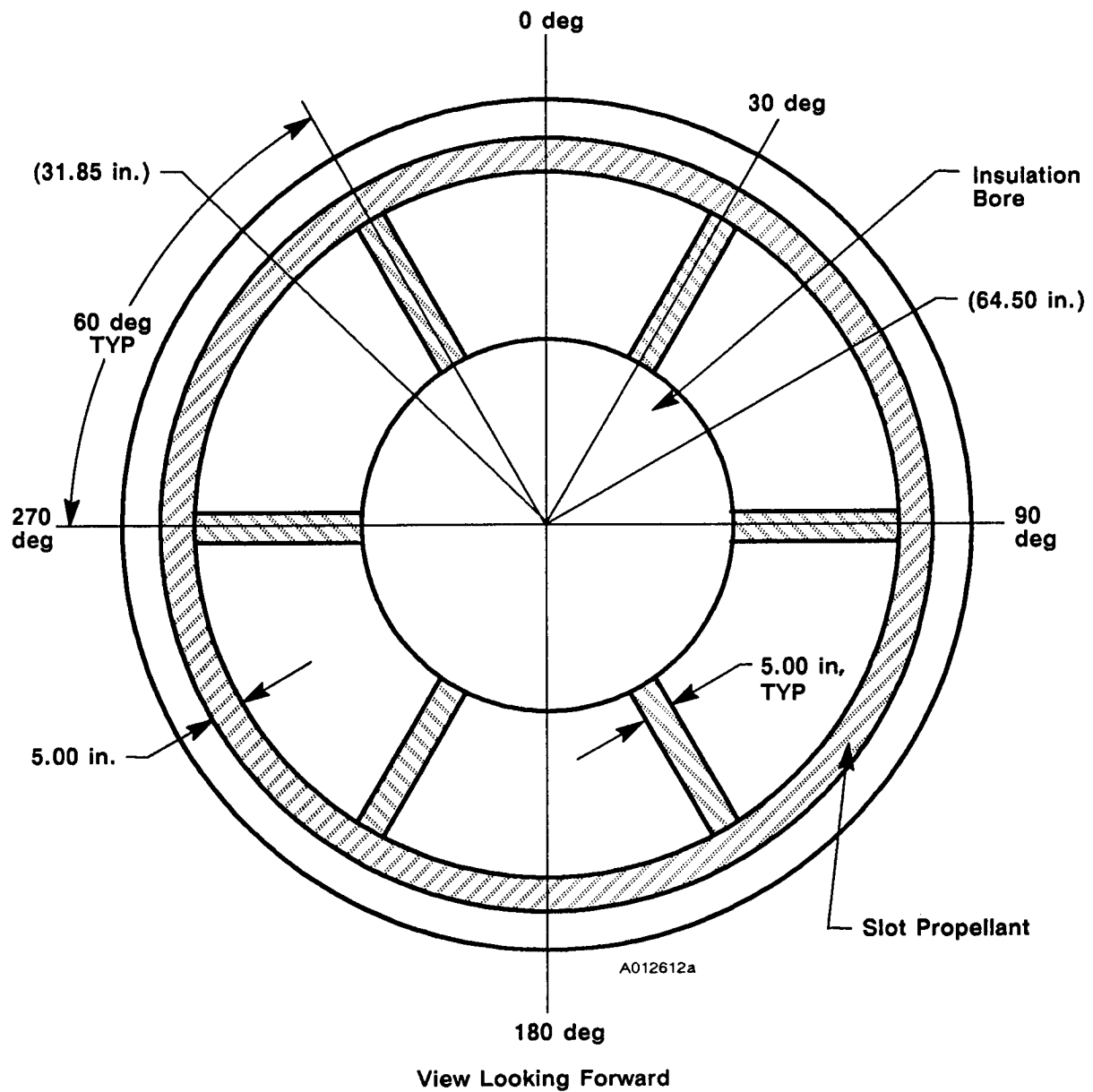


Figure 1.1-6. TPTA 1.1 Slot Propellant Configuration

close to the predicted values and no anomalies were noted in the test article or in its performance.

Because of the extensive amount of data generated during this program, it was decided that the appendixes, issued as Volume II, would not be distributed with this report. Copies of Volume II may be obtained by contacting the Print Crib at Morton Thiokol, Space Operations, ext. 3231.

2

OBJECTIVES

The objectives of the TPTA 1.1 test were to provide data which can be used in subsequent TPTA tests to verify the sealing capability of RSRM joints and to provide facility checkout data. Instrumentation used during the test in support of specific test objectives is shown in Drawing 7U75234.

Primary qualification objectives of this test included:

- a. Certifying that the nominal nozzle-to-case joint insulation design protects the seals from visible degradation by motor combustion gases during an MEOP ignition pressure transient (Reference CPW1-3600A, paragraph 3.2.1.8.1.1.d).
- b. Certifying that the nozzle-to-case joint insulation maintains structural integrity and does not shed fibrous or particulate matter during assembly (CPW1-3600A, paragraphs 3.2.1.8.1.1.c, -d, and -f).
- c. Certifying by inspection that aft segment-to-aft skirt interfaces are compatible (CPW1-3600A, paragraph 3.2.1.3.d).

Primary development test objectives include:

- d. Certifying that the primary O-ring will seal under high Q pressure and ETA loading conditions in a fail-safe mode (CPW1-3600A, paragraphs 3.2.1.2.1.a, and 3.2.7.2)
- e. Evaluating the effect of the seal leak test on the field and nozzle-to-case joint seals and insulation (CPW1-3600A, paragraphs 3.2.1.2.1.c, and 3.2.1.8.1.1.b).
- f. Evaluating the performance of the DM-8 configured field joint insulation (CPW1-3600A, paragraphs 3.2.1.8.1.1.c, -d, and -f).
- g. Verifying that field and nozzle-to-case joint gap opening rates and total deflections fall within analytical predicted limits.

- h. Obtaining data on induced stress in the J-insulation bonded interface and propellant liner insulation (PLI) bondline in the field joint and insulation-to-case bondlines in the field and nozzle-to-case joints.
- i. Demonstrating assembly/disassembly and reusability of joints (CPW1-3600A, paragraph 3.2.5.1).
- j. Obtaining data on the function of the field joint seal system with ignition and strut loads applied.
- k. Establishing a SRM joint performance historical data base.
- l. Demonstrating that no additional case joint deformation exists from multiple tests (ratcheting).
- m. Demonstrating the adequacy of assembly/disassembly tooling and procedures.
- n. Verifying the TPTA ballistic model.
- o. Verifying the function of the TPTA facility under test conditions.
- p. Evaluating the condition of the hardware and components from post-test measurements, inspection and data.
- q. Obtaining data to verify structural models on the effect of high Q ET loads on joint deflection.

USBI Objectives

Primary USBI test objectives for the ETA ring and aft skirt included:

- a. Determining whether yielding of the 360-deg ETA ring components or of the fasteners has occurred during the strut loading sequence or transient motor pressure rise.
- b. Providing information for the historical data base.
- c. Obtaining data from transient loading to compare to static analyses and tests.
- d. Determining out-of-roundness of the motor case before and after ring installation.
- e. Obtaining data to establish the reusability of the aft skirt.

APPLICABLE DOCUMENTS

The latest revisions of the following documents, unless otherwise specified, are applicable to the extent specified herein.

Morton Thiokol Manuals

GS&HM

General Safety and Health Manual

Morton Thiokol Drawings

1U50776	Igniter, Rocket Motor - Test Configuration
7U52480	Instrumentation Installation (TPTA)
7U52488	Fixed Housing Assembly, Insulated
7U52490	Aft Dome, Insulated, Inert-Loaded
7U52494	Forward Dome, Insulated, Inert-Loaded
7U52826	ETA, Modified
7U52831	Stiffener, Modified
7U52933	Cartridge Assembly
7U52985	Safety and Arming Device, Rocket Motor
7U75170	Assembly Fixture SRM Field Joint
7U75234	Instrumentation Kit, Installation
7U75326	Guide Pin Assembly
7U75442	Cylinder, Live Loaded, Forward
7U75455	Cylinder, Live Loaded, Aft
7U75708	Test Assembly TPTA
7U75709	Test Subassembly TPTA

Morton Thiokol Specifications

STW5-2678	Specification Sealant Liquid Epoxy Resin, Asbestos-Float-Filled
STW7-2692	Leak Testing Ignition System Seals, Space Shuttle Project, Solid Rocket Motor

MORTON THIOKOL INC.

Space Operations

STW7-3432	Refurbishment Requirements, RSRM Full-Scale Test Article
STW7-3447	RSRM Leak Testing Case Field Joint
STW7-3448	RSRM Leak Testing Case-to-Nozzle Joint

Morton Thiokol Documents

ETP-0129	Nonvented Joint Inspection Requirements
ETP-0161	TPTA Assembly Measurement Requirements
TWA-792	Receive, Stack, Destack and Ship Transient Pressure Test Article (TPTA) - Operation and Maintenance Documentation
TWR-15937	TPTA Test Requirements Specification
TWR-16201	Guidelines for Quality Assurance of JES, NJES, TPTA, and STA-3 Motors
TWR-16235	Safety, Reliability and Quality Assurance Plan
TWR-16302	Space Shuttle Solid Rocket Motor Project, RSRM, Safety Plan
TWR-16503	Operating Procedure, Field Joint Separation Tool, Vertical Installation and Removal
TWR-16544	Operating Procedure, Field Joint Assembly Fixture, Installation and Removal
TWR-16579	Operating Procedure, Nozzle Removal Tool
TWR-16674	TPTA and Pathfinder Mechanical Loads
TWR-17001	Nozzle Joint Environment Simulator (NJES) 2B, Final Test Report
TWR-16501	Joint Environment Simulator (JES) 3A, Final Test Report

USBI-BPC Documents

10100-0047	360-deg ETA Ring Installation, Morton Thiokol/ MSFC Test Articles
------------	--

USBI Drawings

10100-0047-602	360-deg ETA Ring
10166-0033-601	Aft Skirt
10183-0098	Instrumentation of 360-deg ETA Ring for TPTA Test
10183-0099	Instrumentation of Aft Skirt for TPTA Test

REVISION _____

88842-8.12

DOC NO.	TWR-17927	VOL
SEC	PAGE	15

U.S. Government Documents

CR01-5300.35	MSFC Quality Assurance Plan for SRM/SRB Redesign
DPD-400	Contractor Test Reports
JSC-07700-10-MVP-01	Shuttle Master Verification Plan, General Approach and Guidelines
SE-019-019-2H	Verification Plan, Solid Rocket Booster Shuttle Master Verification Plan, Vol. IV (JSC-07700-MVP-4)
MIL-STD-45662	Calibration System Requirements

SUMMARY AND CONCLUSIONS

4.1 SUMMARY

4.1.1 Static Hot-Firing Test (TPTA 1.1)

All objectives but one of the static hot-firing test were met. The strut loading system malfunctioned and no strut loads were applied during the static hot-firing test. The pressure rise rate and maximum pressure were compatible with the predicted values. The 1,000-kips axial load had no significant effect on joint performance compared with the JES and NJES tests. The maximum pressure was 913.3 psia. An overview of the static hot-firing and cold-gas high Q test results are provided in Table 4.1-1.

4.1.1.1 Ballistic Performance. Ballistic performance was as predicted. The maximum average chamber pressure was 913.3 psia, which compares well with the predicted maximum average pressure of 910.2 psia. The maximum average pressure rise rate achieved was 141.0 psia/10 ms, which was well above the required minimum value of 115.9 psia/10 ms. A detailed description of the ballistic results are discussed in Section 7.1.

4.1.1.2 Joint Performance. All the joints except Joint C were conditioned to temperatures between 75 and 84°F. The required temperature conditioning was 70 ±5°F. Joint C was at ambient temperature. The effect of the 1,000-kips axial load on joints A, B, and D gaps was insignificant. The results noted at the joints are detailed in Section 7.2 and summarized as follows:

- a. Forward dome/forward cylinder (Joint E). There was pressure to the primary O-ring, and no evidence of gas leakage past the primary O-ring or of erosion of the O-ring. Maximum inter-O-ring gap opening was 0.009 inch. This joint was conditioned to an average temperature of 84°F prior to test.
- b. Forward cylinder/aft cylinder (Joint A). Hot gases did not get past the J-insulation. The average joint temperature was 76°F prior to test. The insulation was the pressure face. The maximum inter-O-ring

measured gap was 0.001 in. open, which was less than the predicted maximum value of 0.003 inch.

- c. Aft cylinder/ETA (Joint B). Hot gases did not get past the J-insulation. The average joint temperature was 75°F. Pressure was incident on the insulation and there was no O-ring damage. There were heat-affected areas at the 120- and 240-deg locations. Pressure transducers at these locations caused gas paths in the insulation bondline. The predicted inter-O-ring gap opening was less than 0.003 in. and the maximum measured gap was 0.006 in. open with an average value of 0.000 inch.
- d. ETA segment/stiffener segment (Joint C). Inert propellant was the pressure face. Joint C was not conditioned and was at 50°F. This joint has not been disassembled. Maximum inter-O-ring gap deflection was 0.002 in. (open) with an average deflection of 0.000 inch. Inert propellant was the pressure face.
- e. Stiffener segment/aft dome (Joint F). There was pressure to the primary O-ring and no evidence of gas leakage past the primary O-ring or erosion of the O-ring. The average conditioned joint temperature was 84°F. Maximum inter-O-ring gap opening was 0.006 inch.
- f. Aft dome/fixed housing (Joint D). There was pressure to the wiper O-ring, which sealed. The average joint temperature was 82°F. NBR slivers were found in the area of the wiper O-ring groove. They were caused by cured 913 adhesive that protruded above the steel housing. An unintentional blowhole filled with black viscous material (determined to be decomposed polysulfide) was noted leading to the wiper O-ring at the 188-deg location. The wiper O-ring experienced no blowby or heat effects. Other voids were noted in the bondline. This is believed to be due to the short vent slots. These slots were shorter than currently planned for flight. Upon disassembly, an inexplicable large void was found in the bondline between the steel and glass phenolic of the fixed housing. The void and NBR slivers did not affect the test. Predicted gap opening upstream of the primary O-ring was 0.008 in. and the maximum measured gap opening was 0.009 inch. Predicted gap downstream of the primary O-ring was 0.002 in. and the

Table 4.1-1. TPTA Test Summary

<u>TPTA 1.1 Static Hot Fire</u>		<u>TPTA 1.1A Cold-Gas High Q</u>
<u>OBJECTIVES</u>		
Provide data which can be used in subsequent TPTA tests to verify the sealing capability of RSRM joints and to provide facility checkout data.		
<u>RESULTS</u>		
Due to a malfunction of the strut load application system, all objectives of the static hot-fire test were not met. All objectives of the cold-gas high Q Test were met. The CF O-rings and primary O-rings sealed without indication of any leakage past the O-rings. The test facility performed acceptably.		
<u>TEST DESCRIPTION</u>		
Igniter	Standard flight HPM igniter with CO ₂ quench port	NA
Propellant description	TP-H1214 propellant strips on 45 cartridge fins and slot propellant joints	NA
Amount	413.9 lbm	NA
<u>STRUT LOADS*</u>		
P8 (max/min)	NA	157.30 kips/28.71 kips
P9 (max/min)	NA	-245.48 kips/-158.01 kips
P10 (max/min)	NA	255.20 kips/245.55 kips
<u>BALLISTICS</u>		
Max chamber pressure	913.3 psia	612 psia
Max rise rate	141.0 psi/10 ms	NA
Results	Performed as predicted	NA
<u>JOINT A</u>		
<u>Structures</u>		
Description	CF configuration hardware	CF configuration hardware
Joint Conditioning	76°F	80°F
Inter-O-ring deflection (max/avg)	0.001 in. (open)/0.001 in. (close)	0.005 in. (open)/0.003 in. (open)
Max pressure between CF and primary O-rings	14.0 psia	611.4 psia
Max inter-O-ring pressure	15.7 psia	19.0 psia
Pressure face	Insulation	Insulation and primary O-ring
O-ring material	Fluorocarbon	Fluorocarbon
Results	No O-ring damage or blowby	No O-ring damage or leaks
<u>Insulation</u>		
Description	Unvented DM-8 J-insulation nominal joint, pressure-sensitive adhesive on tang and clevis circumferentially 360 deg	Unvented DM-8 J-insulation nominal joint, pressure-sensitive adhesive on tang and clevis circumferentially 360 deg
Intentional defects	None	None
*(+) = strut compression (-) = strut tension		
Note: TPTA 1.1 measurements taken between 0 to 0.6 sec into test TPTA 1.1A measurements taken between 9 and 14 sec into test		

88842-4.1

REVISION _____

DOC NO. TWR-17927

VOL

SEC

PAGE

19

Table 4.1-1. TPTA Test Summary (Cont)

	<u>TPTA 1.1 Static Hot Fire</u>	<u>Cold-Gas High Q</u>
<u>JOINT B</u>		
<u>Structures</u>		
Description	CF configuration hardware	CF configuration hardware
Joint conditioning	75°F	79°F
Inter O-ring deflection (max/avg)	0.006 in. (open)/0.000 in.	0.004 in. (open)/0.003 in. (open)
Max pressure between CF and primary O-rings	9.7 psia	612.5 psia
Max inter-O-ring pressure	28.5 psia	16.2 psia
Pressure face	Insulation	Insulation and primary O-ring
O-ring material	Fluorocarbon	Fluorocarbon
Results	No O-ring damage or blowby	No O-ring damage or leaks
<u>Insulation</u>		
Description	Unvented DM-8 J-insulation nominal joint, pressure-sensitive adhesive tang and clevis circumferentially 360 deg	Unvented DM-8 J-insulation nominal joint, pressure-sensitive adhesive on tang and clevis circumferentially 360 deg
Intentional defects	None	None
<u>JOINT C</u>		
<u>Structures</u>		
Description	HPM configuration; factory joint without insulation	HPM configuration; factory joint without insulation
Joint conditioning	Ambient (50°F)	Ambient (64°F)
Inter-O-ring deflection (max/avg)	0.002 in. (open)/0.000 in.	0.004 in. (open)/0.003 in. (open)
Max inter-O-ring pressure	14.7 psia	12.1 psia
Pressure face	Inert propellant	Inert propellant
O-ring material	Fluorocarbon	Fluorocarbon
Results	No O-ring damage or blowby	No O-ring damage or leaks
<u>Insulation</u>		
Description	Unvented HPM nominal factory joint	Unvented HPM nominal factory joint
Intentional defects	None	None
<u>JOINT D (Nozzle-to-Case)</u>		
<u>Structures</u>		
Description	RSRM baseline (radial bolt) configuration	RSRM baseline (radial bolt) configuration
Joint conditioning	82°F	83°F
Inter-O-ring deflection (max/avg)	0.004 in. (open)/0.004 in. (open)	0.002 in. (open)/0.001 in. (open)
Max pressure between wiper and primary O-rings	20.3 psia	127.7 psia
Max inter-O-ring pressure	16.6 psia	15.3 psia
Pressure face	Wiper O-ring	Wiper O-ring
O-ring material	Fluorocarbon	Fluorocarbon
Results	No O-ring damage or blowby. Short vent slots cause a blowhole in the polysulfide	No O-ring damage or leaks
<u>Insulation</u>		
Description	RSRM unvented design	RSRM unvented design
Intentional defects	None	None

Note: TPTA 1.1 measurements taken between 0 to 0.6 sec into test
TPTA 1.1A measurements taken between 9.0 to 14.0 sec into test

88842-4.2

REVISION _____

DOC NO. TWR-17927	VOL _____
SEC _____	PAGE 20

maximum measured gap opening was 0.004 inch. Predictions are based on bolt loads of 45 kips on the radial bolt and 140 kips on the axial bolt. The bolts were not torqued with ultrasonics and probably had a low torque applied, which can affect the gap opening.

4.1.1.3 Insulation Performance. The J-insulation functioned nominally as designed and did not permit hot gases to reach the O-rings. Details of insulation are provided in Section 7.3.

4.1.1.4 Nozzle Performance. During the static hot-firing test sequence, approximately 12 sec after ignition, the nozzle was plugged by the quench port injector plug. The motor pressure stabilized at 420 psia for approximately 11 min before it was uneventfully depressurized, using the auxiliary system. Aside from these anomalies, the nozzle functioned nominally.

4.1.2 Cold-Gas High Q Test (TPTA 1.1A)

After the static hot-firing test, the TPTA was pressurized using GN_2 gas. All the joints except Joint C were between 79 and 89°F during the test. The maximum chamber pressure was 612 psia, and the V_2 volume was pressurized to 612 psia with an external GN_2 source, at which time the high Q dynamic strut loads were applied to the ETA section. The following maximum and minimum loads were applied during the cold-gas high Q load cycles between 12.1 and 12.7 sec:

<u>Strut</u>	<u>Maximum (kips)</u>	<u>Minimum (kips)</u>	<u>Peak-to-Peak (kips)</u>
P8	157.30	28.71	128.59
P9	-245.48	-158.01	87.47
P10	255.20	245.55	9.65

NOTE: The sign convention for the applied strut loads as shown above and in all data plots is as follows:

(+) = Strut compression

(-) = Strut tension

Table 4.1-2 compares results of the static-hot test and the cold-gas high Q test. Section 7.1 contains a detailed description of the cold-gas high Q test. There was an insignificant effect of strut loads on joint gap deflections.

Table 4.1-2. TPTA 1.1 Static Hot-Firing Test Summary

Test TPTA-1.1	913.3 psia	141 psi/10 ms				
Joint	Temperature	O-rings	Joint Design	Results	Damage	Inter-O-ring Gap Deflection
Joint E Forward Dome/ Forward Cylinder	Conditioned to average of 83°F	Primary fluorocarbon Secondary saturated polysiloxane	HPM vented, no putty. Full shims of 0.050 in. installed	Pressure to primary O-ring. Primary O-ring sealed	None	Maximum measured gap opening 0.009 in.
Joint A Forward Cylinder/ Aft Cylinder	Conditioned to average of 76°F	CF fluorocarbon Primary fluorocarbon Secondary fluorocarbon	CF joint. DM-8 J-insulation nonvented design. Full shims of 0.040 in. installed. V-2 volume filler installed (fluorocarbon). Average interference was 0.018 in.	Pressure to J-insulation. J-insulation sealed	None	Maximum measured gap opening 0.001 in. Average measured gap 0.001 in. close. Maximum Δgap of 0.002 in. open. Average Δgap of 0.001 in. open.
Joint B Aft Cylinder/ ET Segment	Conditioned to average of 75°F	CF fluorocarbon Primary fluorocarbon Secondary fluorocarbon	CF joint. DM-8 J-insulation nonvented design. Full shims of 0.040 in. installed. V-2 volume filler installed (Silicone). Right hand 360-deg ETA ring installed. Average interference was 0.007 in.	Pressure to J-insulation. J-insulation sealed	None	Maximum measured gap opening 0.006 in. open. Average measured gap 0.000 in. Maximum Δgap of 0.006 in. open. Average Δgap of 0.001 in. open
Joint C ET Segment/ Stiffener Segment	Not conditioned Ambient 50°F	Primary fluorocarbon Secondary fluorocarbon	Full shims of 0.045 in. installed	Pressure to inert propellant	None	Maximum measured gap opening 0.002 in. Average measured gap 0.000 in. Average Δgap of 0.003 in. open. Maximum Δgap of 0.004 in. open.
Joint F Stiffener Segment/ Aft Dome	Conditioned to average of 83°F	Primary fluorocarbon Secondary unsaturated polysiloxane	HPM vented, no putty. Full shims of 0.045 in. installed	Pressure to primary O-ring. Primary O-ring sealed	None	Maximum measured gap opening 0.006 in.
Joint D Aft Dome/ Fixed Housing	Conditioned to average of 82°F	Wiper fluorocarbon Primary fluorocarbon Secondary fluorocarbon	DM-8 unvented nozzle-to- case joint. Ultrasonic not used to torque the bolts	Gas path through the poly- sulfide with pressure to wiper O-ring. Wiper O-ring sealed. Vent slots were shorter than flight design, causing a gas path through the polysulfide.	None	Maximum gap opening aft primary O-ring 0.004 in. Average gap opening aft primary O-ring 0.004 in. Maximum gap opening forward primary O-ring 0.009 in. Average gap opening forward primary O-ring 0.008 in.

REVISION

DOC NO. **TWR-17927**
 SEC

PAGE
22

88842-14.2

4.1.2.1 Joint Performance. It was determined that high Q strut loads, which are higher than lift-off loads, have an insignificant effect on the CF hardware joint gap opening. The results noted at the joints are detailed in Section 7.2 and summarized as follows:

- a. Forward dome/forward cylinder (Joint E). There was pressure to the insulation and primary O-ring, and there was no evidence of gas leakage past the primary O-ring or erosion of the O-ring. This joint was at 89°F during the test. Maximum inter-O-ring gap opening was 0.003 inch.
- b. Forward cylinder/aft cylinder (Joint A). Slot pressure was 612 psia and pressure between the CF and primary O-rings was 611 psia. The primary O-ring sealed. The average joint temperature was 80°F prior to test. Maximum gap opening forward of the primary O-ring was 0.007 in. and the maximum inter-O-ring gap opening was 0.005 inch. Average inter-O-ring gap opening was 0.003 inch. The maximum disassembly load for Joint A was 95.1 kips. This was the total separation force measured on the separation tool.
- c. Aft cylinder/ETA (Joint B). Maximum pressure forward of the CF O-ring was 635 psia. Pressure between the CF and primary O-rings was 613 psia and the primary O-ring sealed. The average joint temperature was 79°F. Maximum slot pressure was 614 psia. Maximum gap opening forward of the primary O-ring was 0.005 in. and the maximum inter-O-ring gap opening was 0.004 inch. The average inter-O-ring gap opening was 0.002 inch. The maximum strut load effect was determined to be 0.0004 inch. The maximum joint disassembly load was 54.0 kips.
- d. ETA segment/stiffener segment (Joint C). Pressure was incident on the inert propellant. These segments have not been disassembled because they have inert propellant within the joint. Joint C was at ambient temperature (64°F) prior to the test. The maximum gap opening forward of the primary O-ring was 0.006 inch. The maximum inter-O-ring gap opening was 0.004 in., with an average of 0.003 inch. Inert propellant was the pressure face.

- e. Stiffener segment/aft dome (Joint F). There was pressure to insulation and no evidence of gas leakage past the primary O-ring or erosion of the O-ring. This joint was at 89°F during the test. Maximum inter-O-ring gap was 0.007 in. (open).
- f. Aft dome/fixed housing (Joint D). Pressure between the wiper and primary O-rings was 128 psia and inter-O-ring pressure was 15 psia. The pressure rise between the wiper and primary O-rings is believed to be due to gas seepage through the phenolics over the period of time that the test article was pressurized. The average joint temperature was 83°F. The maximum gap opening forward of the primary O-ring was 0.004 in., and the maximum inter-O-ring gap opening was 0.002 inch. The average inter-O-ring gap opening was 0.001 inch. The disassembly load for this joint is unknown.

4.2 CONCLUSIONS BY OBJECTIVES

The results of the qualification test objectives are as follows:

<u>Objective</u>	<u>Conclusion</u>
a. Certifying that the nominal nozzle-to-case joint insulation design protects the seals from visible degradation by motor combustion gases during an MEOP ignition pressure transient.	The nozzle-to-case insulation performed as designed with only minor heat effects and erosion. The seals remained intact and the case hardware sustained no thermal damage.
b. Certifying that the nozzle-to-case joint insulation maintains structural integrity and does not shed fibrous or particulate matter during assembly.	When tested at a conditioned temperature of 82°F, inspection revealed that the nozzle-to-case joint sealing system showed no evidence of structural damage or shedding of fibrous or particulate matter.
c. Certifying by inspection that aft segment-to-aft skirt interfaces are compatible.	Inspection showed that aft segment-to-aft skirt interfaces are compatible and that hardware integrity was maintained.
d. Certifying that the primary O-ring will seal under high Q pressure and ETA loading conditions in a fail-safe mode.	There was no evidence of gas leak past the primary O-ring in the field or nozzle-to-case joints.
e. Evaluating the effect of the seal leak test on the field and nozzle-to-case joint seals and insulation.	Post-test inspection showed no evidence of damage to the field joint or nozzle-to-case joint seals as a result of leak test procedures.

- f. Evaluating the performance of the DM-8 configured field joint insulation.
- g. Verifying that field and nozzle-to-case joint gap opening rate and total deflections fall within analytical predicted limits.
- h. Obtaining data on induced stress in the J-insulation bonded interface and PLI bondline in the field joint and insulation-to-case bondlines in the field and nozzle-to-case joints.
- i. Demonstrating assembly/disassembly and reusability of joints.
- j. Obtaining data on the function of the field joint seal system

The DM-8 configured field functioned nominally.

During the static hot-firing test, at the nozzle-to-case joint, gap openings forward of the primary O-ring were no greater than 0.009 in. which was larger than the analytical value of 0.008 inch. The maximum gap opening forward of the primary O-ring for the high Q test was 0.004 inch. Gap openings in the inter-O-ring region for the static firing test were no greater than 0.004 in. which were larger than the analytical value of 0.002 inch. The maximum inter-O-ring gap for the high Q test was 0.002 in. open.

Ignition-induced stresses were obtained in the field and nozzle-to-case joints at 1) J-insulation bonded interface, 2) the PLI bondline and 3) the insulation-to-case bondlines.

Field joints can be successfully assembled and disassembled in the vertical position without sustaining damage.

The strut loads during ignition could not be evaluated since

- with ignition and strut loads applied.
- k. Establishing SRM joint performance historical data base.
- l. Demonstrating that no additional case joint deformation exists from multiple tests (ratcheting).
- m. Demonstrating adequacy of assembly/disassembly tooling and procedures.
- n. Verifying the TPTA ballistic model.
- o. Verifying the function of the TPTA facility under test conditions.
- no strut loads were applied due to a system malfunction.
- Evaluated and acceptable data were compiled into the historical data base for correlation of joint performance to other RSRM tests.
- Case joint permanent deformation did not render the hardware unusable.
- The FJAF shaped the tang to the same configuration as the clevis and provided protection to the O-rings as the field joints were mated. No hardware was damaged on disassembly. Joint A separation load was 95.1 kips while Joint B separation load was 54.0 kips. Separation forces for Joint D are unknown.
- A maximum headend pressure of 913.3 psia was achieved during the static hot-firing test; the predicted value was 910.2 psia. The pressure rise rate was 141.0 psi/10 ms, which exceeded the minimum requirements.
- The MSFC test facility was found to be suitable for testing the RSRM throughout the TPTA test program.

p. Evaluating the condition of the hardware and components from post-test measurements, inspection, and data.

All test hardware was in good condition after the test except that the nozzle fixed housing had a large void between the glass phenolic and steel.

q. Obtaining data to verify structural models on the effect of high Q ET loads on joint deflection.

Data were obtained for verification of the structural models.

USBI Objectives

a. Determining whether yielding of the 360-deg ETA ring components or of the fasteners has occurred during the strut loading sequence or transient motor pressure rise.

No yielding of the 360-deg ETA ring components or fasteners was noted as a result of the test.

b. Providing information for the historical data base.

A historical data base was set up with the test.

c. Obtaining data from transient loading to compare to static analyses and tests.

Data were obtained for comparison of transient loading with static analysis and tests.

d. Determining out-of-roundness of motor case before and after ring installation.

No significant motor out-of-roundness was noted.

e. Obtaining data to establish the reusability of the aft skirt.

Data obtained are being analyzed to determine whether the aft skirt could be reused.

4.3 CORRELATION OF RESULTS BY CEI REQUIREMENTS

The TPTA 1.1 and 1.1A tests were performed in accordance with the Contract End Item (CEI) specifications CPW1-3600A, dated 3 Aug 1987. Results in the TPTA 1.1 and 1.1A tests satisfy most of the planned verification effort and support further TPTA tests. Paragraphs 3.2.1.2.1.a, and -c, 3.2.1.3.d, 3.2.5.1, 3.2.7.2, and 3.2.1.8.1.1.b, -c, -d, and -f are quoted as follows, with the results from Section 7.

<u>CEI Specification Paragraph</u>	<u>Planned Verification Effort</u>	<u>Test Results</u>
<u>3.2.1.2.1.a Pressure seals</u>	Case field and nozzle-to-case joint sealing shall accommodate any structural deflections which may occur. Sealing shall not require, but shall accommodate, pressure assistance.	Nominal case field and nozzle-to-case joints were used to establish a data base. Further TPTA tests will meet this planned verification effort.
<u>3.2.1.2.1.c Pressure seals</u>	The seal verification approach must not degrade the performance or integrity of the system.	Post-test inspection showed no evidence of damage to the case field or nozzle-to-case joint seals.
<u>3.2.1.3.d Case</u>	The case shall meet the SRB forward and aft skirt interfaces as defined in ICD 3-44001 and ICD 3-44003.	Inspection revealed that the aft segment-to-aft skirt interfaces were found to be compatible.
<u>3.2.1.8.1.1.b Leak test compatibility</u>	The leak test method shall be compatible with the joint insulation to verify joint seals.	Post-test inspection revealed no damage to the joint seals as a result of the leak tests.

3.2.1.8.1.1.c
Assembly
configuration

The insulation shall ensure that system performance and structural integrity is maintained during the assembly process and operation.

Pretest assembly and post-test inspection confirmed that the insulation maintained structural integrity by providing thermal protection.

3.2.1.8.1.1.d
Seal protection

Insulation shall protect primary and secondary seals from visible degradation from motor combustion gas.

Post-test inspection revealed that there was no damage to the O-rings, demonstrating good protection by the insulation.

3.2.1.8.1.1.f
Materials

Insulation materials shall not shed fibrous or particulate matter during assembly which could prevent sealing.

No detectable particulate matter or fibers shed from the insulation.

3.2.5.1
Assembly/
disassembly of
segments

The RSRM shall be capable of assembly/disassembly in both the vertical and horizontal position. The RSRM shall be capable of vertical assembly in a manner to meet the alignment criteria of USBI-10183-0022 without a requirement for optical equipment.

Vertical assembly of the aft segment to the aft skirt was accomplished without using optical equipment.

3.2.7.2
Induced
environment

Certify that the primary O-ring will seal under high Q pressure in a fail-safe mode.

The primary O-rings sealed in all the joints.

INSTRUMENTATION

5.1 INTRODUCTION

The instrumentation for the TPTA 1.1 and 1.1A tests was designed to provide data to verify the sealing capability of RSRM joints and to provide facility checkout data. The instrumentation was designed and installed in accordance with Drawings 7U52480 and 7U75234. The instruments and recording channels are summarized below:

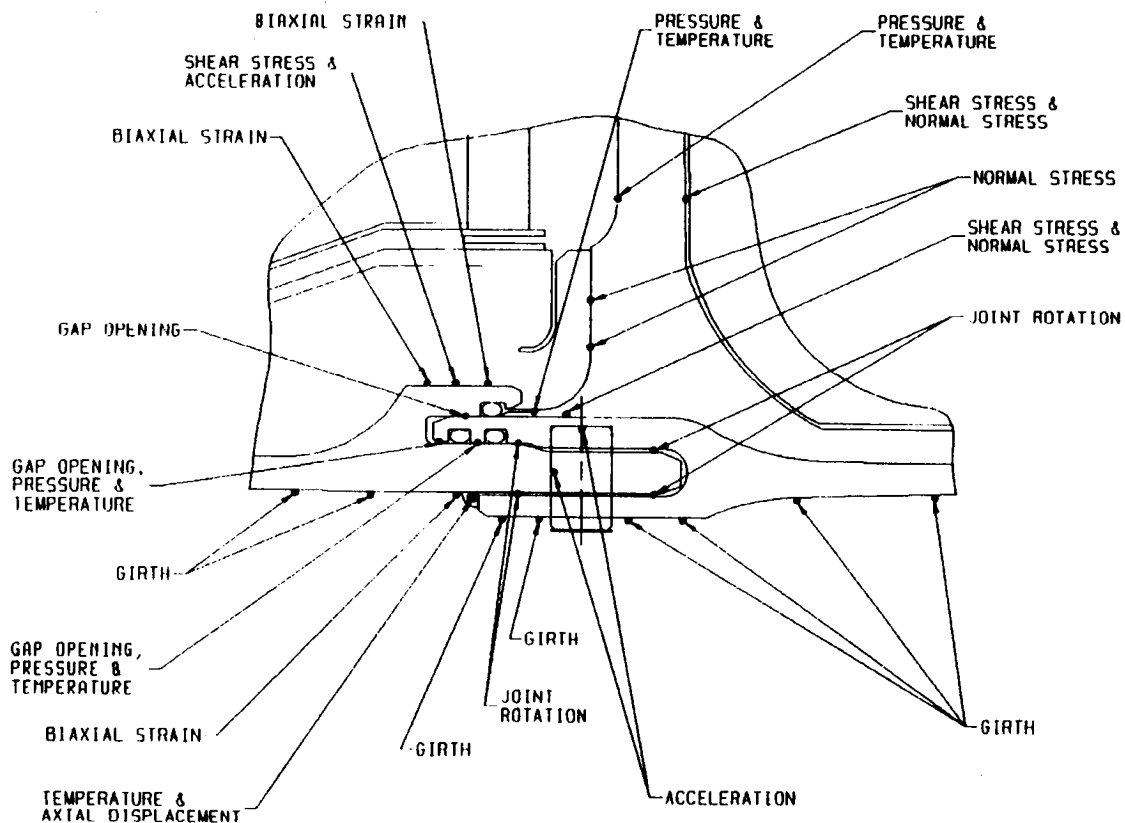
Instr Code	Description	Recording Channels Needed		
		FM	Digital	Data Logger
AXXX	Acceleration	38		
DXXX	Deflection	27	239	
PXXX	Pressure	8	36	
SXXX	Strain		430	
TXXX	Temperature	<u>6</u>	<u>24</u>	<u>26</u>
		79	729	26

5.2 OBJECTIVES

The instrumentation for the test was designed to measure pressures, temperatures, acceleration, joint rotation, gap opening, joint and membrane radial growth, joint axial growth, joint skip, hoop and axial strain, and normal and shear stresses in specific locations. Figures 5.2-1 through 5.2-3 show instrument locations on the three test joints. Figures 5.2-4 through 5.2-7 illustrate case instrumentation and instrumentation on other the joints.

5.3 INSTRUMENTATION DISCUSSION

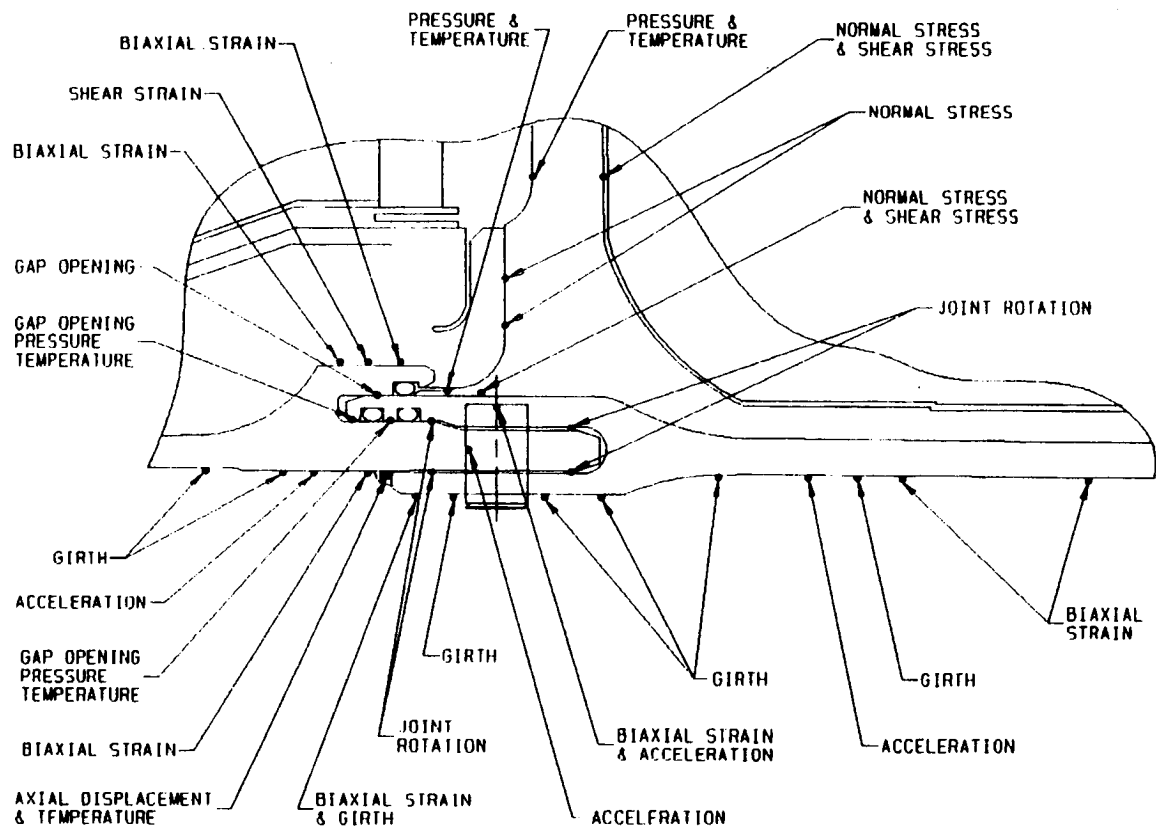
The data collected were sufficient to analyze the sealing capabilities of the joints. Appendix B contains a listing of all instrumentation used. Instruments that failed prior to the test were not mandatory gages and are listed in Table 5.3-1. The remainder of the instruments performed as expected during the test.



JOINT A
(STA 1171.40)

FIG. 14-006, TWR-2, TPTA-1.1

Figure 5.2-1. Joint A Instrumentation

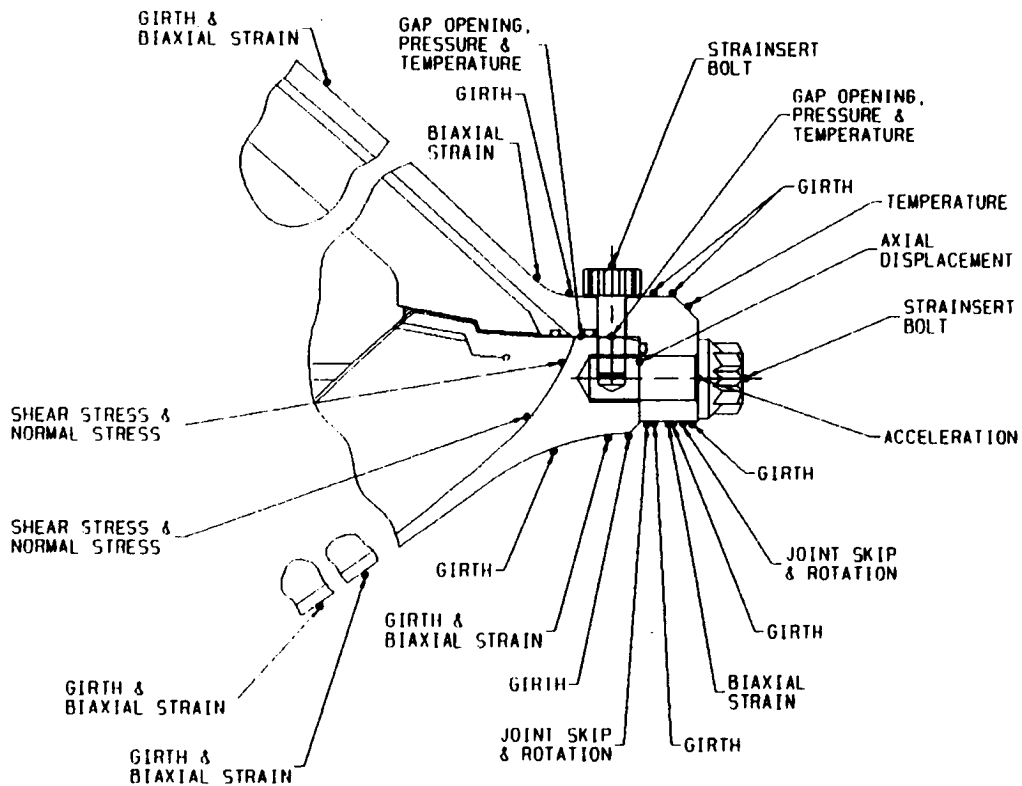


JOINT B

(STA 1491.48)

TOL 14406, TWR, 3, IPTA, 1, 1

Figure 5.2-2. Joint B Instrumentation



JOINT D
(STA 1875.20)

TUL 14486, TWR. 5, TPTA. 1.1

Figure 5.2-3. Joint D Instrumentation

REVISION _____

DOC NO. TWR-17927
SEC _____

VOL _____
PAGE 34

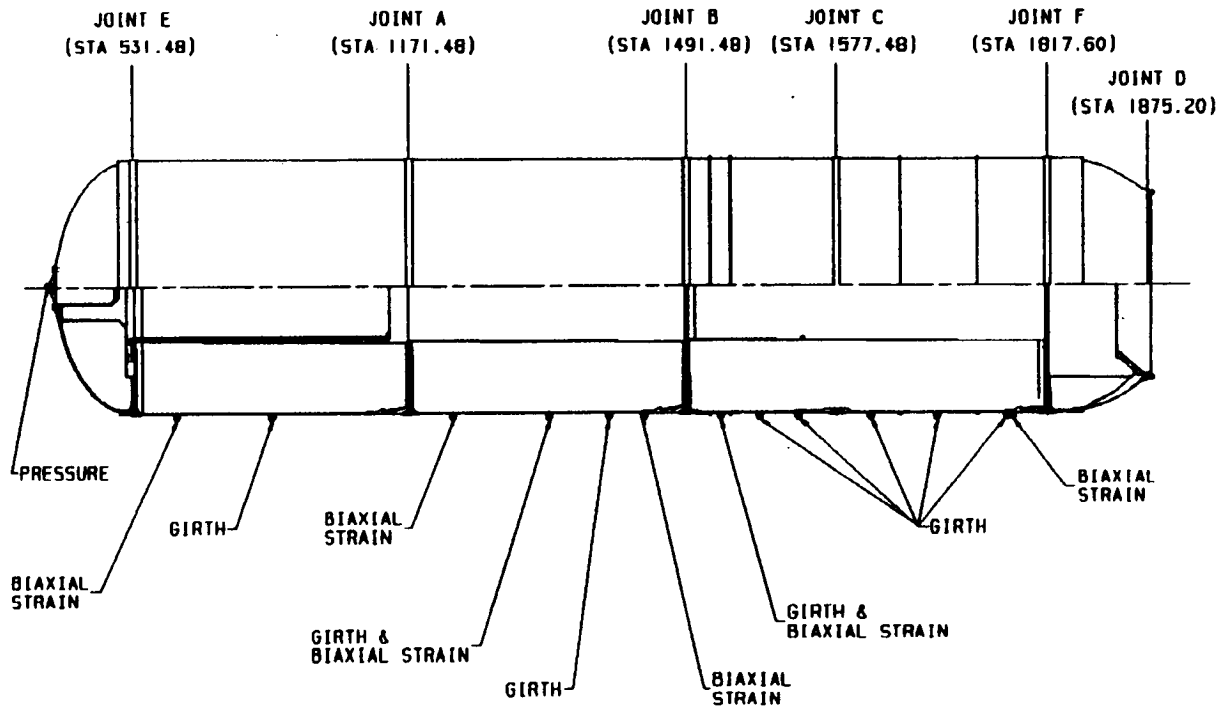


Figure 5.2-4. TPTA Case Measurements

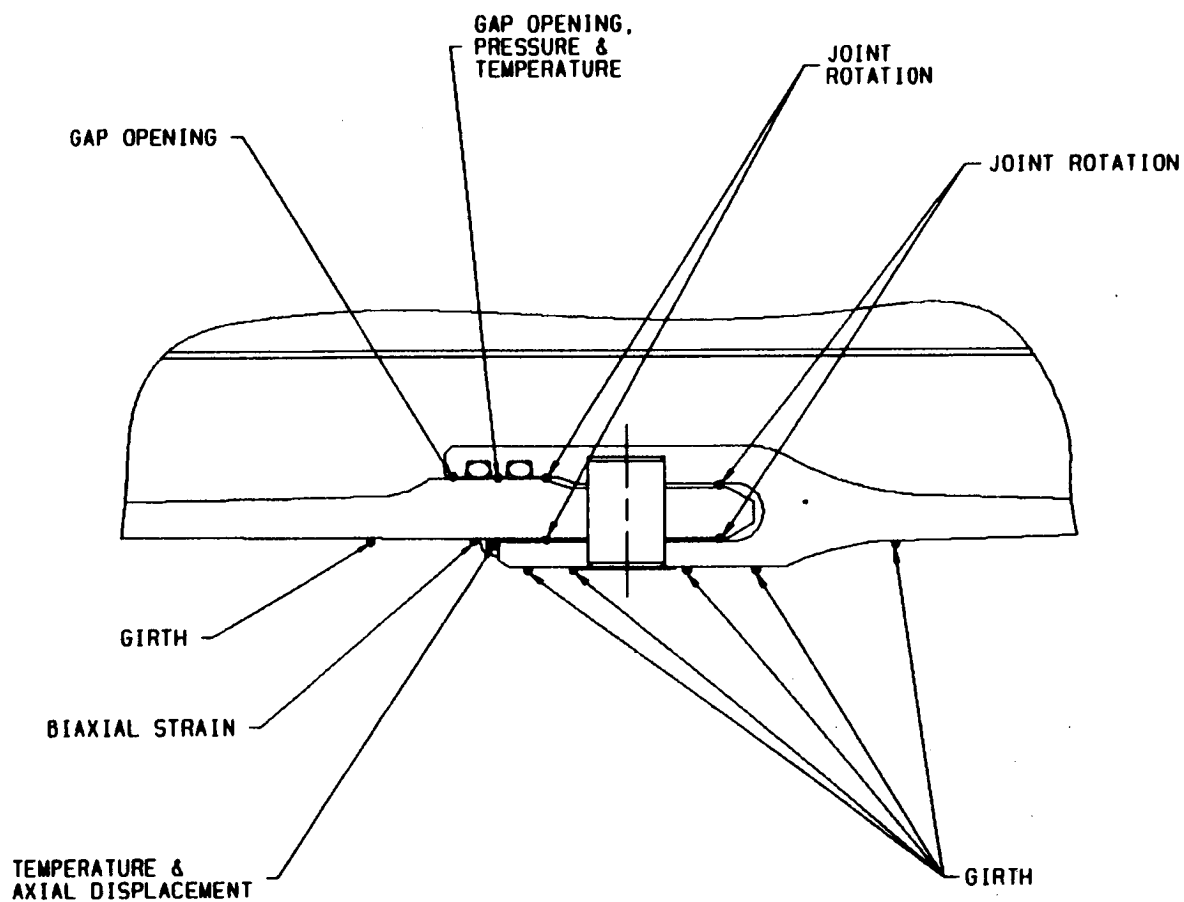


Figure 5.2-5. Joint C Instrumentation

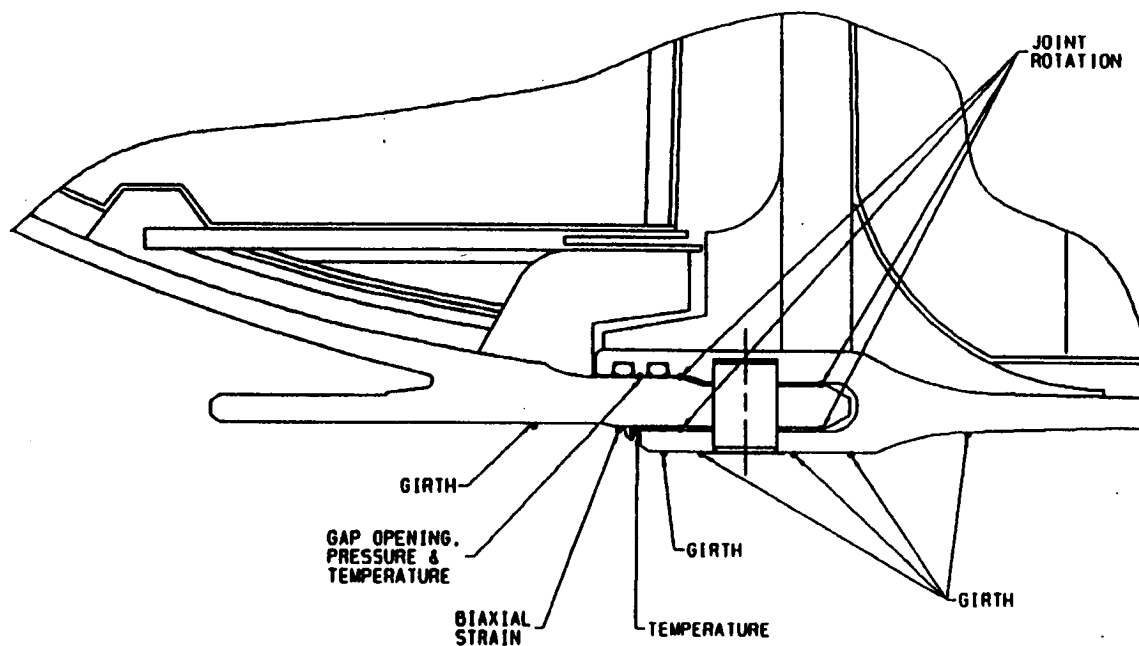


Figure 5.2-6. Joint E Instrumentation

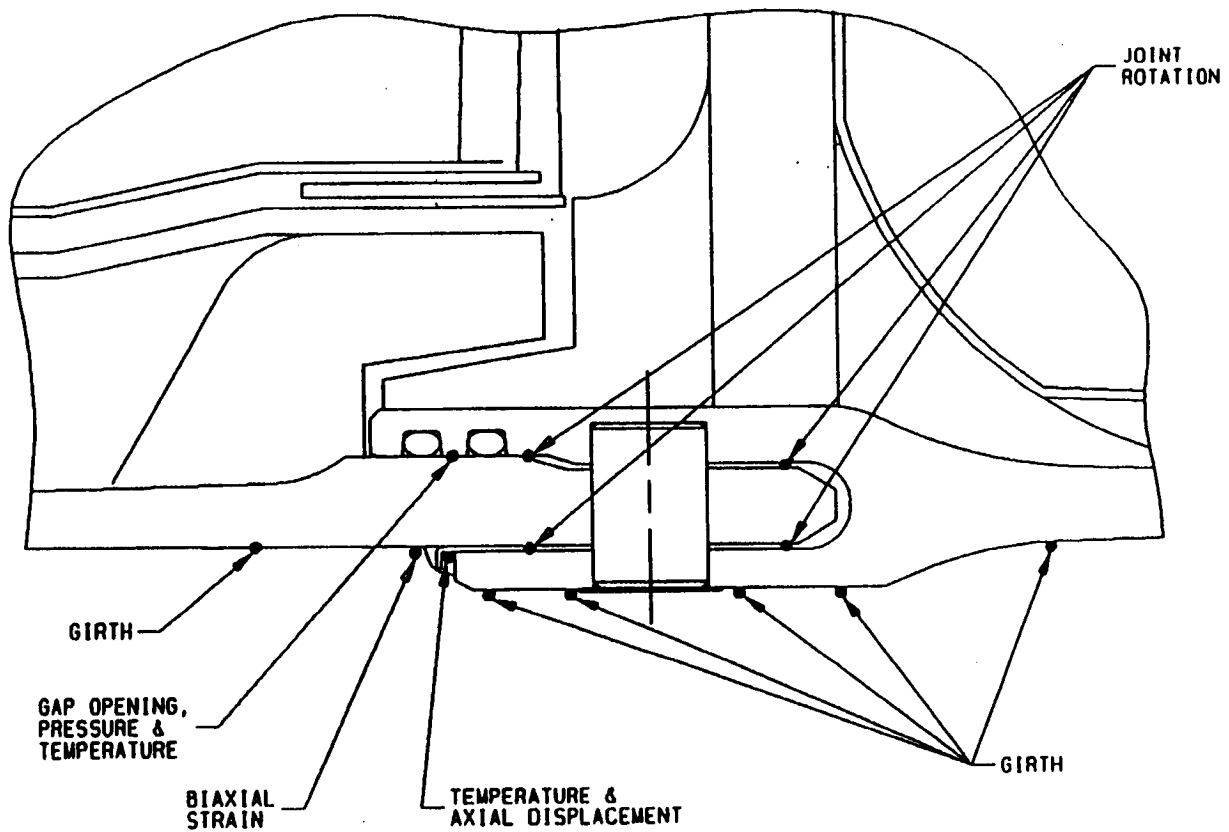


Figure 5.2-7. Joint F Instrumentation

Table 5.3-1. Inoperable Instruments

Damaged during transport or assembly:

- 2 Proximity gages - D125, D127
- 6 Shear gages - S169, S170, S171, S455, S458, S459
- 6 Button transducers - S174, S181, S447, S450, S452, S463
- 6 Strain gages - S049, S813, S814, S815, S816, S820
- 1 Girth gage - D073

Operable at assembly - found inoperable later:

- 4 Button transducers - P076, P077, P078, P081
- 4 Thermocouples - T162, T163, T164, T167

Not installed:

- 16 Strainert bolts (not available) - S289 to S296, S413 to S420
- 13 Bryner differential gages (time constraints) -
D029, D099, D120, D148, D195, D196, D197, D199, D224, D225,
D226, D227, D297
- 3 Strain gages (inaccessibility) - S433, S434, S435
- 1 Girth gage (inaccessibility) - D316

Operable at checkout - inoperable through data acquisition:

- D033, D042, D229, S243, S320, S523, S534, S821

The data from the slot temperature thermocouples shows lower than predicted temperatures. The thermocouples functioned for the duration of the test. The reason for the discrepancy in these thermocouple readings is not well understood and further evaluation is being done in this area.

Button transducers in the J-insulation area protruded from the insulation enough to cause some sooting at these locations. The sooting did not affect the performance of these gages. Button transducers also read tang contact pressure. These will be relocated farther down the flat area in order to obtain a better reading of pressure upstream of the CF O-ring.

On a walk-down of the motor after the test, several of the pressure transducers were discovered to be loose. The engineering requires that

these transducers be torqued to the motor 50 to 70 in.-lb. The fact that these transducers were loose did not affect the data.

5.4 CONCLUSIONS AND RECOMMENDATIONS

It is recommended for subsequent tests that J-insulation button transducers be set deeper into the insulation to prevent sooting in this area. The pressure transducer torquing requirements for subsequent TPTA tests have been increased to 150 to 170 in.-lb to prevent the instruments from coming loose.

Overall, the instruments performed as expected.

6

PHOTOGRAPHY

Photographic coverage was required to document the test and configuration, instrumentation, and any damage or leakage that occurred.

Still color photographs of the test configuration and joint assembly were taken prior to and after the test. As a minimum, the tang and clevis ends of each test joint and the aft dome fixed housing joint surfaces were photographed at each 45-deg location, and at any anomalous conditions.

Color motion pictures of the test were taken with 3 documentary and 12 high-speed cameras. Cameras were set up to ensure good pictorial documentation of the motor (Figure 6-1).

Camera Coverage

<u>Camera</u>	<u>Camera Type</u>	<u>Camera Speed</u>	<u>Coverage</u>	<u>Priority*</u>
1-3	Documentary	Real-time	TPTA assembly at 45, 135, 270 deg	R
4-15	High-speed	400 fps	360 deg on joint, 3 per joint	M
16-17	Video	Real-time	TPTA Assembly	R

*M - mandatory

R - required

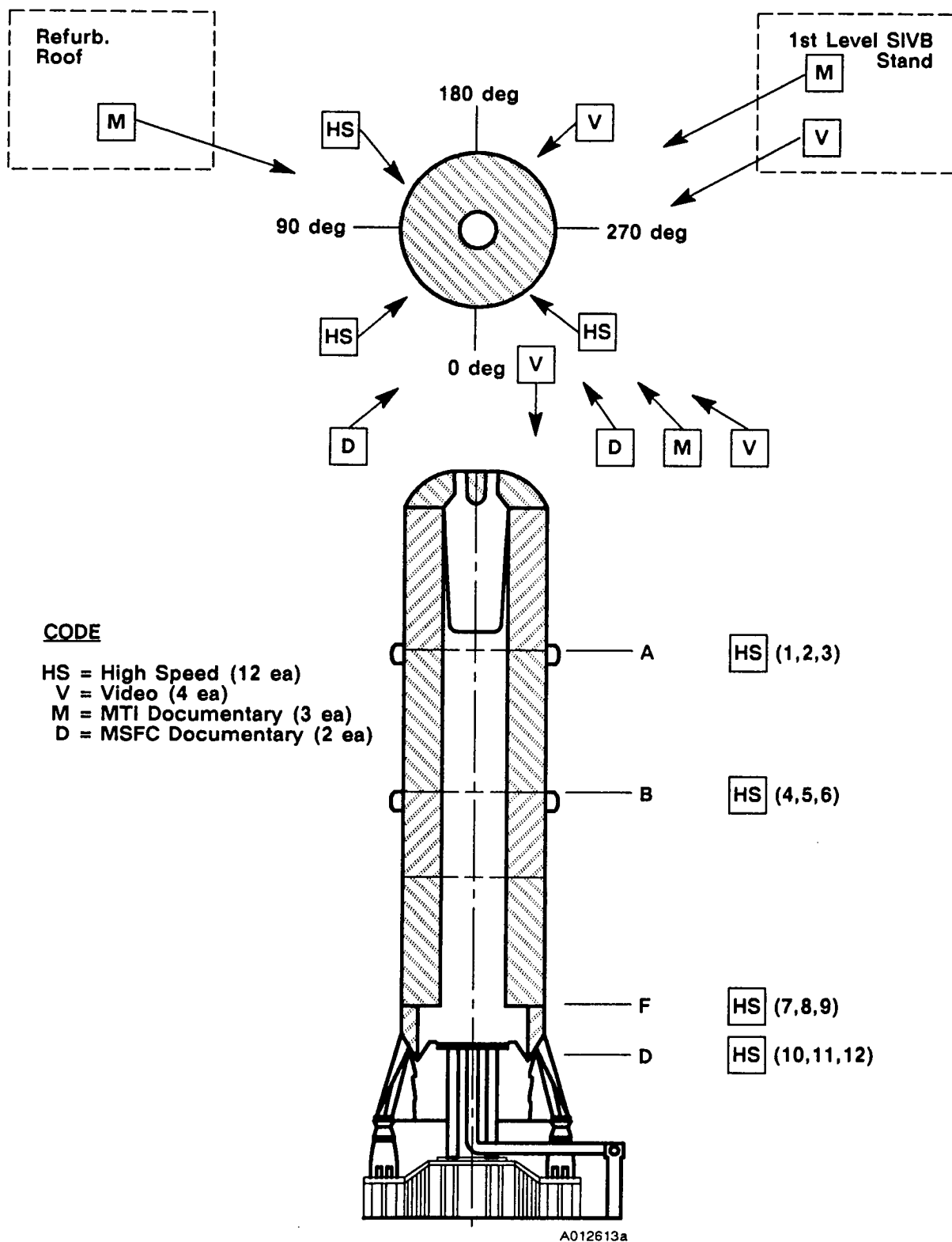


Figure 6-1. Camera Coverage

TEST RESULTS AND DISCUSSION

7.1 BALLISTICS

7.1.1 Ballistics Introduction

The TPTA propellant, TP-H1214, is an 87-percent solids hydroxyl-terminated polybutadiene (HTPB) polymer propellant formulation. The burn rate is achieved by the adjustment of the percentage of the fine (3.2 micron) ammonium perchlorate. The propellant for TPTA 1.1 was obtained from mix F400001 and produced a subscale motor (TU-628) burn rate of 1.366 in./sec at 1,000 psi.

The propellant configuration used in TPTA 1.1 consisted of a cartridge containing 3,600 slabs of propellant (nominal dimensions - 5.0 by 5.0 by 0.35 in.) and a cartwheel configuration of propellant arranged in each of the two motor slots. The slabs of propellant on the cartridge were located on 45 fins. The total weight of the propellant on the cartridge was 205.2 lbm. The propellant located in the two slots had a nominal thickness of 0.20 in. and a total weight of 71.6 lbm. The total weight of the TP-H1214 propellant in the TPTA motor was 276.8 lbm and the total weight of propellant, including the igniter with TP-H1178 propellant, was 413.9 lbm.

7.1.2 Ballistics Objectives

The primary test objective for TPTA 1.1 with regard to ballistics was to verify the TPTA ballistics model. Secondary objectives for the test were to obtain a pressure rise rate comparable to 3 sigma for full-scale SRM operating at MEOP.

7.1.3 Ballistics Results and Discussion

The propellant configuration used in TPTA 1.1 was discussed in Section 7.1.1.

The predicted and measured maximum chamber pressures agreed very well during the first second of the test. Figure 7.1-1 shows this comparison. A maximum average pressure rise rate of 141.0 psi/10 ms was achieved.

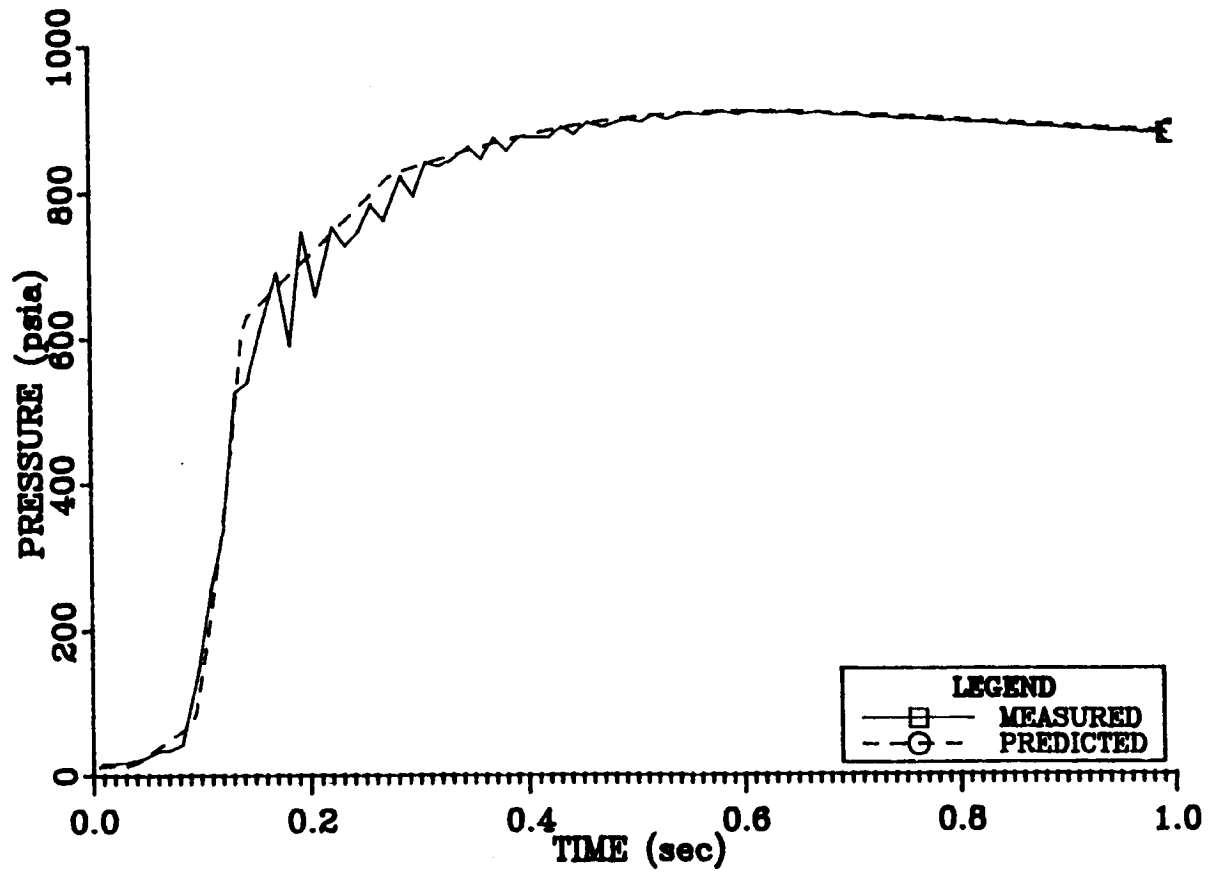


Figure 7.1-1. TPTA 1.1 Pressure Versus Time for 1 sec

The theoretical rise rate of 115.9 psi/10 ms minimum was predicted by the ballistics model. This pressure rise rate occurred at 0.113 sec. Note from Figure 7.1-1 that this is prior to the onset of the pressure oscillations, which are felt to be secondary effects caused by acoustic waves in the motor. The maximum average chamber pressure was 913.3 psia which compares well to the predicted value of 910.2 psia.

The full-duration prediction differed somewhat from the measured pressure traces during the blowdown phase (Figure 7.1-2). It is felt that these differences reflect difficulties in modeling the quenching system used in the TPTA motor. The quench system introduced a flow of nitrogen gas as the motor reached a pressure of 700 psia during blowdown. Theoretically this was to occur at 3.5 sec. The pressure reached 700 psia at an average time of 3.9 sec. It can be seen in Figure 7.1-1 that at approximately 8 sec the predicted and actual curves begin to deviate. Difficulties can be seen with the actual blowdown shortly after 10 sec when the actual curve has an elbow-type turn due to unexpected plugging of the nozzle. Consideration is being given to modifying the model to predict blowdown more accurately.

7.1.4 Ballistics Conclusions and Recommendations

The ballistics performance objectives to verify the TPTA ballistics model, obtain a maximum rise rate greater than 115.9 psia/10 ms, and a headend pressure comparable to that previously seen by the nozzle case joint were all met. The ballistics predictions for the first second of the test were very close to the actual motor performance. The problems which were encountered during blowdown due to the plugging of the nozzle could be eliminated by increasing the nozzle throat diameter. However, this situation will not arise if the motor nozzle throat is closed, as is being planned for subsequent tests.

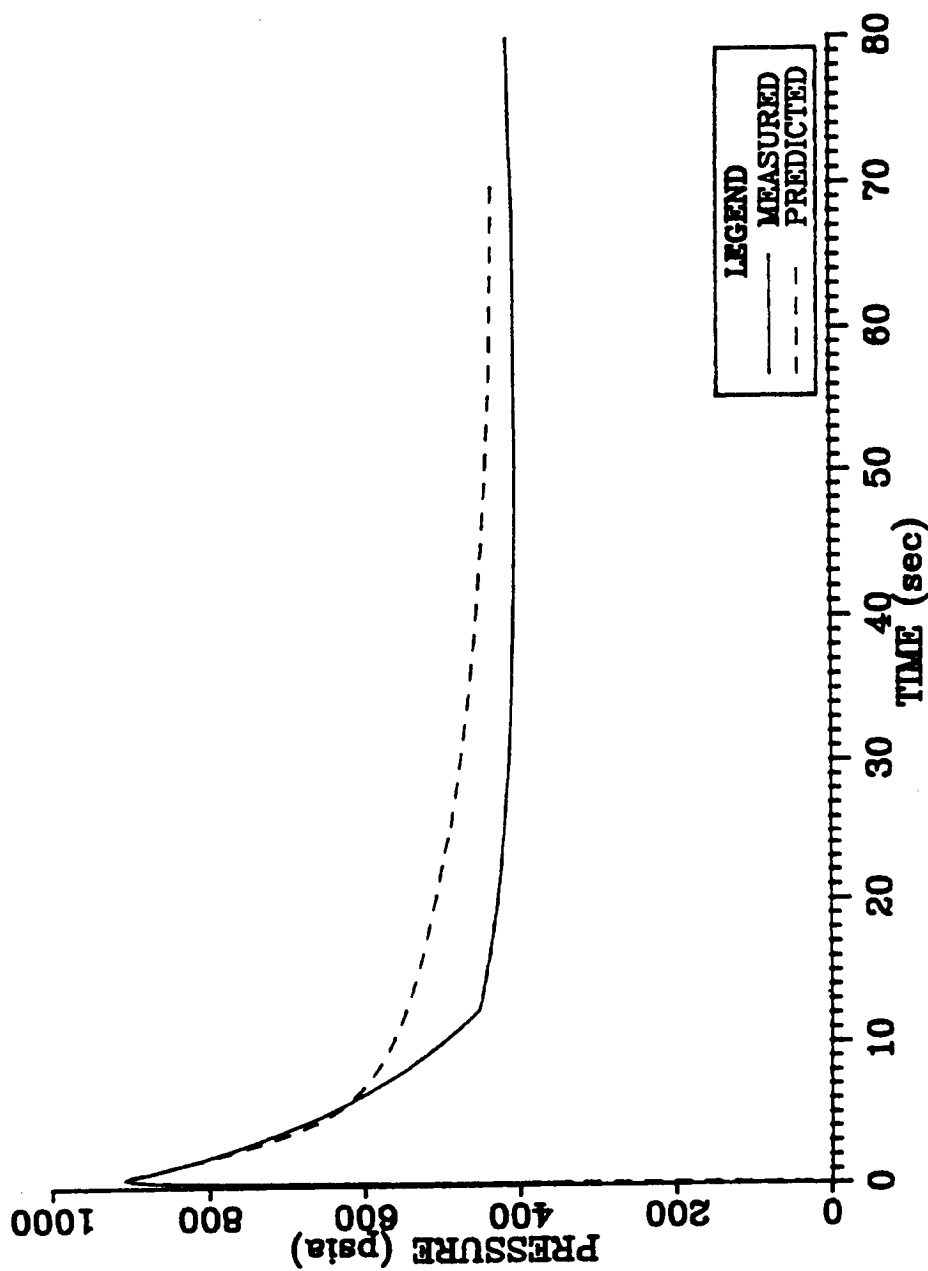


Figure 7.1-2. TPIA 1.1 Pressure Versus Time

7.2 STRUCTURES EVALUATION

7.2.1 Structures Introduction and Objectives

7.2.1.1 Structures Introduction. This section contains a comprehensive report of the performance and response of the Transient Pressure Test Article (TPTA) during the TPTA 1.1 and TPTA 1.1A series of tests. TPTA 1.1 refers to the first short-duration hot-fire launch load test of the TPTA, while TPTA 1.1A is a statically-pressurized simulated high Q loading condition. The major purpose of the tests was to observe and record the response of RSRM hardware to simulated launch and flight loads. Additionally, these tests will assess the performance of the new (360-deg) ETA ring and the modified booster aft skirt.

Test data obtained from the first series of TPTA tests will be useful to Structural Applications in the following areas. First, the testing will provide engineering data on the physical behavior of RSRM field joints and the RSRM baseline nozzle-to-case joint under strut loading conditions and with an axial load applied to the case. These two loading sources (strut and axial) are loads that have not been addressed in either the previous Joint Environmental Simulator (JES) tests or in the "full-up" horizontal SRM testing. Second, these tests will show what effect, if any, the redesigned booster hardware, redesigned ETA ring, and flight aft skirt have on the behavior of the RSRM hardware. Previous vertical testing has not included the aft skirt in the test configuration; in horizontal testing, the aft skirt was free of constraints as it is in the flight configuration. In these tests, the TPTA is restrained at the base of the aft skirt in the same manner as it is on the launch pad and this allows a good representation of the launch configuration. Additionally, data will be obtained to validate existing analytical models of RSRM hardware. Appendixes C and D contain test data for the TPTA 1.1 and TPTA 1.1A tests, respectively.

7.2.1.2 Structures Objectives. The objectives were as follows:

- a. Certify that the primary O-ring will seal under high Q pressure and ETA loading conditions in a fail-safe mode.

- b. Verify that the field and nozzle-to-case joint gap opening rate and total deflections fall within analytical predicted limits.
- c. Obtain data on the function of the field joint seal system with ignition and strut loads applied.
- d. Establish SRM joint performance historical data base.
- e. Evaluate condition of hardware and components from post-test measurements, inspection, and data.
- f. Obtain data to verify structural models on the effect of high Q ET loads on joint deflection.

7.2.2 Structures Conclusions and Recommendations

Joint A, the forward cylinder-to-aft cylinder joint, contained all fluoro-carbon O-rings. Joint A was the new CF joint design with the DM-8 J-insulation configuration. No defects or anomalies were introduced into this joint. The joint was temperature conditioned and, at the time of the static hot-firing, was at an average temperature of 75°F. Maximum chamber pressure was recorded at 913.3 psia. Slot pressure traces matched the chamber pressure traces. There were no leaks to the CF O-ring. Disassembly inspection revealed no soot on the J-insulation surface, confirming that there were no leaks to the CF O-ring. Pressures recorded forward and aft of the primary O-ring experienced no pressure increase. No damage was found to the primary, secondary, or CF O-ring. At the separation of Joint A, no major anomalies occurred. It was determined that the 1,000-kips axial load does not have a significant effect on the field joint and nozzle-to-case joint performance.

The maximum inter-O-ring gap opening measured in Joint A was 0.005 in. during the cold-gas high Q test. Gap opening measurements, in general, open during the initial pressure transient oscillations. Gap openings measured forward of the primary O-ring opened and closed. This measurement was linear with pressure. The inter-O-ring gap opening of 0.005 in. was slightly higher from test than the predicted opening of 0.003 inch. The gap openings forward of the primary O-ring were also higher than predicted. Maximum measured opening forward of the primary O-ring for Joint A was 0.007 in. with the

predicted being 0.002 inch. One gage forward of the primary O-ring measured 0.002 in. open. It is possible, due to the chamfer on the top of the inner clevis leg, for the LVDT probe to slip off onto the chamfer with the axial growth of the joint. With the axial growth of Joint A taken into account, an error of 0.006 in. is possible in the measurements, which would reduce the large measurements significantly. The average axial growth for Joint A was 0.025 in., which matched with the predicted value of 0.025 inch. The axial and radial girth gages showed a linear trend with pressure.

The nonlinear joint movements seen in Joint A are not completely understood; however, the maximum measured inter-O-ring gap opening of 0.005 in. is less than the maximum design allowable of 0.009 inch. The erratic movement of the LVDTs observed during the pressure transient oscillations is also not completely understood.

Joint B, the aft cylinder-to-ETA segment joint, contained all fluoro-carbon O-rings. Joint B was also the CF joint design with the DM-8 J-insulation configuration. The ETA segment had a right-hand, 360-deg ETA ring installed. The J-insulation in Joint B also sealed. Disassembly inspection of Joint B revealed no soot on the J-insulation sealing surface, confirming that there were no leaks to the CF O-ring.

Pressures recorded forward and aft of the primary O-ring experienced no pressure increase. No damage was found to the primary, secondary, or CF O-rings. At the separation of Joint B, no major anomalies occurred.

Inter-O-ring gap openings varied from 0.006 in. open to 0.005 in. close on Joint B during the static hot-firing test. The inter-O-ring gap measurements, in general, open during the pressure transient oscillations with a smoother reading than Joint A. As in Joint A, the LVDTs forward of the primary O-ring opened and then closed linearly with pressure. The inter-O-ring gap movement of Joint B is more linear than Joint A. In Joint B, the maximum gap opening occurs at maximum chamber pressure, which did not always occur in Joint A; however, the general joint movement is very similar between the two joints. The axial and radial girth gages in Joint B, as in Joint A, showed a linear trend with pressure. The average axial growth of Joint B was 0.043 inch.

The joint movements seen in Joint B are not completely understood; however, the maximum measured inter-O-ring gap opening of 0.006 in. open is less than the maximum design allowable of 0.009 inch. The LVDT movements in Joint B were less erratic than the movements in Joint A.

Joint C, the ETA segment/stiffener segment also contained fluorocarbon O-rings. This was a simulated factory joint. In both the TPTA 1.1 and 1.1A tests, the insulation at the bore was the pressure face. The maximum gap deflection was 0.003 in. (close) during the static hot-firing test and 0.004 in. open during the cold-gas high Q test.

During the cold-gas high Q test in Joint D, 127.7 psia was recorded between the wiper and primary O-rings.

7.2.3 Structures Results

7.2.3.1 TPTA 1.1 Post-Test Inspection Results. The results of post-test inspections are as follows in the order of disassembly.

Igniter

Prior to the test, a grease bead was applied around the igniter seal attach bolts and the igniter cover plate. There was no indication of leakage on any bolts or around the cover plate. This confirmed that there was no leakage past the inner and outer Gask-O-Seal® and all Stat-O-Seals® on the igniter cover plate.

Joint E

Joint E is the forward dome-to-case joint which is a conventional (non-capture feature) tang/clevis joint with two O-rings and no insulation sealing (completely vented). Prior to test, a grease bead fillet was applied between the tang and the top of the outer clevis leg to indicate gas leakage past the secondary O-ring. Post-test inspection revealed no leak through the grease bead. The major anomaly with this joint disassembly was the presence of a heavy deposit of brass metal shavings at the 86-deg station. Slivers were present on both the tang and clevis, embedded in grease forward of the pinhole and around the forward edges of the pinhole. It is surmised that the brass shavings are a result of excessive force employed in the use

of the brass alignment pins during joint assembly. This is of particular concern to the Structural Design group because the presence of errant metal shavings near the O-rings could cause damage to the O-rings and/or inhibit their sealing capabilities. Additional metal slivers, which appeared to be motor case steel (D6AC), were present at the 222-deg station. Metal shavings were located at the forward lip of the pinhole and again are thought to be the result of excessive force during assembly. Light soot extending to the top lip of the primary O-ring groove was present at the following degree locations: 2 to 6, 12 to 22, 50 to 64, 74 to 78, 86 to 132, 146 to 168, 174 to 176, 180 to 230, and 254 to 298. There were no soot deposits past the primary O-ring groove forward lip. There was no corrosion or damage apparent in the O-ring grooves. There was a heavy grease coat on the entire tang and clevis as well as grease in the clevis root and on top of the inner clevis leg. There was heavy grease between the O-rings at 210 to 216 deg. There was no apparent O-ring damage.

Joint A

Joint A is a case-to-case RSRM (CF) joint with three O-rings and the J-insulation configuration. As in Joint E, a grease bead was applied between the tang and top of the outer clevis leg. After the test, there was no indication of hot gas passing through the grease bead. The joint was generally very clean with no penetration of soot past the J-insulation. There were burnish marks from the shim installation tool on the tang outside diameter approximately every other pinhole. There was also intermittent burnishing on the inner clevis leg in the interference fit region. There were quantities of a brown/pink substance (grease) in the clevis root intermittently all around, as well as 0.25 in. of water. This is typical of conditioned joints in the manner accomplished on this test. There was no corrosion. The V_2 filler at 80 deg had come loose after joint separation and was left hanging down. There was a sliver of D6AC steel at 130 deg. The LVDT measuring inter-O-ring displacement at 57 deg apparently caused a small divot (approximately 0.03 in. diameter) in the inner clevis leg between the primary and secondary O-ring grooves. The divot was deep enough to be felt with a fingernail (estimated depth of 0.001 to 0.002 in.). Inter-O-ring

grease coverage was nominal to light. Grease was heavy on the outer tang surface and nominal on the inner tang surface.

Joint B

Joint B is the case-to-ETA segment joint in the RSRM (CF) configuration with three O-rings and the J-insulation configuration. The grease bead applied between the tang and top of the outer clevis leg indicated no leak past the secondary O-ring. The joint was generally very clean with no apparent damage or anomalies. There were slight burnish marks on the outside diameter (OD) of the tang approximately every other pinhole. There was surface corrosion on the tang OD of 1.00 in. in length at 264 deg, 0.50 in. in length at 358 deg, and other light surface corrosion intermittently all around. There was corrosion of 1.50 in. in length forward of the leak check hole, which resulted from grease removal for instrumentation installation. Grease coverage on the tang OD was heavy, while the inside diameter (ID) had nominal coverage. There was no significant corrosion present on the tang. There were several gaps in the silicone V₂ filler (0 deg - 6 in. gap, 135 deg - 6 in. gap, and 178 deg - 0.5 in. gap) and one place with no gap (45 deg - no gap). There was no apparent corrosion on the clevis with the grease coverage nominal except for a heavy coat in the root. There was approximately 0.25 in. of water in the clevis root. There was no apparent damage to any O-ring. There were metal slivers in the pinholes at 228, 248, and 252 deg, as well as a cloth string in the pinhole at 262 deg. There was intermittent burnishing of the clevis interference fit region circumferentially. There was no apparent damage to the primary, secondary, or CF O-rings.

Joint F

Joint F is the stiffener segment-to-aft dome joint which is a conventional (noncapture feature) tang/clevis factory joint with two O-rings and no insulation sealing (completely vented). A grease bead was applied between the tang and top of the outer clevis leg prior to test. Post-test inspection revealed no hot gas leak through the grease. This joint was basically very clean and had no major anomalies. There was light soot on the top of

the clevis leg intermittently around the circumference. Light soot extended over the top edge of the inner clevis leg to the primary O-ring in the following degree locations: 62 to 64, 66 to 68, 74, 152 to 154, 160, 220, 311, and 340 to 354. There was a heavy coat of grease on the top of the inner clevis leg, while the grease coverage between the O-rings and at the clevis root was nominal. Heavy grease was present on the tang OD, but not as heavy on the ID, though heavy for a sealing surface. There was no corrosion present and no apparent damage to either primary or secondary O-ring.

Joint D

Joint D is the aft dome-to-fixed housing joint, which is the current RSRM baseline configuration with three O-rings and radial bolts. Prior to the test, a grease bead fillet was applied between the fixed housing and aft dome as a gas leak indicator past the secondary O-ring. Post-test inspection revealed no leakage through the grease bead. The major anomaly with this joint disassembly was the presence of a leak path at the 188-deg station, which extended through the polysulfide adhesive all the way to the wiper O-ring. There was no apparent damage or heat effect to the wiper O-ring as a result of this leak. Sooty grease and/or polysulfide extended down the upstream side of the wiper O-ring groove, approximately one-third of the way across the bottom of the groove at the 188-deg station, and for approximately 8 deg on either side. Beyond this region the sooty grease and/or polysulfide extended approximately one-quarter to one-half of the way down the upstream side of the wiper O-ring groove. Grease was light on the wiper O-ring and it was lightly stuck to the sooty grease/polysulfide at 188 ± 8 deg. Polysulfide extended past the upstream lip of the wiper O-ring groove all around except at 40 deg for 1 in. circumferentially, and at 353 deg twice for 0.5 and 1 in. The break in the polysulfide bead at 40 deg was adjacent to a void in the polysulfide, while the breaks at 353 deg probably happened during disassembly since the edge of the adhesive appeared torn away. The primary O-ring had scuff marks across the diameter at every radial bolt hole. Most of the scuff marks appeared as though the grease had been simply pushed away, while some appeared more severe and there may

actually have been a very small amount of O-ring material rubbed away. There was a piece of yellow material (a paint chip or piece of tape) located at 188 deg between the primary and wiper O-rings. There were soot smudges (believed to be grease from the bolts) located at 63 deg between the primary and wiper O-rings, at the 180-deg radial and wiper O-rings, at the 180-, 212-, and 241-deg radial bolt holes, and at the 248-deg leak check port between the primary and secondary O-rings. Other lighter soot smudges were present intermittently in the sealing region around the entire circumference.

During the final stage of joint separation, the fixed housing was lifted by the crane and allowed to become slightly off-level with the 225-deg side low and 45-deg side high. The difference in elevation from side to side was estimated to be 2 to 4 in. before the crane was stopped. The fixed housing was lowered slightly and the crew surmised that the hydraulic rams on the low side were binding. Several technicians were stationed around the circumference and shook the fixed housing while the crane lifted and successfully freed the fixed housing. There were burnishing marks in the aft dome interference fit region, with the most severe at the 209-deg station. The burnish marks in this area start lightly at 188 deg, gradually progress to the most severe marks at 209 deg, then fall off to light marks by 227 deg. Other less severe burnish marks are present at 18 ± 5 deg and at 97 deg. Very light burnishing was present intermittently around the entire circumference. Grease on the exposed metal and O-rings was generally light with no apparent damage other than possible light scuffs to the primary O-rings, as previously mentioned. There were grease accumulations in the secondary O-ring groove at 32, 45, and 187 deg, and at 188 deg in the primary O-ring groove with no apparent damage to the groove surfaces.

Thrust Piston

The thrust piston had already been cleaned and greased prior to inspection and was not marked with angular reference locations around the circumference, making exact location of anomalies difficult. Sporadic corrosion was present around the outside diameter, and a 0.25-in. wide vertical burnishing mark was observed at one location. At one location adjacent to the most heat-affected insulation, the outside metal circumference appeared to be slightly etched

or stained with black/brown residue which was determined to be heat-affected polysulfide. It was also reported that during disassembly one portion of the insulation flap that covers the thrust piston-to-seal ring interface was missing.

Seal Ring

The seal ring had already been cleaned and greased and the O-rings removed prior to this inspection. Again, the seal ring was not marked with any angular reference locations. There were 22 visible shim marks around the circumference below the secondary O-ring. They were 0.75-in. wide starting at the upper end of the lower transition zone and extending up to as close as 0.0313 in. to the downstream lip of the secondary O-ring. Some shim marks were barely visible, while others made a deep enough impression to be felt with a fingernail. There was a gouge approximately 0.0313 in. wide and 0.0156 in. deep in the upper transition area for approximately 30 deg in the circumferential direction. There was no apparent damage or corrosion to either of the O-ring grooves, although it was difficult to see any small imperfections due to the heavy grease coverage.

7.2.3.2 Static Hot-Fire Test (TPTA 1.1). The static hot-fire test was subject to two major anomalies occurring during the course of the test. First, during the buildup of strut loads which simulate pre-ignition main engine buildup, the strut load actuation system aborted unexpectedly, and effectively eliminated any effect from strut loads to the test article. The basic problem stemmed from the test sequencer which apparently only verifies that the strut load activation system is starting up, and does not reverify that the system is functioning properly prior to giving the ignition command. The strut load actuators did initiate the pre-ignition loads profile properly, but aborted shortly before ignition (Figure 7.2-1). The ignition command was given and the motor fired without strut loads.

The second anomaly occurred while activating the GN_2 quench system. Test planning calls for the GN_2 headend quench system to be activated when the headend pressure has decayed to 700 psig, at which time a small (approximately 2-in. diameter) insulative cover which protects the quench injector is ejected to allow operation of the injector. The quench injector port

TPTA 1.1
ACTUATOR LOADS (FLA1100 = P8 FLA1101 = P9 FLA1102 = P10)
19 NOVEMBER 1987

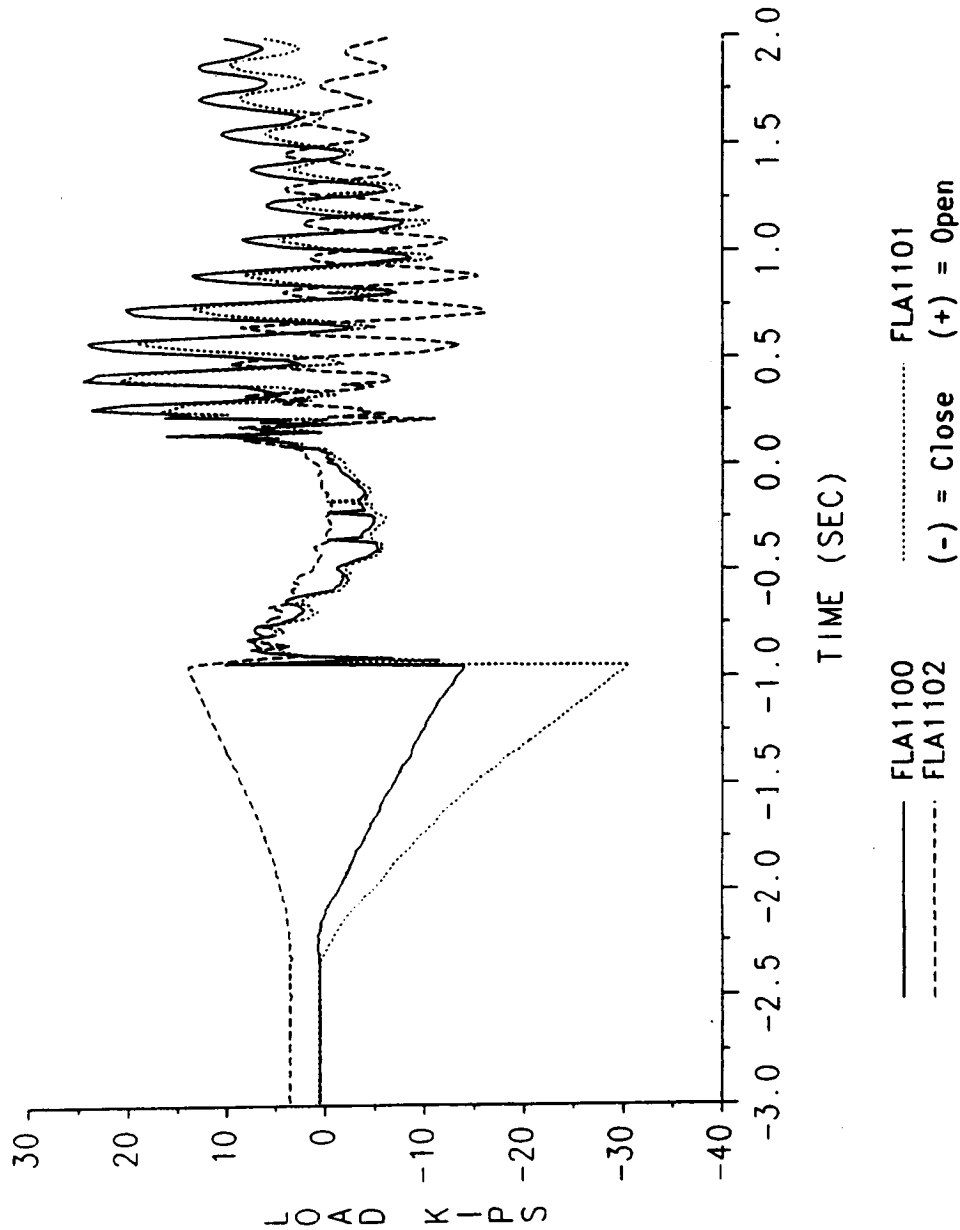


Figure 7.2-1. TPTA 1.1 Lift-Off Strut Loads Profile

plug, released into the test article internal cavity, traveled down the length of the motor segments, into the exhaust pipe, and became lodged in the 2-in. nozzle near the exit of the exhaust system. This caused the venting of the test article to cease 12 sec after ignition and remain pressurized at approximately 420 psia for roughly 11 min, at which time the auxiliary vent valve was opened allowing the test article to continue the vent/purge sequence.

Aside from the aforementioned anomalies, the test article performed nominally achieving a maximum pressure of 913.3 psia at 0.609 sec into the test. The predicted maximum pressure based on actual propellant weight was 910.2 psia.

7.2.3.3 Cold-Gas High Q Test (TPA 1.1A). The test article was pressurized using an external GN₂ source to a maximum pressure of 612 psia, at which time strut load actuators applied the high Q dynamic strut loads. The system performed as intended and applied the specified load profile with no apparent anomalies (Figure 7.2-2).

Post-test joint inspection indicated no major anomalies other than the presence of a leak path through the polysulfide adhesive to the wiper O-ring in the nozzle-to-case joint (Joint D).

TPTA 1.1A MAX-Q FINAL
LOAD VS TIME
GAGES FLA1100 FLA1101 FLA1102
24 NOVEMBER 1987

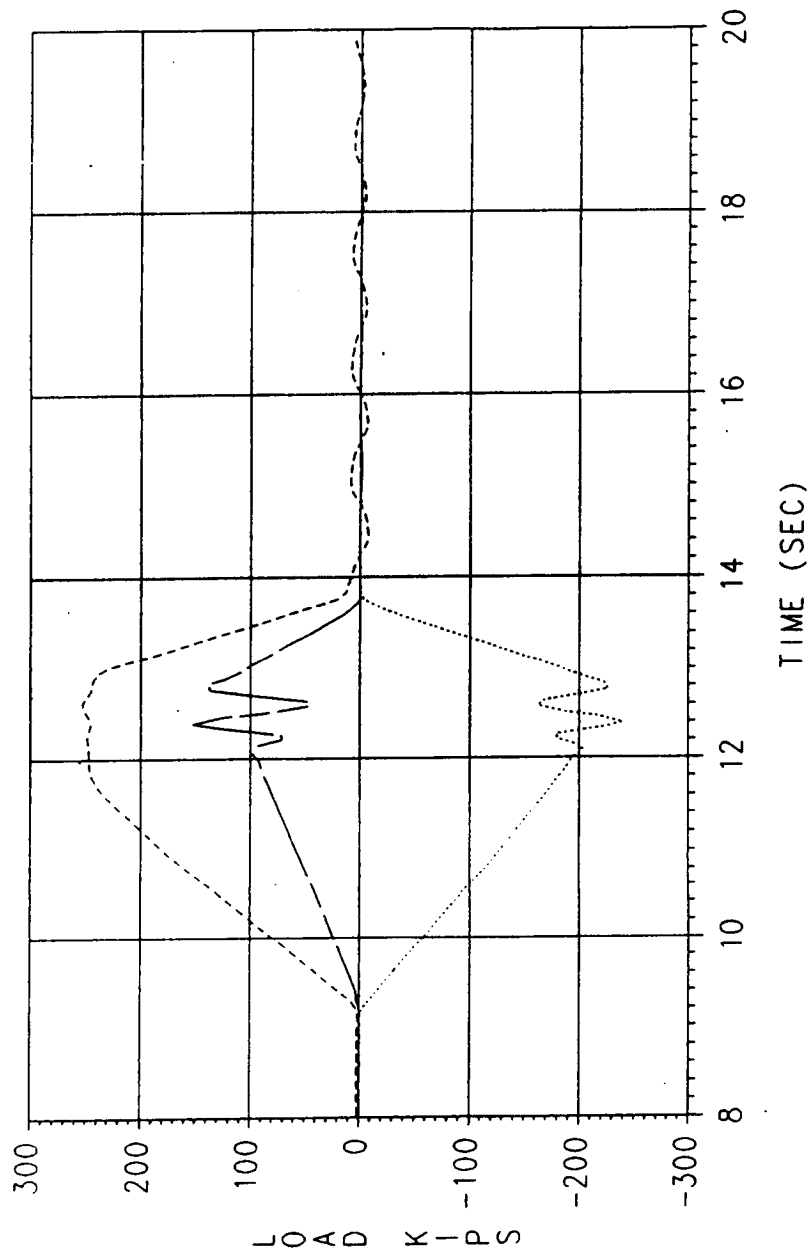


Figure 7.2-2. TPTA 1.1A High Q Strut Load Profile

7.2.3.4 Test Joint Instrumentation Measurement Results

7.2.3.4.1 Test Joint Temperatures

7.2.3.4.1.1 TPTA 1.1 test joint temperatures. All the joints except Joint C were required to be at $70 \pm 5^{\circ}\text{F}$ at $T = 0$ sec. Average test joint temperatures varied between 75 and 82°F .

Joint A Temperatures (TPTA 1.1)

The temperatures recorded above the primary O-ring and between the primary and secondary O-rings experienced little change. The average conditioned joint temperature was 75°F . At time $T = 0$ of the test, the temperature forward and aft of the primary O-ring measured 80 and 75°F , respectively. Table 7.2-1 contains Joint A temperatures at $T = 0$ sec. At maximum chamber pressure during the test, the temperature forward and aft of the primary O-ring measured 78 and 75°F , respectively. The maximum slot temperature of Joint A was $1,483^{\circ}\text{F}$ at maximum chamber pressure. The maximum inter-O-ring temperature was 79°F . All temperatures for Joint A recorded at maximum chamber pressure are given in Table 7.2-2.

Joint B Temperatures (TPTA 1.1)

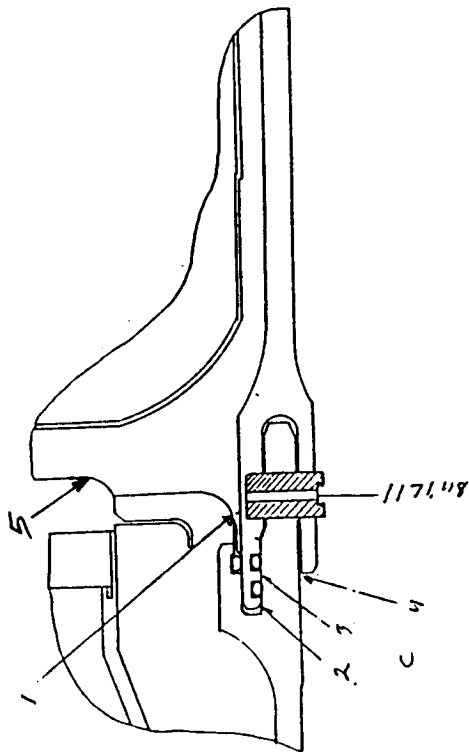
The average conditioned joint temperature was 75°F . At time $T = 0$ sec, the average temperatures forward and aft of the primary O-ring measured 79 and 75°F , respectively. Joint B temperatures at $T = 0$ sec are listed in Table 7.2-3. The temperatures recorded for Joint B saw little change from when they were recorded at time $T = 0$ of the test to maximum chamber pressure. Table 7.2-4 shows the temperatures for Joint B recorded at maximum chamber pressure. The maximum inter-O-ring temperature was 78°F .

Joint D Temperatures (TPTA 1.1)

The average conditioned joint temperature was 82°F . The average temperature recorded forward and aft of the primary O-ring at time $T = 0$ was 82°F . Joint D temperatures did not change during the test. Table 7.2-5 shows the temperatures for Joint D at $T = 0$ sec, and Table 7.2-6 lists the joint temperatures at maximum chamber pressure. The maximum inter-O-ring temperature was 83°F .

Table 7.2-1. TPTA 1.1 Joint A Temperatures at T=0 sec

TEST NAME: TPTA 1.1
JOINT: A
DESCRIPTION: TEMPERATURE SUMMARY AT t=0.0

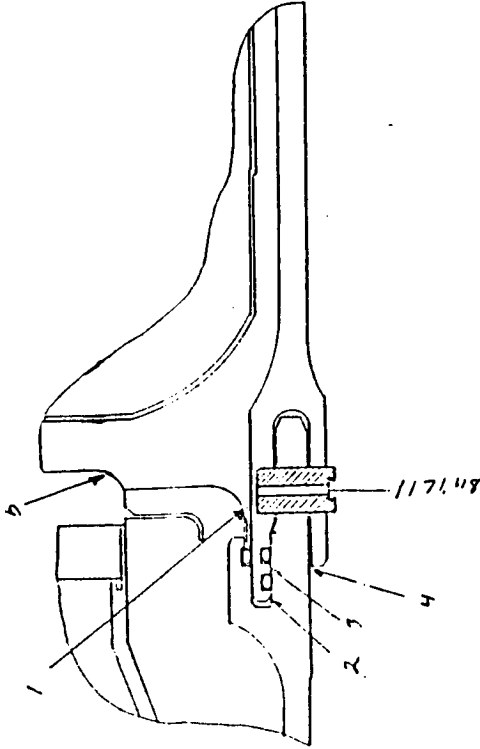


TEMPERATURE LOCAT	GAGE NUMBER	CIRCUMFERENTIAL LOCATION (DEG)	MAXIMUM TEMPERATURE (DEG F)	TIME OF MAX TEMP (SEC)
1	T0162	135.0	ND	ND
1	T0163	235.0	ND	ND
1	T0164	341.0	ND	ND
2	T0073	135.0	79.7	0.000
2	T0074	341.0	ND	ND
3	T0075	45.0	80.0	0.000
3	T0111	157.0	71.1	0.000
4	T0077	0.0	ND	ND
4	T0107	45.0	ND	ND
4	T0078	90.0	ND	ND
4	T0108	135.0	ND	ND
4	T0079	180.0	ND	ND
4	T0109	225.0	ND	ND
4	T0080	270.0	ND	ND
4	T0110	315.0	ND	ND
5	T0205	21.0	58.2	0.000
5	T0206	147.0	33.5	0.000
5	T0207	261.0	51.5	0.000

ND = No data

Table 7.2-2. TPTA 1.1 Joint A Temperatures at Maximum Chamber

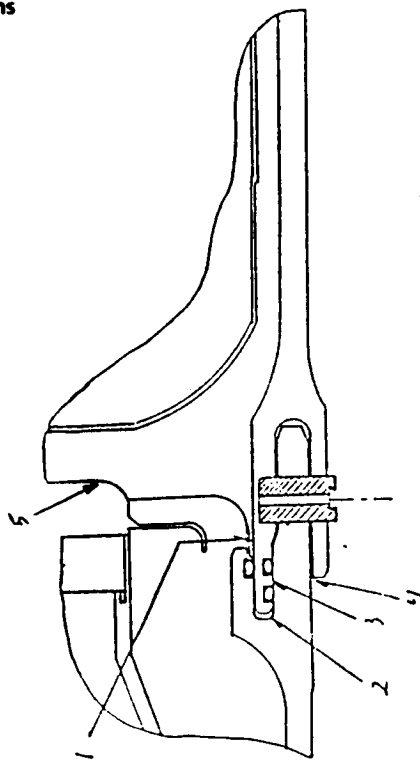
TEST NAME: TPTA 1.1
JOINT: A
DESCRIPTION: TEMPERATURE SUMMARY
MAXIMUM PRESSURE: 909.7 PSIA
DESIRED PRESSURE: 913.3 PSIA
TIME PRESSURE OCCURED: 0.6 SECONDS



TEMPERATURE LOCAT	GAGE NUMBER	CIRCUMFERENTIAL LOCATION (DEG)	TEMPERATURE (DEG F)
1	T0162	135.0	ND
1	T0163	235.0	ND
1	T0164	341.0	ND
2	T0073	135.0	78.0
2	T0074	341.0	ND
3	T0075	45.0	79.0
3	T0111	157.0	70.6
4	T0077	0.0	ND
4	T0107	45.0	ND
4	T0078	90.0	ND
4	T0108	135.0	ND
4	T0079	180.0	ND
4	T0109	225.0	ND
4	T0080	270.0	ND
4	T0110	315.0	ND
5	T0205	21.0	1015.3
5	T0206	147.0	204.9
5	T0207	261.0	1482.8

ND = No data

Table 7.2-3. TPTA 1.1 Joint B Temperatures at T=0 sec



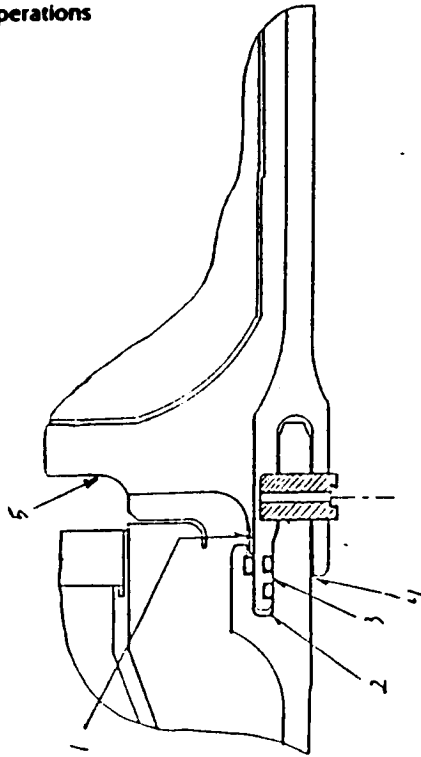
TEST NAME: TPTA 1.1
JOINT: B
DESCRIPTION: TEMPERATURE SUMMARY (T=0.0)

TEMPERATURE LOCAT	GAGE NUMBER	CIRCUMFERENTIAL LOCATION (DEG)	MAXIMUM TEMPERATURE (DEG F)	TIME OF MAX TEMP (SEC)
1	T0165	135.0	ND	ND
1	T0166	235.0	ND	ND
1	T0167	341.0	ND	ND
2	T0085	135.0	77.7	0.000
2	T0086	341.0	79.4	0.000
3	T0087	45.0	79.6	0.000
3	T0120	157.0	71.1	0.000
4	T0089	0.0	ND	ND
4	T0116	45.0	ND	ND
4	T0090	90.0	ND	ND
4	T0117	135.0	ND	ND
4	T0091	180.0	ND	ND
4	T0118	225.0	ND	ND
4	T0092	270.0	ND	ND
4	T0119	315.0	ND	ND
5	T0184	111.0	ND	0.000
5	T0185	291.0	46.2	0.000

ND = No data

Table 7.2-4. TPTA 1.1 Joint B Temperatures at Maximum Chamber Pressure

TEST NAME: TPTA 1.1
JOINT: B
DESCRIPTION: TEMPERATURE SUMMARY
MAXIMUM PRESSURE: 909.7 PSIA
DESIRED PRESSURE: 913.3 PSIA
TIME PRESSURE OCCURED: 0.6 SECONDS



TEMPERATURE LOCAT	GAGE NUMBER	CIRCUMFERENTIAL LOCATION (DEG)	TEMPERATURE (DEG F)
1	T0165	135.0	ND
1	T0166	235.0	ND
1	T0167	341.0	ND
2	T0085	135.0	76.1
2	T0086	341.0	78.2
3	T0087	45.0	78.3
3	T0120	157.0	70.7
4	T0089	0.0	ND
4	T0116	45.0	ND
4	T0090	90.0	ND
4	T0117	135.0	ND
4	T0091	180.0	ND
4	T0118	225.0	ND
4	T0092	270.0	ND
4	T0119	315.0	ND
5	T0184	111.0	2269.6
5	T0185	291.0	1479.6

ND = No data

Table 7.2-5. TPTA 1.1 Joint D Temperatures at T=0 sec

TEST NAME: TPTA 1.1
JOINT: D
DESCRIPTION: TEMPERATURE SUMMARY AT t=0.0

TEMPERATURE LOCAT	GAGE NUMBER	CIRCUMFERENTIAL LOCATION (DEG)	MAXIMUM TEMPERATURE (DEG F)	TIME OF MAX TEMP (SEC)
1	T0135	75.6	ND	ND
1	T0136	165.6	82.2	0.000
1	T0137	255.6	81.6	0.000
1	T0138	345.6	82.4	0.000
2	T0139	68.4	82.0	0.000
2	T0140	158.4	82.5	0.000
2	T0141	248.4	82.0	0.000
2	T0142	338.4	82.9	0.000
3	T0131	45.0	ND	ND
3	T0132	135.0	ND	ND
3	T0133	225.0	ND	ND
3	T0134	315.0	ND	ND

ND = No data

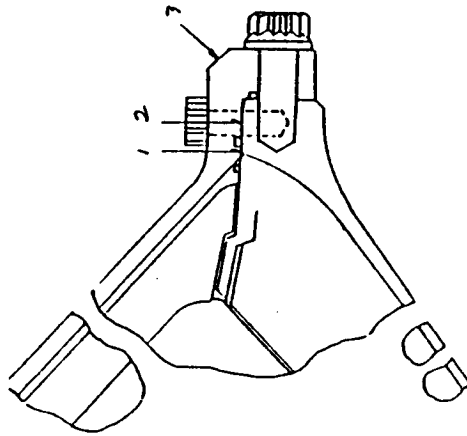
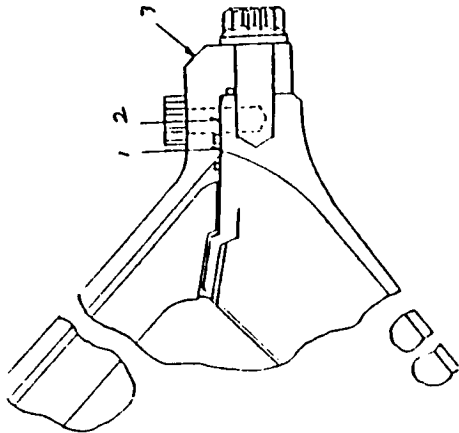


Table 7.2-6. TPTA 1.1 Joint D Temperatures at Maximum Chamber Pressure

TEST NAME: TPTA 1.1
JOINT: D
DESCRIPTION: TEMPERATURE SUMMARY
THE TIME RANGE IS 0.0 TO 6.0 SECONDS



TEMPERATURE LOCAT	GAGE NUMBER	CIRCUMFERENTIAL LOCATION (DEG)	MAXIMUM TEMPERATURE (DEG F)	TIME OF MAX TEMP (SEC)
1	T0135	75.6	ND	ND
1	T0136	165.6	83.8	0.174
1	T0137	255.6	84.1	0.137
1	T0138	345.6	84.1	0.162
2	T0139	68.4	82.2	0.087
2	T0140	158.4	82.8	0.087
2	T0141	248.4	82.5	0.237
2	T0142	338.4	83.1	0.349
3	T0131	45.0	ND	ND
3	T0132	135.0	ND	ND
3	T0133	225.0	ND	ND
3	T0134	315.0	ND	ND

ND = No data

7.2.3.4.1.2 TPTA 1.1A test joint temperatures. All joints were at ambient conditions at time $T = 0$. The average temperatures of Joints A, B, and D were 80, 79, and 83°F, respectively, at the beginning of the test. Temperatures did not change significantly during the test.

7.2.3.4.2 Test Joint Pressures

7.2.3.4.2.1 TPTA 1.1 test joint pressures. Test joint pressures at maximum chamber pressure of 913.3 psia were recorded at approximately 0.6 sec into the test. No pressure data were obtained in the slot for Joint A. Joint B slot pressure averaged 914.6 psia. The pressure reached the insulation only on both Joints A and B. The CF O-ring did not experience any gas pressure to determine its sealing capability. Tables 7.2-7 and 7.2-8 display pressures for Joints A and B at maximum chamber pressure.

Joint D pressure forward of the primary O-ring reached a maximum of 22.5 psia. The wiper O-ring sealed and had no damage. The maximum inter-O-ring pressure was 14.0 psia. Table 7.2-9 lists Joint D pressures at maximum chamber pressure.

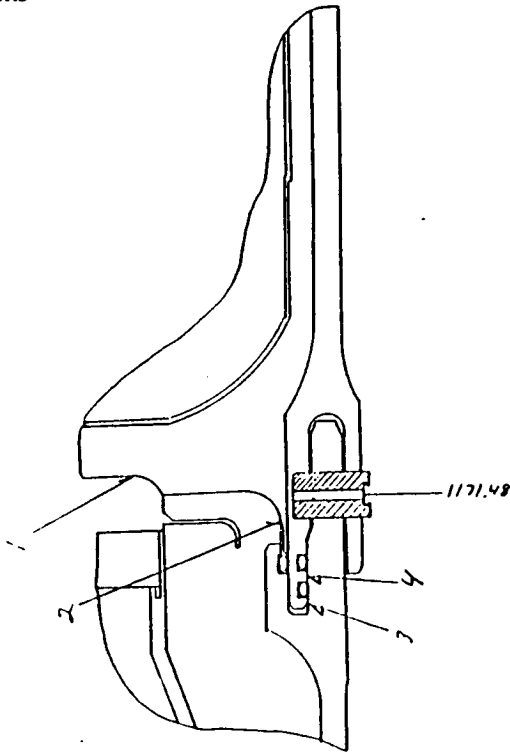
7.2.3.4.2.2 TPTA 1.1A test joint pressures. In both test Joints A and B, the inter-O-ring pressure was introduced with an external GN_2 source. The maximum pressure between the CF and primary O-rings for Joint A was 611.4 psia. Joint A maximum inter-O-ring pressure was 19.5 psia. In Joint B, the maximum pressure between the CF and primary O-rings was 612.5 psia, while the maximum inter-O-ring pressure was 17.6 psia.

In Joint D, the maximum pressure between the CF and primary O-rings was 127.7 psia. This pressure is believed to have been caused by seepage of nitrogen gas through the phenolics over a period of time. There was no damage to the O-rings and the primary O-ring sealed. Maximum inter-O-ring pressure was 15.5 psia. Tables 7.2-10 through 7.2-12 list the TPTA 1.1A test joint pressures at maximum chamber pressure.

7.2.3.4.3 Test Joint Deflections. The LVDTs that are of major interest and importance are those that measure gap opening above the primary O-ring, between the primary and secondary O-rings, and at the CF O-ring. Data from

Table 7.2-7. TPTA 1.1 Joint A Pressures at Maximum Chamber Pressure

TEST NAME: TPTA 1.1
JOINT: A
DESCRIPTION: PRESSURE SUMMARY
MAXIMUM PRESSURE: 909.7 PSIA
DESIRED PRESSURE: 913.3 PSIA
TIME PRESSURE OCCURED: 0.6 SECONDS

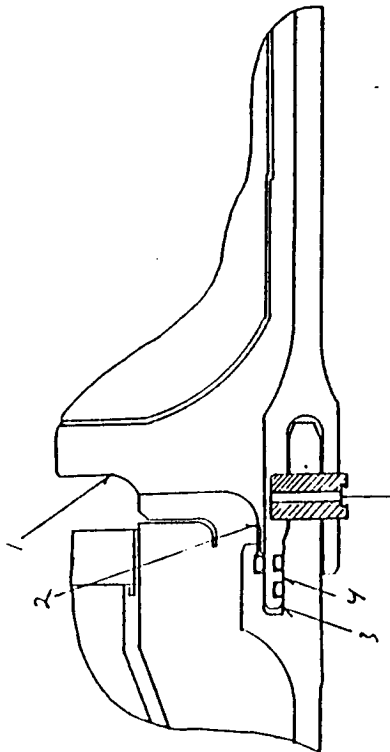


PRESSURE LOCAT	GAGE NUMBER	CIRCUMFERENTIAL LOCATION (DEG)	PRESSURE (PSIA)
1	P0048	111.0	ND
1	P0049	291.0	ND
2	P0076	135.0	ND
2	P0077	235.0	ND
2	P0078	341.0	ND
3	P0037	135.0	7.9
3	P0038	241.0	8.5
4	P0039	45.0	15.9
4	P0050	157.0	15.5

ND = No data

Table 7.2-8. TPTA 1.1 Joint B Pressures at Maximum Chamber Pressure

TEST NAME: TPTA 1.1
JOINT: B
DESCRIPTION: PRESSURE
MAXIMUM PRESSURE: 909.7 PSIA
DESIRED PRESSURE: 913.3 PSIA
TIME PRESSURE OCCURED: 0.6 SECONDS



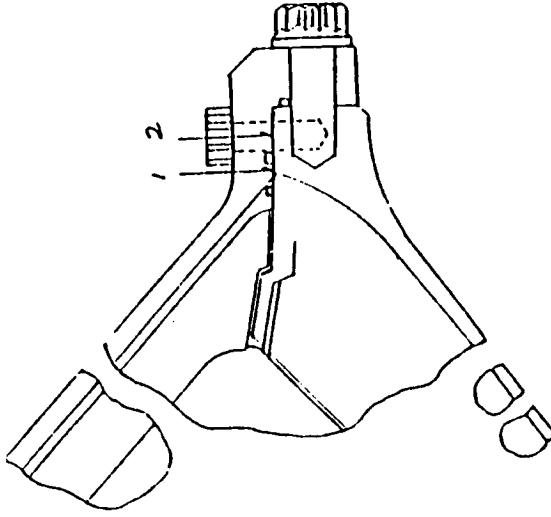
PRESSURE LOCAT	GAGE NUMBER	CIRCUMFERENTIAL		PRESSURE (PSIA)
		LOCATION (DEG)		
1	P0051	111.0		910.1
1	P0052	291.0		909.7
2	P0079	135.0		924.1
2	P0080	235.0		796.9
2	P0081	341.0		ND
3	P0044	135.0		9.3
3	P0045	341.0		10.0
4	P0046	45.0		ND
4	P0053	157.0		28.5

ND = No data

Table 7.2-9. TPTA 1.1 Joint D Pressures at Maximum Chamber Pressure

TEST NAME: TPTA 1.1
JOINT: D
DESCRIPTION: PRESSURE SUMMARY

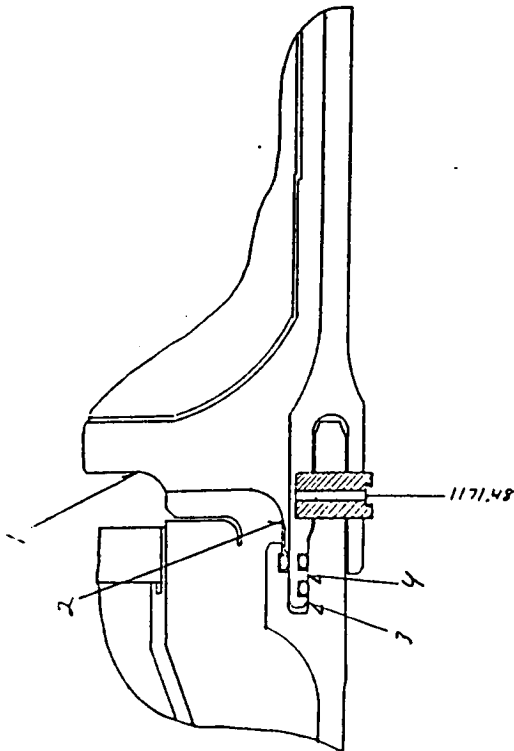
THE TIME RANGE IS 0.0 TO 6.0 SECONDS



PRESSURE LOCAT	GAGE NUMBER	CIRCUMFERENTIAL LOCATION (DEG)	MAXIMUM PRESSURE (PSIA)	TIME OF MAX PRES (SEC)
1	P0055	75.6	22.4	0.158
1	P0056	165.6	15.8	0.158
1	P0057	255.6	22.5	0.134
1	P0058	345.6	20.3	0.146
2	P0059	68.4	20.1	0.084
2	P0060	158.4	15.4	0.084
2	P0061	248.4	14.6	0.071
2	P0062	338.4	16.4	0.096

Table 7.2-10. TPTA 1.1A Joint A Pressures at Maximum Load

TEST NAME: TPTA 1.1A
JOINT: A
DESCRIPTION: PRESSURE SUMMARY
THE TIME RANGE IS 9.0 TO 14.0 SECONDS



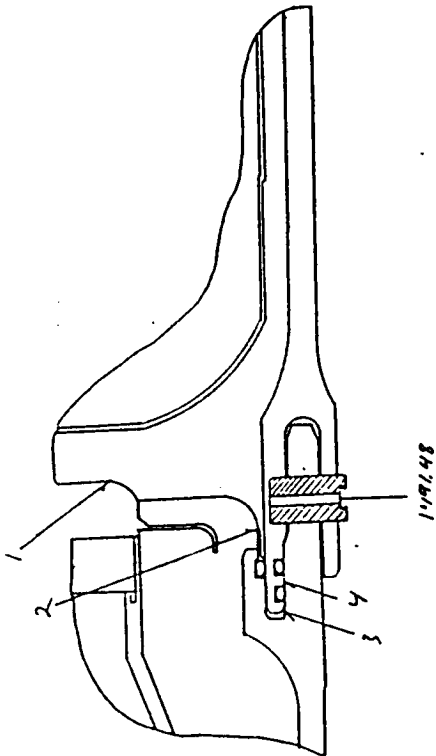
PRESSURE LOCAT	GAGE NUMBER	CIRCUMFERENTIAL LOCATION (DEG)	MAXIMUM PRESSURE (PSIA)	TIME OF MAX PRES (SEC)
1	P0048	111.0	ND	ND
1	P0049	291.0	ND	ND
2	P0076	135.0	ND	ND
2	P0077	235.0	ND	ND
2	P0078	341.0	ND	ND
3	P0037	135.0	ND	ND
3	P0038	241.0	611.4	9.612
4	P0039	45.0	18.5	12.988
4	P0050	157.0	19.5	9.150

ND = No data

Table 7.2-11. TPTA 1.1A Joint B Pressures at Maximum Load

TEST NAME: TPTA 1.1A
JOINT: B
DESCRIPTION: PRESSURE

THE TIME RANGE IS 9.0 TO 14.0 SECONDS



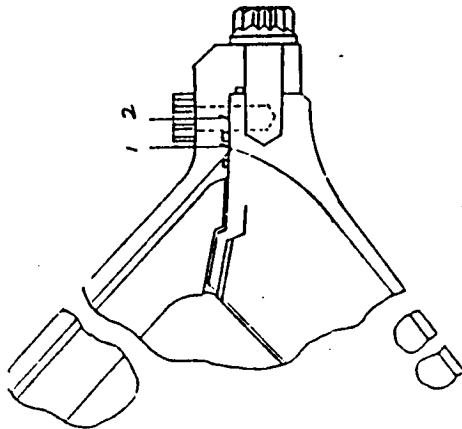
PRESSURE LOCAT	GAGE NUMBER	CIRCUMFERENTIAL LOCATION (DEG)	MAXIMUM PRESSURE (PSIA)	TIME OF MAX PRES (SEC)
1	P0051	111.0	614.2	9.250
1	P0052	291.0	610.4	9.000
2	P0079	135.0	569.2	9.012
2	P0080	235.0	635.0	10.050
2	P0081	341.0	ND	ND
3	P0044	135.0	ND	ND
3	P0045	341.0	612.5	9.412
4	P0046	45.0	14.8	10.438
4	P0053	157.0	17.6	13.100

ND = No data

Table 7.2-12. TPTA 1.1A Joint D Pressures at Maximum Load

TEST NAME: TPTA 1.1A
JOINT: D
DESCRIPTION: PRESSURE SUMMARY

THE TIME RANGE IS 9.0 TO 14.0 SECONDS



PRESSURE LOCAT	GAGE NUMBER	CIRCUMFERENTIAL LOCATION (DEG)	MAXIMUM PRESSURE (PSIA)	TIME OF MAX PRES (SEC)
1	P0055	75.6	127.5	10.175
1	P0056	165.6	127.7	10.462
1	P0057	255.6	127.5	9.450
1	P0058	345.6	128.0	12.576
2	P0059	68.4	15.5	11.112
2	P0060	158.4	15.4	10.038
2	P0061	248.4	15.6	10.288
2	P0062	338.4	15.6	10.438

these locations allow an overall characterization of the sealing system capabilities and behavior at each joint when subjected to launch/flight loading conditions. Several representative LVDTs will be examined to show the effect of the ignition transient and strut loading on test Joints A, B, and D. The response of these LVDTs and proximity gages will be plotted against time along with the dominant applied load (pressure or strut load) in order to observe the correlation between load and gage response.

Data from LVDTs measuring primary and primary/secondary gap deflection are output in inches and employ the following sign conventions:

Positive deflection (+) = Gap closing

Negative deflection (-) = Gap opening

Data from proximity gages measuring CF gap deflection are output in mils and employ the following sign convention:

Positive deflection (+) = Gap opening

Negative deflection (-) = Gap closing

7.2.3.4.3.1 TPTA 1.1 test joint deflections

Joint A Deflections (TPTA 1.1)

There is an easily discernible correlation between the ignition transient and joint gap deflection. Gages at the primary O-ring in general show trends similar to those shown by gages D0079 and D0081 (Figures 7.2-3 and 7.2-4). The gages shown directly track the ignition transient pressure rise with a gap opening response. As the motor case pressure decays to the point at which the exhaust nozzle became plugged, the gages show either a steady unchanging response or a slight relaxing of the opening response previously brought on by the ignition transient.

The response of gages between the primary and secondary O-rings is not as easily defined as that of the primary O-ring. Some LVDTs show an initial tendency for gap closing while others show an initial trend towards gap opening. However, once the initial transient has passed, most of the primary/secondary gages show a bias towards a gradual gap closing as the

TPTA 1.1 FINAL
D0079(STAT= 1169.15, 121 DEG) D0081(STAT= 1169.15, 323 DEG)
19 NOVEMBER 1987

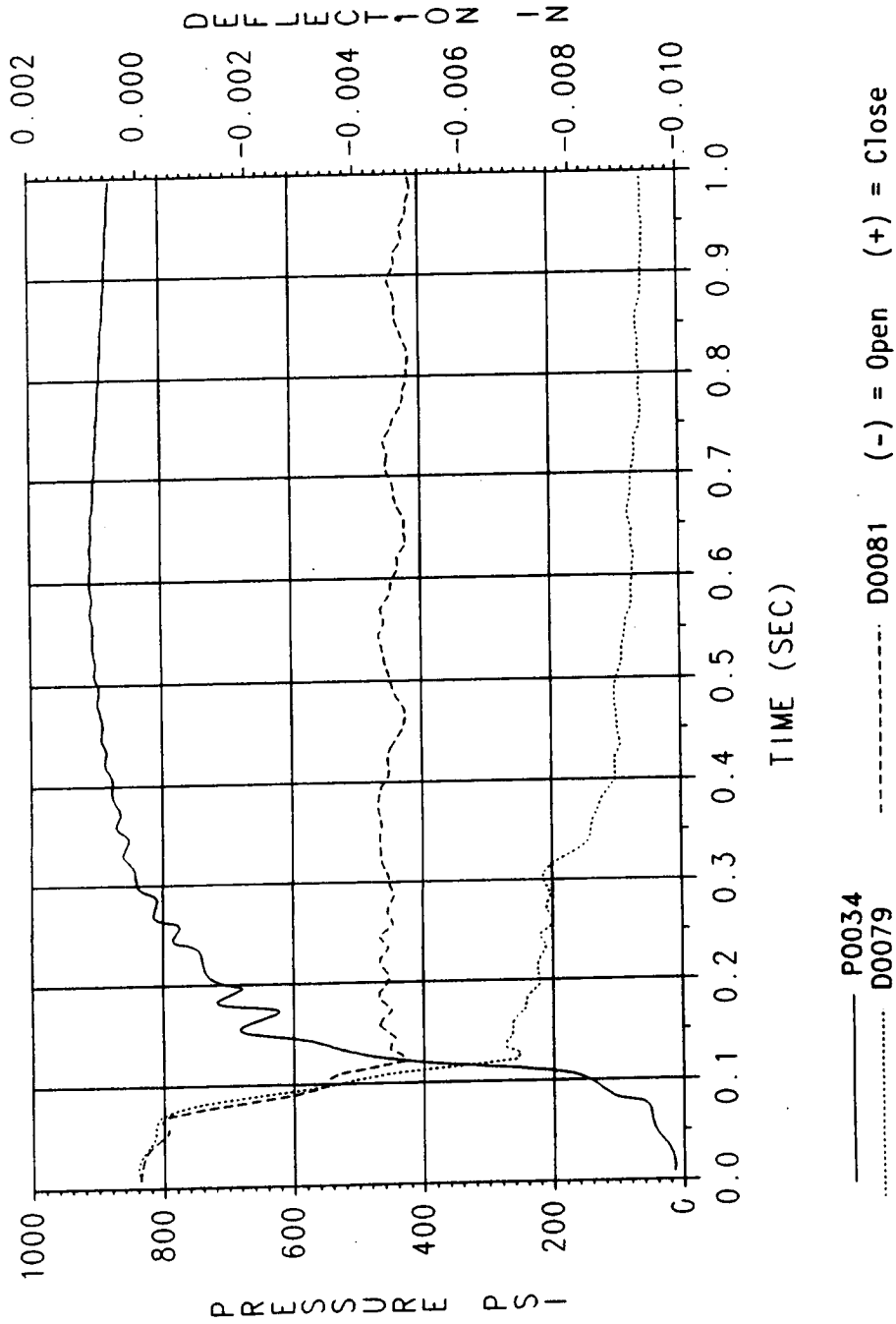
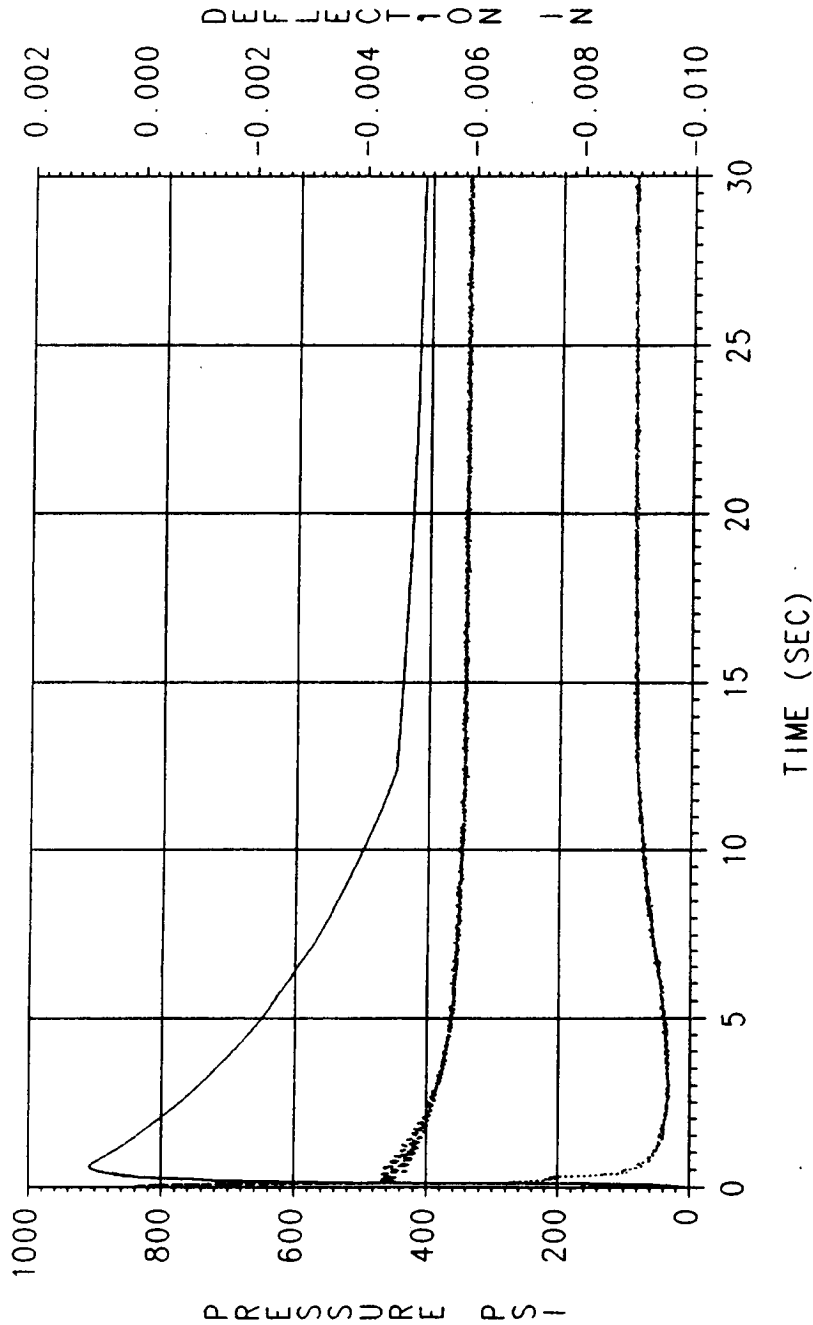


Figure 7.2-3. TPTA 1.1 Joint A Gap Deflection at Primary O-ring (0-1 sec)

TPTA 1.1 FINAL
D0079(STAT= 1169.15, 121 DEG) D0081(STAT= 1169.15, 323 DEG)
19 NOVEMBER 1987



----- P0034 (-) = Open (+) = Close
..... D0079

Figure 7.2-4. TPTA 1.1 Joint A Gap Deflection at Primary O-ring (0-30 sec)

internal pressure decays (Figures 7.2-5 and 7.2-6). These gages also show discontinuities, well-defined though small in magnitude, at approximately 0.10 sec, which occur as the motor case pressure overcomes the static axial weight of the test article causing joint reconfiguration as the axial slack in the joint is taken up.

Proximity gages near the CF O-ring show varied responses, as did the primary/secondary gages. However, data from certain gages lead one to believe that output from some proximity gages may be suspect. For example, gages D0127 and D0141 (Figures 7.2-7 and 7.2-8) both show an initial tendency towards gap closing, followed by a slight turn towards gap opening, until 9.0 sec when gage D0141 spikes to zero, then settles at 0.0005 in. closed. The spike is obviously a gage malfunction and should be ignored. In addition to this discrepancy, the positive sign of measurements from gage D0127 indicates a condition of gap opening, but examination of the time displacement plot indicates that the gage was zeroed to a value of 0.006 in. open. These are typical of the pitfalls associated with the use of output data from the CF proximity gages.

The maximum values of gap opening and closing response for Joint A are summarized in the Table 7.2-13. These values are taken in the time span from 0.0 to 120.0 sec. The maximum readings from the CF proximity gages should be taken in light of the discussion of the previous paragraph. Table 7.2-14 shows a good comparison of TPTA 1.1 Joint A deflections with JES-3A.

Joint B Deflections (TPTA 1.1).

Joint B primary O-ring LVDTs show the same trend as those at Joint A, but with larger absolute magnitudes and the presence of "ringing" after the firing (Figures 7.2-9 and 7.2-10). The LVDTs track the ignition transient pressure rise with an initial gap response of approximately 0.001 to 0.002 in. open (varying circumferentially). In evidence is the presence of regular damped oscillatory motion ("ringing") after the firing, indicating that one of the natural frequencies of the the test article was disturbed.

Joint B primary/secondary LVDTs show tendencies both to open or close depending on the particular gage under scrutiny. As shown in Figure 7.2-11,

TPTA 1.1 FINAL
D082(STAT= 1169.77, 115 DEG) D084(STAT= 1169.77, 317 DEG)
19 NOVEMBER 1987

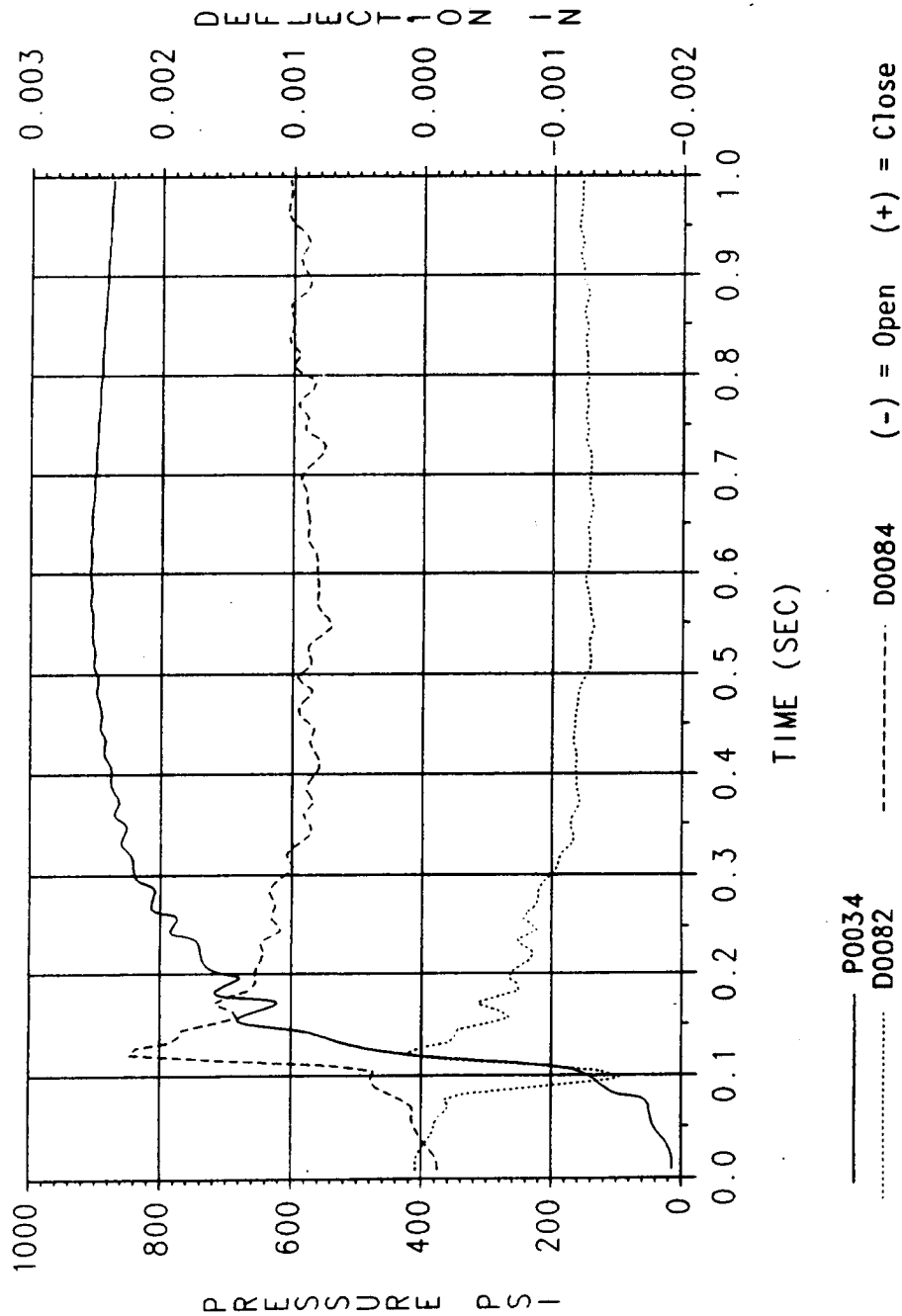
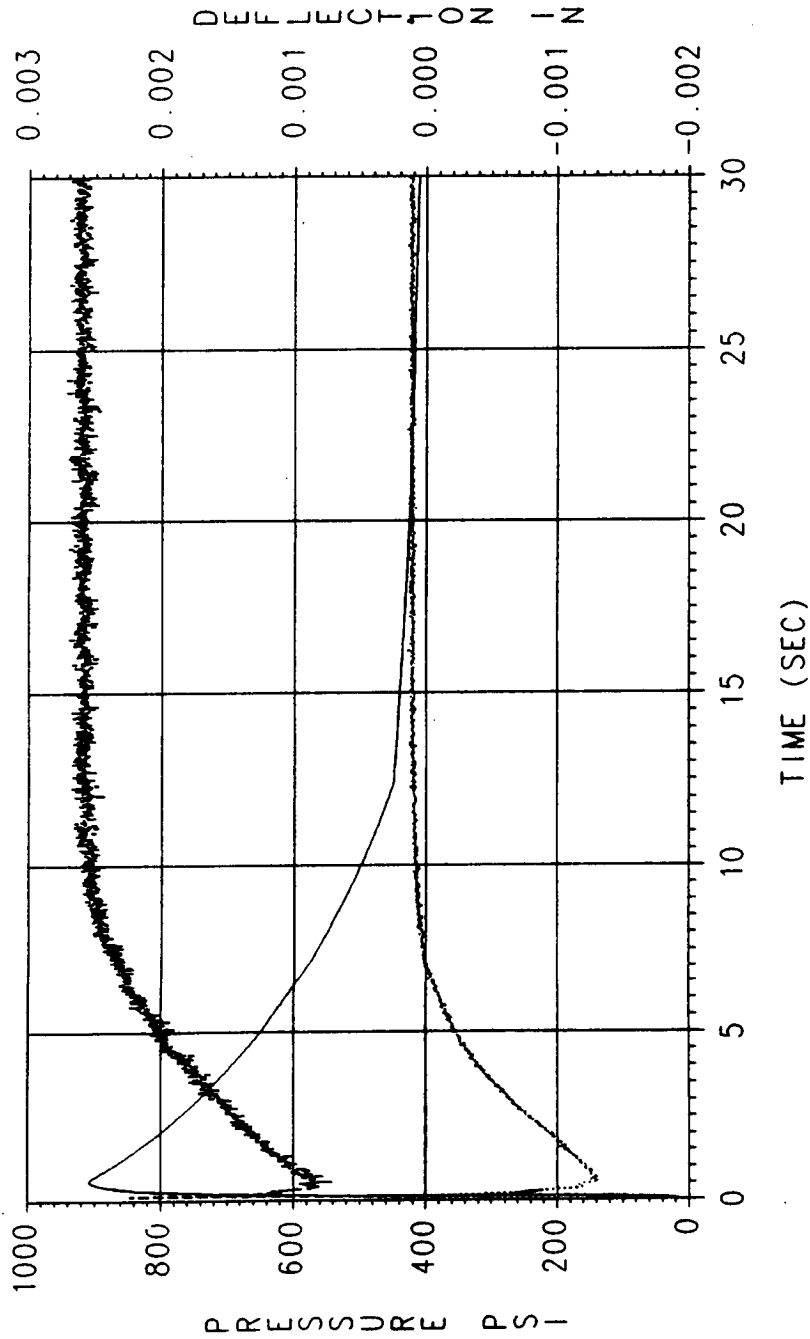


Figure 7.2-5. TPTA 1.1 Joint A Deflection at Primary/Secondary O-rings (0-1 sec)

TPTA 1.1 FINAL

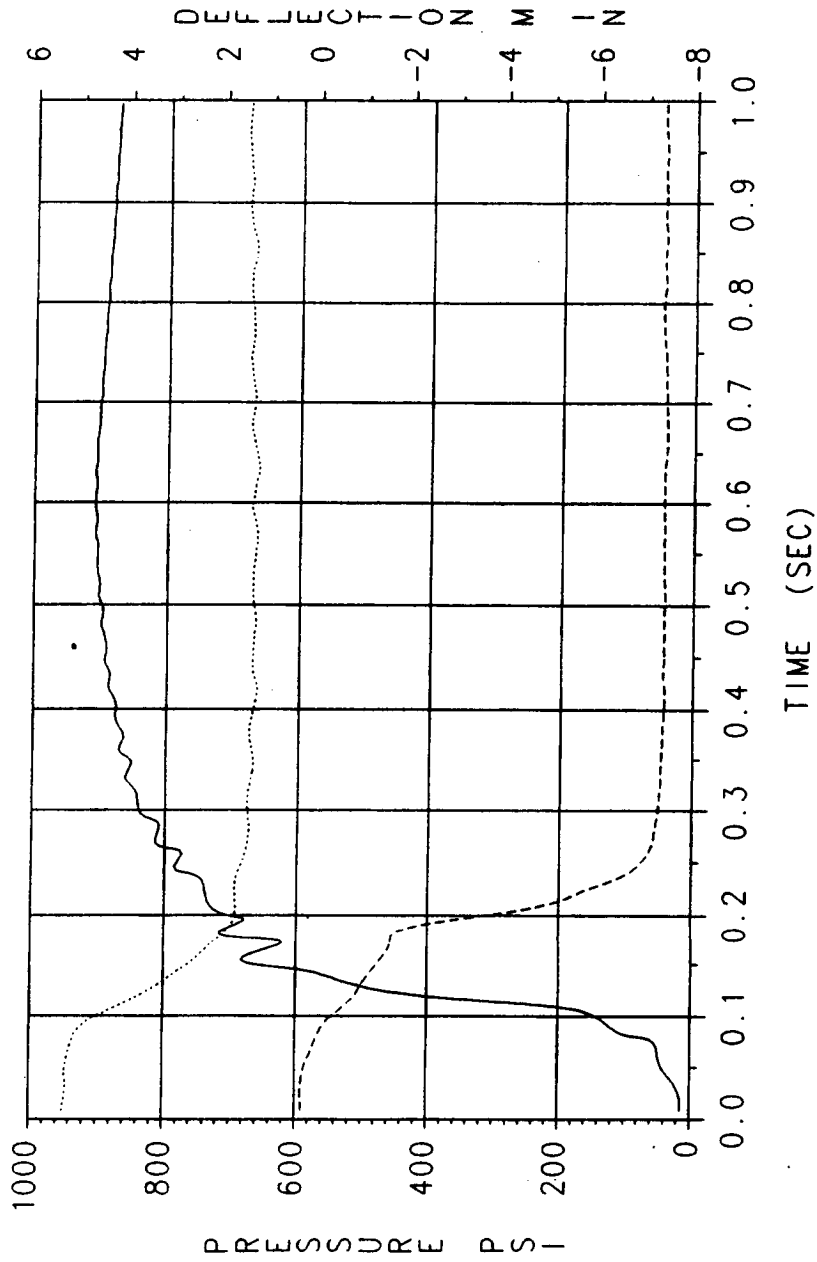
D082(STAT= 1169.77, 115 DEG) D084(STAT= 1169.77, 317 DEG)
19 NOVEMBER 1987



— P0034
..... D0082
----- D0084
(-) = Open (+) = Close

Figure 7.2-6. TPTA 1.1 Joint A Gap Deflection at Primary/Secondary O-rings (0-30 sec)

TPTA 1.1 FINAL
D127(STAT= 1169.57, 180 DEG) D141(STAT= 1169.57, 60 DEG)
19 NOVEMBER 1987



— P0034 (—) = Close (+) = Open
... D0127
--- D0141

Figure 7.2-7. TPTA 1.1 Joint A Gap Deflection at CF O-ring (0-1 sec)

TPTA 1.1 FINAL
D127(STAT= 1169.57, 180 DEG) D141(STAT= 1169.57, 60 DEG)
19 NOVEMBER 1987

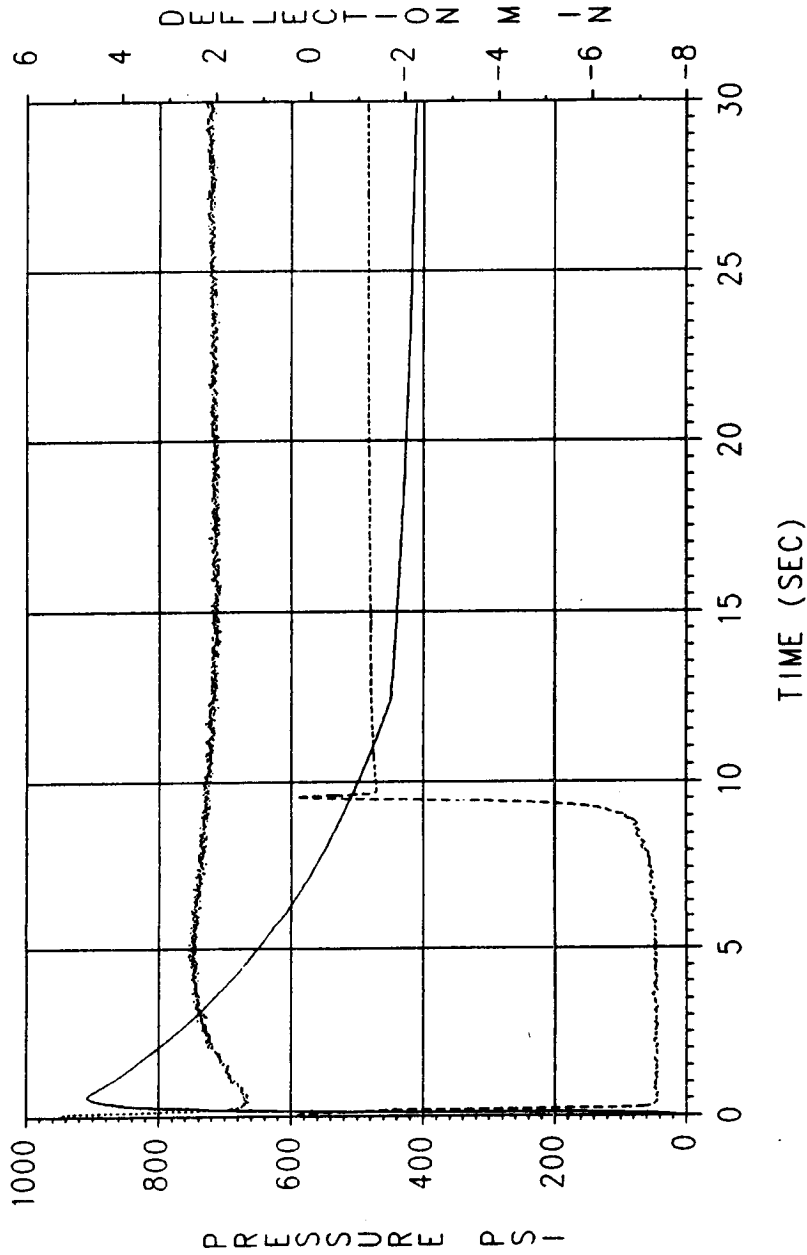
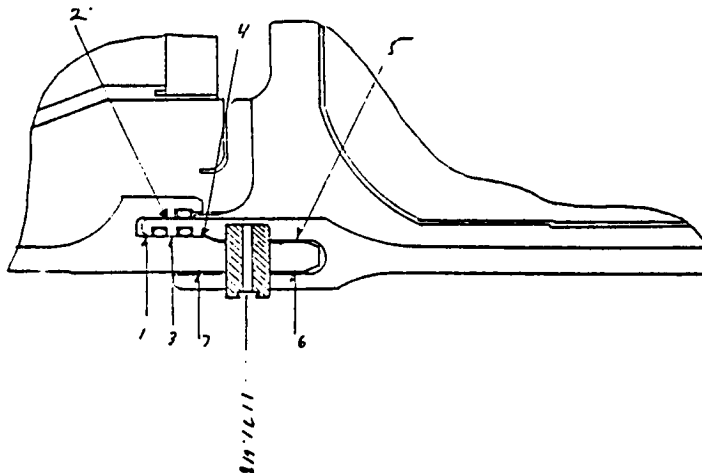


Figure 7.2-8. TPTA 1.1 Joint A Gap Deflection at CF O-ring (0-30 sec)

Table 7.2-13. TPTA 1.1 Joint A Maximum Gap Summary

TEST NAME: TPTA 1.1
 JOINT: A
 DESCRIPTION: DISPLACEMENT SUMMARY
 MODEL PRESSURE 913.3 PSIA
 MAXIMUM PRESSURE: 909.7 PSIA
 DESIRED PRESSURE: 913.3 PSIA
 TIME PRESSURE OCCURRED: 0.6 SECONDS



LOCAT	FROM STATION	TO STATION	GAGE NUMBER	ANGULAR LOCATION	DEFLECTION (IN)
1	1169.2		D0143	63.0	- 0.005 OPEN
1	1169.2		D0079	121.0	- 0.009 OPEN
1	1169.2		D0080	183.0	- 0.002 OPEN
1	1169.2		D0144	223.0	- 0.006 OPEN
1	1169.2		D0081	323.0	- 0.005 OPEN
2	1169.6		D0141	60.0	- 0.007 OPEN
2	1169.6		D0125	118.0	ND
2	1169.6		D0126	180.0	- 0.001 OPEN
2	1169.6		D0142	220.0	0.000 CLOSE
2	1169.6		D0127	320.0	0.001 CLOSE
3	1169.8		D0145	57.0	- 0.000 OPEN
3	1169.8		D0082	115.0	- 0.001 OPEN
3	1169.8		D0083	177.0	0.001 CLOSE
3	1169.8		D0146	201.0	0.001 CLOSE
3	1169.8		D0147	217.0	0.002 CLOSE
3	1169.8		D0084	317.0	0.001 CLOSE
4	1170.4		D0150	59.0	0.003 CLOSE
4	1170.4		D0092	117.0	0.010 CLOSE
4	1170.4		D0151	219.0	0.008 CLOSE
4	1170.4		D0093	319.0	0.004 CLOSE
5	1172.7		D0152	61.0	0.004 CLOSE
5	1172.7		D0090	119.0	0.004 CLOSE
5	1172.7		D0153	221.0	0.004 CLOSE
5	1172.7		D0091	321.0	0.004 CLOSE
6	1172.7		D0154	59.0	- 0.023 OPEN
6	1172.7		D0096	117.0	- 0.026 OPEN
6	1172.7		D0155	219.0	- 0.020 OPEN
6	1172.7		D0097	319.0	- 0.020 OPEN
7	1170.4		D0156	61.0	- 0.003 OPEN
7	1170.4		D0094	119.0	0.001 CLOSE
7	1170.4		D0157	221.0	0.002 CLOSE
7	1170.4		D0095	321.0	- 0.001 OPEN

ND = No data

Table 7.2-14. Comparison of TPTA Joint A Gaps With JES-3A*

Max Chamber Pressure = 913.3 psia

Description: Maximum deflections at time = 0 to 1 sec

Pressure Face: Insulation

Deflection Location	Gage Number	Circumferential Location (deg)	Deflection (in.)	
			TPTA 1.1	JES-3A*
Forward of Primary	D079	121	0.010 (open)	0.012 (open)
	D080	183	0.004 (open)	0.012 (open)
	D081	323	0.006 (open)	0.004 (open)
		Average	0.007 (open)	0.009 (open)
Interference Fit	D125	118	ND	ND
	D126	180	0.003 (open)	0.002 (close)
	D127	320	0.005 (close)	0.004 (close)
		Average	0.001 (close)	0.003 (close)
Inter-O-ring	D082	115	0.002 (open)	0.004 (close)
	D083	117	0.002 (close)	0.006 (open)
	D084	317	0.003 (close)	0.003 (open)
		Average	0.001 (close)	0.002 (open)

*Deflection normalized with pressure of 913.3 psia

Note: ND = No data

TPTA 1.1
GAGES D0164 D0165 D0168

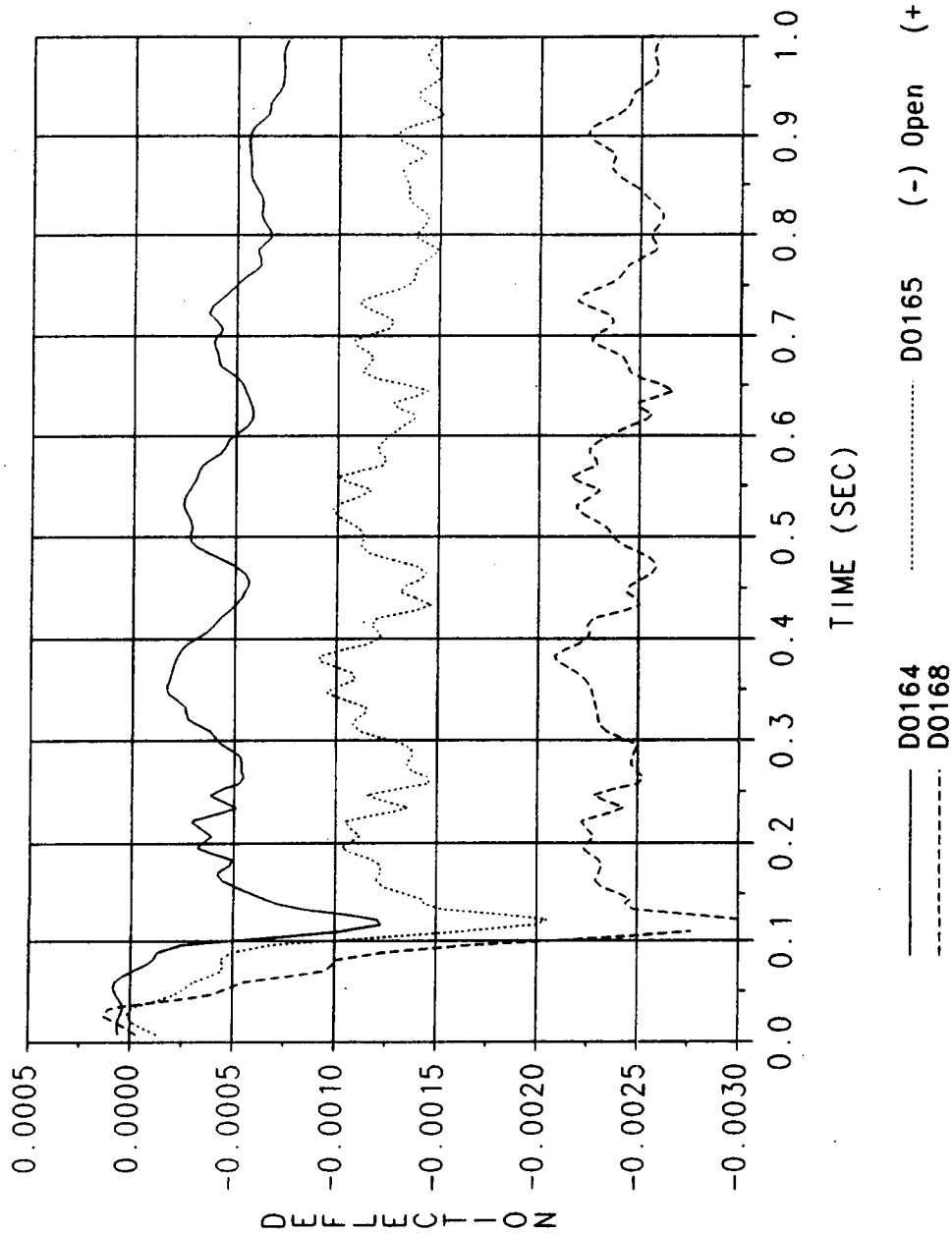


Figure 7.2-9. TPTA 1.1 Joint B Gap Deflection at Primary O-ring (0-1 sec)

TPTA 1.1
GAGES D0164 D0165 D0168

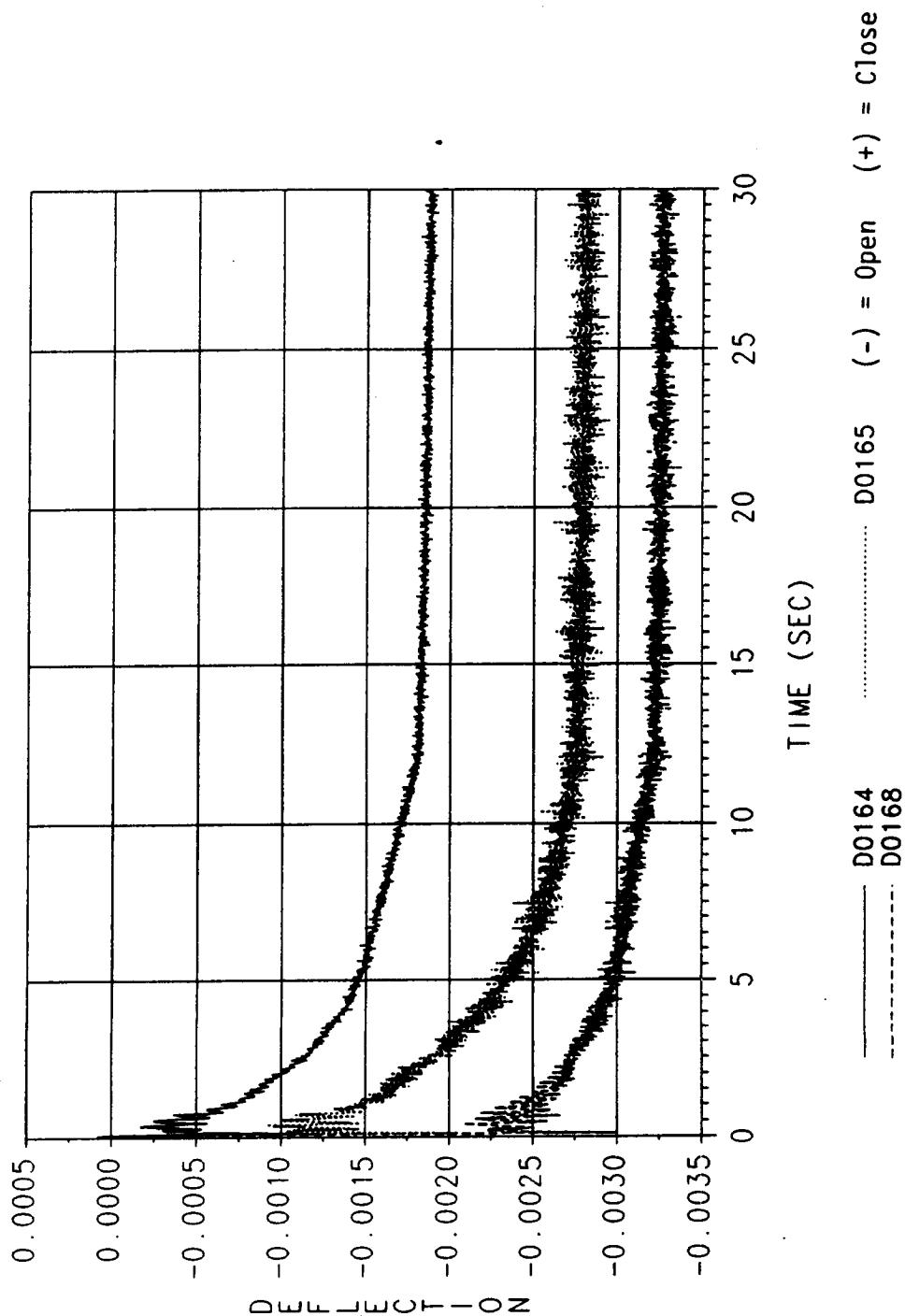


Figure 7.2-10. TPTA Joint B Gap Deflection at Primary O-ring (0-30 sec)

TPTA 1.1 FINAL

D112(STAT=1489.77, 115 DEG) D334(STAT=1555.48)

19 NOVEMBER 1987

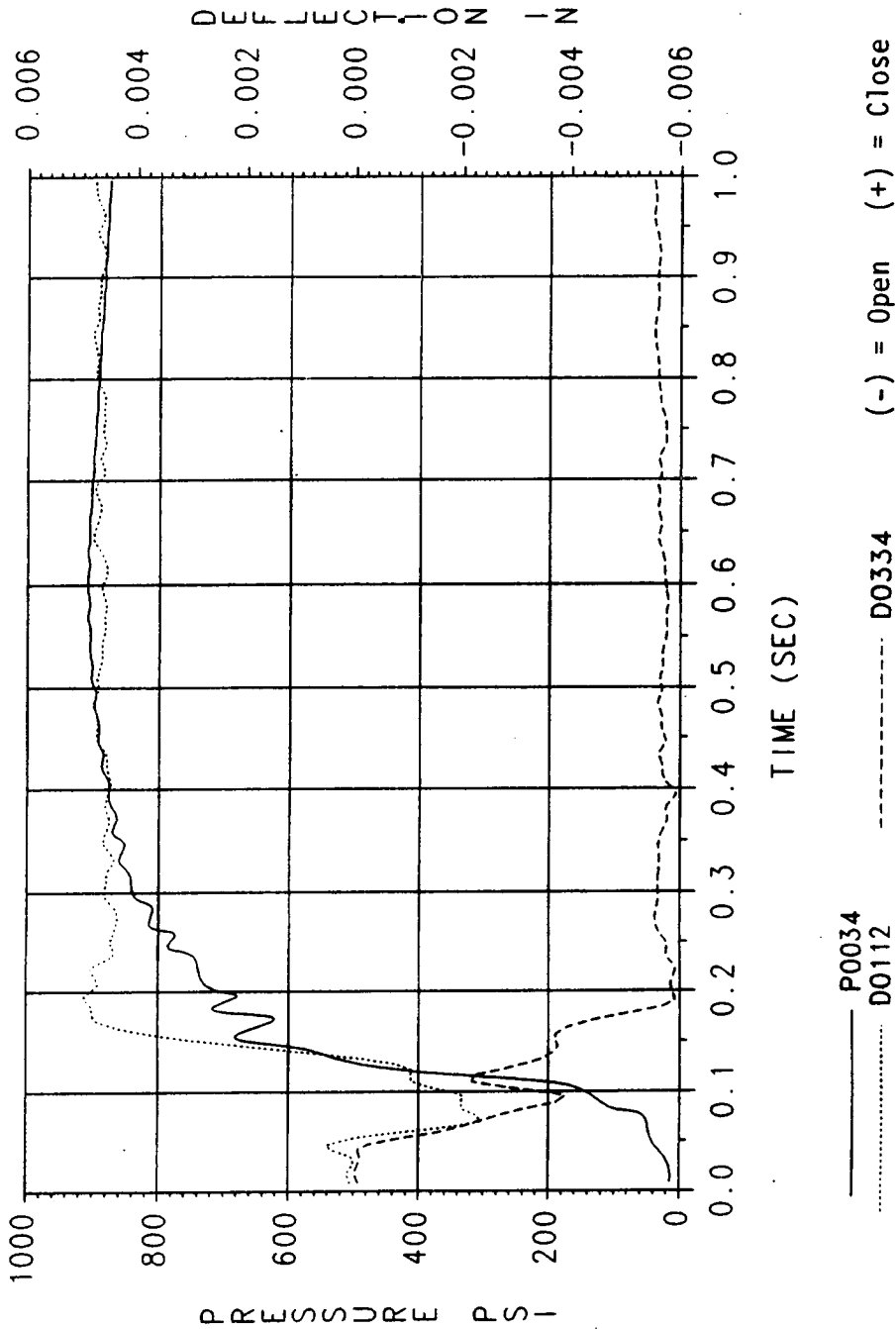


Figure 7.2-11. TPTA 1.1 Joint B Gap Deflection at Primary/Secondary O-rings (0-1 sec)

gages D0012 and D0334 begin to move in the gap opening direction, but at approximately 0.08 sec, gage D0112 turns up (closes) and quickly settles to about 0.005 in. closed, while D0334 continues down (opening) and settles at 0.006 in. open (Figure 7.2-12). The time at which the gages turn in divergent directions also coincides with the approximate pressure at which the internal pressure overcomes the axial weight of the stack and releases the axial "slack" in the joint. This indicates that some nonlinear phenomenon such as "pin skip" is the cause of this apparent disparity.

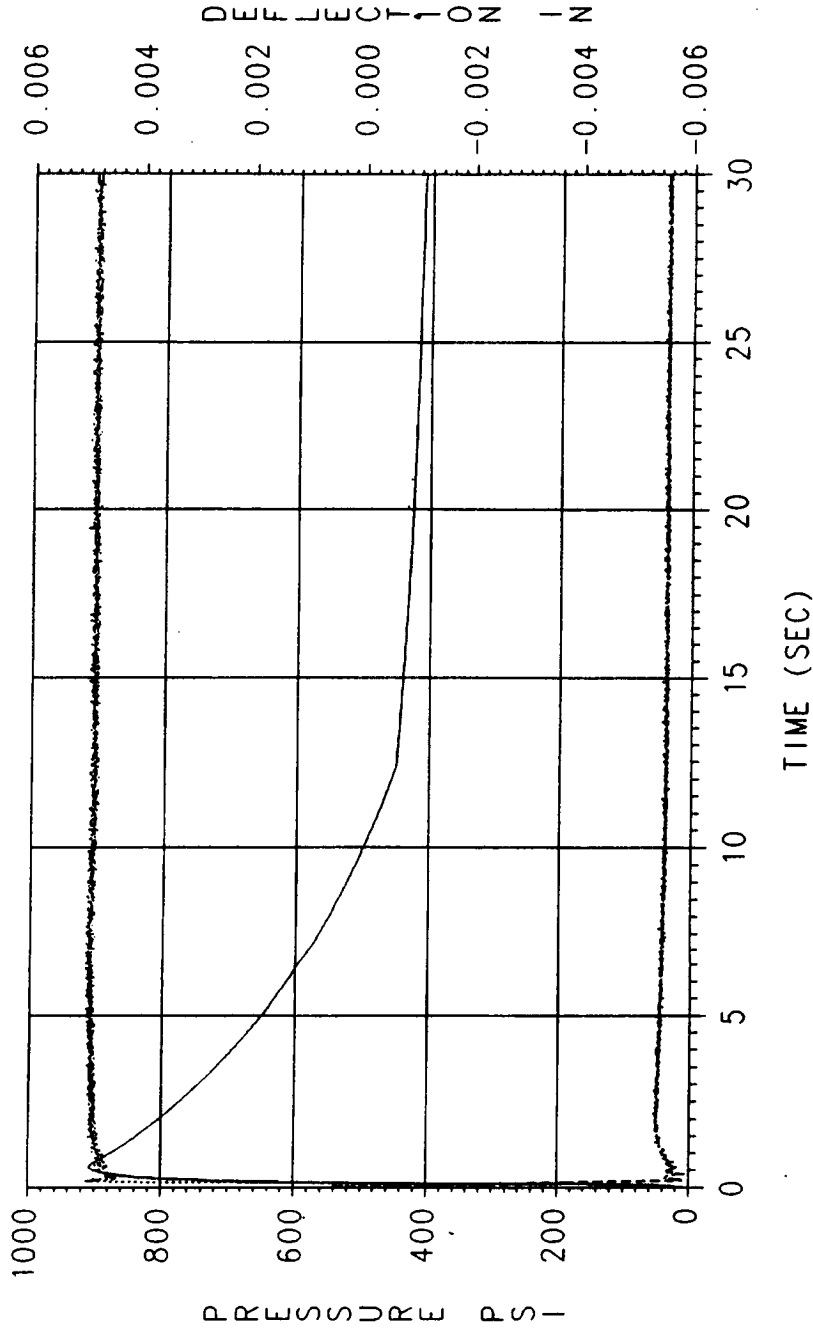
CF gages at Joint B in general show a stable linear response after the initial ignition transient. The gages typically track the initial pressure rise with a closing response (Figures 7.2-13 and 7.2-14, gage D0160), then relax slightly and stabilize for the remainder of the test. As in Joint A, there are a certain number of suspect gages, such as D0130 (Figures 7.2-13 and 7.2-14), which show only the slightest response at the point of ignition, then apparently settle to zero. The output from these gages should be carefully scrutinized.

The values of gap opening and closing response at maximum chamber pressure for Joint B are summarized in Table 7.2-15. These values are taken in the time span from 0.0 to 120.0 sec. Again, the maximum readings from the CF proximity gages should be taken in light of the discussion of the previous paragraph. Table 7.2-14 demonstrates a good comparison between the TPTA 1.1 and JES-3A Joint A deflection. Table 7.2-16 illustrates a good comparison between Joint B gaps in the TPTA 1.1 test and the JES-3A test.

Joint D Deflections (TPTA 1.1)

Joint D deflections were as expected. The average gap forward of the wiper O-ring was 0.008 in. and the average inter-O-ring gap was 0.004 inch. Table 7.2-17 summarizes Joint D gaps at maximum chamber pressure. These values matched well with the NJES-2B test data. Table 7.2-18 lists the deflection values for the TPTA 1.1 test.

TPTA 1.1 FINAL
D112(STAT= 1489.77, 115 DEG) D334(STAT= 1555.48)
19 NOVEMBER 1987

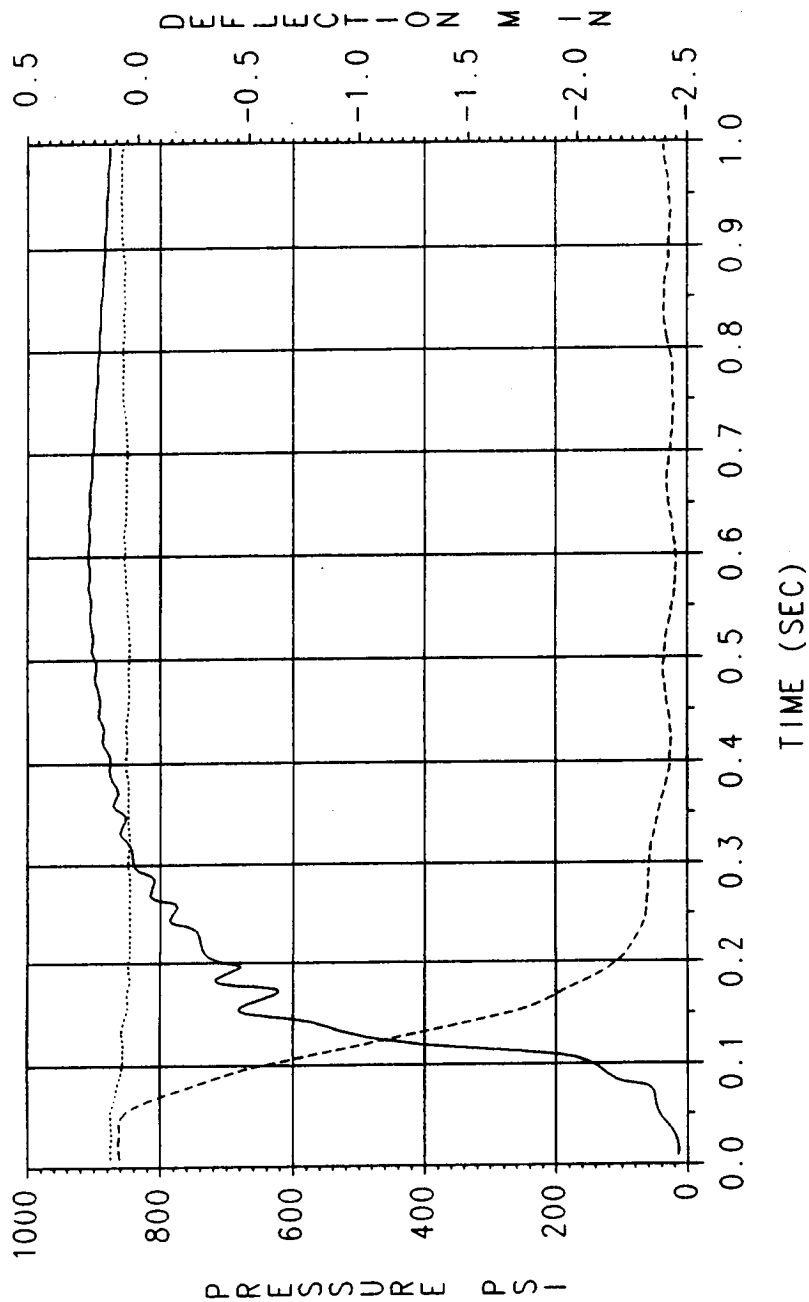


_____ P0034
 D0112
 ----- D0334
 (-) = Open (+) = Close

Figure 7.2-12. TPTA 1.1 Joint B Gap Deflection at Primary/Secondary O-rings (0-30 sec)

TPTA 1.1 FINAL

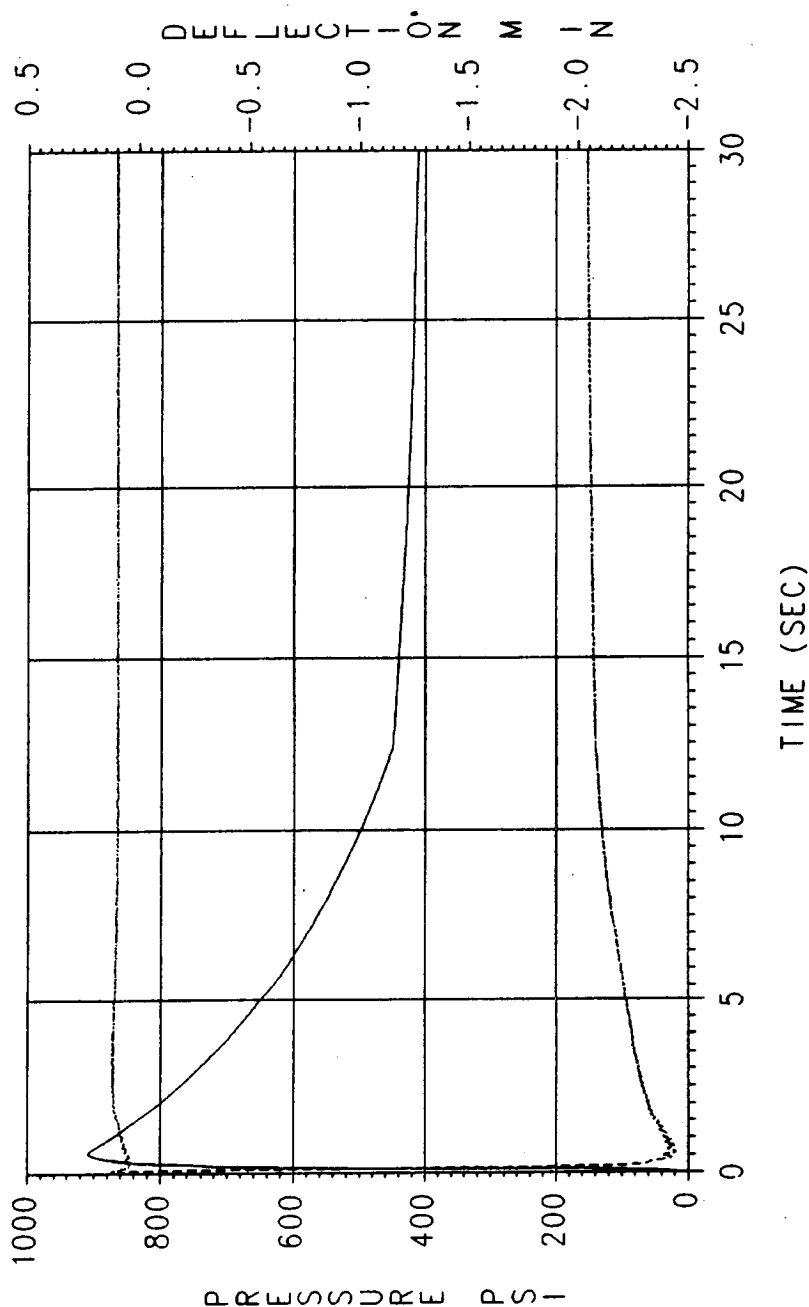
D130(STAT= 1489.57, 320 DEG) D160(STAT= 1489.57, 220 DEG)
19 NOVEMBER 1987



— P0034
- - - D0130
- - - D0160 (-) = Close (+) = Open

Figure 7.2-13. TPTA 1.1 Joint B Gap Deflection at CF O-ring (0-1 sec)

TPTA 1.1 FINAL
D130(STAT= 1489.57, 320 DEG) D160(STAT= 1489.57, 220 DEG)
19 NOVEMBER 1987



—— P0034
----- D0130
(-) = Close (+) = Open

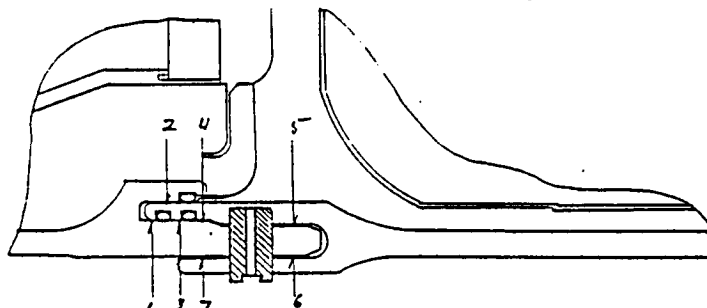
Figure 7.2-14. TPTA 1.1 Joint B Gap Deflection at CF O-ring (0-30 sec)

MORTON THIKOL INC.

Space Operations

Table 7.2-15. TPTA 1.1 Joint B Maximum Gap Summary

TEST NAME: TPTA 1.1
 JOINT: B
 DESCRIPTION: DEFLECTION SUMMARY
 MODEL PRESSURE 913.3 PSIA
 MAXIMUM PRESSURE: 909.7 PSIA
 DESIRED PRESSURE: 913.3 PSIA
 TIME PRESSURE OCCURED: 0.6 SECONDS



LOCAT	FROM STATION	TO STATION	GAGE NUMBER	ANGULAR LOCATION	DEFLECTION (IN)
1	1489.2		D0163	3.0	-0.001 OPEN
1	1489.2		D0164	63.0	-0.001 OPEN
1	1489.2		D0165	121.0	-0.001 OPEN
1	1489.2		D0116	183.0	-0.001 OPEN
1	1489.2		D0166	223.0	0.000 OPEN
1	1489.2		D0167	243.0	-0.001 OPEN
1	1489.2		D0168	269.0	-0.002 OPEN
1	1489.2		D0117	323.0	-0.003 OPEN
2	1489.2		D0158	0.0	0.000 CLOSE
2	1489.2		D0159	60.0	0.000 CLOSE
2	1489.2		D0128	118.0	0.000 CLOSE
2	1489.2		D0129	180.0	0.002 OPEN
2	1489.2		D0160	220.0	0.002 OPEN
2	1489.2		D0161	240.0	0.000 OPEN
2	1489.2		D0162	266.0	0.002 OPEN
2	1489.2		D0130	320.0	0.001 CLOSE
3	1489.8		D0333	25.0	0.002 CLOSE
3	1489.8		D0169	57.0	0.002 CLOSE
3	1489.8		D0112	115.0	0.005 CLOSE
3	1489.8		D0334	139.0	-0.006 OPEN
3	1489.8		D0113	177.0	-0.001 OPEN
3	1489.8		D0351	201.0	0.000 OPEN
3	1489.8		D0171	217.0	0.000 OPEN
3	1489.8		D0172	237.0	0.000 OPEN
3	1489.8		D0173	263.0	-0.001 OPEN
3	1489.8		D0335	287.0	0.001 CLOSE
3	1489.8		D0336	307.0	0.001 CLOSE
3	1489.8		D0114	317.0	0.001 CLOSE
3	1489.8		D0174	357.0	0.001 CLOSE
4	1490.4		D0176	59.0	0.008 CLOSE
4	1490.4		D0104	117.0	0.012 CLOSE
4	1490.4		D0017	179.0	0.005 CLOSE
4	1490.4		D0177	219.0	0.002 CLOSE
4	1490.4		D0178	239.0	0.011 CLOSE
4	1490.4		D0179	265.0	0.007 CLOSE
4	1490.4		D0105	319.0	0.005 CLOSE
4	1490.4		D0175	359.0	0.000 CLOSE
5	1492.7		D0180	1.0	0.003 CLOSE
5	1492.7		D0181	61.0	0.004 CLOSE
5	1492.7		D0102	119.0	0.003 CLOSE
5	1492.7		D0018	181.0	0.004 CLOSE
5	1492.7		D0182	221.0	0.004 CLOSE
5	1492.7		D0183	241.0	0.004 CLOSE
5	1492.7		D0184	267.0	0.004 CLOSE
5	1492.7		D0103	321.0	0.004 CLOSE
6	1492.7		D0186	59.0	-0.023 OPEN
6	1492.7		D0108	117.0	-0.026 OPEN
6	1492.7		D0019	179.0	-0.020 OPEN
6	1492.7		D0187	219.0	-0.019 OPEN
6	1492.7		D0188	239.0	-0.016 OPEN
6	1492.7		D0189	265.0	-0.021 OPEN
6	1492.7		D0109	319.0	-0.027 OPEN
6	1492.7		D0185	359.0	-0.020 OPEN
7	1490.4		D0190	1.0	0.004 CLOSE
7	1490.4		D0191	61.0	0.000 CLOSE
7	1490.4		D0106	119.0	0.003 CLOSE
7	1490.4		D0020	181.0	0.000 OPEN
7	1490.4		D0192	221.0	0.001 CLOSE
7	1490.4		D0193	241.0	0.006 CLOSE
7	1490.4		D0194	267.0	0.002 CLOSE
7	1490.4		D0107	321.0	-0.002 OPEN

ORIGINAL PAGE IS
OF POOR QUALITY

ND = No data

Table 7.2-16. Comparison of TPTA 1.1 Joint B Gaps with JES-3A*

Max Chamber Pressure = 913.3 psia

Description: Maximum deflections at time = 0 to 1 sec

Pressure Face: Insulation

Deflection Location	Gage Number	Circumferential Location (deg)	Deflection (in.)	
			TPTA 1.1	JES-3A*
Forward of Primary	D115	123	NA	0.007 (open)
	D116	183	ND	0.007 (open)
	D117	323	0.003 (open)	0.002 (open)
		Average	0.003 (open)	0.005 (open)
Interference Fit	D128	118	0.001 (close)	0.005 (close)
	D129	180	0.002 (open)	0.001 (close)
	D130	320	0.000 --	0.001 (close)
		Average	0.001 (open)	0.001 (close)
Inter-O-ring	D333	25	0.003 (close)	0.001 (open)
	D169	57	0.002 (close)	0.004 (open)
	D112	115	0.005 (close)	0.005 (open)
	D334	139	0.006 (open)	0.005 (close)
	D113	177	0.001 (open)	0.002 (close)
	D171	217	0.001 (open)	0.007 (close)
	D172	237	0.001 (close)	0.002 (open)
	D173	263	0.002 (open)	0.001 (open)
	D335	287	0.001 (close)	0.001 (open)
	D336	307	0.002 (close)	0.001 (open)
	D114	317	0.001 (close)	0.001 (open)
	D174	357	0.002 (close)	0.001 (open)
		Average	0.001 (close)	0.000 --

*JES-3A had a 270-deg ETA ring installed and TPTA 1.1 had a 360-deg ETA ring installed.

Deflections normalized with pressure of 913.3 psia.

Note: ND = No data

NA = Not applicable

Table 7.2-17. Comparison of TPTA 1.1 Joint D Gaps With NJES-2B*

Max Chamber Pressure = 913.3 psia

Description: Maximum deflections at time = 0 to 1 sec

Pressure Face: Wiper O-ring

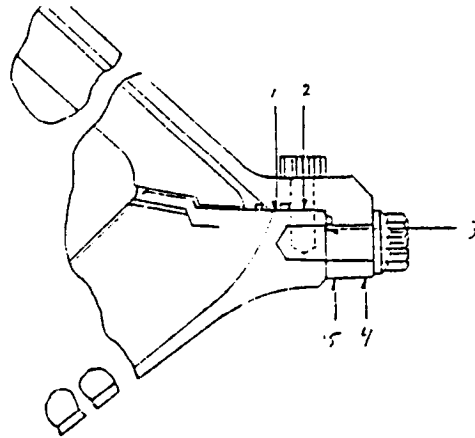
Deflection Location	Gage Number	Circumferential Location (deg)	Gap Opening (in.)	
			TPTA 1.1	NJES-2B*
Forward of Primary	D249	14.4	0.009	0.008
	D250	46.8	0.008	0.007
	D251	104.4	0.008	ND
	D252	136.8	0.008	0.007
	D253	194.4	0.008	0.007
	D254	226.8	0.008	0.007
	D255	284.4	0.008	0.008
	D256	316.8	0.008	0.007
		Average	0.008	0.007
Inter-O-ring	D241	7.2	0.004	0.002
	D242	39.6	0.004	0.003
	D243	97.2	0.004	0.002
	D244	129.6	0.004	0.003
	D245	187.2	0.003	0.003
	D246	219.6	0.004	0.003
	D247	277.2	0.003	0.003
	D248	309.6	0.004	0.002
		Average	0.004	0.003

*NJES-2B had modified HPM hardware

Note: ND = No data

Table 7.2-18. TPTA 1.1 Joint D Maximum Gap Summary

TEST NAME: TPTA 1.1
 JOINT: D
 DESCRIPTION: DISPLACEMENT SUMMARY
 MODEL PRESSURE 913.3 PSIA
 MAXIMUM PRESSURE: 909.7 PSIA
 DESIRED PRESSURE: 913.3 PSIA
 TIME PRESSURE OCCURRED: 0.6 SECONDS



LOCAT	FROM STATION	TO STATION	GAGE NUMBER	ANGULAR LOCATION	DEFLECTION (IN)	
1	1873.3		D0249	14.4	-0.009	OPEN
1	1873.3		D0250	46.8	-0.008	OPEN
1	1873.3		D0251	104.4	-0.008	OPEN
1	1873.3		D0252	136.8	-0.008	OPEN
1	1873.3		D0253	194.4	-0.008	OPEN
1	1873.3		D0254	226.8	-0.008	OPEN
1	1873.3		D0255	284.4	-0.008	OPEN
1	1873.3		D0256	316.8	-0.008	OPEN
2	1874.3		D0241	7.2	-0.004	OPEN
2	1874.3		D0242	39.6	-0.004	OPEN
2	1874.3		D0243	97.2	-0.004	OPEN
2	1874.3		D0244	129.6	-0.004	OPEN
2	1874.3		D0245	187.2	-0.003	OPEN
2	1874.3		D0246	219.6	-0.004	OPEN
2	1874.3		D0247	277.2	-0.003	OPEN
2	1874.3		D0248	309.6	-0.004	OPEN
3	1875.2		D0257	317.0	-0.003	OPEN
3	1875.2		D0258	59.0	-0.003	OPEN
3	1875.2		D0259	117.0	-0.003	OPEN
3	1875.2		D0260	219.0	0.000	OPEN
3	1875.2		D0261	319.0	-0.003	OPEN
3	1875.2		D0262	61.0	-0.004	OPEN
3	1875.2		D0263	119.0	-0.003	OPEN
3	1875.2		D0264	221.0	-0.004	OPEN
4	1876.6		D0317	7.2	0.000	CLOSE
4	1876.6		D0318	46.8	0.000	CLOSE
4	1876.6		D0319	97.2	0.000	CLOSE
4	1876.6		D0320	136.8	0.000	CLOSE
4	1876.6		D0321	187.2	0.000	CLOSE
4	1876.6		D0322	226.8	0.000	CLOSE
4	1876.6		D0323	277.2	0.000	CLOSE
4	1876.6		D0324	316.8	0.000	OPEN
5	1875.4		D0265	7.2	0.000	CLOSE
5	1875.4		D0266	46.8	0.000	OPEN
5	1875.4		D0267	97.2	0.000	CLOSE
5	1875.4		D0268	136.8	0.000	CLOSE
5	1875.4		D0269	187.2	0.000	CLOSE
5	1875.4		D0270	226.8	0.000	CLOSE
5	1875.4		D0271	277.2	0.000	CLOSE
5	1875.4		D0272	316.8	0.000	CLOSE

7.2.3.4.3.2 TPTA 1.1A test joint deflections

Joint A Deflections (TPTA 1.1A)

The effect of strut loads on gap deflection at Joint A is, at worst, almost undiscernible. Absolute gap deflections due to internal pressure and strut loads range from 0.002 in. open to 0.007 in. open forward of the primary O-ring, 0.002 in. open to 0.005 in. open between the primary and secondary O-rings, and 0.002 in. open at the CF O-ring. The LVDTs maintain a steady deflection value due to internal pressure until 12.0 sec when the strut loads are applied and most gages respond with a small glitch of approximately 0.0003 in. maximum peak-to-peak (Figures 7.2-15 through 7.2-17). The maximum values of gap deflection at Joint A (due to internal pressure and strut loads) and the peak-to-peak gap deflection response (due to strut loads) are summarized in Table 7.2-19. These values are taken in the time span from 8.0 to 20.0 sec.

Joint B Deflections (TPTA 1.1A)

Joint B gap opening response due to strut loads is similar to that of Joint A. Gap openings range from 0.001 in. open to 0.005 in. open forward of the primary O-ring, 0.001 in. open to 0.004 in. open between the primary and secondary O-rings, and 0.003 in. open to 0.003 in. close at the CF O-ring. As in TPTA 1.1, it appears that some of the proximity gages may have been improperly zeroed, judging by the relatively large range of values due to pressure loads. However, the peak-to-peak deflections due to strut loads are, nevertheless, well within the expected range. As at Joint A, most LVDTs maintain a steady deflection value due to internal pressure until 12.0 sec when the strut loads are applied and most gages respond with a small glitch of approximately 0.0003 in. maximum peak-to-peak (Figures 7.2-18 through 7.2-20). The maximum values of gap deflection at Joint B (due to internal pressure and strut loads) and the peak-to-peak gap deflection response (due to strut loads) are summarized in Table 7.2-20. These values are taken in the time span from 8.0 to 20.0 sec.

TPTA1.1A MAX-Q FINAL(REVISED)
D0143(ST=1169.15, 63 DEG) D0079(ST=1169.15, 121 DEG)
D0080(ST=1169.15, 183 DEG) D0144(ST=1169.15, 223 DEG)
24 NOVEMBER 1987

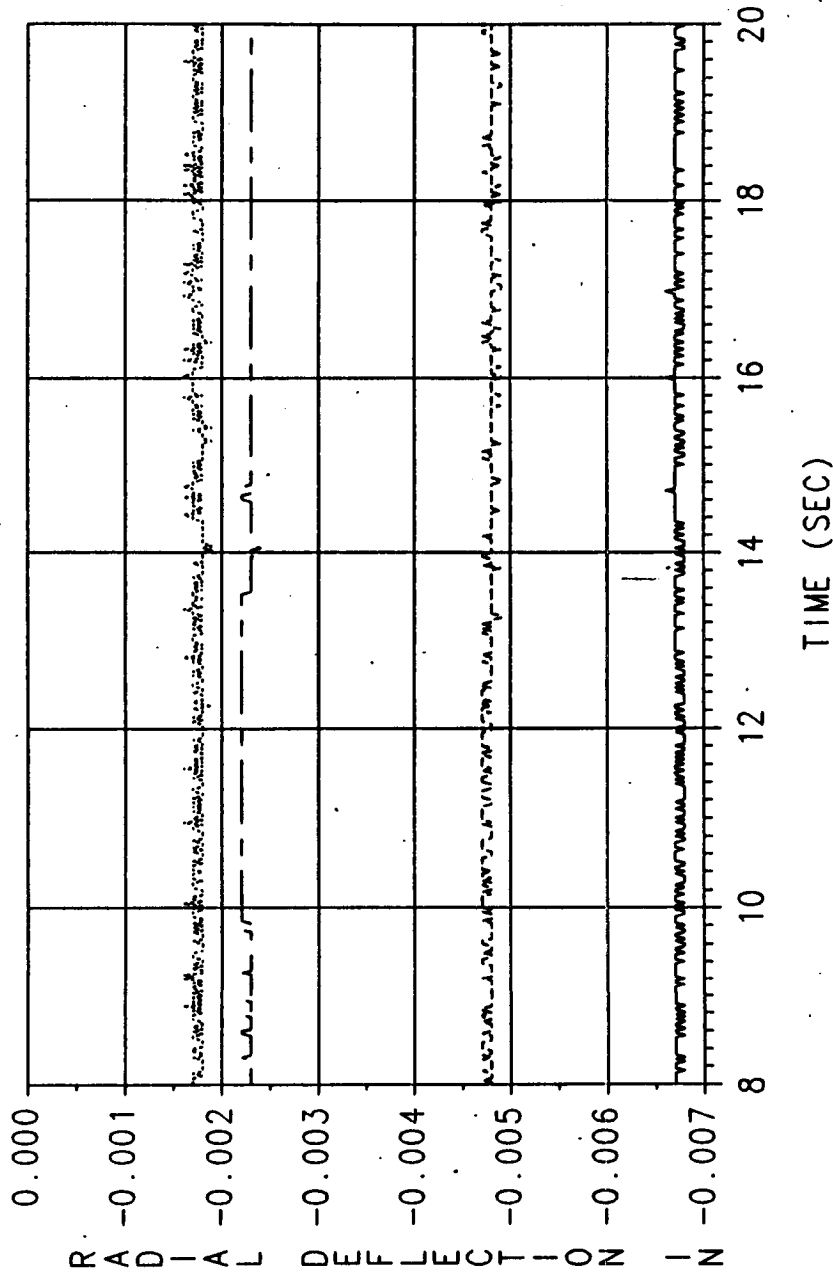


Figure 7.2-15. TPTA 1.1A Joint A Gap Deflection at Primary 0-ring (8-20 sec)

TPTA1.1A MAX-Q FINAL(REVISED)
D0145(ST=1169.77, 57 DEG) D0082(ST=1169.77, 115 DEG)
D0083(ST=1169.77, 177 DEG) D0146(ST=1169.77, 201 DEG)
24 NOVEMBER 1987

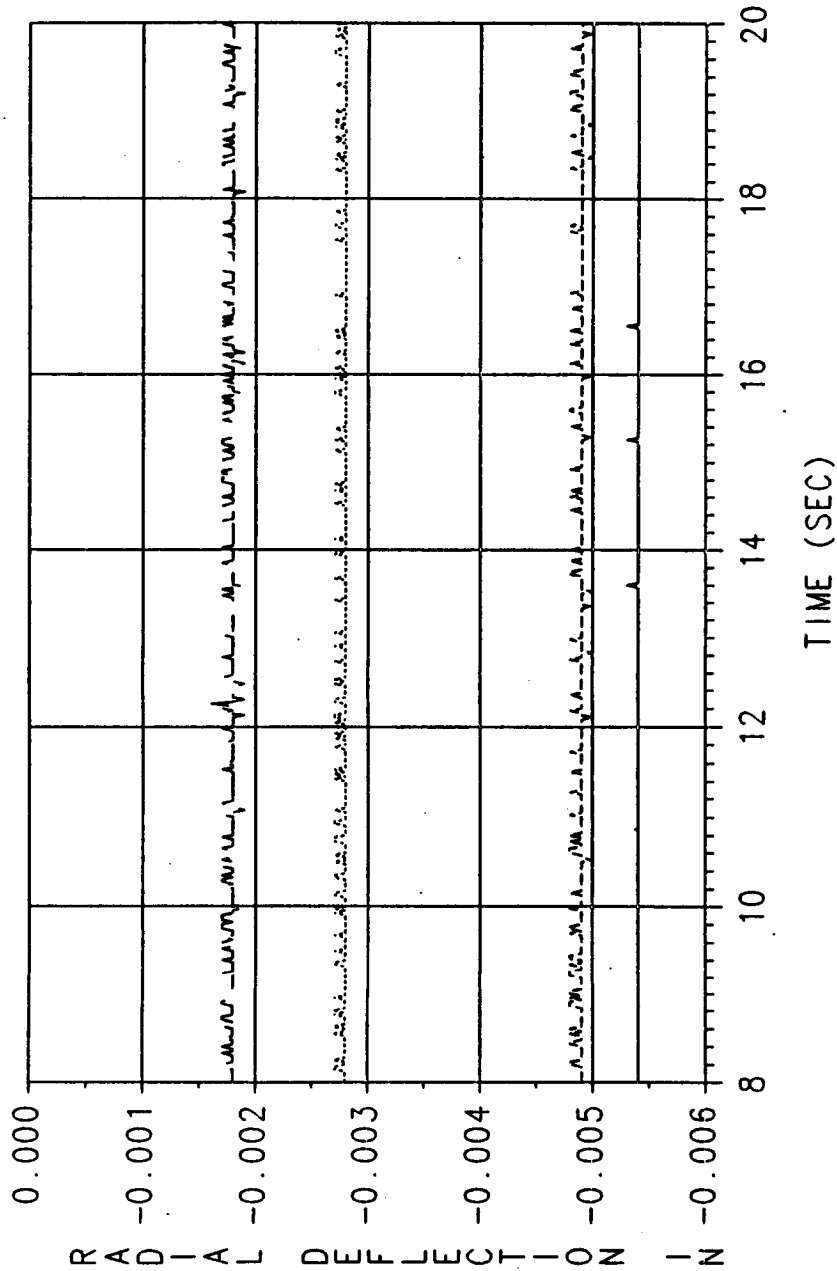


Figure 7.2-16. TPTA 1.1A Joint A Gap Deflection at Primary/Secondary 0-rings (8-20 sec)

TPTA1.1A MAX-Q FINAL(REVISED)
D0141(ST=1169.57, 60 DEG) D0126(ST=1169.57, 180 DEG)
D0142(ST=1169.57, 220 DEG) D0127(ST=1169.57, 320 DEG)
24 NOVEMBER 1987

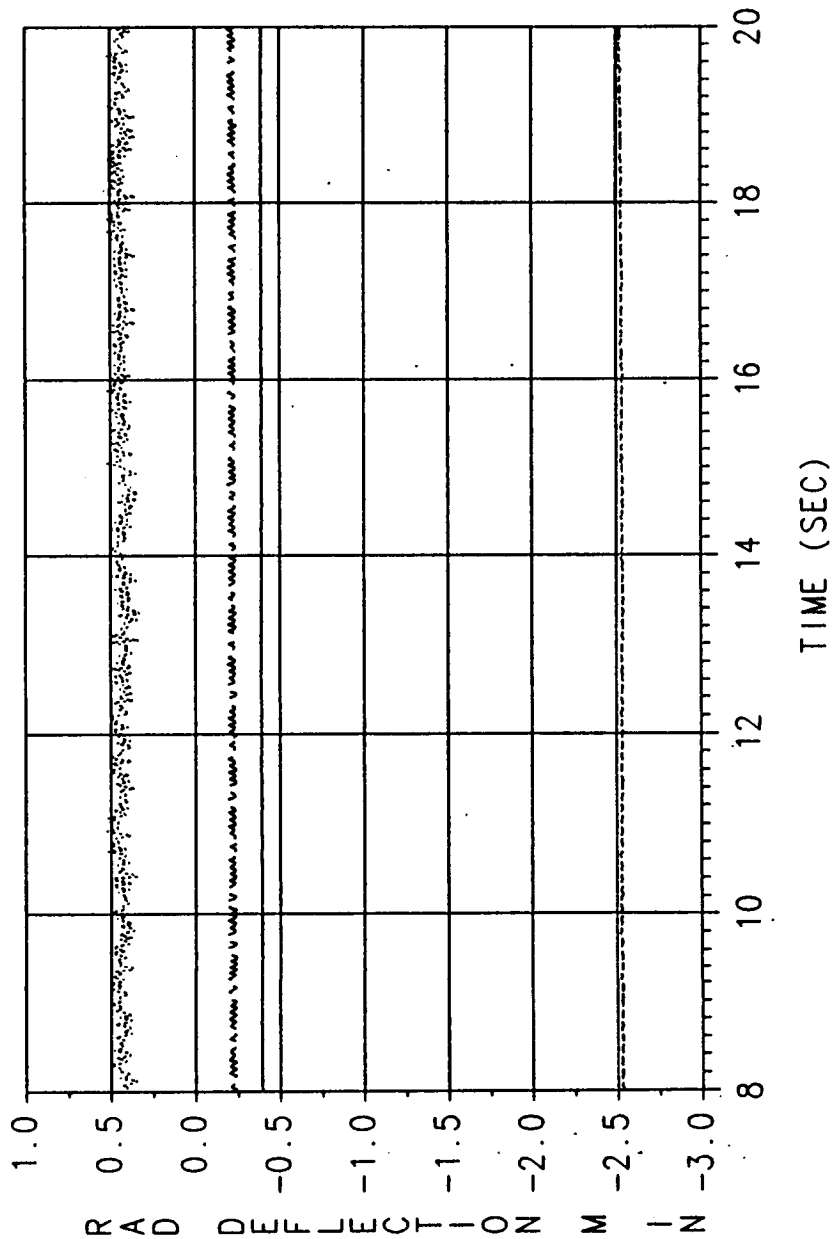
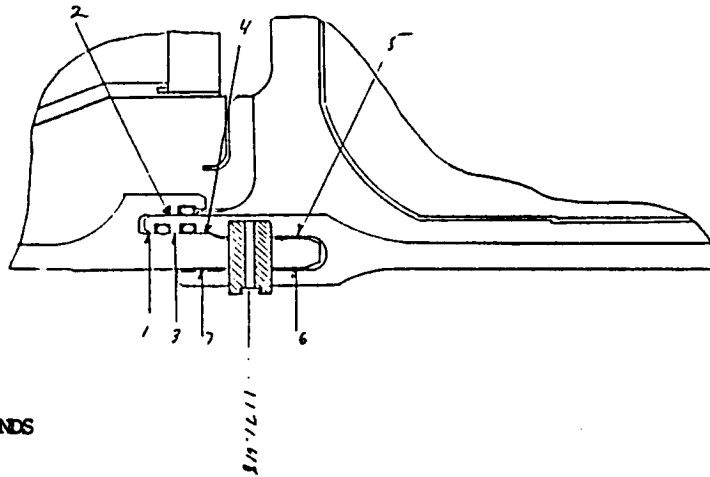


Figure 7.2-17. TPTA 1.1A Joint A Gap Deflection at CF O-ring (8-20 sec)

Table 7.2-19. TPTA 1.1 Joint A Maximum Gap Summary



TEST NAME: TPTA 1.1A
 JOINT: A
 DESCRIPTION: DISPLACEMENT SUMMARY
 MODEL PRESSURE
 THE TIME RANGE IS 9.0 TO 14.0 SECONDS

LOCAT	FROM STATION	TO STATION	GAGE NUMBER	ANGULAR LOCATION	DEFLECTION (IN)
1	1169.2		D0143	63.0	-0.005 OPEN
1	1169.2		D0079	121.0	-0.007 OPEN
1	1169.2		D0080	183.0	-0.002 OPEN
1	1169.2		D0144	223.0	-0.002 OPEN
1	1169.2		D0081	323.0	-0.005 OPEN
2	1169.6		D0141	60.0	-0.002 OPEN
2	1169.6		D0125	118.0	ND
2	1169.6		D0126	180.0	-0.000 OPEN
2	1169.6		D0142	220.0	-0.000 OPEN
2	1169.6		D0127	320.0	0.000 CLOSE
3	1169.8		D0145	57.0	-0.005 OPEN
3	1169.8		D0082	115.0	-0.005 OPEN
3	1169.8		D0083	177.0	-0.003 OPEN
3	1169.8		D0146	201.0	-0.002 OPEN
3	1169.8		D0147	217.0	-0.002 OPEN
3	1169.8		D0084	317.0	-0.003 OPEN
4	1170.4		D0150	59.0	0.001 CLOSE
4	1170.4		D0092	117.0	0.006 CLOSE
4	1170.4		D0151	219.0	0.004 CLOSE
4	1170.4		D0093	319.0	0.001 CLOSE
5	1172.7		D0152	61.0	0.003 CLOSE
5	1172.7		D0090	119.0	0.003 CLOSE
5	1172.7		D0153	221.0	0.003 CLOSE
5	1172.7		D0091	321.0	0.003 CLOSE
6	1172.7		D0154	59.0	-0.003 OPEN
6	1172.7		D0096	117.0	-0.006 OPEN
6	1172.7		D0155	219.0	-0.004 OPEN
6	1172.7		D0097	319.0	-0.003 OPEN
7	1170.4		D0156	61.0	0.003 CLOSE
7	1170.4		D0094	119.0	0.006 CLOSE
7	1170.4		D0157	221.0	0.005 CLOSE
7	1170.4		D0095	321.0	0.003 CLOSE

ND = No data

TPTA1.1A MAX-Q FINAL(REVISED)
D0166(ST=1489.15, 223 DEG) D0167(ST=1489.15, 243 DEG)
D0168(ST=1489.15, 269 DEG) D0117(ST=1489.15, 323 DEG)
24 NOVEMBER 1987

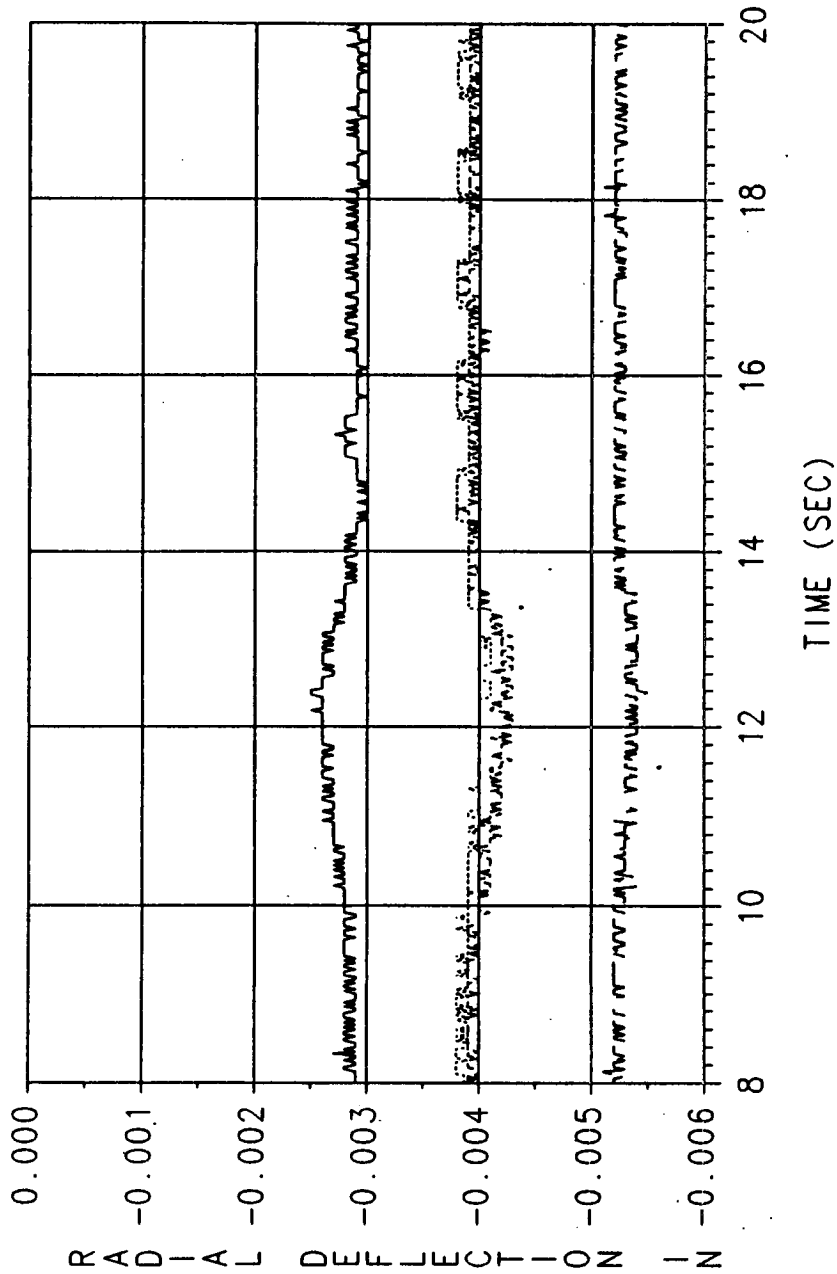


Figure 7.2-18. TPTA 1.1A Joint B Gap Deflection at Primary O-ring (8-20 sec)

TPTA1.1A MAX-Q FINAL(REVISED)
D0113(ST=1489.77, 177 DEG) D0351(ST=1489.77, 201 DEG)
D0171(ST=1489.77, 217 DEG) D0172(ST=1489.77, 237 DEG)
24 NOVEMBER 1987

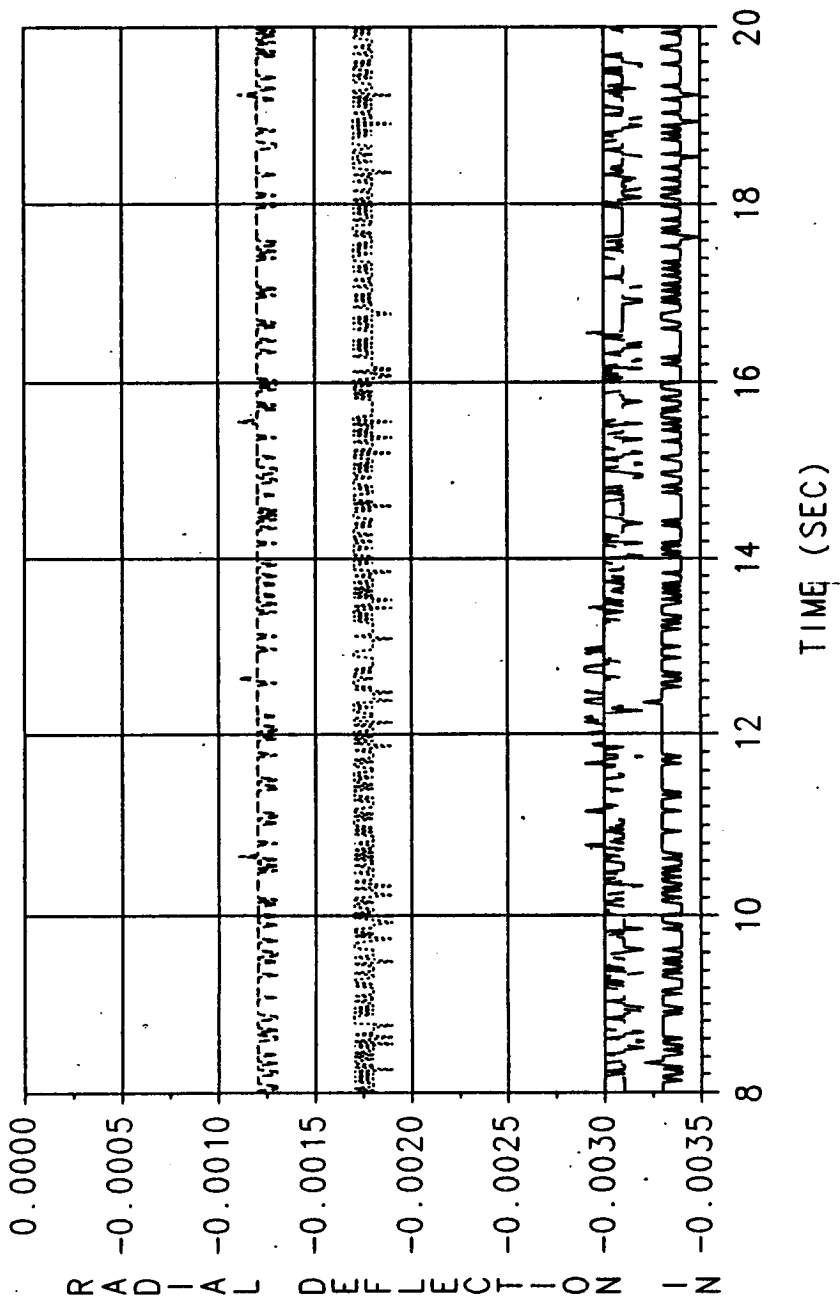
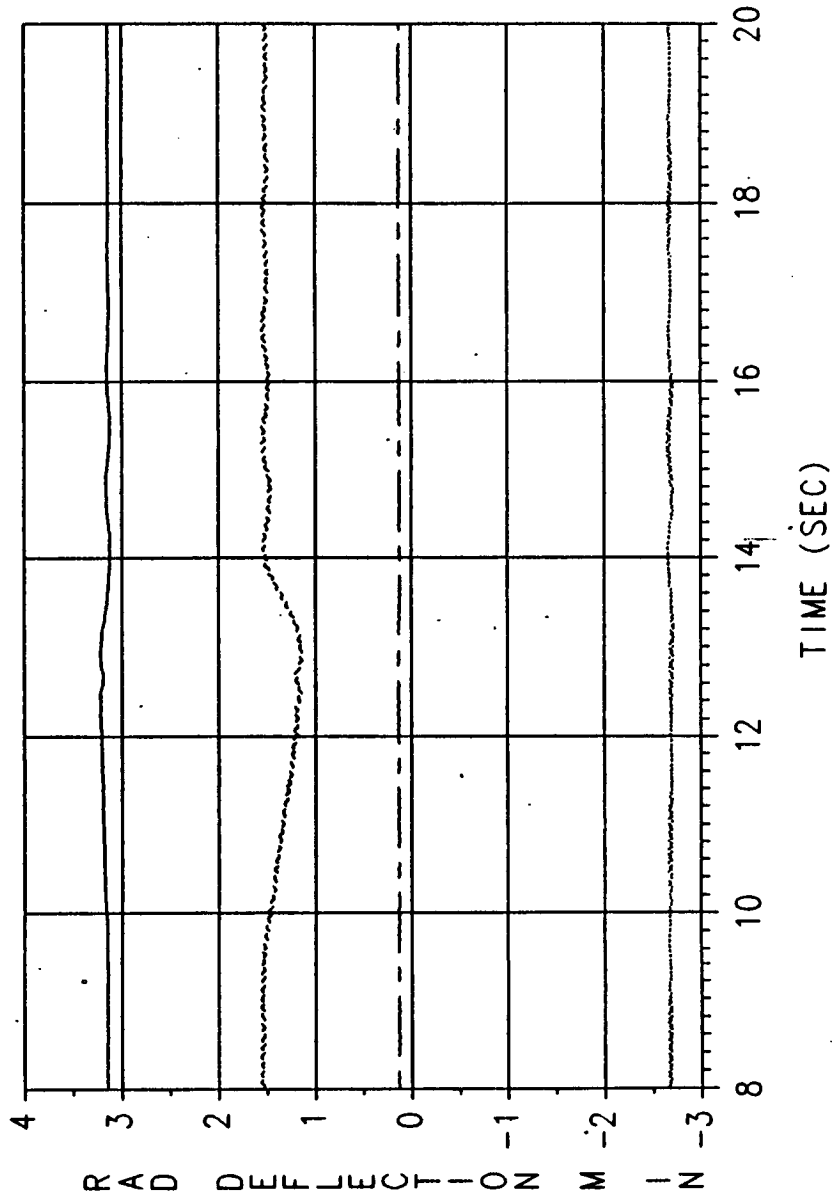


Figure 7.2-19. TPTA 1.1A Joint B Gap Deflection at Primary/Secondary O-rings (8-20 sec)

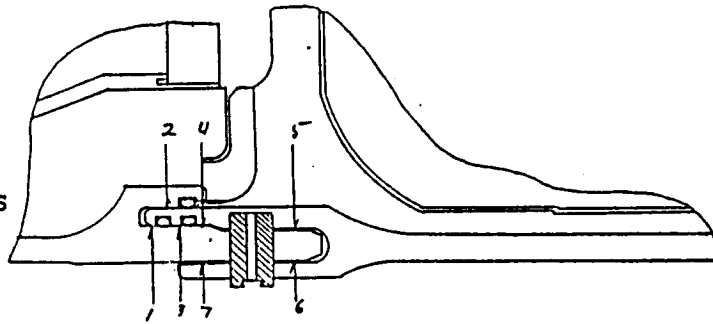
TPTA1.1A MAX-Q FINAL(REVISED)
D0158(ST=1489.57, 0 DEG) D0159(ST=1489.57, 60 DEG)
D0128(ST=1489.57, 118 DEG) D0129(ST=1489.57, 180 DEG)
24 NOVEMBER 1987



—— D0128 D0129 - - - - D0158 - - - - D0159
Figure 7.2-20. TPTA 1.1A Joint B Gap Deflection at CF 0-ring (8-20 sec)

Table 7.2-20. TPTA 1.1 Joint B Maximum Gap Summary

TEST NAME: TPTA 1.1A
 JOINT: B
 DESCRIPTION: DEFLECTION SUMMARY
 MODEL PRESSURE
 THE TIME RANGE IS 9.0 TO 14.0 SECONDS



LOCAT	FROM STATION	TO STATION	GAGE NUMBER	ANGULAR LOCATION	DEFLECTION (IN)
1	1489.2		D0163	3.0	-0.002 OPEN
1	1489.2		D0164	63.0	-0.001 OPEN
1	1489.2		D0165	121.0	-0.004 OPEN
1	1489.2		D0118	183.0	ND
1	1489.2		D0166	223.0	-0.004 OPEN
1	1489.2		D0167	243.0	-0.004 OPEN
1	1489.2		D0168	269.0	-0.005 OPEN
1	1489.2		D0117	323.0	-0.003 OPEN
2	1489.2		D0158	0.0	0.002 CLOSE
2	1489.2		D0159	60.0	0.000 CLOSE
2	1489.2		D0128	118.0	0.003 CLOSE
2	1489.2		D0129	180.0	-0.003 OPEN
2	1489.2		D0160	220.0	-0.003 OPEN
2	1489.2		D0161	240.0	0.001 CLOSE
2	1489.2		D0162	266.0	-0.002 OPEN
2	1489.2		D0130	320.0	0.000 CLOSE
3	1489.8		D0333	25.0	-0.001 OPEN
3	1489.8		D0169	57.0	-0.003 OPEN
3	1489.8		D0112	115.0	-0.002 OPEN
3	1489.8		D0334	139.0	-0.002 OPEN
3	1489.8		D0113	177.0	-0.003 OPEN
3	1489.8		D0351	201.0	-0.003 OPEN
3	1489.8		D0171	217.0	-0.002 OPEN
3	1489.8		D0172	237.0	-0.001 OPEN
3	1489.8		D0173	263.0	-0.003 OPEN
3	1489.8		D0335	287.0	-0.004 OPEN
3	1489.8		D0336	307.0	-0.003 OPEN
3	1489.8		D0114	317.0	-0.003 OPEN
3	1489.8		D0174	357.0	-0.002 OPEN
4	1490.4		D0176	59.0	0.002 CLOSE
4	1490.4		D0104	117.0	0.010 CLOSE
4	1490.4		D0017	179.0	0.002 CLOSE
4	1490.4		D0177	219.0	0.002 CLOSE
4	1490.4		D0178	239.0	0.010 CLOSE
4	1490.4		D0179	265.0	0.005 CLOSE
4	1490.4		D0105	319.0	0.004 CLOSE
4	1490.4		D0175	359.0	0.008 CLOSE
5	1492.7		D0180	1.0	0.002 CLOSE
5	1492.7		D0181	61.0	0.002 CLOSE
5	1492.7		D0102	119.0	0.003 CLOSE
5	1492.7		D0018	181.0	0.002 CLOSE
5	1492.7		D0182	221.0	0.002 CLOSE
5	1492.7		D0183	241.0	0.003 CLOSE
5	1492.7		D0184	267.0	0.003 CLOSE
5	1492.7		D0103	321.0	0.003 CLOSE
6	1492.7		D0186	59.0	-0.004 OPEN
6	1492.7		D0108	117.0	-0.011 OPEN
6	1492.7		D0019	179.0	-0.006 OPEN
6	1492.7		D0187	219.0	-0.011 OPEN
6	1492.7		D0188	239.0	-0.013 OPEN
6	1492.7		D0189	265.0	-0.011 OPEN
6	1492.7		D0109	319.0	-0.008 OPEN
6	1492.7		D0185	359.0	-0.007 OPEN
7	1490.4		D0190	1.0	0.005 CLOSE
7	1490.4		D0191	61.0	0.004 CLOSE
7	1490.4		D0106	119.0	0.005 CLOSE
7	1490.4		D0020	181.0	0.003 CLOSE
7	1490.4		D0192	221.0	0.002 CLOSE
7	1490.4		D0193	241.0	0.005 CLOSE
7	1490.4		D0194	267.0	0.004 CLOSE
7	1490.4		D0107	321.0	0.003 CLOSE

ND = No data

ORIGINAL PAGE IS
 OF POOR QUALITY

Joint D Deflections (TPTA 1.1A)

Maximum Joint D deflections were lower during the TPTA 1.1A test when compared to the TPTA 1.1 test. This is due to a lower chamber pressure.

Maximum deflections of Joint D are listed in Table 7.2-21. The maximum inter-O-ring gap opening was 0.002 inch.

7.2.3.4.4 Axial Growth. The axial growth of the two test joints, or relative movement of the tang and clevis in the axial direction, was measured at three equally-spaced locations around each joint. The maximum average axial growth recorded for Joints A and B during the TPTA 1.1 test was 0.026 and 0.043 in., respectively. Analysis predicted 0.034 in. for Joint A and 0.010 for Joint B. Table 7.2-22 lists all maximum axial growth measurements recorded from the TPTA 1.1 test. Maximum axial growth recorded for TPTA 1.1A test is listed in Table 7.2-23. The maximum average axial growth recorded for Joints A and B during the TPTA 1.1A test was 0.025 and 0.019 in., respectively. Table 7.2-24 demonstrates that the axial growth of Joints A and B in the TPTA 1.1 test were higher than in the JES-3A test. Effects of the 1,000-kips axial load on the axial growth were insignificant.

7.2.3.4.5 Radial Growth. Girth gages were placed around test Joints A and B to measure the radial growth of the joint. All girth gages were placed on the exterior of the joint. The girth gages measure average hoop strain, which is then converted to radial growth by the equation:

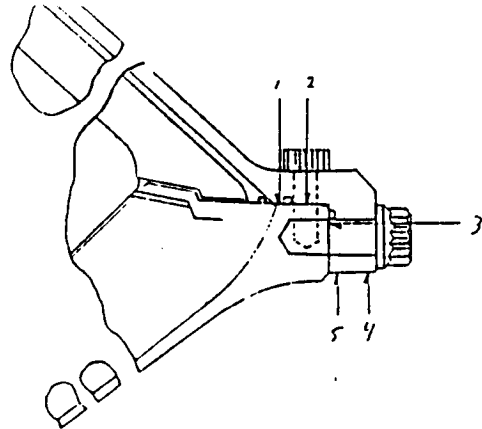
$$\Delta r = \epsilon R_o$$

where ϵ is the girth strain and R_o is the case radius. The 1,000-kips axial load did not induce significant effects on the radial growth.

7.2.3.4.5.1 Joint A radial growth (TPTA 1.1). Girth gages on and around Joint A indicate that maximum peak-to-peak radial growth of the joint due to the ignition pressure rise was consistently in the range of 0.150 to 0.196 inch. Table 7.2-25 shows the girth gage measurements for test Joint A. On the majority of the gages, the initial strain response is a positive (radially inward) spike followed by a negative (radially outward) response, at which time the gage settles. Typical gage data (D035, D036, D038 and D039) are shown in Figures 7.2-21 and 7.2-22.

Table 7.2-21. TPTA 1.1 Joint D Maximum Gap Summary

TEST NAME: TPTA 1.1A
 JOINT: D
 DESCRIPTION: DISPLACEMENT SUMMARY
 MODEL PRESSURE
 THE TIME RANGE IS 9.0 TO 14.0 SECONDS



LOCAT	FROM STATION	TO STATION	GAGE NUMBER	ANGULAR LOCATION	DEFLECTION (IN)	
1	1873.3		D0249	14.4	-0.004	OPEN
1	1873.3		D0250	46.8	-0.004	OPEN
1	1873.3		D0251	104.4	-0.004	OPEN
1	1873.3		D0252	136.8	-0.004	OPEN
1	1873.3		D0253	194.4	-0.004	OPEN
1	1873.3		D0254	226.8	-0.004	OPEN
1	1873.3		D0255	284.4	-0.004	OPEN
1	1873.3		D0256	316.8	-0.004	OPEN
2	1874.3		D0241	7.2	-0.001	OPEN
2	1874.3		D0242	39.6	-0.001	OPEN
2	1874.3		D0243	97.2	-0.002	OPEN
2	1874.3		D0244	129.6	-0.001	OPEN
2	1874.3		D0245	187.2	-0.001	OPEN
2	1874.3		D0246	219.6	-0.001	OPEN
2	1874.3		D0247	277.2	-0.001	OPEN
2	1874.3		D0248	309.6	-0.001	OPEN
3	1875.2		D0257	317.0	-0.001	OPEN
3	1875.2		D0258	59.0	-0.001	OPEN
3	1875.2		D0259	117.0	-0.001	OPEN
3	1875.2		D0260	219.0	0.000	CLOSE
3	1875.2		D0261	319.0	0.000	OPEN
3	1875.2		D0262	61.0	-0.001	OPEN
3	1875.2		D0263	119.0	-0.001	OPEN
3	1875.2		D0264	221.0	-0.001	OPEN
4	1876.6		D0317	7.2	0.000	CLOSE
4	1876.6		D0318	46.8	0.000	CLOSE
4	1876.6		D0319	97.2	0.000	CLOSE
4	1876.6		D0320	136.8	0.000	CLOSE
4	1876.6		D0321	187.2	0.000	CLOSE
4	1876.6		D0322	226.8	0.000	CLOSE
4	1876.6		D0323	277.2	0.000	CLOSE
4	1876.6		D0324	316.8	ND	OPEN
5	1875.4		D0265	7.2	0.000	CLOSE
5	1875.4		D0266	46.8	0.000	CLOSE
5	1875.4		D0267	97.2	0.000	CLOSE
5	1875.4		D0268	136.8	0.000	CLOSE
5	1875.4		D0269	187.2	0.000	CLOSE
5	1875.4		D0270	226.8	0.000	CLOSE
5	1875.4		D0271	277.2	0.000	CLOSE
5	1875.4		D0272	316.8	0.000	CLOSE

ND = No data

Table 7.2-22. TPTA 1.1 Maximum Axial Growth
in Joints A and B

<u>Axial Deflection Joint</u>	<u>Station</u>	<u>Gage Number</u>	<u>Circumferential Location (deg)</u>	<u>Axial Deflection (in.)</u>	<u>Average (in.)</u>
A	1169.8	D0145	60.0	ND	0.026
	1169.8	D0098	118.0	0.029	
	1169.8	D0149	220.0	0.022	
	1169.8	D0099	320.0	ND	
B	1489.8	D0195	0.0	ND	0.043
	1489.8	D0196	60.0	ND	
	1489.8	D0119	118.0	0.054	
	1489.8	D0029	180.0	ND	
	1489.8	D0197	220.0	ND	
	1489.8	D0198	240.0	0.032	
	1489.8	D0199	260.0	ND	
	1489.8	D0120	320.0	ND	

 ND = No data

Table 7.2-23. TPTA 1.1A Maximum Axial Growth in Joints A and B

<u>Axial Deflection Joint</u>	<u>Station</u>	<u>Gage Number</u>	<u>Circumferential Location (deg)</u>	<u>Axial Deflection (in.)</u>	<u>Average</u>
A	1169.8	D0148	60.0	ND	0.025
	1169.8	D0098	118.0	0.027	
	1169.8	D0149	220.0	0.022	
	1169.8	D0099	320.0	ND	
B	1489.8	S0195	0.0	ND	0.019
	1489.8	D0196	60.0	ND	
	1489.8	D0119	118.0	0.011	
	1489.8	D0029	180.0	ND	
	1489.8	D0197	220.0	ND	
	1489.8	D0198	240.0	0.027	
	1489.8	D0199	260.0	ND	
	1489.8	D0120	320.0	ND	

ND = no data

Table 7.2-24. Comparison of Maximum Axial Growth
in Joints A and B of TPTA 1.1 Test With JES-3A Test

Test Joint	Station	Gage Number	Circumferential Location (deg)	Axial Deflection (in.)	
				TPTA 1.1	JES-3A
A	1169.8	D0148	60.0	ND	NA
	1169.8	D0098	118.0	0.029	NA
	1169.8	D0149	220.0	0.022	NA
	1169.8	D0099	320.0	ND	0.022
	Average:			0.026	0.022
B	1489.8	D0195	0.0	ND	NA
	1489.8	D0196	60.0	ND	NA
	1489.8	D0119	118.0	0.054	0.024
	1489.8	D0029	180.0	ND	0.024
	1489.8	D0197	220.0	ND	NA
	1489.8	D0198	240.0	0.032	NA
	1489.8	D0199	260.0	ND	NA
	1489.8	D0120	320.0	ND	0.024
Average:				0.043	0.024

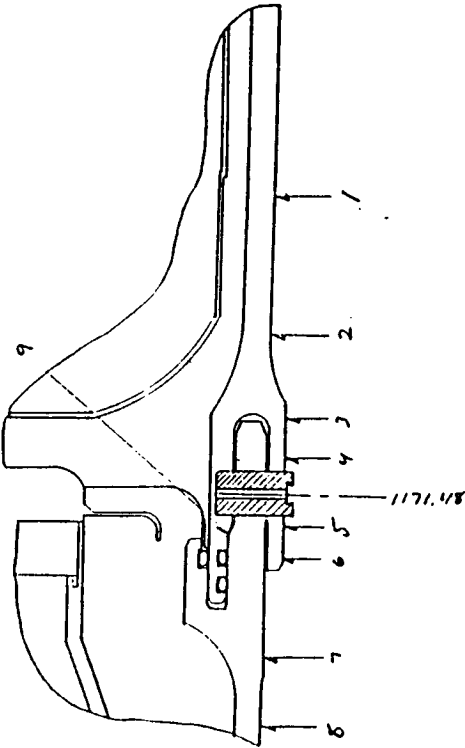
All JES-3A data is normalized with TPTA 1.1 chamber pressure

NA = Not applicable

ND = No data

Table 7.2-25. TPTA 1.1 Joint A Radial Growth

TEST NAME: TPTA 1.1
JOINT: A
DESCRIPTION: GIRTH GAGE SUMMARY
MODEL PRESSURE 913.3 PSIA
MAXIMUM PRESSURE: 909.7 PSIA
DESIRED PRESSURE: 913.3 PSIA
TIME PRESSURE OCCURED: 0.6 SECONDS



GIRTH GAGE LOCATION	GAGE NUMBER	STATION	RADIUS (IN)	RADIAL GROWTH (IN)	TEST STRAIN (UTN/IN)
1	D0039	1172.3	73.1	-0.196	-2680
2	D0038	1175.0	73.1	-0.175	-2392
3	D0037	1173.2	73.4	-0.168	-2282
4	D0066	1172.3	73.4	-0.162	-2209
5	D0065	1170.8	73.4	-0.152	-2067
6	D0036	1170.1	73.4	-0.150	-2048
7	D0035	1168.0	73.1	-0.168	-2304
8	D0034	1166.8	73.1	-0.178	-2441
9	D0089	1170.6	72.3	ND	ND

ND = No data
(-) = Growth

TPTA 1.1 FINAL

D0032(STAT=1251.48) D0034(STAT=1166.78)

D0035(STAT=1168.03) D0036(STAT=1170.07)

19 NOVEMBER 1987

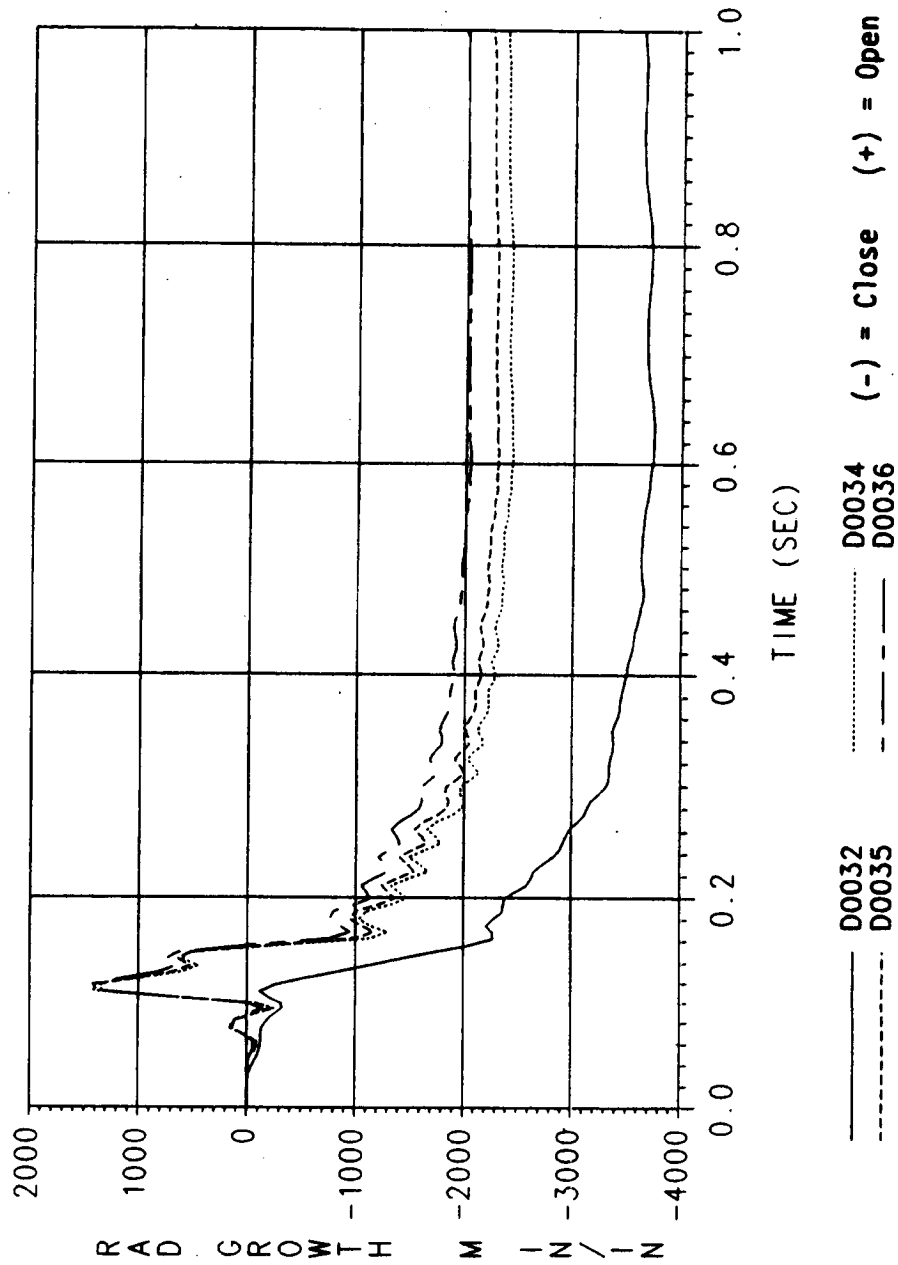


Figure 7.2-21. TPTA 1.1 Joint A Girth Gages (0-1 sec)

TPTA 1.1 FINAL
D0037(STAT=1173.16) D0038(STAT=1175.03)
D0039(STAT=1177.28) D0043(STAT=1493.16)
19 NOVEMBER 1987

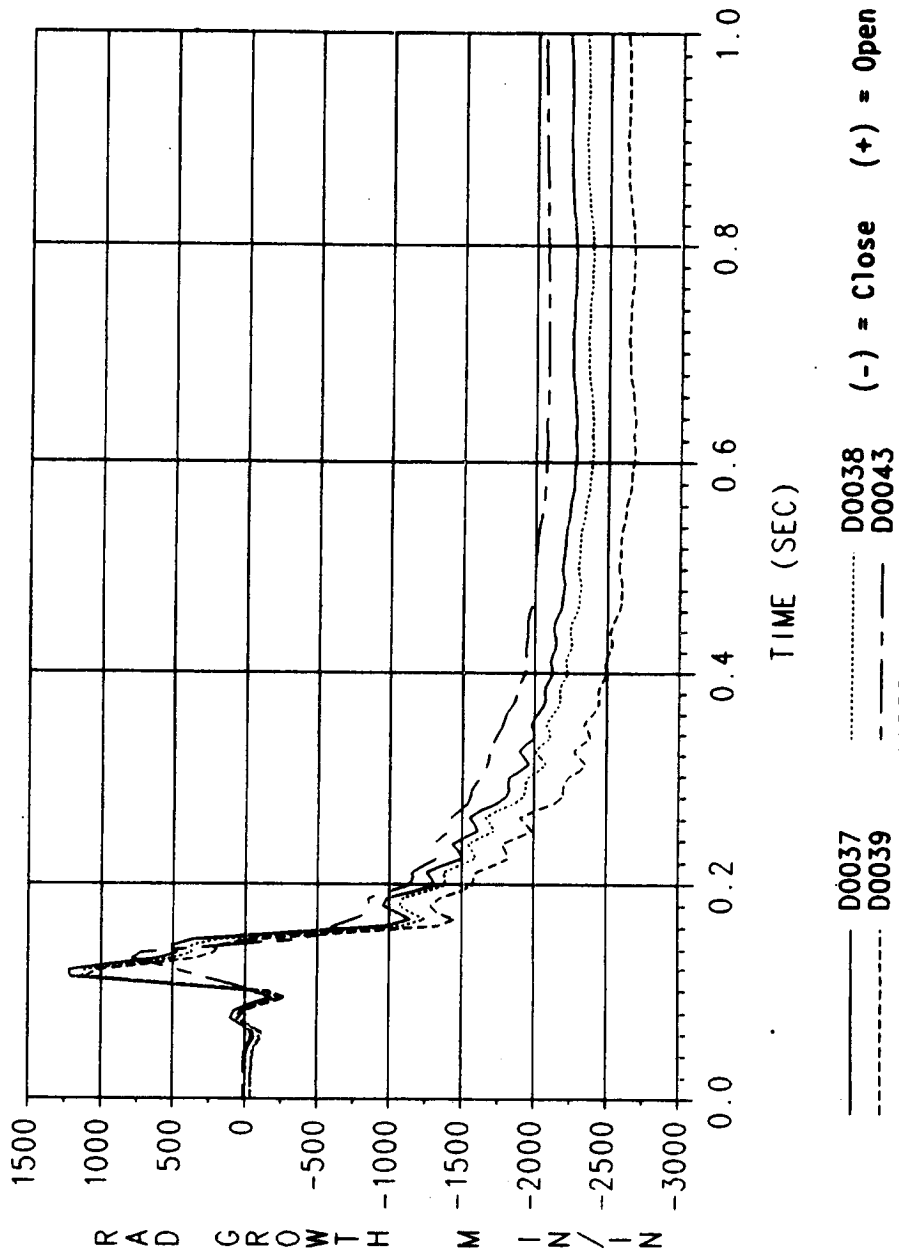


Figure 7.2-22. TPTA 1.1 Joint A Girth Gages (0-30 sec)

7.2.3.4.5.2 Joint B radial growth (TPTA 1.1). As seen in Table 7.2-26, girth gages in Joint B show a radial growth ranging from 0.146 to 0.178 inch. The Joint B girth gages indicated similar radial growth as those of Joint A with respect to time. Table 7.2-27 compares girth gage radial growths of Joints A and B with those of the JES-3A test. With all measurements normalized to the TPTA 1.1 test pressure, the radial growth of the tang is slightly lower on the TPTA 1.1 test than on the JES-3A test. Data from typical gages D044, D045, D067 and D068 are illustrated in Figures 7.2-23 and 7.2-24.

7.2.3.4.5.3 Joint D radial growth (TPTA 1.1). Joint D had a radial growth varying from 0.029 in. to 0.169 inch. Radial growth measurements are listed in Table 7.2-28. Table 7.2-29 compares data from the TPTA 1.1 and NJES-2B tests. There was no significant difference in the data obtained from these two tests.

7.2.3.4.5.4 Joints A, B, and D radial growth (TPTA 1.1A). Radial growth measurements for the TPTA 1.1A test are listed in Table 7.2-30 for Joint A, Table 7.2-31 for Joint B, and Table 7.2-32 for Joint D. All measurements were within the expected range. Typical radial growths for Joints A and B are shown in Figures 7.2-25 and 7.2-26.

7.2.3.4.6 Strain Gages

Joint A Tang Area Strains

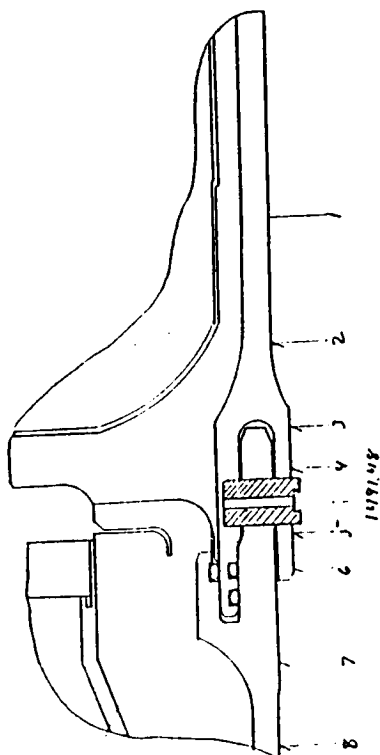
Several hoop and axial strain gages on the inside of Joint A were placed on the CF hook under the insulation. Tables 7.2-33 and 7.2-34 display the hoop and axial strains recorded, as well as hoop and axial stress for the TPTA 1.1 and 1.1A tests, respectively. At three different locations on Joint A, hoop and axial strain gages were mounted to measure strain on the tang just above the outer clevis leg.

Joint A Outer Clevis Strains

Hoop and axial strain gages were placed on the outer clevis leg around several pinholes on Joint A. Tables 7.2-35 and 7.2-36 display the hoop and

Table 7.2-26. TPTA 1.1 Joint B Radial Growth

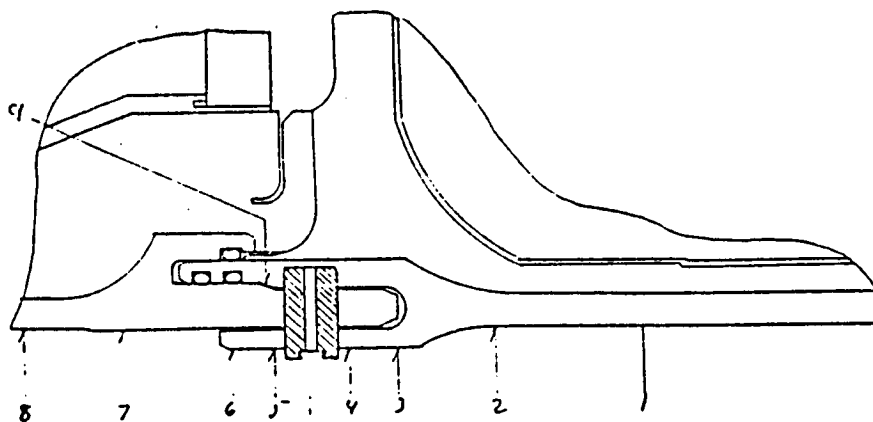
TEST NAME: TPTA 1.1
JOINT: B
DESCRIPTION: GIRTH GAGE SUMMARY
MODEL PRESSURE 913.3 PSIA
MAXIMUM PRESSURE: 909.7 PSIA
DESIRED PRESSURE: 913.3 PSIA
TIME PRESSURE OCCURRED: 0.6 SECONDS



GIRTH GAGE LOCATION	GAGE NUMBER	STATION	RADIUS (IN)	RADIAL GROWTH (IN)	TEST STRAIN (UIN/IN)
1	D0045	1497.3	73.1	-0.159	-2180
2	D0044	1495.0	73.1	-0.155	-2117
3	D0043	1493.2	73.4	-0.152	-2076
4	D0068	1492.2	73.4	-0.150	-2048
5	D0067	1490.8	73.4	-0.146	-1991
6	D0042	1490.7	73.4	ND	NA
7	D0041	1488.0	73.1	-0.168	-2294
8	D0040	1486.8	73.1	-0.178	-2439

ND = No data
NA = Not applicable
(-) = Growth

Table 7.2-27. Comparison of Joints A and B Radial Growth in TPTA 1.1 Test With JES-3A Test



Test Joint	Girth Gage Location	Gage Number	Station	Radial Growth (in.)		
				TPTA 1.1	JES-3A	Difference
A	1	D0039	1172.3	-0.196	-0.217	-0.021
	2	D0038	1175.0	-0.175	-0.193	-0.018
	3	D0037	1173.2	-0.168	-0.181	-0.013
	4	D0066	1172.3	-0.162	NA	NA
	5	D0065	1170.8	-0.152	NA	NA
	6	D0036	1170.1	-0.150	NA	NA
	7	D0035	1168.0	-0.168	NA	NA
	8	D0034	1166.8	-0.178	-0.192	-0.014
	9	D0089	1170.6	ND	NA	NA
B	1	D0045	1497.3	-0.159	-0.177	-0.018
	2	D0044	1495.0	-0.155	-0.126	-0.029
	3	D0043	1493.2	-0.152	-0.123	-0.029
	4	D0068	1492.2	-0.150	-0.167	-0.017
	5	D0067	1490.8	-0.146	-0.157	-0.011
	6	D0042	1490.7	0.038	NA	NA
	7	D0041	1488.0	-0.168	NA	NA
	8	D0040	1486.8	-0.178	-0.188	-0.010

(-) = Growth

NA = Not applicable

ND = No data

All JES-3A growth data normalized with TPTA 1.1 chamber pressure

TPTA 1.1 FINAL

D0044(STAT=1495.03) D0045(STAT=1497.28)

D0063(STAT= 611.48) D0065(STAT=1170.78)

19 NOVEMBER 1987

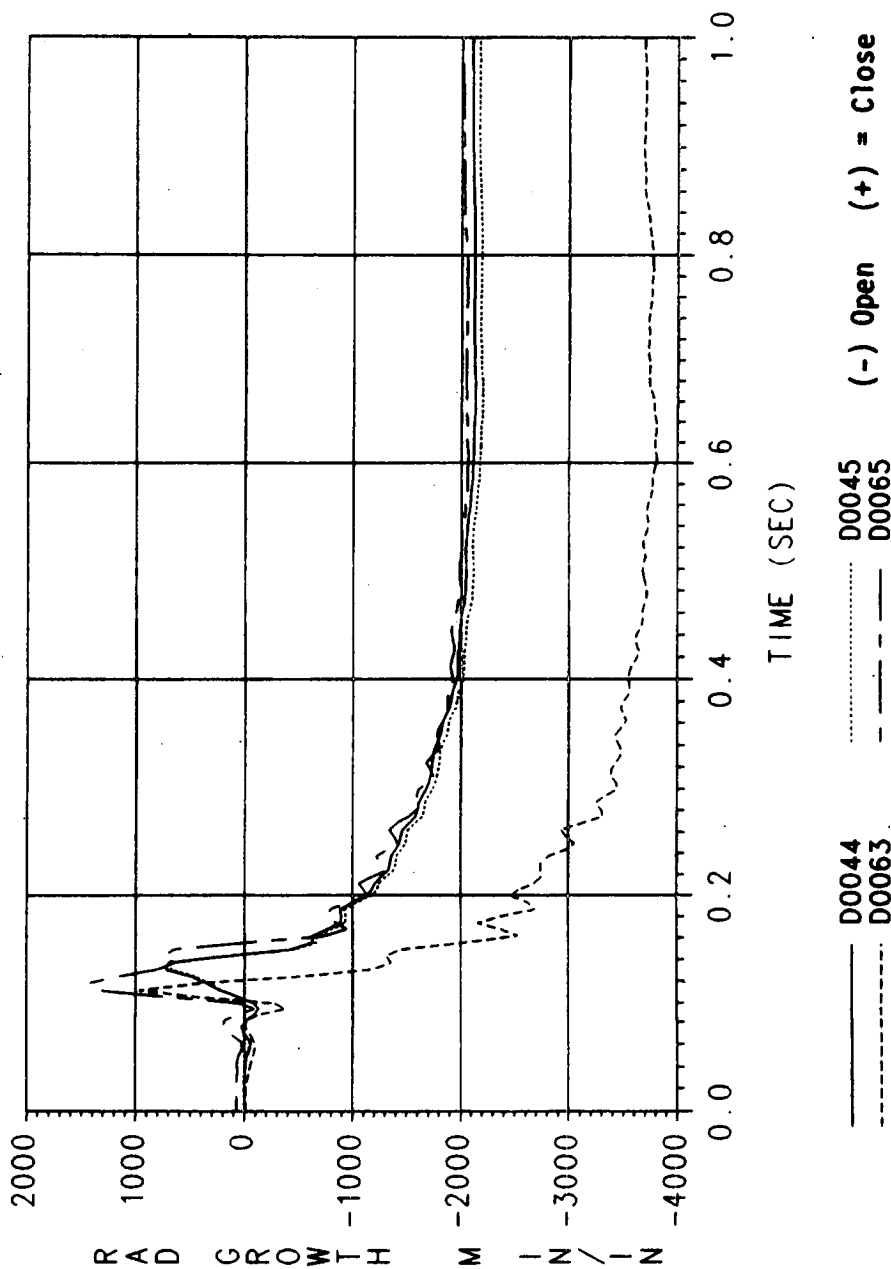


Figure 7.2-23. TPTA 1.1 Joint B Girth Gages (0-1 sec)

TPTA 1.1 FINAL
D0066(STAT=1172.25) D0067(STAT=1490.78)
D0068(STAT=1492.25) D0069(STAT= 528.03)
19 NOVEMBER 1987

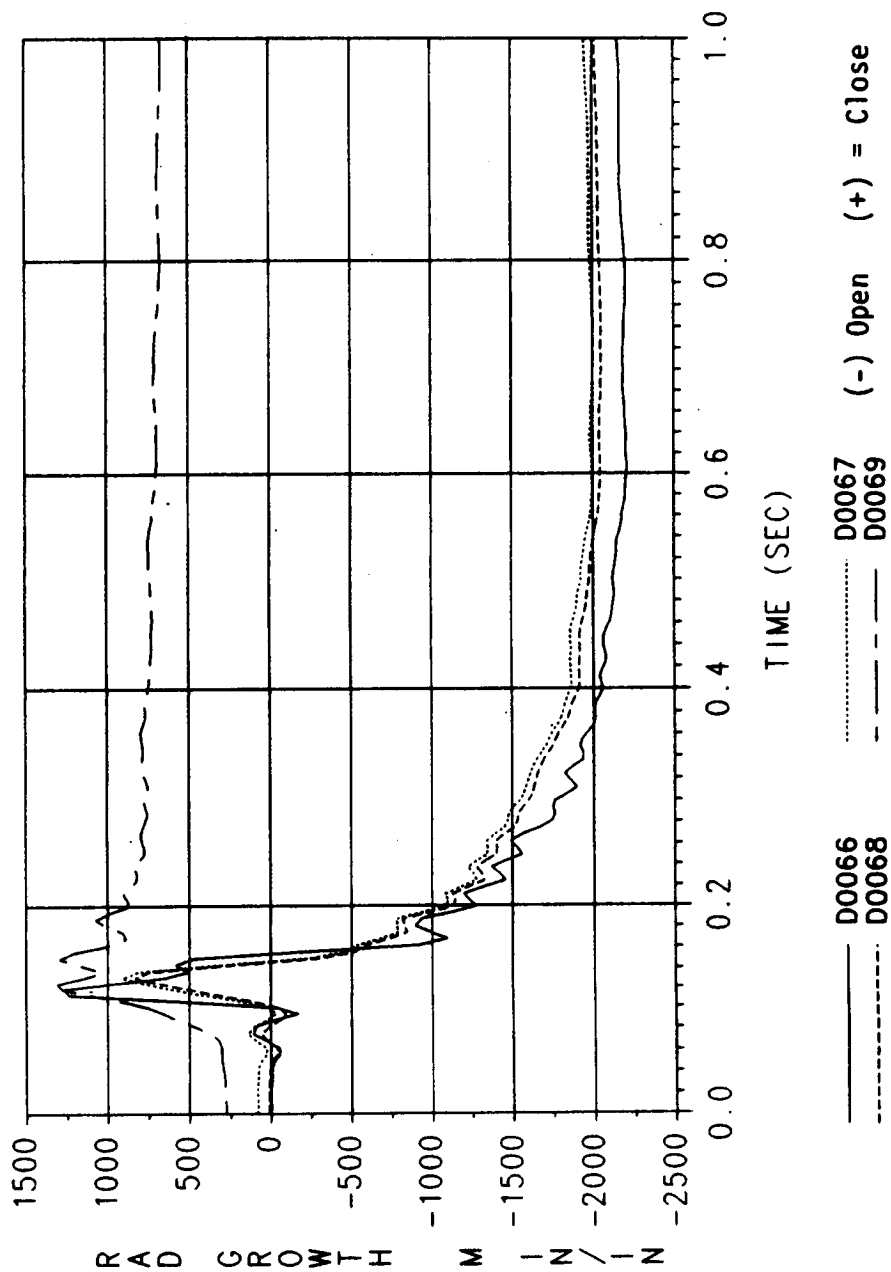
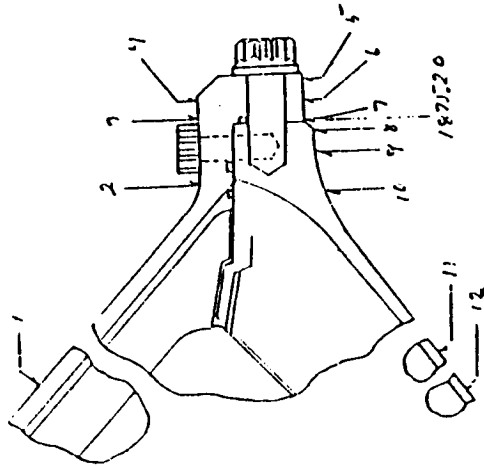


Figure 7.2-24. TPTA 1.1 Joint B Girth Gages (0-30 sec)

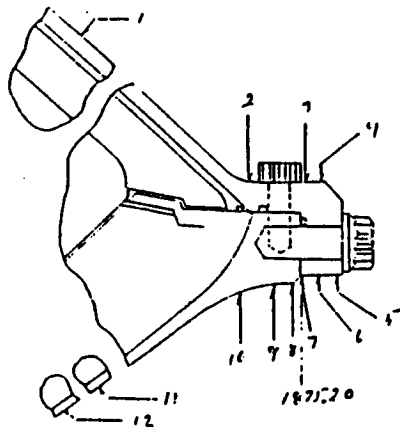
Table 7.2-28. TPTA 1.1 Joint D Radial Growth

TEST NAME: TPTA 1.1
JOINT: D
DESCRIPTION: GIRTH GAGE SUMMARY
MODEL PRESSURE: 896.2 PSIG
THE TIME RANGE IS 0.0 TO 6.0 SECONDS



GIRTH GAGE LOCATION	GAGE NUMBER	STATION	RADIUS (IN)	RADIAL GROWTH (IN)	TEST STRAIN (UIN/IN)
1	D0308	1865.2	44.0	0.029	653
2	D0307	1872.9	50.5	-0.101	-2006
3	D0274	1875.7	50.5	-0.148	-2934
4	D0273	1876.3	50.5	-0.147	-2904
5	D0309	1876.8	54.4	-0.152	-2790
6	D0310	1876.8	54.4	-0.142	-2605
7	D0311	1875.7	54.4	-0.133	-2443
8	D0312	1874.8	54.8	-0.118	-2155
9	D0313	1874.2	54.8	-0.111	-2030
10	D0314	1872.5	55.0	-0.093	-1682
11	D0315	1859.2	63.8	-0.169	-2642
12	D0316	1846.3	69.9	ND	ND

ND = No data
(-) = Growth

Table 7.2-29. Comparison of Joint D Radial Growth
in TPTA 1.1 Test With NJES-2B Test

Girth Gage Location	Gage Number	Station	Radial Growth (in.)		
			TPTA 1.1	NJES-2B	Difference
1	D0308	1865.2	0.029	0.042	-0.013
2	D0307	1872.9	-0.101	-0.088	0.013
3	D0274	1875.7	-0.148	-0.129	0.019
4	D0273	1876.3	-0.147	-0.138	0.009
5	D0309	1876.8	-0.152	-0.142	0.010
6	D0310	1876.8	-0.142	-0.135	0.007
7	D0311	1875.7	-0.133	-0.127	0.006
8	D0312	1874.8	-0.118	-0.118	0.000
9	D0313	1874.2	-0.111	-0.112	-0.001
10	D0314	1872.5	-0.093	-0.095	-0.002
11	D0315	1859.2	-0.169	-0.191	-0.022
12	D0316	1846.3	ND	NA	NA

(-) = Growth

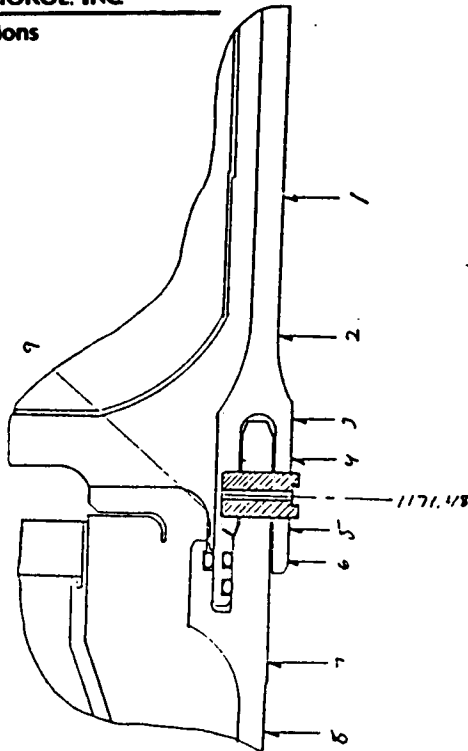
NA = Not applicable

ND = No data

All JES-3A growth data normalized with TPTA 1.1 chamber pressure

Table 7.2-30. TPTA 1.1A Joint A Radial Growth

TEST NAME: TPTA 1.1A
JOINT: A
DESCRIPTION: GIRTH GAGE SUMMARY
THE TIME RANGE IS 9.0 TO 14.0 SECONDS

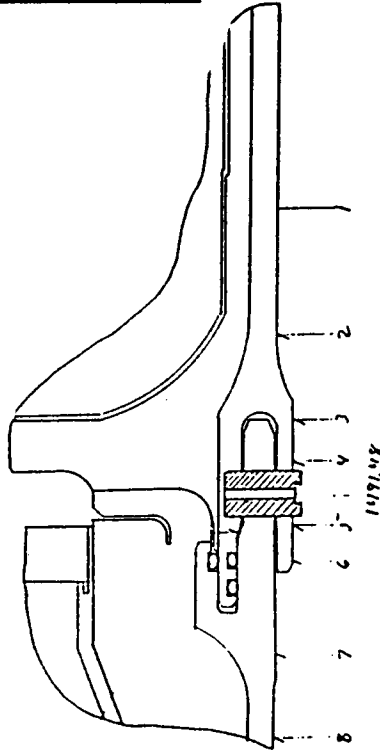


ND = No data
(-) = Growth

GIRTH GAGE LOCATION	GAGE NUMBER	STATION	RADIUS (IN)	RADIAL GROWTH (IN)	TEST STRAIN (UTIN/IN)
1	D0039	1172.3	73.1	-0.132	-1803
2	D0038	1175.0	73.1	-0.115	-1572
3	D0037	1173.2	73.4	-0.112	-1526
4	D0066	1172.3	73.4	-0.108	-1473
5	D0065	1170.8	73.4	-0.117	-1592
6	D0036	1170.1	73.4	-0.104	-1420
7	D0035	1168.0	73.1	-0.130	-1775
8	D0034	1166.8	73.1	-0.121	-1661
9	D0089	1170.6	72.3	ND	ND

Table 7.2-31. TPTA 1.1A Joint B Radial Growth

TEST NAME: TPTA 1.1A
JOINT: B
DESCRIPTION: GIRTH GAGE SUMMARY
THE TIME RANGE IS 9.0 TO 14.0 SECONDS

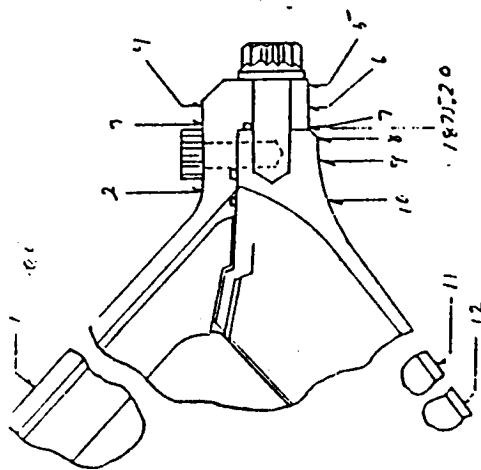


GIRTH GAGE LOCATION	GAGE NUMBER	STATION	RADIUS (IN)	RADIAL GROWTH (IN)	TEST STRAIN (UIN/IN)
1	D0045	1497.3	73.1	-0.113	-1542
2	D0044	1495.0	73.1	-0.108	-1475
3	D0043	1493.2	73.4	-0.105	-1432
4	D0068	1492.2	73.4	-0.103	-1406
5	D0067	1490.8	73.4	ND	ND
6	D0042	1490.7	73.4	ND	ND
7	D0041	1488.0	73.1	-0.116	-1593
8	D0040	1486.8	73.1	-0.123	-1684

ND = No data
(-) = Growth

Table 7.2-32. TPTA 1.1A Joint D Radial Growth

TEST NAME: TPTA 1.1A
JOINT: D
DESCRIPTION: GIRTH GAGE SUMMARY
THE TIME RANGE IS 9.0 TO 14.0 SECONDS



GIRTH GAGE LOCATION	GAGE NUMBER	STATION	RADIUS (IN)	RADIAL GROWTH (IN)	TEST STRAIN (UIN/IN)
1	D0308	1865.2	44.0	0.024	552
2	D0307	1872.9	50.5	-0.061	-1209
3	D0274	1875.7	50.5	-0.096	-1893
4	D0273	1876.3	50.5	-0.099	-1967
5	D0309	1876.8	54.4	-0.103	-1886
6	D0310	1876.8	54.4	-0.096	-1771
7	D0311	1875.7	54.4	-0.090	-1662
8	D0312	1874.8	54.8	-0.080	-1466
9	D0313	1874.2	54.8	-0.075	-1362
10	D0314	1872.5	55.0	-0.064	-1158
11	D0315	1859.2	63.8	-0.114	-1787
12	D0316	1846.3	69.9	ND	ND

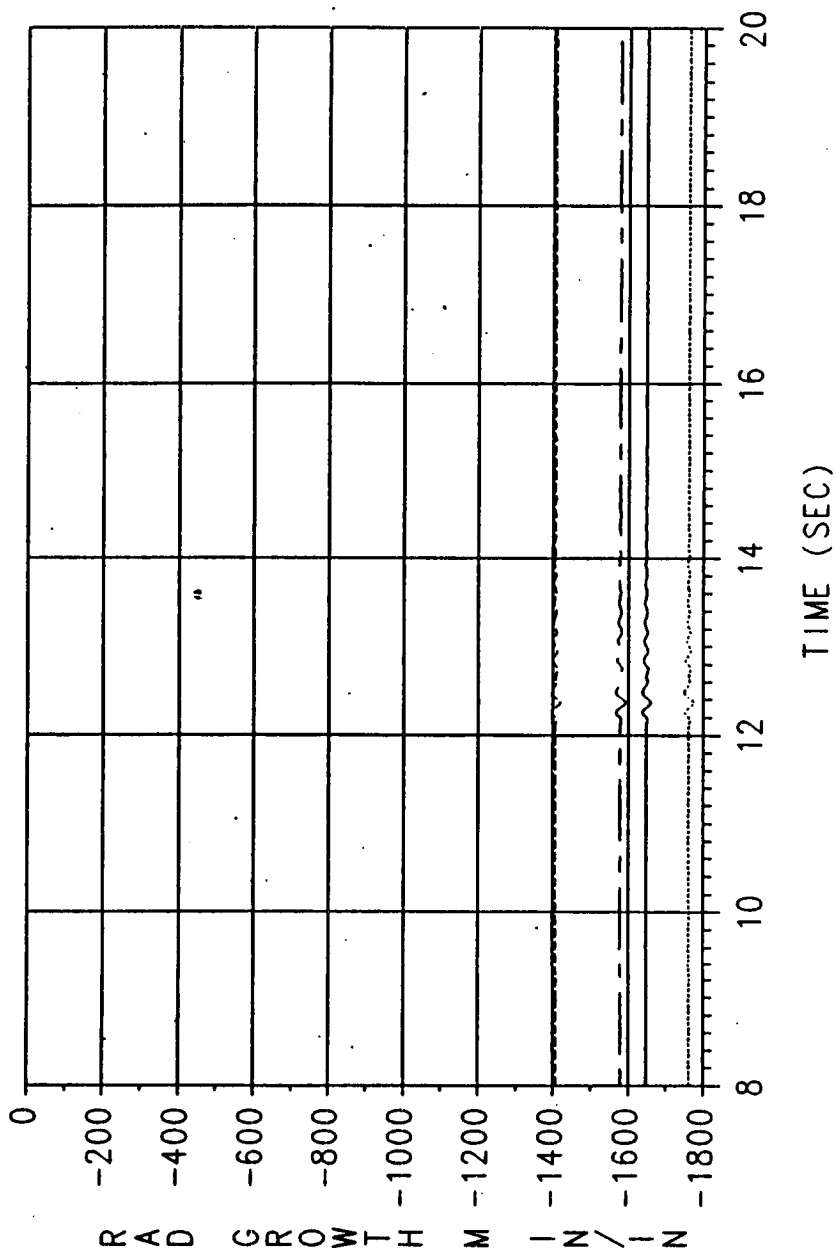
ND = No data
(-) = Growth

TPTA1.1A MAX-Q FINAL(REVISED)

D0034(ST=1166.78) D0035(ST=1168.03)

D0036(ST=1170.07) D0065(ST=1170.78)

24 NOVEMBER 1987



— D0034 D0035 ----- D0036 - - - - D0065

Figure 7.2-25. TPTA 1.1A Joint A Radial Growth (8-20 sec)

TPTA1.1A MAX-Q FINAL(REVISED)

D0043(ST=1493.16) D0044(ST=1495.03)

D0045(ST=1497.28) D0133(ST=1511.48)

24 NOVEMBER 1987

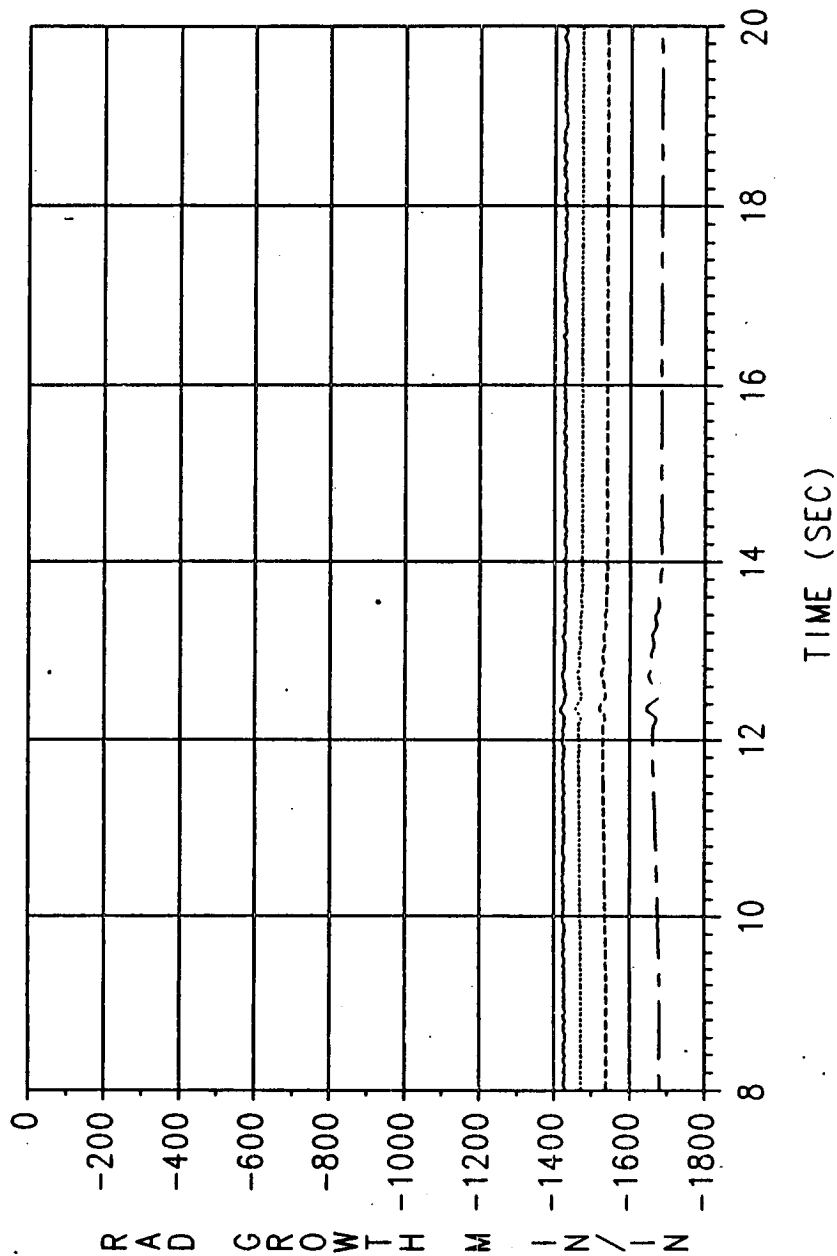


Figure 7.2-26. TPTA 1.1A Joint B Radial Growth (8-20 sec)

Table 7.2-33. TPTA 1.1 Joint A Tang Area Stresses

TEST NAME TPTA 1.1
JOINT A
DESCRIPTION BIAXIAL GAGES
MODEL PRESSURE 913.3 PSIA
MAXIMUM PRESSURE: 909.7 PSIA
DESIRED PRESSURE: 913.3 PSIA
TIME PRESSURE OCCURRED: 0.6 SECONDS

LOCAT	ANGULAR LOCATION	HOOP GAGE	AXIAL GAGE	TEST DATA			
				HOOP STRESS (KSI)	AXIAL STRESS (KSI)	HOOP STRAIN (UIN/IN)	AXIAL STRAIN (UIN/IN)
1	118.0	S0037	S0036	-71.7	-17.8	-2210	122
1	320.0	S0041	S0040	-80.9	-22.8	-2470	50
			AVERAGE:	-76.3	-20.3	-2340	86
2	118.0	S0031	S0030	-77.3	-17.8	-2398	181
2	320.0	S0035	S0034	-78.3	-9.6	-2513	462
			AVERAGE:	-77.8	-13.7	-2456	321
3	60.0	S0067	S0066	-79.6	-43.0	-2224	-637
3	118.0	S0565	S0564	-71.6	-34.9	-2038	-448
3	240.0	S0071	S0070	-83.4	-37.7	-2404	-421
3	320.0	S0073	S0072	-72.9	-32.1	-2110	-341
			AVERAGE:	-76.9	-36.9	-2194	-462

(+) = Compression
(-) = Tension

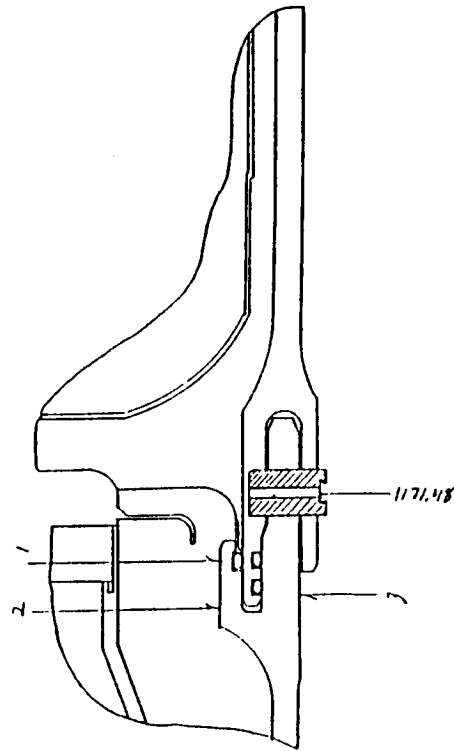
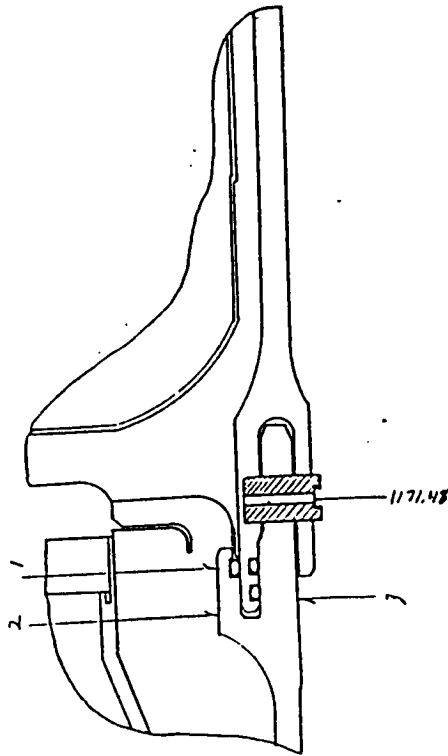


Table 7.2-34. TPTA 1.1A Joint A Tang Area Stresses

TEST NAME: TPTA 1.1A
JOINT: A
DESCRIPTION: BIAXIAL GAGES
THE TIME RANGE IS 9.0 TO 14.0 SECONDS

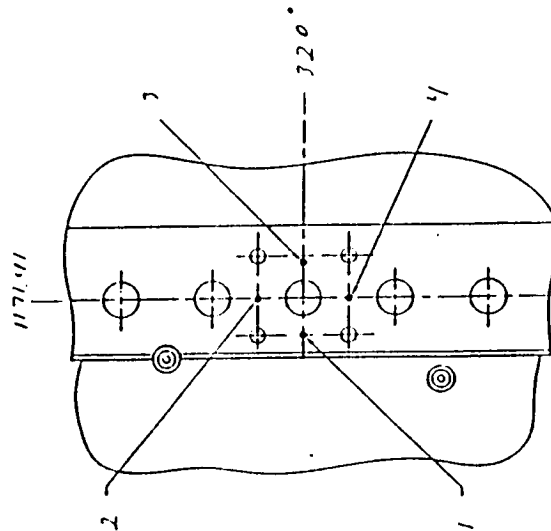


LOCAT	ANGULAR LOCATION	HOOP GAGE	AXIAL GAGE	HOOP STRESS (KSI)	AXIAL STRESS (KSI)	TEST DATA	
						HOOP STRAIN (UIN/IN)	AXIAL STRAIN (UIN/IN)
1	118.0	S0037	S0036	-49.9	-8.0	-1582	231
1	320.0	S0041	S0040	-76.5	-17.7	-2374	175
			AVERAGE:	-63.2	-12.9	-1978	203
2	118.0	S0031	S0030	-53.0	-2.0	-1747	463
2	320.0	S0035	S0034	-48.1	5.6	-1658	666
			AVERAGE:	-50.5	1.8	-1702	565
3	60.0	S0067	S0066	-49.2	-18.5	-1455	-126
3	118.0	S0565	S0564	-34.1	-20.1	-935	-329
3	240.0	S0071	S0070	-54.1	-22.1	-1583	-196
3	320.0	S0073	S0072	-46.7	-15.6	-1402	-52
			AVERAGE:	-46.0	-19.1	-1344	-176

(+) = Compression
(-) = Tension

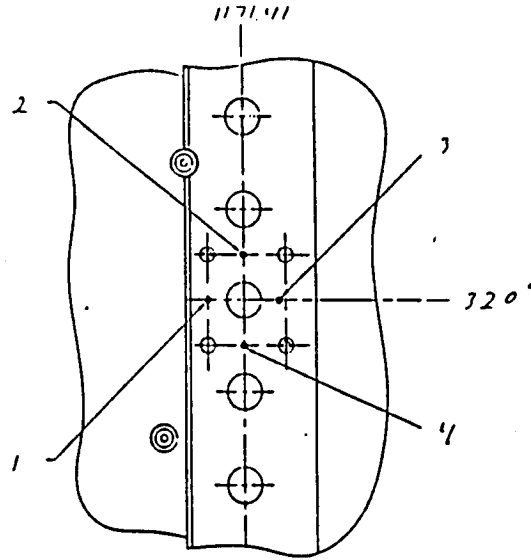
Table 7.2-35. TPTA 1.1 Joint A Outer Clevis Leg Stresses

LOCAT	ANGULAR LOCATION	HOOP GAGE	AXIAL GAGE	TEST DATA			
				HOOP STRESS (KSI)	AXIAL STRESS (KSI)	HOOP STRAIN (UTN/IN)	AXIAL STRAIN (UTN/IN)
1	320.0	S0101	S0100 AVERAGE:	-88.9 -88.9	29.1 29.1	-3254 -3254	1860 1860
2	320.0	S0099	S0098 AVERAGE:	-43.9 -43.9	-44.7 -44.7	-1015 -1015	-1053 -1053
3	320.0	S0103	S0102 AVERAGE:	-74.0 -74.0	-40.4 -40.4	-2062 -2062	-607 -607
4	320.0	S0318	S0317 AVERAGE:	-43.2 -43.2	-41.5 -41.5	-1027 -1027	-949 -949



(+) = Compression
(-) = Tension

Table 7.2-36. TPTA 1.1A Joint A Outer Clevis Leg Stresses



Locat	Angular Location	Hoop Gage	Axial Gage	Hoop Stress (ksi)	Axial Stress (ksi)	Test Data	
						Hoop Strain (μin./in.)	Axial Strain (μin./in.)
1	320.0	S0101	S0100	-60.7	30.2	-2,324	1,612
2	320.0	S0099	S0098	-27.4	-30.4	-608	-741
3	320.0	S0103	S0102	-47.4	-26.0	-1,320	-392
4	320.0	S0318	S0317	-19.6	-23.6	-417	-592

(+) => Compression
(-) => Tension

axial strains recorded, as well as hoop and axial stress for the TPTA 1.1 and 1.1A tests, respectively.

Joint A Pinhole Strains

At the 320-deg pinhole on Joint A, sets of hoop and axial strain gages were placed around a pinhole to measure strains. Tables 7.2-37 and 7.2-38 display the hoop and axial strains measured around the 320-deg pinhole as well as the hoop and axial stress for the TPTA 1.1 and 1.1A tests, respectively.

Joint B Inner Clevis Strain Gages, Tang Area Strain, Joint Line Loads, and Alignment Hole Strains

Several hoop and axial strain gages on the inside of Joint B were placed on the CF hook and on the inside clevis leg under the insulation. Tables 7.2-39 and 7.2-40 display the hoop and axial strains recorded as well as hoop and axial stress for the TPTA 1.1 and 1.1A tests, respectively.

Joint B Pinhole Strains

At the 320-deg pinhole on Joint B, hoop and axial strain gages were placed around a pinhole to measure strains. Table 7.2-41, displays the hoop and axial strains measured around the 320-deg pinhole for the TPTA 1.1 test. Table 7.2-42 shows the pinhole strains and stresses for the TPTA 1.1A test.

Joint D Strains

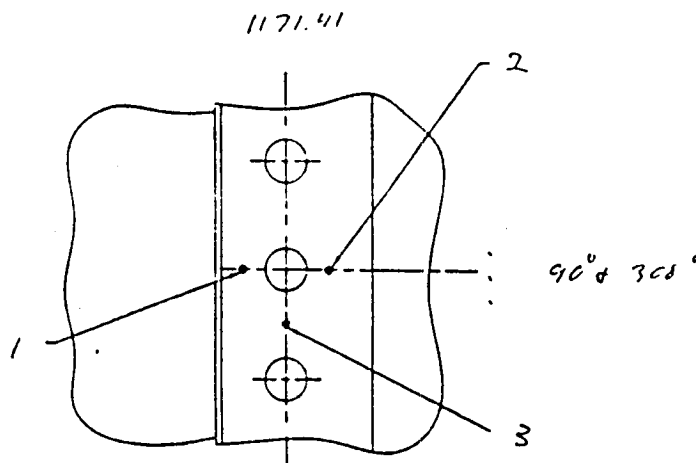
Strains were measured at the fixed housing and aft dome of test Joint D. Tables 7.2-43 and 7.2-44 list test data for the TPTA 1.1 and 1.1A tests, respectively.

7.2.3.4.7 Case Data

Case Membrane Girth Gage

Girth gages were placed at the center of the cylinder segment and at the center of the ETA segment. The strains were converted into radial growths and are also shown in Table 7.2-45. Some case gages, most notably D0133 (Figures 7.2-27 and 7.2-28), do not show the aforementioned initial positive

Table 7.2-37. TPTA 1.1 Joint A Pin Hole Stresses

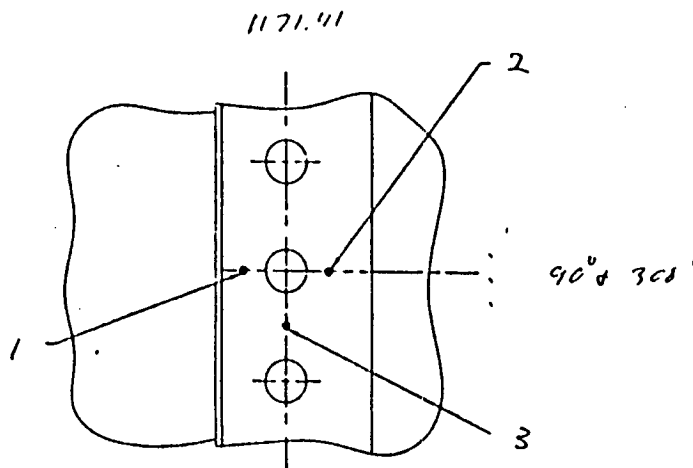


Locat	Angular Location	Hoop Gage	Axial Gage	Hoop Stress (ksi)	Axial Stress (ksi)	Test Data	
						Hoop Strain (μin./in.)	Axial Strain (μin./in.)
1	90.0	S0302	S0301	-88.7	35.6	-3,313	2,073
1	308.0	S0310	S0309	-16.0	22.0	-754	895
2	90.0	S0306	S0305	-84.6	-40.6	-2,413	-508
2	308.0	S0314	S0313	-82.9	-39.8	-2,365	-497
3	90.0	S0308	S0307	-42.2	-47.2	-936	-1,151
3	308.0	S0316	S0315	-44.0	-45.8	-1,007	-1,088

(+) => Compression

(-) => Tension

Table 7.2-38. TPTA 1.1A Joint A Pin Hole Stresses



Locat	Angular Location	Hoop Gage	Axial Gage	Hoop Stress (ksi)	Axial Stress (ksi)	Test Data	
						Hoop Strain (μ in./in.)	Axial Strain (μ in./in.)
1	90.0	S0302	S0301	-63.2	33.1	-2,439	1,736
1	308.0	S0310	S0309	-8.2	13.9	-411	545
2	90.0	S0306	S0305	-56.5	-22.6	-1,656	-190
2	308.0	S0314	S0313	-54.4	-26.3	-1,551	-332
3	90.0	S0308	S0307	-25.7	-31.8	-539	-803
3	308.0	S0316	S0315	-28.9	-38.7	-575	-1,003

(+) => Compression

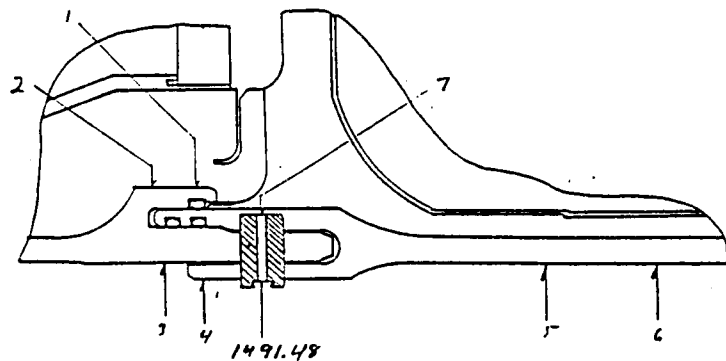
(-) => Tension

MORTON THIOKOL, INC.

Space Operations

Table 7.2-39. TPTA 1.1 Joint B Hoop and Axial Stresses (Inner Clevis Leg, Tang Area and Alignment Holes)

TEST NAME: TPTA 1.1
JOINT: B
DESCRIPTION: BIAXIAL GAGES
MODEL PRESSURE: 913.3 PSIA
MAXIMUM PRESSURE: 909.7 PSIA
DESIRED PRESSURE: 913.3 PSIA
TIME PRESSURE OCCURRED: 0.6 SECONDS

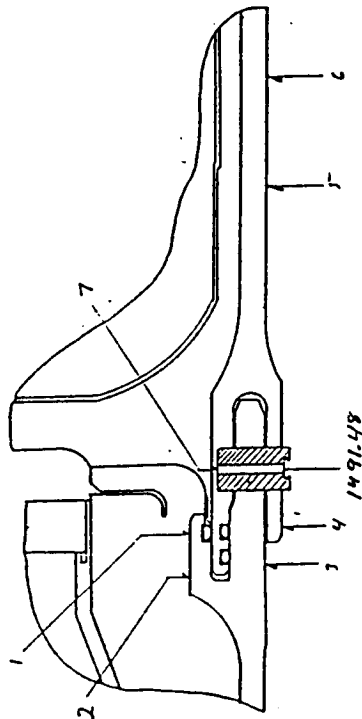


LOCAT	ANGULAR LOCATION	HOOP GAGE	AXIAL GAGE	HOOP STRESS (KSI)	AXIAL STRESS (KSI)	TEST DATA	
						HOOP STRAIN (UIN/IN)	AXIAL STRAIN (UIN/IN)
1	118.0	S0049	S0048	ND	ND	ND	185
1	180.0	S0051	S0050	-19.3	-73.8	95	-2266
1	320.0	S0053	S0052	-114.8	-79.8	-3029	-1512
			AVERAGE:	-67.1	-76.8	-1467	-1198
2	118.0	S0055	S0054	-15.1	-78.8	284	-2477
2	180.0	S0057	S0056	-75.7	-9.0	-2433	458
2	320.0	S0059	S0058	-75.6	-11.2	-2408	382
			AVERAGE:	-55.5	-33.0	-1519	-546
3	0.0	S0567	S0566	-84.3	-39.1	-2419	-460
3	60.0	S0238	S0237	-84.9	-39.4	-2436	-464
3	118.0	S0075	S0074	-75.7	-38.9	-2134	-541
3	180.0	S0240	S0239	-76.6	-41.3	-2141	-611
3	220.0	S0242	S0241	-73.5	-37.1	-2079	-502
3	240.0	S0079	S0078	-84.3	-37.1	-2441	-393
3	266.0	S0244	S0243	-48.6	-119.5	-424	-3498
3	320.0	S0082	S0081	ND	ND	ND	-1860
			AVERAGE:	-75.4	-50.3	-2011	-1041
4	0.0	S0511	S0510	-24.0	-4.1	-758	102
4	82.0	S0513	S0512	-80.3	13.9	-2816	1266
4	180.0	S0515	S0514	-82.1	6.8	-2804	1047
4	220.0	S0517	S0516	-79.7	9.5	-2751	1115
4	240.0	S0519	S0518	-21.7	-5.4	-668	38
4	255.0	S0521	S0520	-6.7	-44.2	217	-1406
4	270.0	S0523	S0522	-76.0	8.1	-2615	1031
4	285.0	S0525	S0524	-45.0	-7.1	-1430	213
4	320.0	S0527	S0526	-70.3	15.4	-2498	1216
			AVERAGE:	-54.0	-0.8	-1791	514
5	0.0	S0529	S0528	-99.0	-85.9	-2442	-1874
5	82.0	S0531	S0530	-93.0	-85.2	-2247	-1909
5	180.0	S0533	S0532	-94.2	-91.8	-2220	-2119
5	220.0	S0535	S0534	ND	ND	ND	ND
5	240.0	S0537	S0536	-93.2	-84.9	-2259	-1898
5	255.0	S0539	S0538	-95.3	-94.6	-2232	-2200
5	270.0	S0541	S0540	-96.5	-90.8	-2308	-2062
5	285.0	S0543	S0542	-95.3	-88.7	-2291	-2003
5	320.0	S0545	S0544	-61.9	-34.3	-1721	-525
6	0.0	S0547	S0546	-80.3	-54.0	-2138	-997
6	82.0	S0549	S0548	-81.1	-54.2	-2160	-995
6	180.0	S0551	S0550	-80.6	-56.5	-2122	-1078
6	220.0	S0553	S0552	-78.3	-54.9	-2060	-1048
6	240.0	S0555	S0554	-51.7	-79.5	-927	-2133
6	255.0	S0557	S0556	-78.9	-56.6	-2066	-1096
6	270.0	S0559	S0558	-80.2	-54.5	-2128	-1016
6	285.0	S0561	S0560	-81.5	-54.7	-2168	-1009
6	320.0	S0563	S0562	-80.4	-56.1	-2121	-1066
			AVERAGE:	-77.0	-57.9	-1988	-1160
7	0.0	S0089	S0088	-104.7	-20.9	-3281	350
7	118.0	S0097	S0096	-112.0	-23.4	-3499	339
7	320.0	S0105	S0104	-109.2	-22.5	-3416	342
			AVERAGE:	-108.6	-22.3	-3399	344

(+) = Compression
(-) = Tension

ND = No data

Table 7.2-40. IPTA 1.1A Joint B Hoop and Axial Stresses (Inner Clevis Leg, Tang Area and Alignment Holes)



(+) = Compression
(-) = Tension

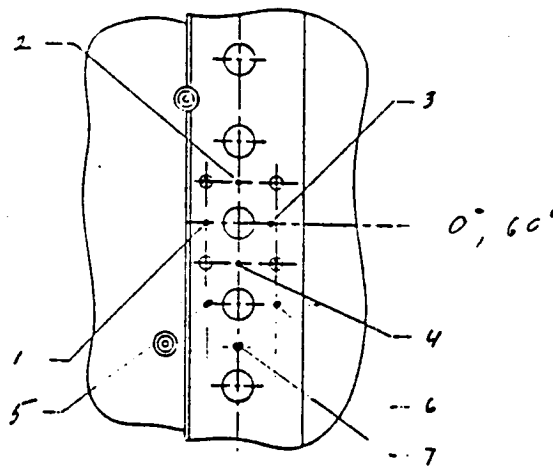
TEST NAME: IPTA 1.1A
JOINT: B
DESCRIPTION: BIAXIAL GAGES
MODEL PRESSURE
THE TIME RANGE IS 9.0 TO 14.0 SECONDS

LOCAT	ANGULAR LOCATION	HOOP GAGE	AXIAL GAGE	TEST DATA			
				HOOP STRESS (KSI)	AXIAL STRESS (KSI)	HOOP STRAIN (UTN/IN)	AXIAL STRAIN (UTN/IN)
1	118.0	S0049	S0048	ND	ND	ND	344
1	180.0	S0051	S0050	ND	ND	351	ND
1	320.0	S0053	S0052	-76.3	-63.5	-1909	-1354
2	118.0	S0055	S0054	2.1	-55.3	623	-1863
2	180.0	S0057	S0056	-49.8	7.8	-1739	759
2	320.0	S0059	S0058	-45.4	6.0	-1573	655
			AVERAGE:	-31.0	-13.8	-896	-150
3	0.0	S0567	S0566	-54.7	-24.2	-1580	-259
3	60.0	S0238	S0237	-55.4	-23.6	-1609	-234
3	118.0	S0075	S0074	-48.8	-19.5	-1430	-163
3	180.0	S0240	S0239	-52.2	-26.6	-1474	-363
3	220.0	S0242	S0241	-48.0	-21.0	-1391	-221
3	240.0	S0079	S0078	-53.9	-21.1	-1586	-166
3	266.0	S0244	S0243	-17.3	-50.1	-75	-1498
3	320.0	S0082	S0081	ND	ND	-1307	-1751
			AVERAGE:	-47.2	-26.6	-1307	-582
4	0.0	S0511	S0510	-13.1	-2.9	-408	36
4	82.0	S0513	S0512	-56.5	13.0	-2015	999
4	180.0	S0515	S0514	-56.3	6.8	-1944	789
4	220.0	S0517	S0516	-56.2	8.1	-1956	833
4	240.0	S0519	S0518	-14.1	-3.0	-439	40
4	255.0	S0521	S0520	-3.6	-26.4	143	-843
4	270.0	S0523	S0522	-50.3	6.9	-1745	732
4	285.0	S0525	S0524	-29.2	-5.5	-919	108

4	320.0	S0527	S0526	-56.6	13.6	-2023	1019
		AVERAGE:		-37.3	1.2	-1256	413
5	0.0	S0529	S0528	-63.1	-55.6	-1548	-1221
5	82.0	S0531	S0530	-62.8	-57.1	-1521	-1274
5	180.0	S0533	S0532	-61.6	-66.4	-1390	-1597
5	220.0	S0535	S0534	ND	ND	ND	ND
5	240.0	S0537	S0536	-64.7	-57.7	-1580	-1276
5	255.0	S0539	S0538	-65.4	-64.0	-1540	-1480
5	270.0	S0541	S0540	-65.6	-58.6	-1602	-1296
5	285.0	S0543	S0542	-68.3	-62.4	-1653	-1397
5	320.0	S0545	S0544	-47.4	-29.3	-1286	-503
6	0.0	S0547	S0546	-58.6	-38.7	-1566	-704
6	82.0	S0549	S0548	-55.3	-36.6	-1476	-666
6	180.0	S0551	S0550	-49.7	-39.8	-1258	-829
6	220.0	S0553	S0552	-56.4	-37.6	-1506	-688
6	240.0	S0555	S0554	-37.5	-57.0	-680	-1525
6	255.0	S0557	S0556	-56.4	-39.8	-1483	-763
6	270.0	S0559	S0558	-58.8	-37.8	-1581	-672
6	285.0	S0561	S0560	-61.7	-42.7	-1630	-806
6	320.0	S0563	S0562	-63.5	-49.5	-1621	-1015
		AVERAGE:		-55.3	-42.2	-1422	-852
7	0.0	S0089	S0088	-76.9	-15.8	-2405	241
7	118.0	S0097	S0096	-74.0	-16.0	-2306	207
7	320.0	S0105	S0104	-77.7	-14.0	-2450	310
		AVERAGE:		-76.2	-15.3	-2387	253

ND = No data

Table 7.2-41. TPTA 1.1 Joint B Pin Hole Stresses



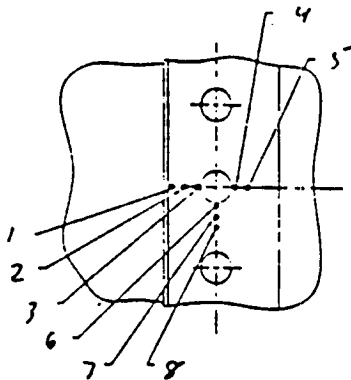
Locat	Angular Location	Hoop Gage	Axial Gage	Hoop Stress (ksi)	Axial Stress (ksi)	Test Data	
						Hoop Strain ($\mu\text{in./in.}$)	Axial Strain ($\mu\text{in./in.}$)
1	0.0	S0465	S0464	-32.8	-12.5	-970	-88
1	60.0	S0320	S0319	ND	ND	ND	ND
2	59.0	S0322	S0321	-48.8	-57.1	-1,056	-1,415
2	359.0	S0467	S0466	-44.9	-36.4	-1,134	-765
3	0.0	S0469	S0468	-75.3	-44.8	-2,061	-740
3	60.0	S0324	S0323	-53.4	-77.2	-1,006	-2,041
4	1.0	S0328	S0327	-35.3	-47.2	-705	-1,221
4	61.0	S0326	S0325	-45.4	-57.1	-944	-1,448
5	2.0	S0812	S0811	-106.4	30.0	-3,846	2,063
6	2.0	S0808	S0807	-78.0	-41.8	-2,183	-613
7	3.0	S0810	S0809	-42.3	-66.4	-745	-1,791

(+) => Compression

(-) => Tension

ND = No data

Table 7.2-41. TPTA 1.1 Joint B Pin Hole Stresses (Cont)

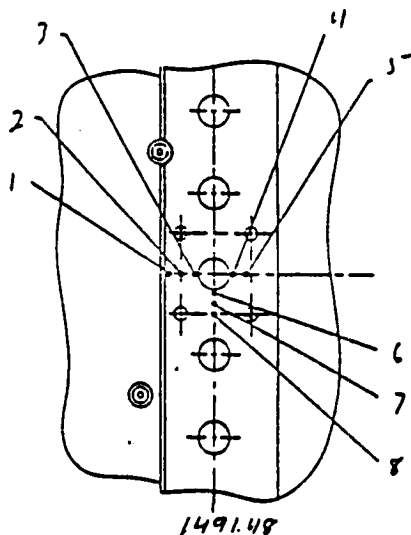


Locat	Angular Location	Hoop Gage	Axial Gage	Hoop Stress (ksi)	Axial Stress (ksi)	Test Data	
						Hoop Strain (μ in./in.)	Axial Strain (μ in./in.)
1	90.0	S0338	S0337	-73.8	5.0	-2,511	905
2	90.0	S0340	S0339	-82.7	27.2	-3,028	1,732
2	308.0	S0330	S0329	-96.3	43.0	-3,639	2,396
3	90.0	S0342	S0341	-55.1	297.0	-4,807	1,452
4	90.0	S0344	S0343	-107.6	-30.2	-3,285	70
5	90.0	S0346	S0345	-83.8	-47.2	-2,320	-735
5	308.0	S0334	S0333	-80.7	-50.6	-2,184	-880
6	90.5	S0348	S0347	-33.7	-71.0	-420	-2,029
7	90.7	S0350	S0349	-40.5	-57.5	-776	-1,511
8	91.0	S0352	S0351	-40.4	-56.2	-784	-1,469
8	309.0	S0336	S0335	-44.2	-53.7	-937	-1,347

(+) => Compression

(-) => Tension

Table 7.2-41. TPTA 1.1 Joint B Pin Hole Stresses (Cont)

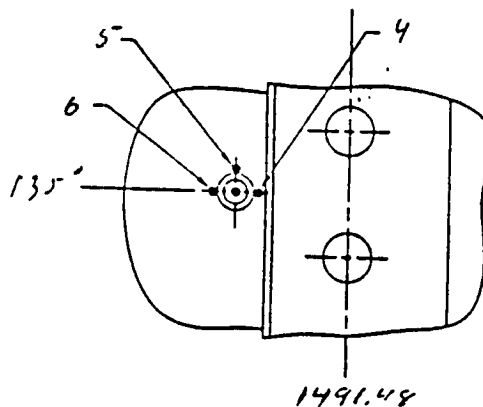
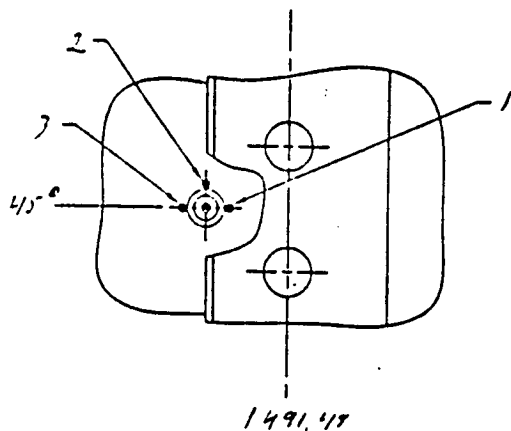


Locat	Angular Location	Hoop Gage	Axial Gage	Hoop Stress (ksi)	Axial Stress (ksi)	Test Data	
						Hoop Strain ($\mu\text{in./in.}$)	Axial Strain ($\mu\text{in./in.}$)
1	320.0	S0133	S0132	-84.3	3.8	-2,848	968
2	320.0	S0135	S0134	-87.2	29.9	-3,206	1,870
3	320.0	S0137	S0136	-146.9	104.7	-5,945	4,961
4	320.0	S0131	S0130	-95.6	-35.2	-2,836	-218
5	320.0	S0139	S0138	-78.3	-45.2	-2,158	-725
6	320.5	S0141	S0140	-17.9	-55.7	-40	-1,679
7	320.7	S0143	S0142	-38.5	-56.7	-717	-1,505
8	321.0	S0145	S0144	-43.1	-50.7	-929	-1,260

(+) => Compression

(-) => Tension

Table 7.2-41. TPTA 1.1 Joint B Pin Hole Stresses (Cont)



Locat	Angular Location	Hoop Gage	Axial Gage	Hoop Stress (ksi)	Axial Stress (ksi)	Test Data	
						Hoop Strain (μ in./in.)	Axial Strain (μ in./in.)
1	45.0		S0813	ND	ND	ND	ND
2	44.6		S0815	ND	ND	ND	ND
3	45.0	S0818	S0817	-91.3	-37.6	-2,665	-342
4	135.0	S0820	S0819	ND	ND	ND	ND
5	134.4	S0822	S0821	1.1	-1.2	50	-53
6	135.0	S0824	S0823	-101.8	-42.0	-2,973	-383

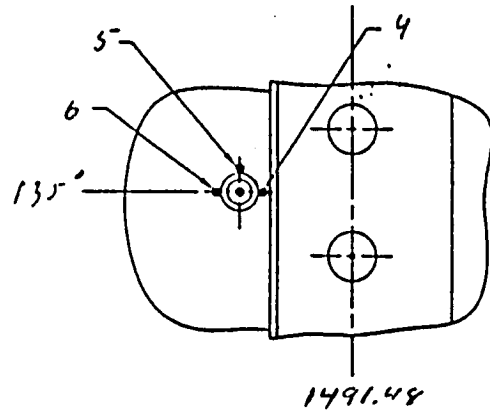
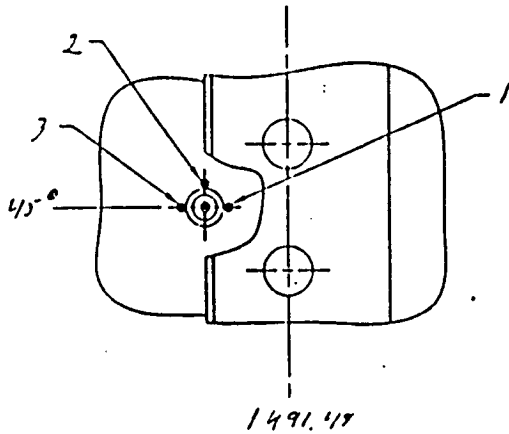
(+) => Compression

(-) => Tension

ND = no data

Note: These are stresses at the leak check port area

Table 7.2-41. TPTA 1.1 Joint B Pin Hole Stresses (Cont)



Locat	Angular Location	Hoop Gage	Axial Gage	Hoop Stress (ksi)	Axial Stress (ksi)	Test Data	
						Hoop Strain (μin./in.)	Axial Strain (μin./in.)
1	45.0		S0813	ND	ND	ND	ND
2	44.6		S0815	ND	ND	ND	ND
3	45.0	S0818	S0817	-59.6	-20.1	-1,787	-73
4	135.0	S0820	S0819	ND	ND	ND	ND
5	134.4	S0822	S0821	-23.5	-6.6	-718	14
6	135.0	S0824	S0823	-68.3	-25.3	-2,025	-159

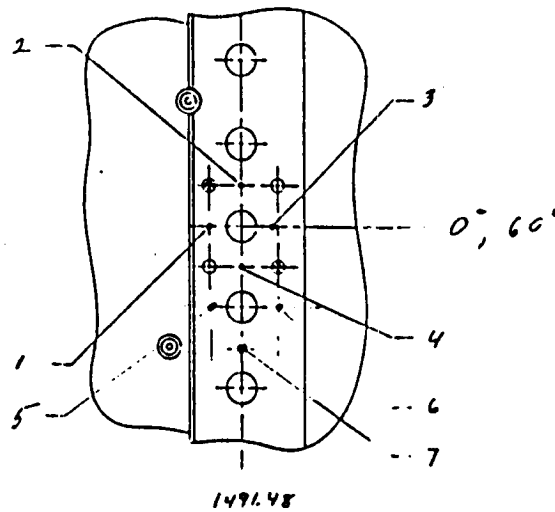
(+) => Compression

(-) => Tension

ND = no data

Note: These are stresses at the leak check port area

Table 7.2-42. TPTA 1.1A Joint B Pin Hole Stresses



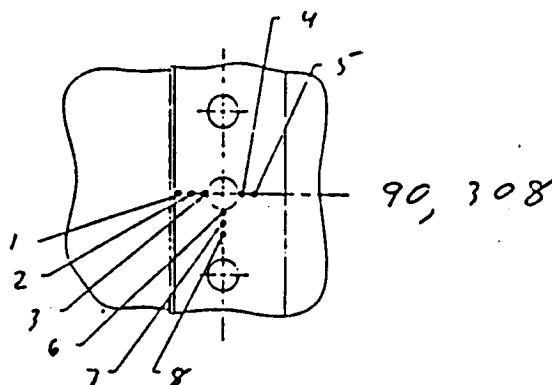
Locat	Angular Location	Hoop Gage	Axial Gage	Hoop Stress (ksi)	Axial Stress (ksi)	Test Data	
						Hoop Strain ($\mu\text{in./in.}$)	Axial Strain ($\mu\text{in./in.}$)
1	0.0	S0465	S0464	-20.3	-9.0	-587	-97
1	60.0	S0320	S0319	ND	ND	ND	ND
2	59.0	S0322	S0321	-30.8	-42.7	-599	-1,116
2	359.0	S0467	S0466	-33.3	-23.8	-873	-461
3	0.0	S0469	S0468	-50.2	-29.8	-1,375	-491
3	60.0	S0324	S0323	-30.0	-47.1	-529	-1,269
4	1.0	S0328	S0327	-23.2	-36.2	-413	-974
4	61.0	S0326	S0325	-28.5	-43.6	-513	-1,169
5	2.0	S0812	S0811	-69.7	25.4	-2,578	1,544
6	2.0	S0808	S0807	-52.1	-25.7	-1,481	-335
7	3.0	S0810	S0809	-26.7	-50.1	-390	-1,404

(+) => Compression

(-) => Tension

ND = no data

Table 7.2-42. TPTA 1.1A Joint B Pin Hole Stresses (Cont)

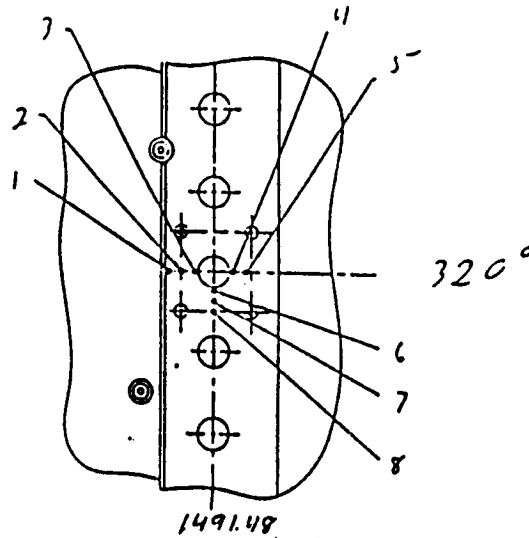


Locat	Angular Location	Hoop Gage	Axial Gage	Hoop Stress (ksi)	Axial Stress (ksi)	Test Data	
						Hoop Strain ($\mu\text{in./in.}$)	Axial Strain ($\mu\text{in./in.}$)
1	90.0	S0338	S0337	-53.8	5.0	-1,843	705
2	90.0	S0340	S0339	-56.9	28.1	-2,176	1,504
2	308.0	S0330	S0329	-78.7	39.5	-3,020	2,104
3	90.0	S0342	S0341	-54.3	145.5	-3,266	5,393
4	90.0	S0344	S0343	-70.9	-19.2	-2,170	68
5	90.0	S0346	S0345	-54.9	-26.3	-1,566	-329
5	308.0	S0334	S0333	-55.0	-34.6	-1,489	-603
6	90.5	S0348	S0347	-20.6	-51.4	-173	-1,507
7	90.7	S0350	S0349	-23.7	-41.2	-379	-1,136
8	91.0	S0352	S0351	-23.9	-41.1	-385	-1,130
8	309.0	S0336	S0335	-32.2	-48.1	-592	-1,280

(+) => Compression

(-) => Tension

Table 7.2-42. TPTA 1.1A Joint B Pin Hole Stresses (Cont)



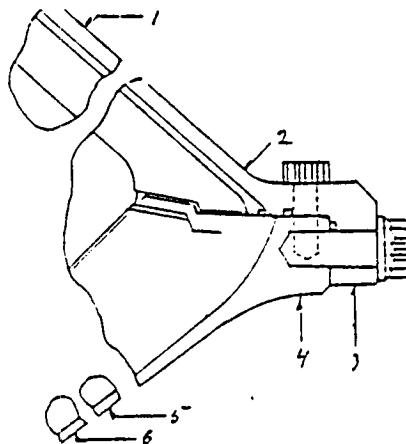
Locat	Angular Location	Hoop Gage	Axial Gage	Hoop Stress (ksi)	Axial Stress (ksi)	Test Data	
						Hoop Strain (μin./in.)	Axial Strain (μin./in.)
1	320.0	S0133	S0132	-64.4	5.1	-2,198	814
2	320.0	S0135	S0134	-61.1	33.0	-2,366	1,712
3	320.0	S0137	S0136	-98.1	190.0	-5,171	7,313
4	320.0	S0131	S0130	-61.6	-12.0	-1,931	214
5	320.0	S0139	S0138	-54.3	-29.8	-1,511	-450
6	320.5	S0141	S0140	34.8	-22.3	1,383	-1,091
7	320.7	S0143	S0142	-27.6	-41.3	-508	-1,100
8	321.0	S0145	S0144	-32.8	-38.6	-709	-958

(+) => Compression

(-) => Tension

Table 7.2-43. TPTA 1.1 Joint D Stresses

TEST NAME: TPTA 1.1
 JOINT: D
 DESCRIPTION: BIAxIAL GAGES
 MODEL PRESSURE 913.3 PSIA
 MAXIMUM PRESSURE: 909.7 PSIA
 DESIRED PRESSURE: 913.3 PSIA
 TIME PRESSURE OCCURRED: 0.6 SECONDS



LOCAT	ANGULAR LOCATION	HOOP GAGE	AXIAL GAGE	HOOP STRESS (KSI)	AXIAL STRESS (KSI)	TEST DATA	
						HOOP STRAIN (UIN/IN)	AXIAL STRAIN (UIN/IN)
1	45.0	S0266	S0265	13.2	-25.9	698	-995
1	135.0	S0268	S0267	11.7	-27.2	661	-1023
			AVERAGE:	12.4	-26.6	679	-1009
2	45.0	S0274	S0273	-38.5	26.1	-1543	1254
2	135.0	S0276	S0275	-38.8	23.3	-1528	1166
2	225.0	S0278	S0277	-37.1	29.3	-1530	1349
2	315.0	S0280	S0279	-37.5	20.9	-1459	1072
			AVERAGE:	-38.0	24.9	-1515	1210
3	45.0	S0282	S0281	-81.9	9.0	-2820	1118
3	135.0	S0284	S0283	-84.3	6.7	-2878	1066
3	235.0	S0286	S0285	-83.1	9.1	-2859	1133
3	315.0	S0288	S0287	-87.9	6.8	-2998	1106
			AVERAGE:	-84.3	7.9	-2889	1106
4	45.0	S0394	S0393	-59.1	11.6	-2085	978
4	135.0	S0396	S0395	-63.6	15.2	-2272	1143
			AVERAGE:	-61.3	13.4	-2178	1061
5	45.0	S0426	S0425	-100.4	-65.7	-2689	-1187
5	135.0	S0428	S0427	-103.5	-67.8	-2772	-1224
			AVERAGE:	-101.9	-66.7	-2730	-1205
6	45.0		S0433	ND	ND	ND	ND
6	135.0		S0435	ND	ND	ND	ND
			AVERAGE:	ND	ND	ND	ND

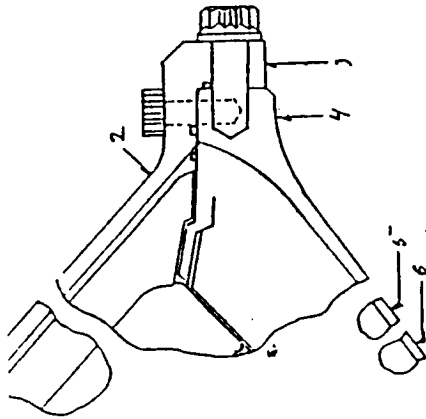
(+) = Compression

(-) = Tension

ND = No data

Table 7.2-44. TPTA 1.1A Joint D Stresses

TEST NAME: TPTA 1.1A
JOINT: D
DESCRIPTION: BIAXIAL GAGES
THE TIME RANGE IS 9.0 TO 14.0 SECONDS

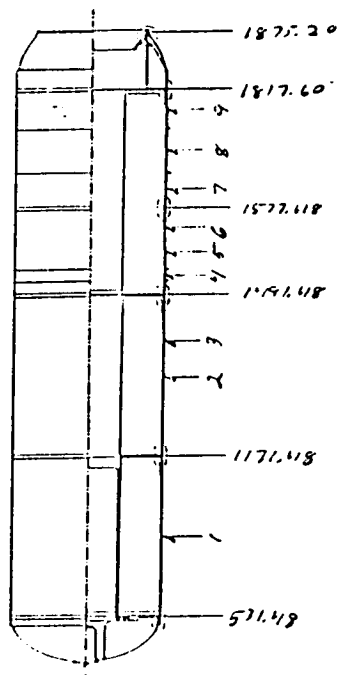


LOCAT	ANGULAR LOCATION	HOOP GAGE	AXIAL GAGE	HOOP STRESS (KSI)	AXIAL STRESS (KSI)	TEST DATA	
						HOOP STRAIN (UIN/IN)	AXIAL STRAIN (UIN/IN)
1	45.0	S0266	S0265	12.9	-16.4	594	-677
1	135.0	S0268	S0267	13.6	-16.7	620	-692
2	45.0	S0274	S0273	-24.0	26.2	-1062	1112
2	135.0	S0276	S0275	-24.8	23.1	-1056	1016
2	225.0	S0278	S0277	-23.7	27.6	-1066	1157
2	315.0	S0280	S0279	-23.5	22.4	-1007	981
		AVERAGE:		-24.0	24.8	-1048	1067
3	45.0	S0282	S0281	-59.1	2.9	-1999	687
3	135.0	S0284	S0283	-55.1	1.1	-1849	588
3	235.0	S0286	S0285	-58.4	2.0	-1965	650
3	315.0	S0288	S0287	-61.5	0.7	-2057	639
		AVERAGE:		-58.5	1.7	-1968	641
4	45.0	S0394	S0393	-41.3	7.5	-1454	665
4	135.0	S0396	S0395	-44.2	8.9	-1562	739
		AVERAGE:		-42.8	8.2	-1508	702
5	45.0	S0426	S0425	-67.7	-44.3	-1813	-801
5	135.0	S0428	S0427	-70.0	-46.1	-1872	-837
		AVERAGE:		-68.8	-45.2	-1843	-819
6	45.0		S0433	ND	ND	ND	ND
6	135.0		S0435	ND	ND	ND	ND

(+) = Compression
(-) = Tension
ND = No data

Table 7.2-45. TPTA 1.1 Case Membrane Girth Gage Data

TEST NAME: TPTA 1.1
JOINT: CASE
DESCRIPTION: GIRTH GAGE SUMMARY
MODEL PRESSURE 913.3 PSIA
MAXIMUM PRESSURE: 909.7 PSIA
DESIRED PRESSURE: 913.3 PSIA
TIME PRESSURE OCCURRED: 0.6 SECONDS



GIRTH GAGE LOCATION	GAGE NUMBER	STATION	RADIUS (IN)	RADIAL GROWTH (IN)	TEST STRAIN (UIN/IN)
1	D0063	611.5	73.1	-0.277	-3794
2	D0032	1251.5	73.1	-0.273	-3734
3	D0132	1286.5	73.1	-0.269	-3685
4	D0133	1511.5	73.1	-0.161	-2203
5	D0033	1533.5	73.1	ND	ND
6	D0134	1555.5	73.1	-0.266	-3639
7	D0135	1596.5	73.1	-0.251	-3433
8	D0136	1634.6	73.1	ND	ND
9	D0137	1674.3	73.1	-0.248	-3396

ND = No data

TPTA 1.1 FINAL

D0072(STAT= 535.03) D0133(STAT=1511.48)

D0134(STAT=1555.48) D0282(STAT= 530.07)

19 NOVEMBER 1987

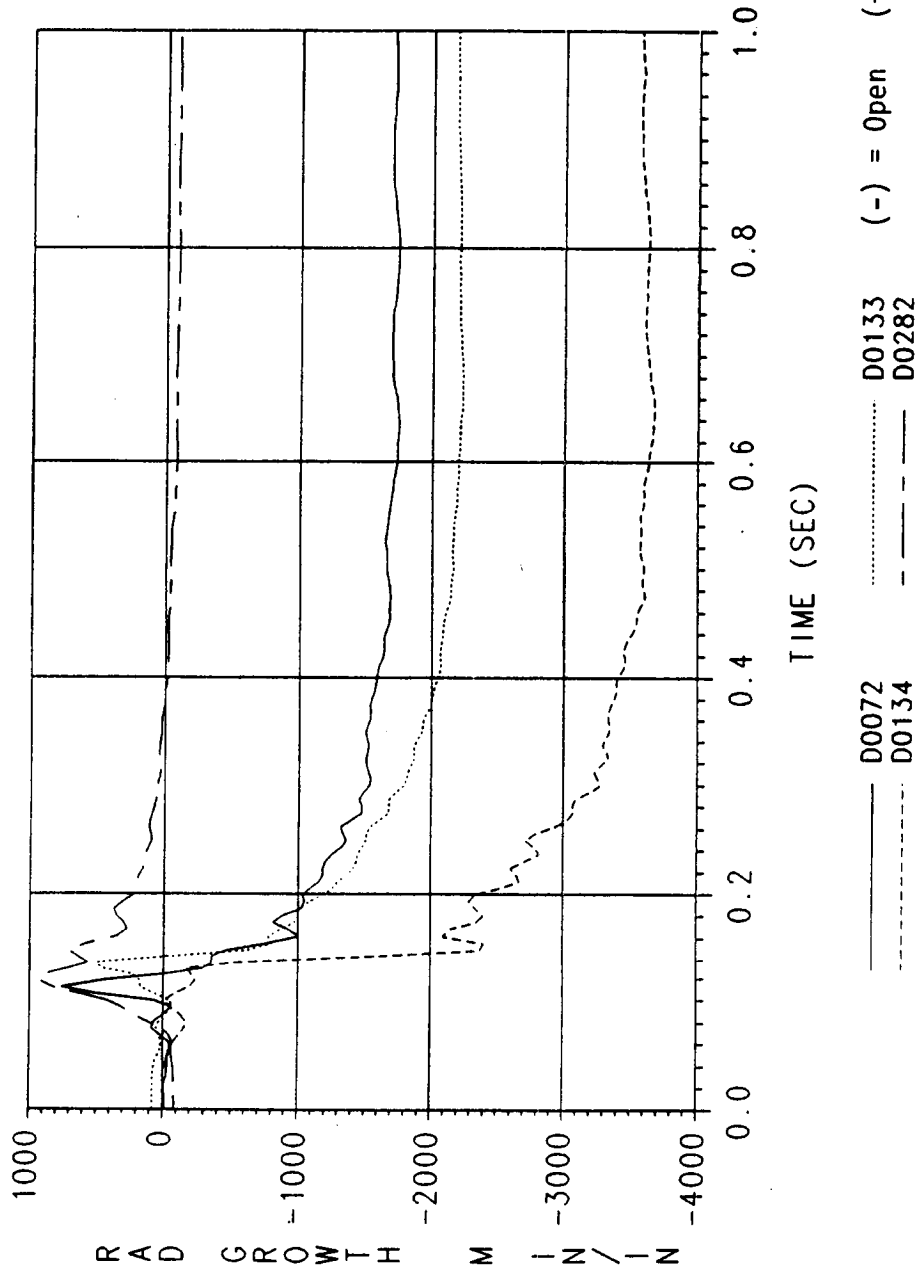


Figure 7.2-27. TPTA 1.1 Case Girth Gages (0-1 sec)

TPTA 1.1 FINAL

D0072(STAT= 535.03) D0133(STAT=1511.48)
D0134(STAT=1555.48) D0282(STAT= 530.07)
19 NOVEMBER 1987

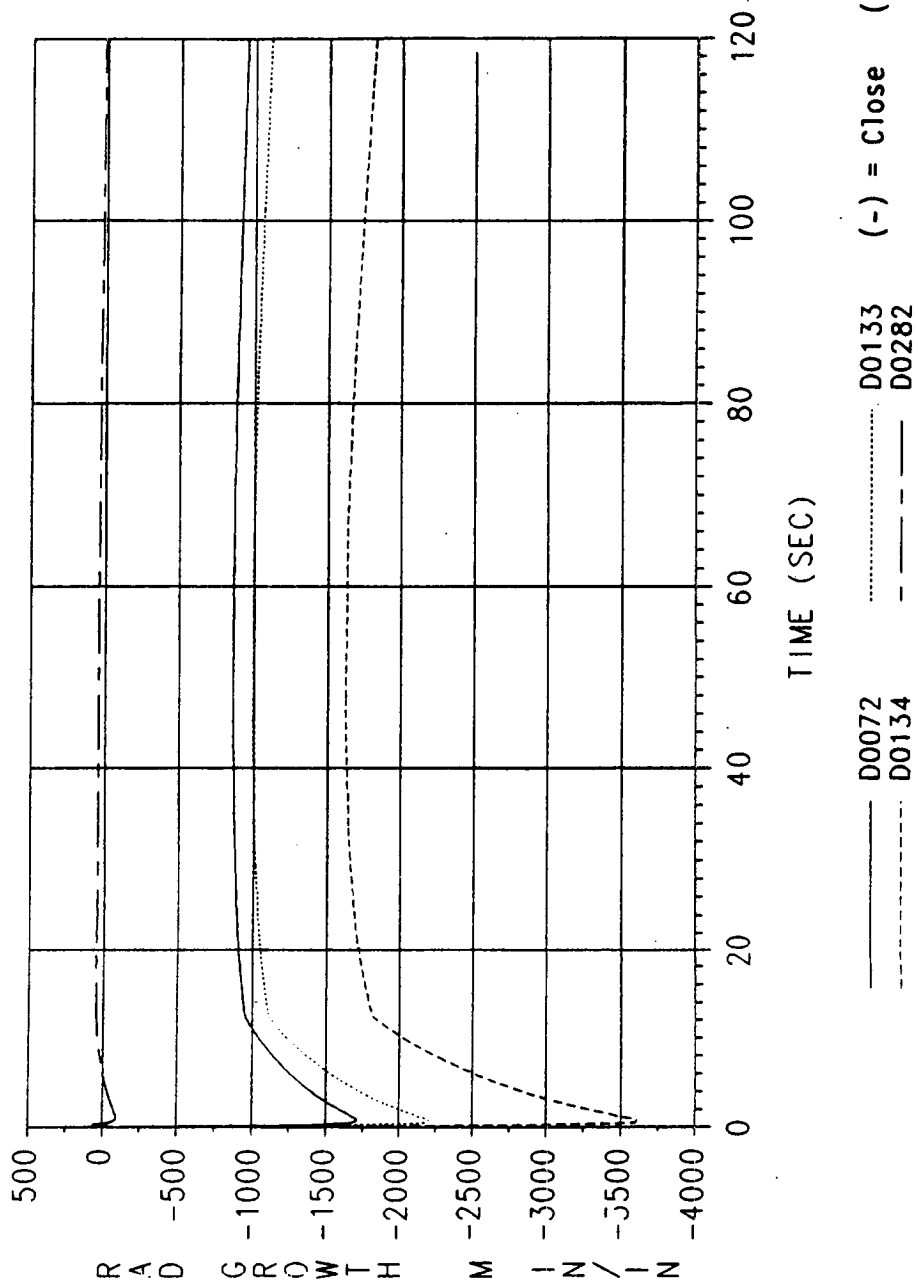


Figure 7.2-28. TPTA 1.1 Case Girth Gages (0-30 sec)

spike, but still indicate a value maximum peak-to-peak radial growth consistent with the joint gages. Table 7.2-46 lists membrane girth gage data for the TPTA 1.1A test.

Case Membrane Strain Gages

Hoop and axial strain gages were mounted in three different circumferential locations: 21 in. above Joint A on the forward cylinder, 21 in. below Joint A on the aft cylinder, and 21 in. above Joint B on the aft cylinder. Table 7.2-47 displays the hoop and axial strains measured as well as stress calculated from the strains. Examining the measurements indicates that the values are consistent. Table 7.2-48 lists membrane strain gage data for the TPTA 1.1A test.

7.2.3.5 Nontest Joint Instrumentation Measurements

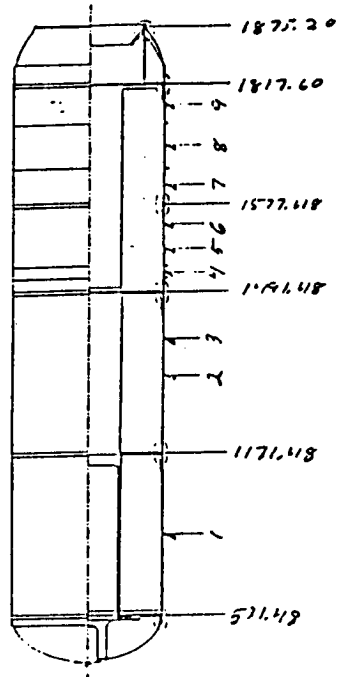
Joint E Forward Dome/Forward Cylinder

This joint is the original HPM design and was fully vented. The primary groove contained a fluorocarbon O-ring and the secondary groove contained a polysiloxane O-ring. At the 0-deg location, a pressure and temperature gage monitored the pressure and temperature between the primary and secondary O-rings. At the 317-deg location, a displacement gage measured the gap opening at the land between the primary and secondary O-rings. This joint was conditioned to 84 and 89°F prior to the static test firing and high Q tests, respectively.

During the TPTA 1.1 test, the maximum pressure recorded was 19.5 psia and the maximum temperature recorded was 85.0°F at the inter-O-ring location. The maximum inter-O-ring deflection recorded was 0.009 in. open. Analysis predicted an opening of 0.000 in. with full shims installed. Full shims of 0.050 in. were installed in this joint. This joint performed as expected with no anomalies. During the TPTA 1.1A test, the maximum inter-O-ring pressure and temperature were 18.0 psia and 88°F, respectively. The maximum inter-O-ring opening was 0.003 inch. All instrumentation readings are recorded in Tables 7.2-49 through 7.2-54.

Table 7.2-46. TPTA 1.1A Case Membrane Girth Gage Data

TEST NAME: TPTA 1.1A
JOINT: CASE
DESCRIPTION: GIRTH GAGE SUMMARY
MODEL PRESSURE
THE TIME RANGE IS 9.0 TO 14.0 SECONDS



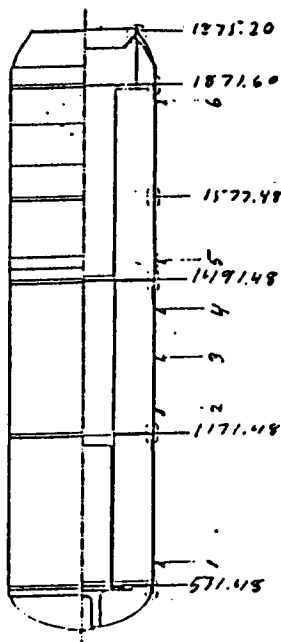
GIRTH GAGE LOCATION	GAGE NUMBER	STATION	RADIUS (IN)	RADIAL GROWTH (IN)	TEST STRAIN (UTN/IN)
1	D0063	611.5	73.1	-0.194	-2653
2	D0032	1251.5	73.1	-0.192	-2629
3	D0132	1286.5	73.1	-0.189	-2587
4	D0133	1511.5	73.1	-0.123	-1686
5	D0033	1533.5	73.1	ND	ND
6	D0134	1555.5	73.1	-0.188	-2576
7	D0135	1596.5	73.1	-0.179	-2445
8	D0136	1634.6	73.1	ND	ND
9	D0137	1674.3	73.1	-0.181	-2473

ND = No data

ORIGINAL PAGE IS
OF POOR QUALITY

Table 7.2-48. TPTA 1.1A Case Membrane Strain Gage Data

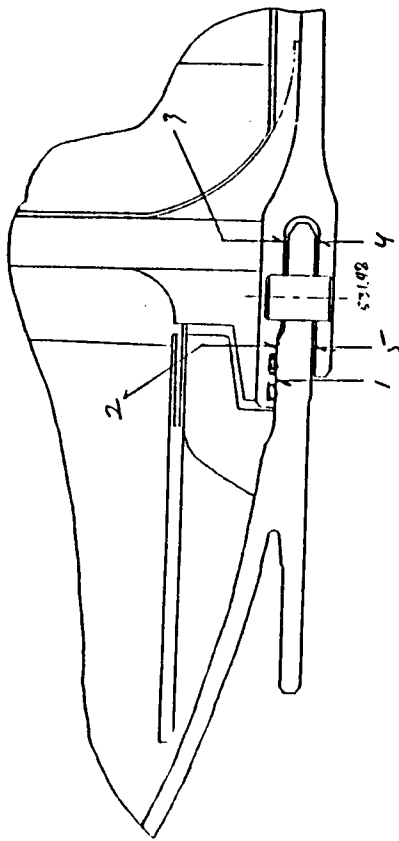
TEST NAME:		TPTA 1.1A		CASE		BIAXIAL GAGES		THE TIME RANGE IS 9.0 TO 14.0 SECONDS		TEST DATA		TEST DATA	
JOINT DESCRIPTION:		ANGULAR LOCATION		HOOP GAGE		AXIAL GAGE		HOOP STRESS (KSI)		AXIAL STRESS (KSI)		HOOP STRAIN (UIN/IN)	
LOCAT		LOCATION		GAGE		GAGE		STRESS (KSI)		STRESS (KSI)		STRAIN (UIN/IN)	
1	0.0	S0471	S0470	-96.2	-49.6	-2710	-691	-2710	-691	-2710	-691	-2710	-691
1	82.0	S0473	S0472	-90.0	-46.9	-2532	-664	-2532	-664	-2532	-664	-2532	-664
1	180.0	S0475	S0474	-94.8	-51.6	-2645	-771	-2645	-771	-2645	-771	-2645	-771
1	270.0	S0477	S0476	-99.2	-52.1	-2786	-745	-2786	-745	-2786	-745	-2786	-745
		AVERAGE:		-95.1	-50.1	-2668	-718	-2668	-718	-2668	-718	-2668	-718
2	0.0	S0479	S0478	-86.9	-48.1	-2416	-735	-2416	-735	-2416	-735	-2416	-735
2	82.0	S0481	S0480	-96.0	-52.6	-2673	-794	-2673	-794	-2673	-794	-2673	-794
2	180.0	S0483	S0482	-90.8	-50.7	-2520	-782	-2520	-782	-2520	-782	-2520	-782
2	270.0	S0485	S0484	-92.2	-48.8	-2584	-705	-2584	-705	-2584	-705	-2584	-705
		AVERAGE:		-91.5	-50.0	-2548	-754	-2548	-754	-2548	-754	-2548	-754
3	9.0	S0775	S0743	-46.5	-91.8	-630	-2596	-630	-2596	-630	-2596	-630	-2596
3	16.0	S0776	S0744	-50.8	-98.6	-708	-2780	-708	-2780	-708	-2780	-708	-2780
3	23.0	S0777	S0745	-53.7	-99.4	-796	-2776	-796	-2776	-796	-2776	-796	-2776
3	30.0	S0778	S0746	-58.7	-109.4	-863	-3058	-863	-3058	-863	-3058	-863	-3058
3	43.0	S0779	S0747	-51.7	-98.6	-738	-2721	-738	-2721	-738	-2721	-738	-2721
3	55.0	S0780	S0748	-47.2	-92.8	-647	-2670	-647	-2670	-647	-2670	-647	-2670
3	70.0	S0781	S0749	-46.8	-92.7	-632	-2624	-632	-2624	-632	-2624	-632	-2624
3	99.0	S0782	S0750	-54.4	-101.7	-798	-2846	-798	-2846	-798	-2846	-798	-2846
3	112.0	S0783	S0751	-48.2	-88.4	-724	-2463	-724	-2463	-724	-2463	-724	-2463
3	117.0	S0784	S0752	-48.8	-94.8	-677	-2674	-677	-2674	-677	-2674	-677	-2674
3	122.0	S0785	S0753	-47.2	-88.3	-690	-2472	-690	-2472	-690	-2472	-690	-2472
3	135.0	S0786	S0754	-53.6	-97.7	-811	-2719	-811	-2719	-811	-2719	-811	-2719
3	155.0	S0787	S0755	-53.2	-100.6	-768	-2820	-768	-2820	-768	-2820	-768	-2820
3	160.0	S0788	S0756	-52.9	-100.4	-761	-2817	-761	-2817	-761	-2817	-761	-2817
3	220.0	S0789	S0757	-54.2	-106.1	-745	-2996	-745	-2996	-745	-2996	-745	-2996
3	266.0	S0790	S0758	-60.6	-120.1	-819	-3398	-819	-3398	-819	-3398	-819	-3398
3	308.0	S0791	S0759	-49.0	-95.5	-679	-2694	-679	-2694	-679	-2694	-679	-2694
3	320.0	S0792	S0760	-54.2	-99.1	-814	-2763	-814	-2763	-814	-2763	-814	-2763
		AVERAGE:		-51.8	-98.7	-739	-2772	-739	-2772	-739	-2772	-739	-2772
4	0.0	S0487	S0486	-46.6	-83.3	-722	-2310	-722	-2310	-722	-2310	-722	-2310
4	82.0	S0489	S0488	-93.0	-52.2	-2577	-811	-2577	-811	-2577	-811	-2577	-811
4	180.0	S0491	S0490	-86.0	-47.7	-2389	-729	-2389	-729	-2389	-729	-2389	-729
4	270.0	S0493	S0492	-95.5	-53.2	-2551	-817	-2551	-817	-2551	-817	-2551	-817
		AVERAGE:		-80.3	-59.1	-2085	-1167	-2085	-1167	-2085	-1167	-2085	-1167



TEST DATA		TEST DATA		TEST DATA		TEST DATA		TEST DATA		TEST DATA		TEST DATA	
HOOP STRESS (KSI)		AXIAL STRESS (KSI)		HOOP STRAIN (UIN/IN)		AXIAL STRAIN (UIN/IN)		HOOP STRESS (KSI)		AXIAL STRESS (KSI)		HOOP STRAIN (UIN/IN)	
5	9.0	S0761	S0793	-68.1	-56.8	-1702	-1211	5	16.0	S0762	S0794	-68.3	-56.8
5	23.0	S0763	S0795	-65.1	-53.0	-1683	-1211	5	30.0	S0764	S0796	-65.1	-53.0
5	30.0	S0765	S0797	-66.1	-51.1	-1692	-1104	5	43.0	S0766	S0798	-66.1	-51.1
5	55.0	S0767	S0799	-67.9	-52.4	-1750	-1026	5	70.0	S0768	S0800	-67.9	-52.4
5	99.0	S0769	S0801	-67.4	-51.8	-1699	-1042	5	112.0	S0770	S0802	-67.4	-51.8
5	117.0	S0771	S0803	-67.8	-53.2	-1714	-1063	5	122.0	S0772	S0804	-67.8	-53.2
5	135.0	S0773	S0805	-66.7	-53.6	-1659	-1099	5	155.0	S0774	S0806	-66.7	-53.6
5	160.0	S0775	S0807	-64.7	-55.0	-1673	-1128	5	220.0	S0776	S0808	-64.7	-55.0
5	220.0	S0777	S0809	-64.5	-52.2	-1628	-1165	5	255.0	S0778	S0810	-64.5	-52.2
5	266.0	S0779	S0811	-65.2	-63.3	-1613	-1598	5	308.0	S0780	S0812	-65.2	-63.3
5	308.0	S0781	S0813	-68.3	-60.0	-1676	-1613	5	320.0	S0782	S0814	-68.3	-60.0
		AVERAGE:		-69.7	-57.8	-1747	-1229			AVERAGE:		-65.7	-54.8
6	0.0	S0503	S0502	-46.4	-38.9	-1157	-834	6	82.0	S0504	S0503	-46.4	-38.9
6	180.0	S0505	S0504	-86.3	-40.5	-2472	-486	6	270.0	S0506	S0505	-86.3	-40.5
6	270.0	S0507	S0506	-93.0	-57.5	-2526	-985	6		S0508	S0507	-93.0	-57.5
6		S0509	S0508	-47.5	-96.3	-620	-2735	6		AVERAGE:		-68.3	-58.3
		AVERAGE:		-68.3	-58.3	-1694	-1260			AVERAGE:		-68.3	-58.3

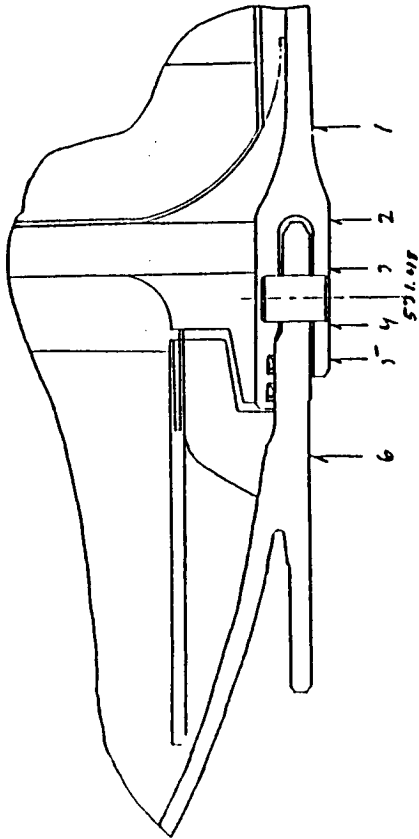
Table 7.2-49. TPTA 1.1 Joint E Maximum Deflections

TEST NAME: TPTA 1.1
JOINT: E
DESCRIPTION: DISPLACEMENT SUMMARY
MODEL PRESSURE: 913.3 PSIA
MAXIMUM PRESSURE: 909.7 PSIA
DESIRED PRESSURE: 913.3 PSIA
TIME PRESSURE OCCURRED: 0.6 SECONDS



LOCAT	FROM STATION	TO STATION	GAGE NUMBER	ANGULAR LOCATION	DEFLECTION (IN)
1	529.8		D0276	317.0	-0.009 OPEN
2	530.4		D0277	319.0	-0.008 OPEN
3	532.7		D0278	321.0	0.003 CLOSE
4	532.7		D0279	319.0	-0.032 OPEN
5	530.4		D0280	321.0	-0.012 OPEN

Table 7.2-50. TPTA 1.1 Joint E Radial Growth



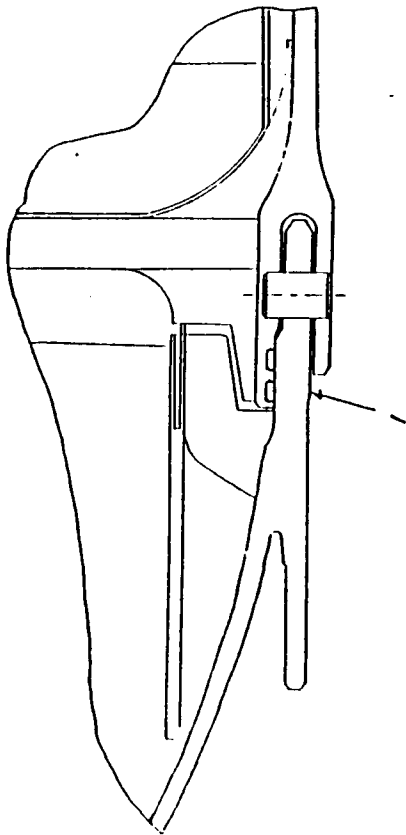
TEST NAME: TPTA 1.1
JOINT: E
DESCRIPTION: GIRTH GAGE SUMMARY
MODEL PRESSURE: 913.3 PSIA
MAXIMUM PRESSURE: 909.7 PSIA
DESIRED PRESSURE: 913.3 PSIA
TIME PRESSURE OCCURED: 0.6 SECONDS

GIRTH GAGE LOCATION	GAGE NUMBER	STATION	RADIUS (IN)	RADIAL GROWTH (IN)	TEST STRAIN (UTN/TN)
1	D0072	535.0	73.1	-0.127	-1736
2	D0285	533.2	73.4	-0.085	-1151
3	D0284	532.3	73.4	ND	ND
4	D0283	530.8	73.4	-0.021	-290
5	D0282	530.1	73.4	-0.006	-77
6	D0069	528.0	73.1	0.051	693

ND = No data

Table 7.2-51. TPTA 1.1 Joint E Stress

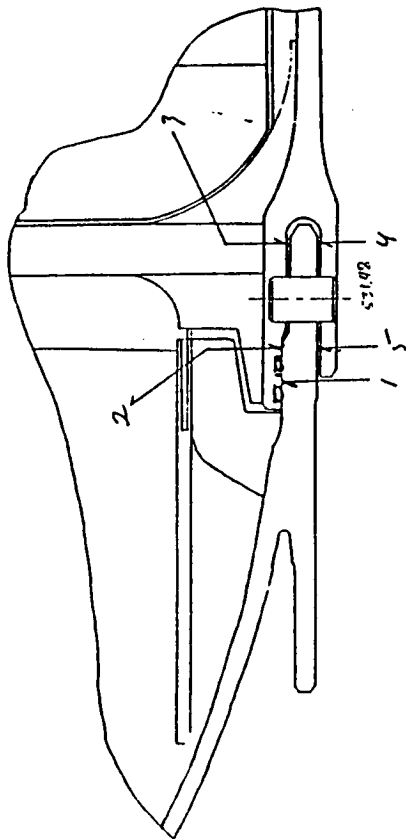
TEST NAME: TPTA 1.1
JOINT: E
DESCRIPTION: BIAXIAL GAGES
MODEL PRESSURE 913.3 PSIA
MAXIMUM PRESSURE: 909.7 PSIA
DESIRED PRESSURE: 913.3 PSIA
TIME PRESSURE OCCURED: 0.6 SECONDS



LOCAT	ANGULAR LOCATION	HOOP GAGE	AXIAL GAGE	HOOP STRESS (KSI)	AXIAL STRESS (KSI)	TEST DATA	
						HOOP STRAIN (UTIN/IN)	AXIAL STRAIN (UTIN/IN)
1	320.0	S0298	S0297	10.0	7.6	257	153

(+) = Compression
(-) = Tension

Table 7.2-52. TPTA 1.1A Joint E Maximum Deflections

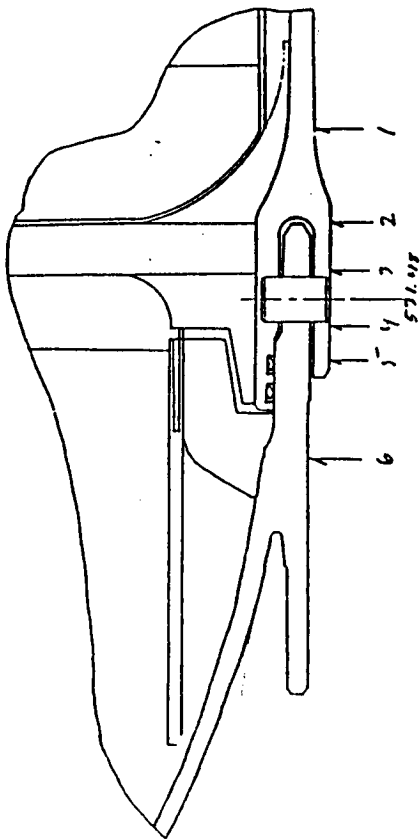


TEST NAME: TPTA 1.1A
JOINT: E
DESCRIPTION: DISPLACEMENT SUMMARY
MODEL PRESSURE
THE TIME RANGE IS 9.0 TO 14.0 SECONDS

LOCAT	FROM STATION	TO STATION	GAGE NUMBER	ANGULAR LOCATION	DEFLECTION (IN)
1	529.8		D0276	317.0	-0.003 OPEN
2	530.4		D0277	319.0	0.002 CLOSE
3	532.7		D0278	321.0	0.002 CLOSE
4	532.7		D0279	319.0	-0.009 OPEN
5	530.4		D0280	321.0	0.001 CLOSE

(+) = Compression
(-) = Tension

Table 7.2-53. TPTA 1.1A Joint E Radial Growth

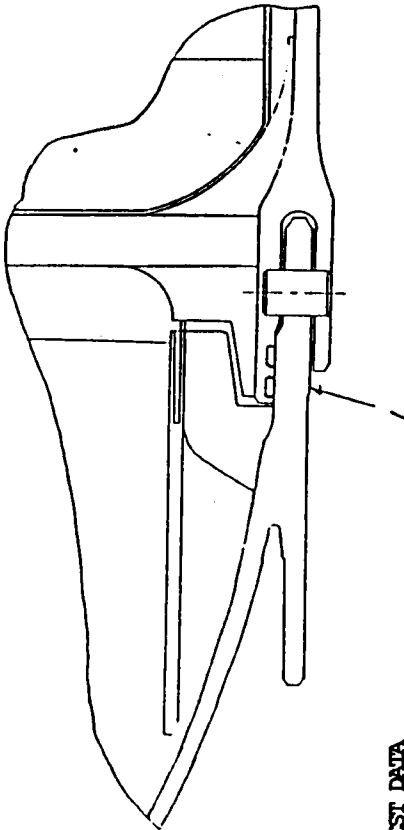


TEST NAME: TPTA 1.1A
JOINT: E
DESCRIPTION: GIRTH GAGE SUMMARY
THE TIME RANGE IS 9.0 TO 14.0 SECONDS

GIRTH GAGE LOCATION	GAGE NUMBER	STATION	RADIUS (IN)	RADIAL GROWTH (IN)	TEST STRAIN (UIN/IN)
1	D0072	535.0	73.1	-0.088	-1210
2	D0285	533.2	73.4	-0.061	-833
3	D0284	532.3	73.4	ND	ND
4	D0283	530.8	73.4	-0.030	-412
5	D0282	530.1	73.4	-0.021	-290
6	D0069	528.0	73.1	0.114	1567

(+) = Compression
(-) = Tension

Table 7.2-54. TPTA 1.1A Joint E Stress



TEST NAME: TPTA 1.1A
JOINT: E
DESCRIPTION: BIAXIAL GAGES
THE TIME RANGE IS 9.0 TO 14.0 SECONDS

LOCAT	ANGULAR LOCATION	HOOP GAGE	HOOP GAGE	AXIAL GAGE	HOOP STRESS (KSI)	AXIAL STRESS (KSI)	TEST DATA	
							HOOP STRAIN (UIN/IN)	AXIAL STRAIN (UIN/IN)
1	320.0	S0298	S0297		6.1	13.0	73	372

(+) = Compression
(-) = Tension

Joint C ETA Segment/Aft Dome

This joint was a nonvented factory joint with fluorocarbon primary and secondary O-rings. This joint had inert propellant. In both the TPTA 1.1 and 1.1A tests, the inert propellant was the pressure face. There was no damage to the O-rings. This joint was not conditioned for the tests. The pretest temperatures were 50 and 64°F for the TPTA 1.1 and 1.1A tests, respectively.

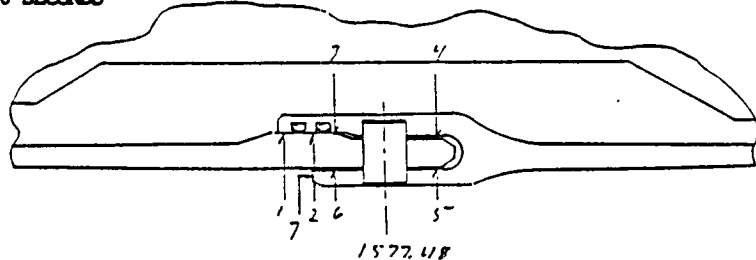
During the TPTA 1.1 test, the maximum inter-O-ring gap deflection was 0.002 in. open, while during the TPTA 1.1A test, the maximum inter-O-ring gap opening was 0.004 inch. Tables 7.2-55 through 7.2-60 list all the major instrumentation recordings for the TPTA 1.1 and 1.1A tests.

Joint F Stiffener Segment/Aft Dome

Joint F was an original HPM design that was fully vented. The primary O-ring was fluorocarbon, while an unsaturated polysiloxane O-ring was used in the secondary O-ring groove. The conditioned pretest temperatures were 84 and 89°F for the TPTA 1.1 and 1.1A tests, respectively. Tables 7.2-61 through 7.2-63 contain all the instrumentation data in this joint for the TPTA 1.1 test. Pressure was incident on the primary O-ring, which sealed without damage. The maximum gap opening was 0.006 in. for the TPTA 1.1 test and 0.007 in. for the TPTA 1.1A test. Tables 7.2-64 through 7.2-66 list data for the TPTA 1.1A test.

Table 7.2-55. TPTA 1.1 Joint C Maximum Deflections

TEST NAME: TPTA 1.1
 JOINT: C
 DESCRIPTION: DISPLACEMENT SUMMARY
 MODEL PRESSURE: 896.2 PSIG
 THE TIME RANGE IS 0.0 TO 6.0 SECONDS



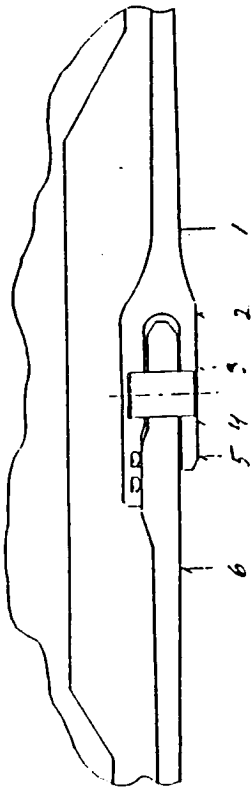
LOCAT	FROM STATION	TO STATION	GAGE NUMBER	ANGULAR LOCATION	DEFLECTION (IN)
1	1575.2		D0200	63.0	-0.003 OPEN
1	1575.2		D0201	121.0	-0.004 OPEN
1	1575.2		D0202	223.0	0.001 CLOSE
1	1575.2		D0203	323.0	-0.002 OPEN
2	1575.8		D0204	57.0	-0.002 OPEN
2	1575.8		D0205	117.0	-0.002 OPEN
2	1575.8		D0206	217.0	0.002 CLOSE
2	1575.8		D0207	317.0	0.003 CLOSE
3	1576.4		D0208	59.0	0.010 CLOSE
3	1576.4		D0209	117.0	0.013 CLOSE
3	1576.4		D0210	219.0	0.009 CLOSE
3	1576.4		D0211	319.0	0.009 CLOSE
4	1578.7		D0212	61.0	***** CLOSE
4	1578.7		D0213	119.0	0.004 CLOSE
4	1578.7		D0214	221.0	0.004 CLOSE
4	1578.7		D0215	321.0	0.004 CLOSE
5	1578.7		D0216	59.0	-0.008 OPEN
5	1578.7		D0217	117.0	-0.011 OPEN
5	1578.7		D0218	219.0	-0.013 OPEN
5	1578.7		D0219	319.0	-0.015 OPEN
6	1576.4		D0220	61.0	0.005 CLOSE
6	1576.4		D0221	119.0	0.007 CLOSE
6	1576.4		D0222	221.0	0.004 CLOSE
6	1576.4		D0223	321.0	0.003 CLOSE
7	1575.8		D0224	60.0	ND
7	1575.8		D0225	118.0	ND
7	1575.8		D0226	220.0	ND
7	1575.8		D0227	320.0	ND

ND = No data

***** = No data

Table 7.2-56. TPTA 1.1 Joint C Radial Growth

TEST NAME: TPTA 1.1
JOINT: C
DESCRIPTION: GIRTH GAGE SUMMARY
MODEL PRESSURE: 896.2 PSIG
THE TIME RANGE IS 0.0 TO 6.0 SECONDS

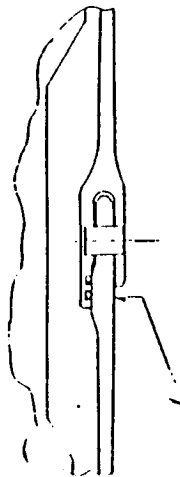
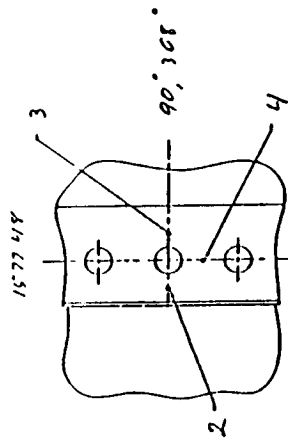


GIRTH GAGE LOCATION	GAGE NUMBER	STATION	RADIUS (IN)	RADIAL GROWTH (IN)	TEST STRAIN (UIN/IN)
1	D0233	1581.0	73.1	-0.186	-2549
2	D0232	1579.2	73.4	-0.179	-2436
3	D0231	1578.3	73.4	-0.174	-2368
4	D0230	1576.8	73.4	-0.165	-2242
5	D0229	1576.1	73.4	ND	ND
6	D0228	1574.0	73.1	-0.179	-2454

ND = No data

Table 7.2-57. TPTA 1.1 Joint C Stresses

TEST NAME: TPTA 1.1
JOINT: C
DESCRIPTION: BIAXIAL GAGES
MODEL PRESSURE: 896.2
THE TIME RANGE IS 0.0 TO 6.0 SECONDS

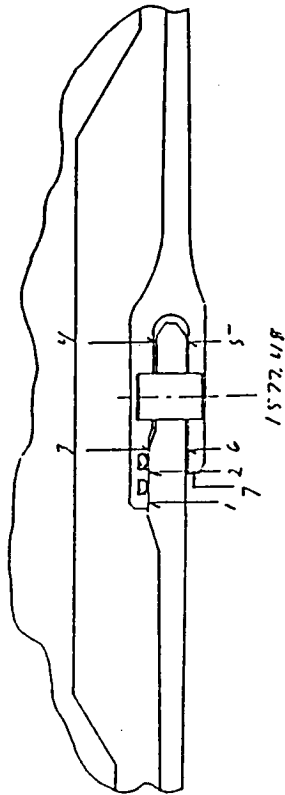


LOCAT	ANGULAR LOCATION	HOOP GAGE	AXIAL GAGE	HOOP STRESS (KSI)	AXIAL STRESS (KSI)	TEST DATA	
						HOOP STRAIN (UIN/IN)	AXIAL STRAIN (UIN/IN)
1	60.0	S0254	S0253	-89.4	-56.1	-2418	-978
1	118.0	S0256	S0255	-97.5	-53.6	-2715	-813
1	220.0	S0258	S0257	-159.0	-303.9	-2261	-8539
1	320.0	S0260	S0259	-90.3	-57.5	-2435	-1012
			AVERAGE:	-109.1	-117.8	-2457	-2835
2	90.0	S0362	S0361	-95.1	32.1	-3490	2020
			AVERAGE:	-95.1	32.1	-3490	2020
3	90.0	S0366	S0365	-28.0	-17.2	-760	-294
			AVERAGE:	-28.0	-17.2	-760	-294
4	91.0	S0368	S0367	-45.2	-56.9	-938	-1445
			AVERAGE:	-45.2	-56.9	-938	-1445
2	308.0	S0370	S0369	-106.0	33.4	-3869	2174
			AVERAGE:	-106.0	33.4	-3869	2174
3	308.0	S0374	S0373	-94.1	-43.2	-2705	-500
			AVERAGE:	-94.1	-43.2	-2705	-500
4	309.0	S0376	S0375	-46.9	-59.4	-968	-1513
			AVERAGE:	-46.9	-59.4	-968	-1513

(+) = Compression
(-) = Tension

Table 7.2-58. TPTA 1.1A Joint C Maximum Deflection

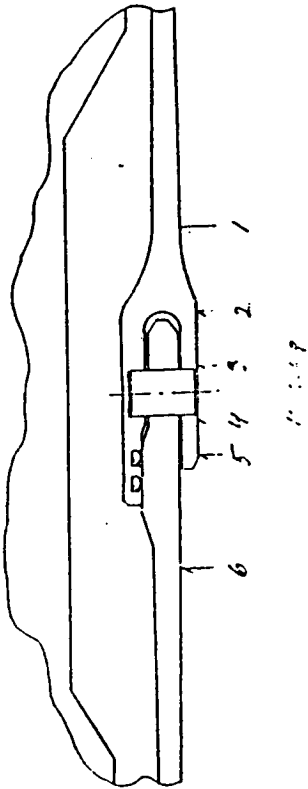
TEST NAME: TPTA 1.1A
JOINT: C
DESCRIPTION: DISPLACEMENT SUMMARY
MODEL PRESSURE
THE TIME RANGE IS 9.0 TO 14.0 SECONDS



LOCAT	FROM STATION	TO STATION	GAGE NUMBER	ANGULAR LOCATION	DEFLECTION (IN)
1	1575.2		D0200	63.0	-0.006 OPEN
1	1575.2		D0201	121.0	-0.004 OPEN
1	1575.2		D0202	223.0	-0.003 OPEN
1	1575.2		D0203	323.0	-0.004 OPEN
2	1575.8		D0204	57.0	-0.002 OPEN
2	1575.8		D0205	117.0	-0.002 OPEN
2	1575.8		D0206	217.0	-0.003 OPEN
2	1575.8		D0207	317.0	-0.004 OPEN
3	1576.4		D0208	59.0	0.004 CLOSE
3	1576.4		D0209	117.0	0.010 CLOSE
3	1576.4		D0210	219.0	0.005 CLOSE
3	1576.4		D0211	319.0	0.003 CLOSE
4	1578.7		D0212	61.0	ND
4	1578.7		D0213	119.0	0.003 CLOSE
4	1578.7		D0214	221.0	0.003 CLOSE
4	1578.7		D0215	321.0	0.003 CLOSE
5	1578.7		D0216	59.0	-0.004 OPEN
5	1578.7		D0217	117.0	-0.006 OPEN
5	1578.7		D0218	219.0	-0.007 OPEN
5	1578.7		D0219	319.0	-0.005 OPEN
6	1576.4		D0220	61.0	0.005 CLOSE
6	1576.4		D0221	119.0	0.007 CLOSE
6	1576.4		D0222	221.0	0.006 CLOSE
6	1576.4		D0223	321.0	0.005 CLOSE
7	1575.8		D0224	60.0	ND
7	1575.8		D0225	118.0	ND
7	1575.8		D0226	220.0	ND
7	1575.8		D0227	320.0	ND

ND = No data

Table 7.2-59. TPTA 1.1A Joint C Radial Growth



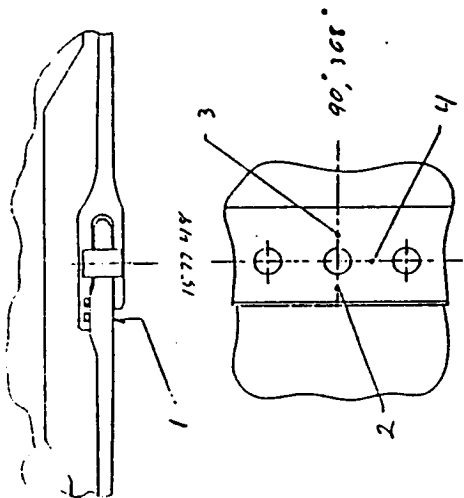
TEST NAME: TPTA 1.1A
JOINT: C
DESCRIPTION: GIRTH GAGE SUMMARY
THE TIME RANGE IS 9.0 TO 14.0 SECONDS

GIRTH GAGE LOCATION	GAGE NUMBER	STATION	RADIUS (IN)	RADIAL GROWTH (IN)	TEST STRAIN (UTN/IN)
1	D0233	1581.0	73.1	-0.126	-1727
2	D0232	1579.2	73.4	-0.120	-1634
3	D0231	1578.3	73.4	-0.116	-1576
4	D0230	1576.8	73.4	-0.109	-1489
5	D0229	1576.1	73.4	ND	ND
6	D0228	1574.0	73.1	-0.122	-1669

ND = No data

Table 7.2-60. TPTA 1.1A Joint C Stresses

TEST NAME: TPTA 1.1A
JOINT: C
DESCRIPTION: BIAXIAL GAGES
THE TIME RANGE IS 9.0 TO 14.0 SECONDS

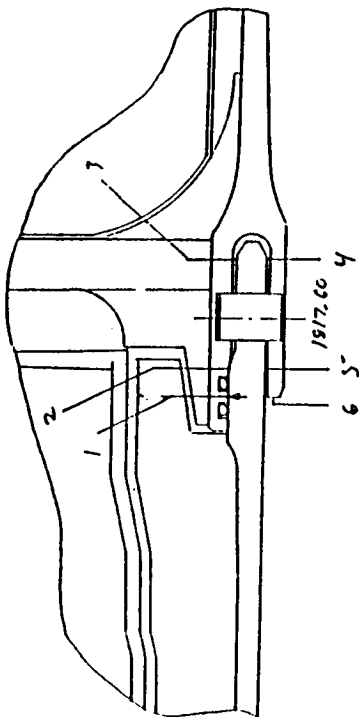


LOCAT	ANGULAR LOCATION	HOOP GAGE	AXIAL GAGE	HOOP STRESS (KSI)	AXIAL STRESS (KSI)	TEST DATA	
						HOOP STRAIN (UIN/IN)	AXIAL STRAIN (UIN/IN)
1	60.0	S0254	S0253	-58.5	-35.6	-1594	-601
1	118.0	S0256	S0255	-64.3	-35.5	-1789	-539
1	220.0	S0258	S0257	-29.9	36.3	-1359	1508
1	320.0	S0260	S0259	-58.2	-35.1	-1589	-587
			AVERAGE:	-52.7	-17.5	-1583	-55
2	90.0	S0362	S0361	-58.7	28.5	-2241	1537
2	308.0	S0370	S0369	-66.8	29.5	-2521	1651
3	90.0	S0366	S0365	-139.6	-46.8	-4187	-163
3	308.0	S0374	S0373	-61.6	-28.3	-1770	-326
4	91.0	S0368	S0367	-27.5	-36.0	-556	-924
4	309.0	S0376	S0375	-28.0	-34.9	-584	-882

(+) = Compression
(-) = Tension

Table 7.2-61. TPTA 1.1 Joint F Maximum Deflections

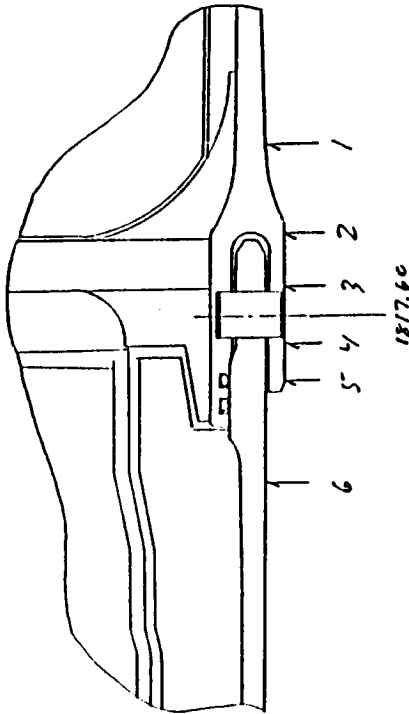
TEST NAME: TPTA 1.1
JOINT: F
DISCREPANCY: 913.3 PSIA
MODEL PRESSURE: 913.3 PSIA
MAXIMUM PRESSURE: 909.7 PSIA
DESIRED PRESSURE: 913.3 PSIA
TIME PRESSURE OCCURED: 0.6 SECONDS



ND = No data

LOCAT	FROM STATION	TO STATION	GAGE NUMBER	ANGULAR LOCATION	DEFLECTION (IN)
1	1815.9		D0292	317.0	-0.006 OPEN
2	1816.6		D0293	319.0	0.002 CLOSE
3	1818.8		D0294	321.0	0.005 CLOSE
4	1818.8		D0295	319.0	-0.015 OPEN
5	1816.6		D0296	321.0	0.001 CLOSE
6	1815.9		D0297	320.0	ND

Table 7.2-62. TPTA 1.1 Joint F Radial Growth



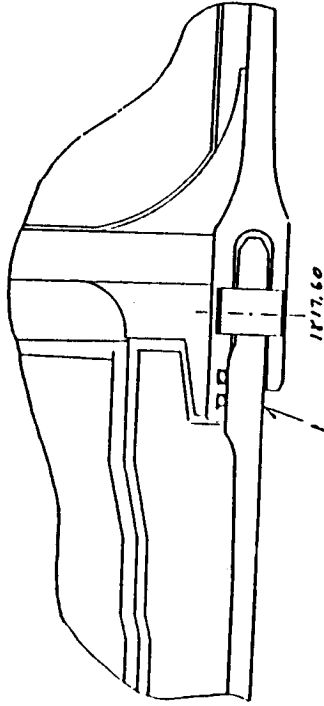
TEST NAME: TPTA 1.1
JOINT: F
DESCRIPTION: GIRTH GAGE SUMMARY
MODEL PRESSURE 913.3 PSIA
MAXIMUM PRESSURE: 909.7 PSIA
DESIRED PRESSURE: 913.3 PSIA
TIME PRESSURE OCCURED: 0.6 SECONDS

GIRTH GAGE LOCATION	GAGE NUMBER	STATION	RADIUS (IN)	RADIAL GROWTH (IN)	TEST STRAIN (UIN/IN)
1	D0075	1821.2	73.1	-0.146	-2003
2	D0301	1819.3	73.4	ND	ND
3	D0300	1818.4	73.4	-0.163	-2213
4	D0299	1816.9	73.4	-0.158	-2151
5	D0298	1816.2	73.4	ND	ND
6	D0073	1812.9	73.1	ND	ND

ND = No data

Table 7.2-63. TPTA 1.1 Joint F Stress

TEST NAME: TPTA 1.1
JOINT: F
DESCRIPTION: BIAXIAL GAGES
MODEL PRESSURE 913.3 PSIA
MAXIMUM PRESSURE: 909.7 PSIA
DESIRED PRESSURE: 913.3 PSIA
TIME PRESSURE OCCURRED: 0.6 SECONDS

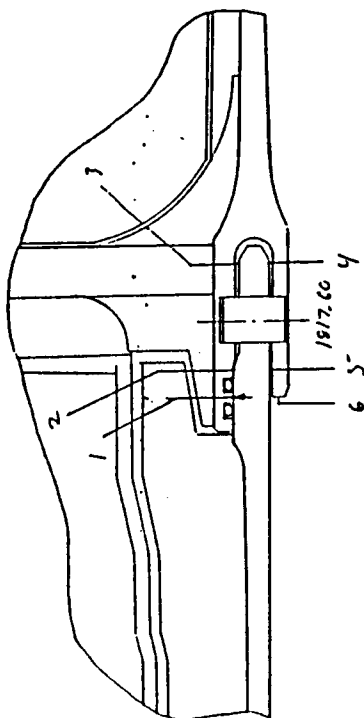


LOCAT	ANGULAR LOCATION	HOOP GAGE	AXIAL GAGE	HOOP STRESS (KSI)	AXIAL STRESS (KSI)	TEST DATA	
						HOOP STRAIN (UIN/IN)	AXIAL STRAIN (UIN/IN)
1	320.0	S0300	S0299	-90.6	-65.2	-2366	-1268
AVERAGE:				-90.6	-65.2	-2366	-1268

(+) = Compression
(-) = Tension

Table 7.2-64. TPTA 1.1A Joint F Maximum Deflections

TEST NAME: TPTA 1.1A
JOINT: F
DESCRIPTION: DISPLACEMENT SUMMARY
MODEL PRESSURE
THE TIME RANGE IS 9.0 TO 14.0 SECONDS

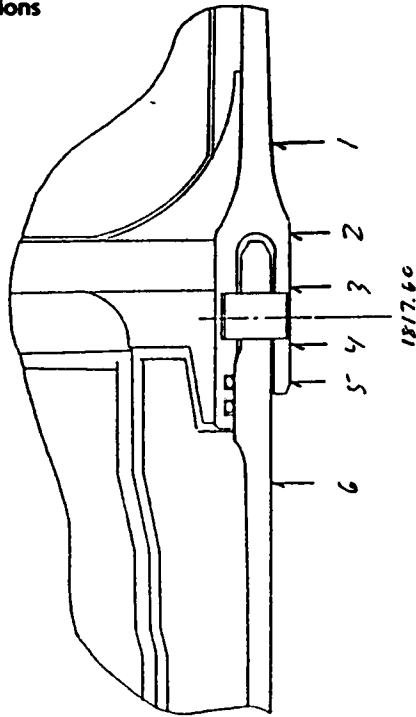


LOCAT	FROM STATION	TO STATION	GAGE NUMBER	ANGULAR LOCATION	DEFLECTION (IN)
1	1815.9		D0292	317.0	-0.007 OPEN
2	1816.6		D0293	319.0	0.002 CLOSE
3	1818.8		D0294	321.0	0.003 CLOSE
4	1818.8		D0295	319.0	-0.013 OPEN
5	1816.6		D0296	321.0	0.002 CLOSE
6	1815.9		D0297	320.0	ND

ND = No data

Table 7.2-65. TPTA 1.1A Joint F Radial Growth

TEST NAME: TPTA 1.1A
JOINT: F
DESCRIPTION: GIRTH GAGE SUMMARY
THE TIME RANGE IS 9.0 TO 14.0 SECONDS

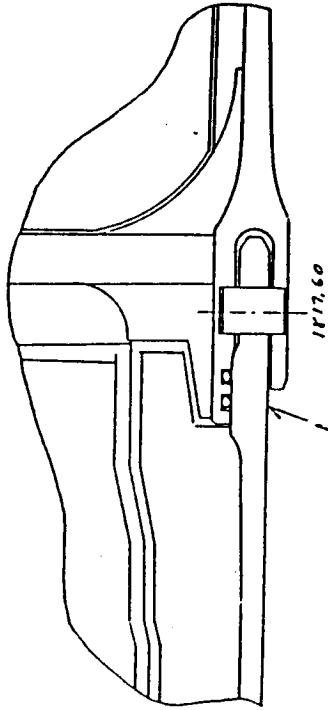


GIRTH GAGE LOCATION	GAGE NUMBER	STATION	RADIUS (IN)	RADIAL GROWTH (IN)	TEST STRAIN (UTN/IN)
1	D0075	1821.2	73.1	-0.099	-1354
2	D0301	1819.3	73.4	ND	ND
3	D0300	1818.4	73.4	-0.107	-1457
4	D0299	1816.9	73.4	-0.108	-1472
5	D0298	1816.2	73.4	ND	ND
6	D0073	1812.9	73.1	ND	ND

ND = No data

Table 7.2-66. TPTA 1.1A Joint F Stress

TEST NAME: TPTA 1.1A
JOINT: F
DESCRIPTION: BIAXIAL GAGES
THE TIME RANGE IS 9.0 TO 14.0 SECONDS



LOCAT	ANGULAR LOCATION	HOOP GAGE	HOOP GAGE	AXIAL GAGE	HOOP STRESS (KSI)	AXIAL STRESS (KSI)	TEST DATA	
							HOOP STRAIN (UIN/IN)	AXIAL STRAIN (UIN/IN)
1	320.0	S0300	S0299	S0299	-63.7	-54.2	-1581	-1169

(+) = Compression
(-) = Tension

7.3 INSULATION EVALUATION

7.3.1 Insulation Objectives

Test objectives of the insulated assemblies were:

- a. Evaluate the DM-8 field joint insulation design during the ignition pressure transient and the high Q condition tests with strut loads applied.
- b. Certify that the nozzle-to-case joint insulation design protects the seals from damage due to the ignition pressure transient.
- c. Evaluate the loads transferred between adjacent insulation components for test joints during disassembly of the bonded joints.

7.3.2 Insulation Conclusions

Conclusions drawn following test evaluation of the TPTA 1.1 test article for insulation are provided in the following paragraphs:

- a. The post-test inspection showed that test Joints A and B sealed properly. Although there were some minor anomalies, damage to the joints and insulation surfaces was minimal. The strut load which was to be applied during the firing malfunctioned and no data were obtained. However, it did function during the high Q test. From the disassembly inspection, it was ascertained that no violation of the J-insulation occurred during the high Q test.
- b. The nozzle-to-case joint also functioned as designed in protecting the O-ring seals from heat effects and degradation. There was a "blowhole" through the bondline, but this only pressurized the wiper O-ring and resulted in no erosion to the seals or NBR.
- c. The loads observed for disassembly were representative of the loads observed during the JES-3 test series. Basically, these were too small to measure accurately, and thus produced no damage to the insulation components.
- d. Dry fits of the joints were made prior to assembly. Joint B showed contact was made along the entire circumference at assembly; however,

Joint A showed very poor contact around the joint circumference, including three areas, each approximately 12 deg circumferential, in which there appeared to be no joint contact. A bore inspection was made after the final mate on Joint A. The gaps then appeared to be a maximum of 1 to 2 deg circumferential with gap openings of approximately 2 to 3 mils. These irregularities caused no anomalies to the function of the joint as it sealed properly.

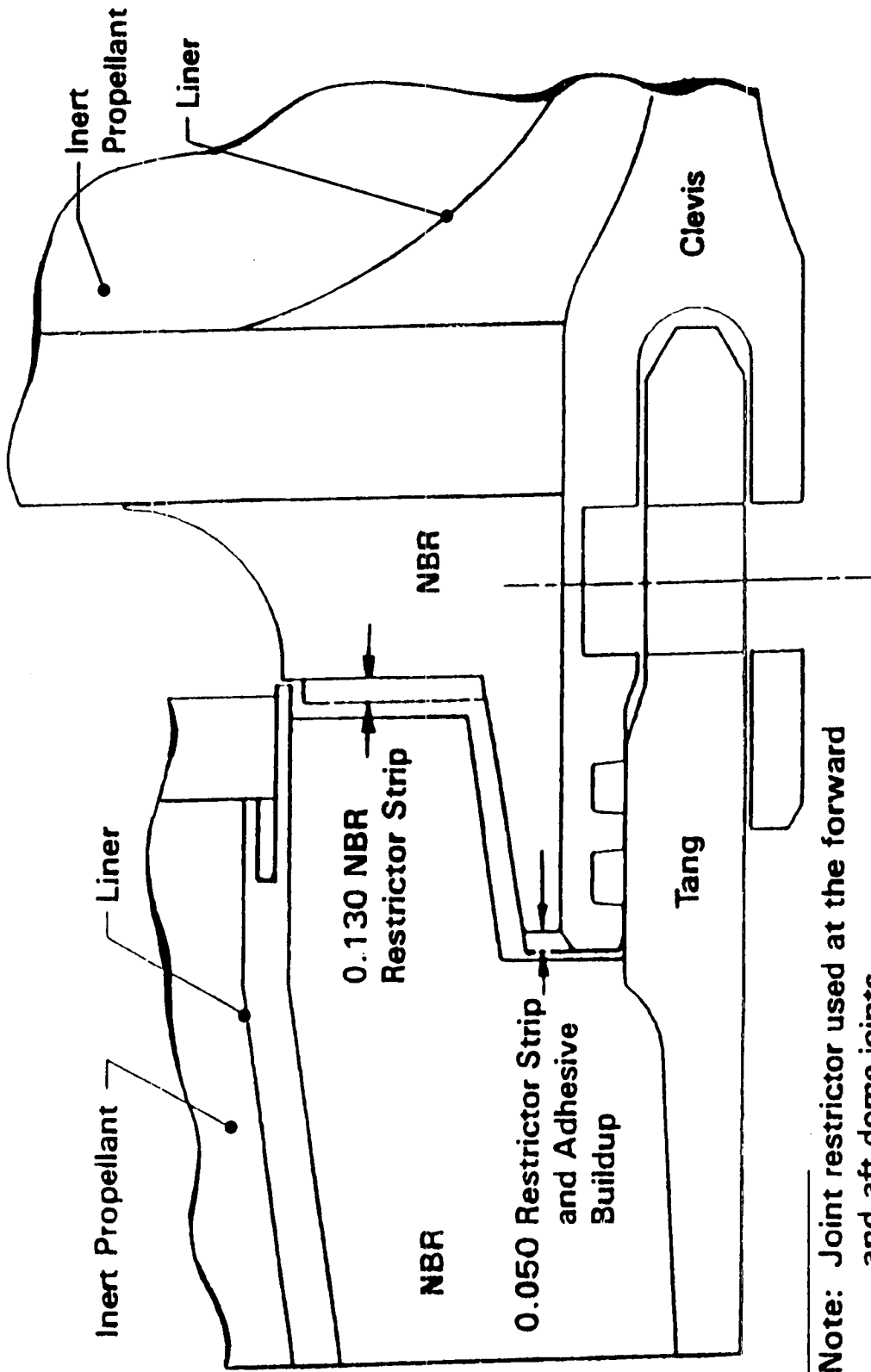
- e. The joint impression test was not used on TPTA 1.1 as it had failed to provide reliable results in previous tests, as in the JES test series.
- f. The increased thickness of insulation in the exposed acreage areas provided good insulation with minimal refurbishment required prior to the next test.

7.3.3 Insulation Results

7.3.3.1 Pretest Test Article Conditions. All segments were new test articles with newly-fabricated insulation. The test article contained the DM-8 baseline J-insulation joint configurations in both test Joints A and B, and the current RSRM configuration nozzle-to-case joint (Joint D) with shorter vent slots. Localized areas of the test joints were made of STW4-2621 (asbestos-filled NBR). Test Joint C, ETA-to-ET stiffener factory joint, was an RSRM baseline nontest joint. A 1.0 in. minimum thickness of NBR was used over all inert propellant with 0.2-in. thick corner patterns. Test Joints E and F were modified HPM configuration nontest joints.

In addition, the following conditions were present on the pretest segment assemblies:

- a. Forward Dome. The forward dome tang was fabricated to the HPM configuration. Since it was a nontest joint, it was made of silica-filled NBR. One unbond condition was found during fabrication and repaired with adhesive.
- b. Forward Cylinder. The forward cylinder clevis (forward dome joint) was fabricated to the HPM configuration using silica-filled NBR. Restrictors were secondarily bonded to the joint face surface (Figure 7.3-1). The silica-filled NBR extrusions used in the clevis end nontest joints were



Note: Joint restrictor used at the forward and aft dome joints

Figure 7.3-1. HPM Configuration - Dome Joints

approaching or had exceeded their initial shelf life prior to cure. Recent experience has shown that silica-filled NBR extrusions have not flowed or bonded well when they approached their shelf life. This led to some unflow conditions on the clevis, as well as a full 360-deg case unbond. The unbond and any serious unflow conditions were repaired with adhesive and brought somewhat back to contour. Since this was a nontest joint, a large amount of time was not spent on returning the joint to drawing specifications. Post-test inspection ensured this had no effect on joint performance.

The forward cylinder tang (Figure 7.3-2) was manufactured as a baseline DM-8 unvented J-insulation configuration. The local area of the joint was made using asbestos-filled NBR.

- c. Aft Cylinder. The aft cylinder tang and clevis joints were fabricated to the baseline DM-8 unvented J-insulation configuration using asbestos-filled NBR in the localized joint areas. The DM-8 clevis joint configuration is shown in Figure 7.3-3. The molded joint surfaces cured differently than anticipated. During layup of the insulation assembly, instrumentation was bonded to the inside diameter (ID) of the inner clevis leg. After cure, it was noted that the NBR did not flow well into these thin areas. Repair areas were filled with asbestos epoxy (STW5-2678) and the joint was hand-worked to restore contour. The restructuring of the clevis occurred largely in the ramp and flat area downstream from the radius, and thus would not be detrimental to the joint assembly (Figure 7.3-4). The areas which were restructured with the epoxy are listed as follows:

<u>Angular Location (deg)</u>	<u>Max Depth From Clevis Edge (Nom 1.14 in.)</u>
0 - 4	2.260
25 - 39	1.313
43 - 52	1.230
57 - 64	1.657
66 - 70	1.278
86 - 92	1.289

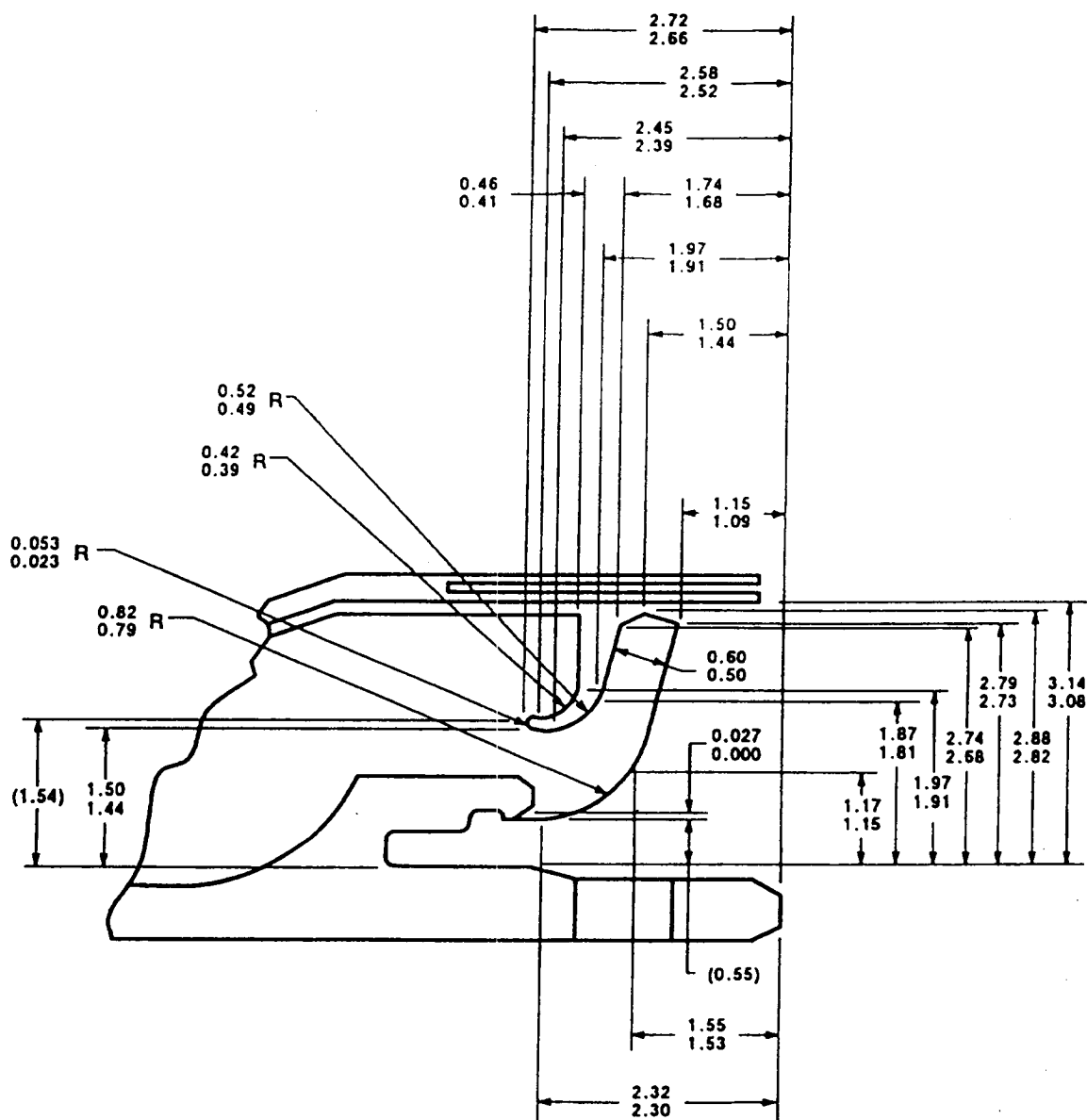


Figure 7.3-2. DM-8 J-insulation Tang Configuration - Insulated Level

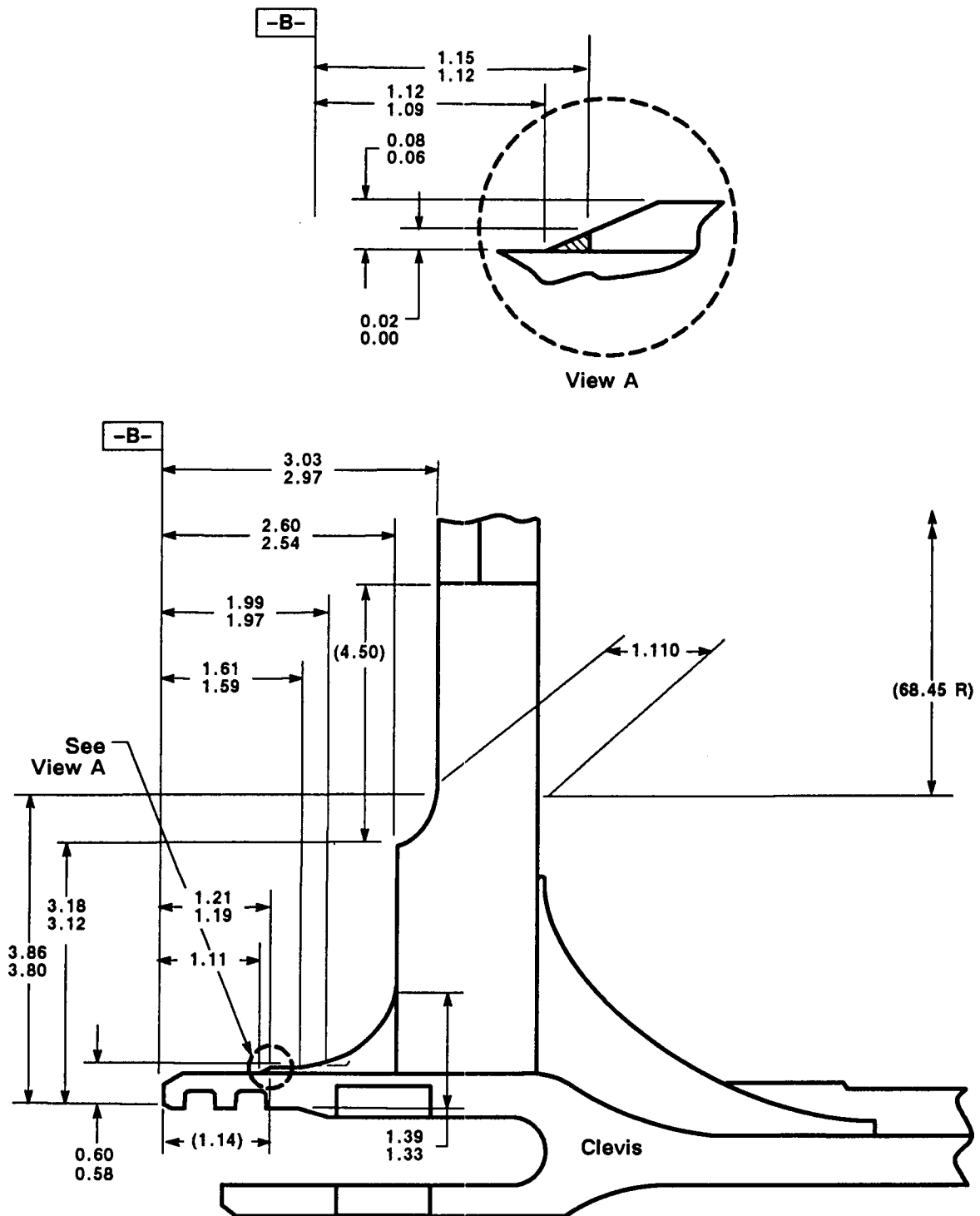


Figure 7.3-3. DM-8 J-insulation Clevis Configuration

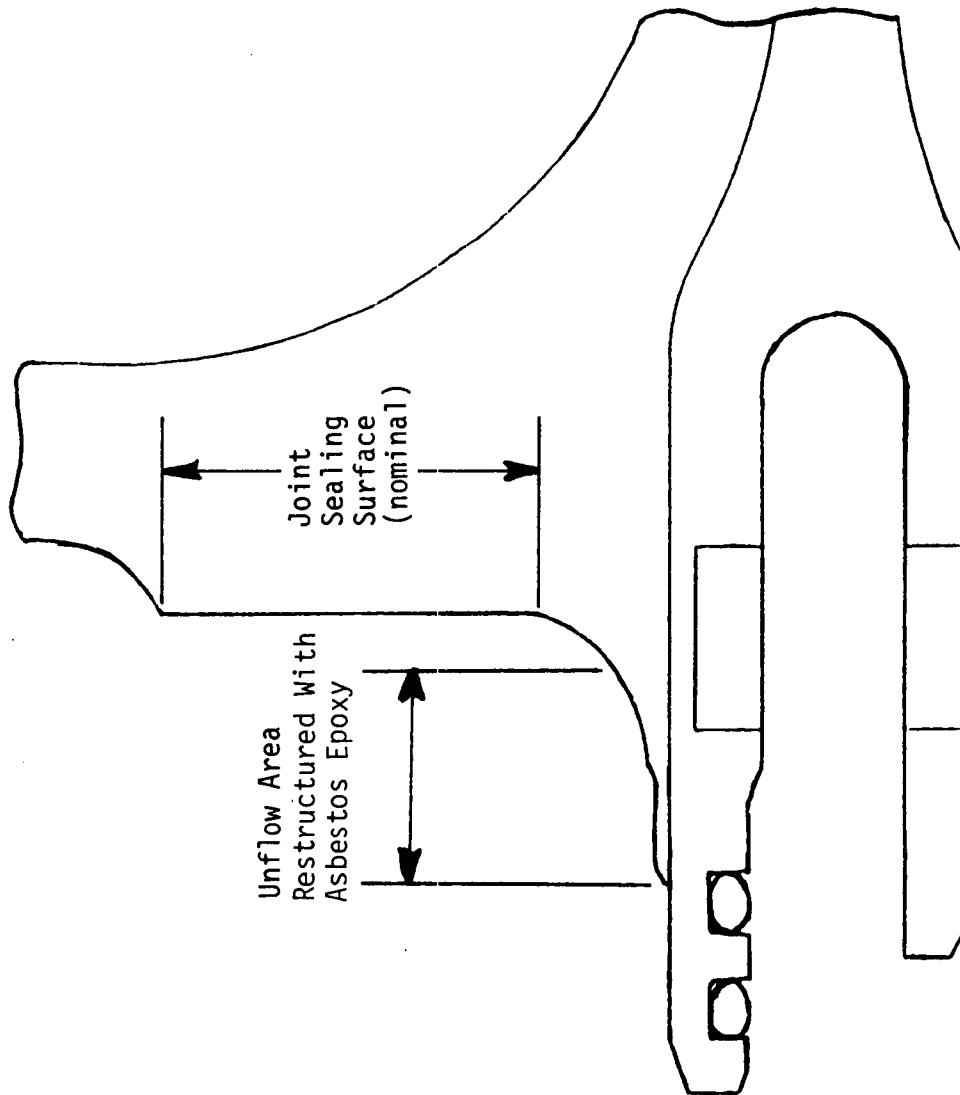


Figure 7.3-4. Joint A Clevis Insulation

<u>Angular Location (deg)</u>	<u>Max Depth From Clevis Edge (Nom 1.14 in.)</u>
94 - 108	1.263
113 - 124	2.165
128 - 132	1.222
237 - 322	2.200
330 - 339	1.570

Due to the hand-working of the clevis, many surfaces were left out of tolerance. These, as well as some out-of-tolerance molded dimensions on the clevis and tang, were compared with DM-8 and JES tolerances and found to be within acceptable limits. This was determined to cause no detrimental effects to the joint assembly and most did not involve the joint sealing surfaces. Section 7.3.3.2 presents a further explanation.

Following the insulation cure process, insulation separations began to form in the clevis joint radius approximately 0.8 in. radially inboard from the ID of the clevis. The separations appeared to be located at the intersection of the NBR plies laid up longitudinally in the radius and the NBR plies laid up radially in the inhibitor (Figure 7.3-5). These separations were intermittent around the entire circumference; however, they were very small and the maximum depth was less than 0.02 inch. Similar separations were seen on JES-3 tests and did not propagate or cause any detrimental effects to the sealing function.

The aft cylinder tang was also manufactured to the baseline DM-8 unvented J-insulation configuration with the local joint area consisting of asbestos-filled NBR.

- d. ETA Stiffener Segment. The ETA stiffener segment clevis was fabricated to the baseline DM-8 unvented J-insulation using asbestos-filled NBR, as it was a test joint. The clevis joint cured in a manner similar to that of the aft cylinder. Instrumentation was bonded at various locations to the ID of the clevis, causing numerous unflow conditions of the NBR. These were repaired with the asbestos epoxy, as was done with the aft cylinder. The surfaces were again abraded back to contour with some

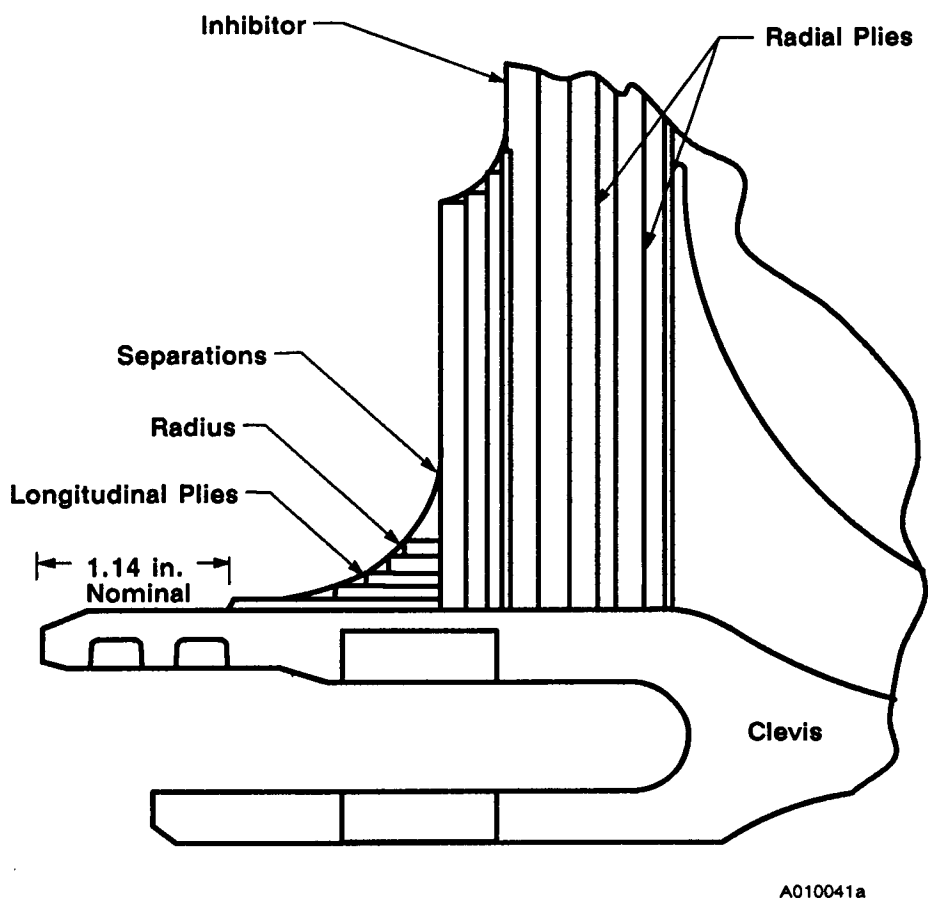


Figure 7.3-5. Test Joint Unbonds, Joint Layup

areas slightly out of tolerance. This was left "as is" since the function of the J-insulation would not be compromised. Locations of the unflow areas are as follows:

<u>Angular Location (deg)</u>	<u>Maximum Depth From Clevis Edge (Nom 1.14 in.)</u>
0 - 24	1.49
30	1.24
120	2.09
136	1.24
138	1.28
182	1.29
190	1.20
192	1.30
196 - 202	1.54
206	1.34
233	1.21
240	1.94

Insulation separations formed in the molded clevis joint radius on the ETA stiffener as was also noticed on the aft cylinder. These were again repaired by filling the cracks with an epoxy adhesive. An insulation-to-case unbond was found at 170 deg and measured 1.00 in. circumferentially by 1.125 in. longitudinally. It was repaired by filling with epoxy adhesive.

The ETA stiffener tang was a nontest joint fabricated to the HPM configuration with restrictors and using silica-filled NBR.

- e. Aft Dome. The aft dome clevis joint insulation was the molded HPM field joint configuration with silica-filled NBR. The nozzle-to-case joint is the current unvented RSRM configuration and is test Joint D (Figure 7.3-6). It was fabricated of asbestos-filled NBR and carbon fiber EPDM and employed two insulation cures, as does a flight motor. It also implements a stress flap for shrinkage of the inert propellant during cure and afterwards. During the manufacture of the aft dome, the flap was trimmed too short. This became evident after casting the inert

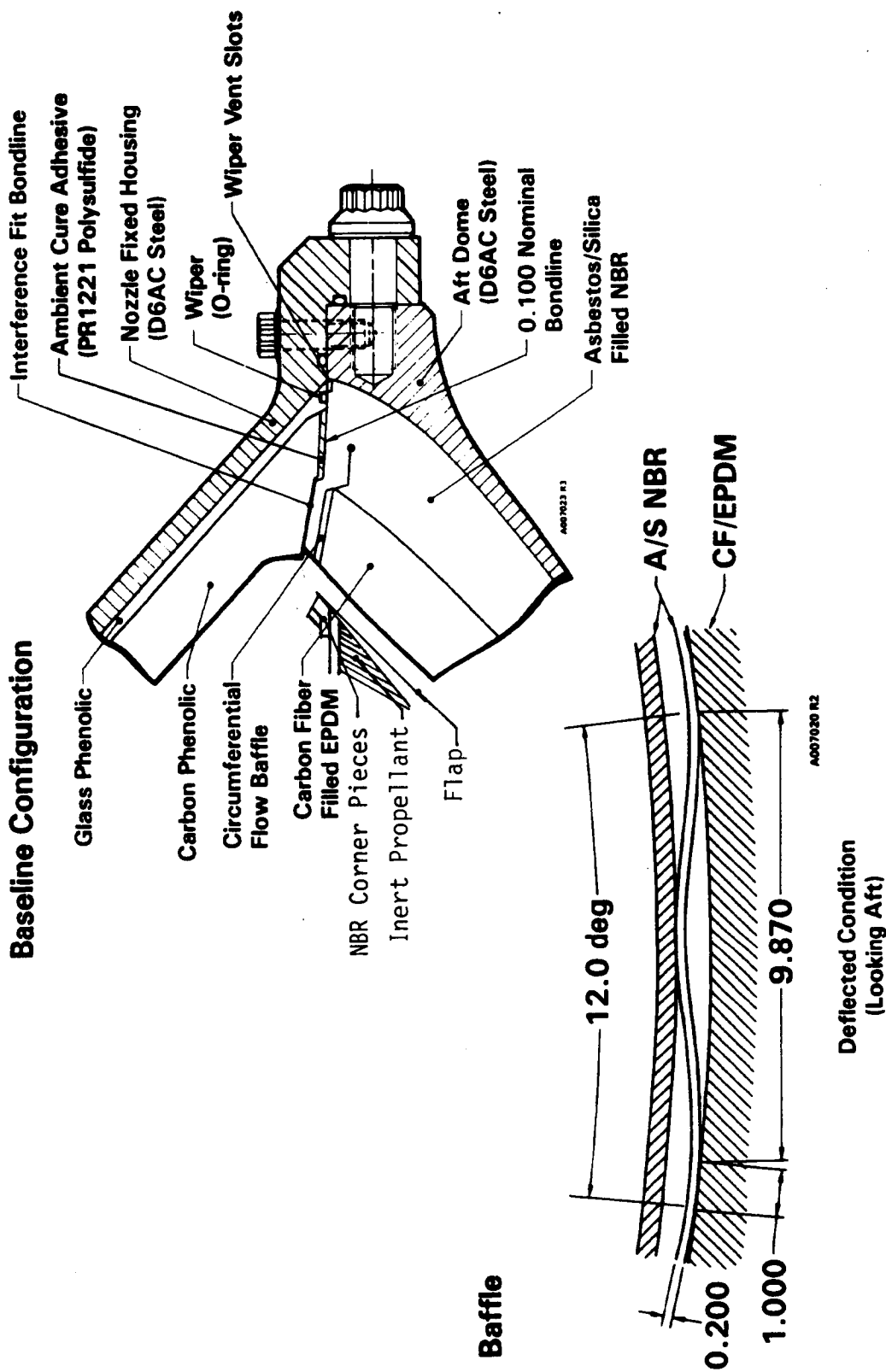


Figure 7.3-6. TPTA 1.1 Insulation, Baseline Configuration

propellant, when silica-filled NBR corner pieces are to be bonded to the flap. The flap was extended by splicing on an extra layer of NBR, making it possible to bond on the corner pieces. However, it was still short of proper tolerance. It was determined that this would not affect the function of the joint, and the flap was left at its current length.

7.3.3.1 Pretest Test Article Conditions. Pretest test article conditions and the assembled joint gaps are described in this section. Joint dimensions were requested on all field joints per ETP-0129 prior to assembly.

a. Test Joint A

1. Joint Gaps. The forward-to-aft cylinder joint, Joint A, is of an unvented J-insulation configuration. The cured configuration of the joint shrank inboard longitudinally and reduced joint surface engagement. Measurements were taken of the tang and clevis surfaces and were evaluated at locations shown in Figure 7.3-7. A summary of the gap analysis is shown in Table 7.3-1. The results are compared to engineering design and DM-8 data. Average, maximum, and minimum joint gaps at Points A and B were within the engineering design tolerances. At Point C the design tolerances ranged from a small gap to slight joint engagement. However, the actual profile showed the gap did not concur with these tolerances, as the minimum gap measurement was larger than the maximum gap specified by Engineering Design. At Point D the joint bondline should provide a minimum engagement of 0.330 in. and the minimum was a gap of 0.078 inches. The J-insulation slot gaps for Joint A at Point A were all larger than the maximum designed gaps or the gaps indicated for DM-8. None of the gap measurements were within the design tolerances, but it must be pointed out that the methods used to obtain the measurements are not totally accurate, making the data inconclusive. The transfer medium inspection showed that better contact was achieved than the profile measurements indicate.

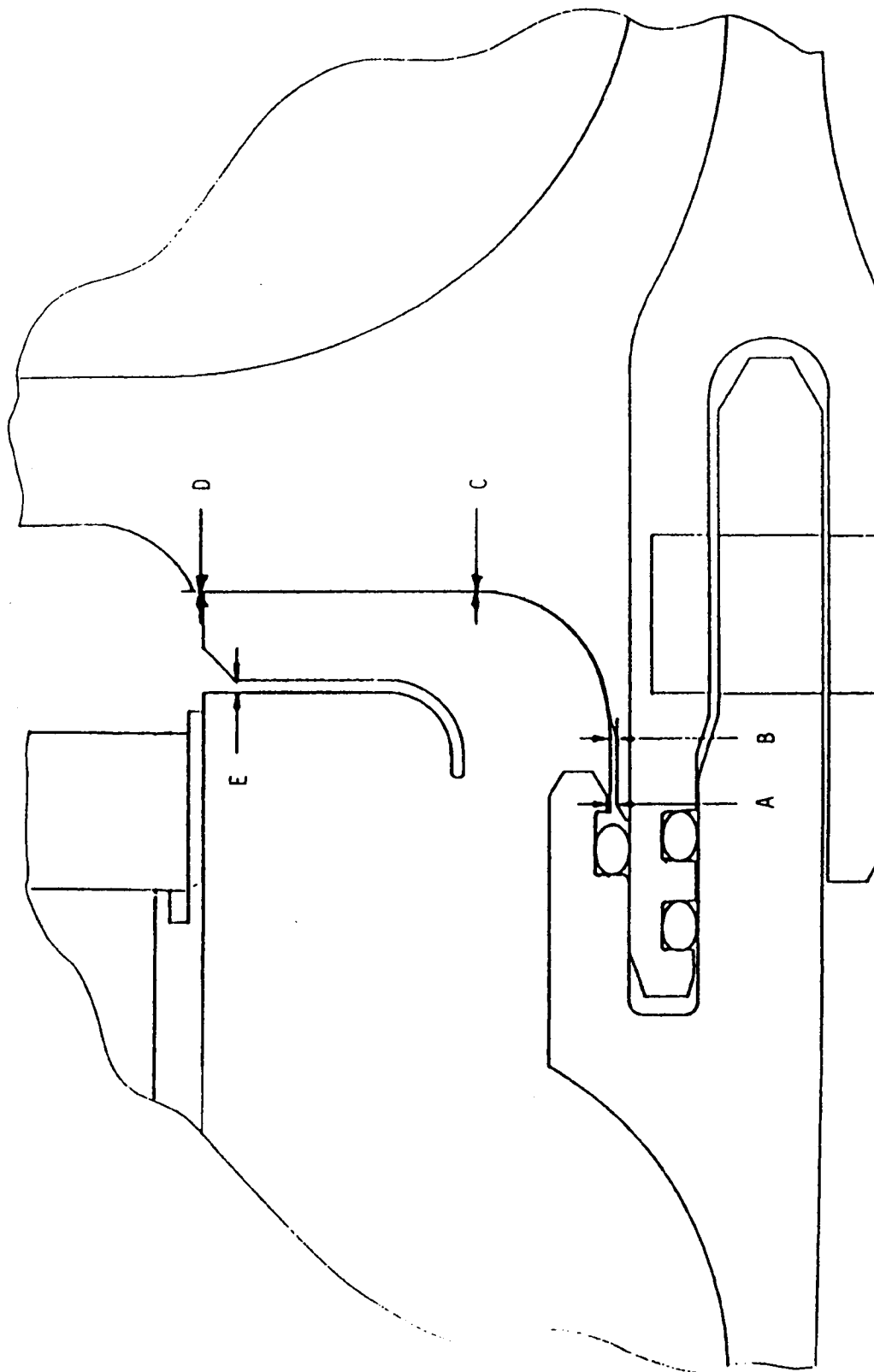


Figure 7.3-7. J-Insulation Gap Locations

Table 7.3-1. J-insulation Joint Gap Analysis Summary

	Gap Location				
	A	B	C	D	E
Engineering Design (75°F)*					
Minimum	0.035	0.035	-0.010	-0.450	-0.050
Maximum	0.098	0.098	0.070	-0.330	0.220
Nominal	0.067	0.067	0.030	-0.390	0.085
Engineering Design (40°F) Loaded level w/ slump**					
Minimum				-0.100	
DM-8 (Ctr/Ctr)					
Minimum	0.038	0.067	-0.096	-0.194	0.194
Maximum	0.060	0.094	0.123	0.020	0.288
Average	0.052	0.081	0.086	-0.124	0.245
Test Joint A (JES-3A)					
Minimum	0.003	0.029	0.128	-0.137	0.240
Maximum	0.073	0.105	0.212	0.029	0.406
Average	0.060	0.084	0.170	-0.016	0.351
Test Joint A (TPTA)					
Minimum	0.050	0.047	0.113	-0.038	0.400
Maximum	0.078	0.097	0.170	0.078	0.452
Average	0.065	0.068	0.142	0.041	0.426
Test Joint B (TPTA)					
Minimum	0.037	0.058	0.088	-0.043	0.333
Maximum	0.073	0.092	0.190	0.029	0.376
Average	0.058	0.072	0.129	-0.013	0.359

Note: Ref Figure 7.3-7

* - Values at the insulated level not accounting for subsequent propellant slump or assembly shrinkage.

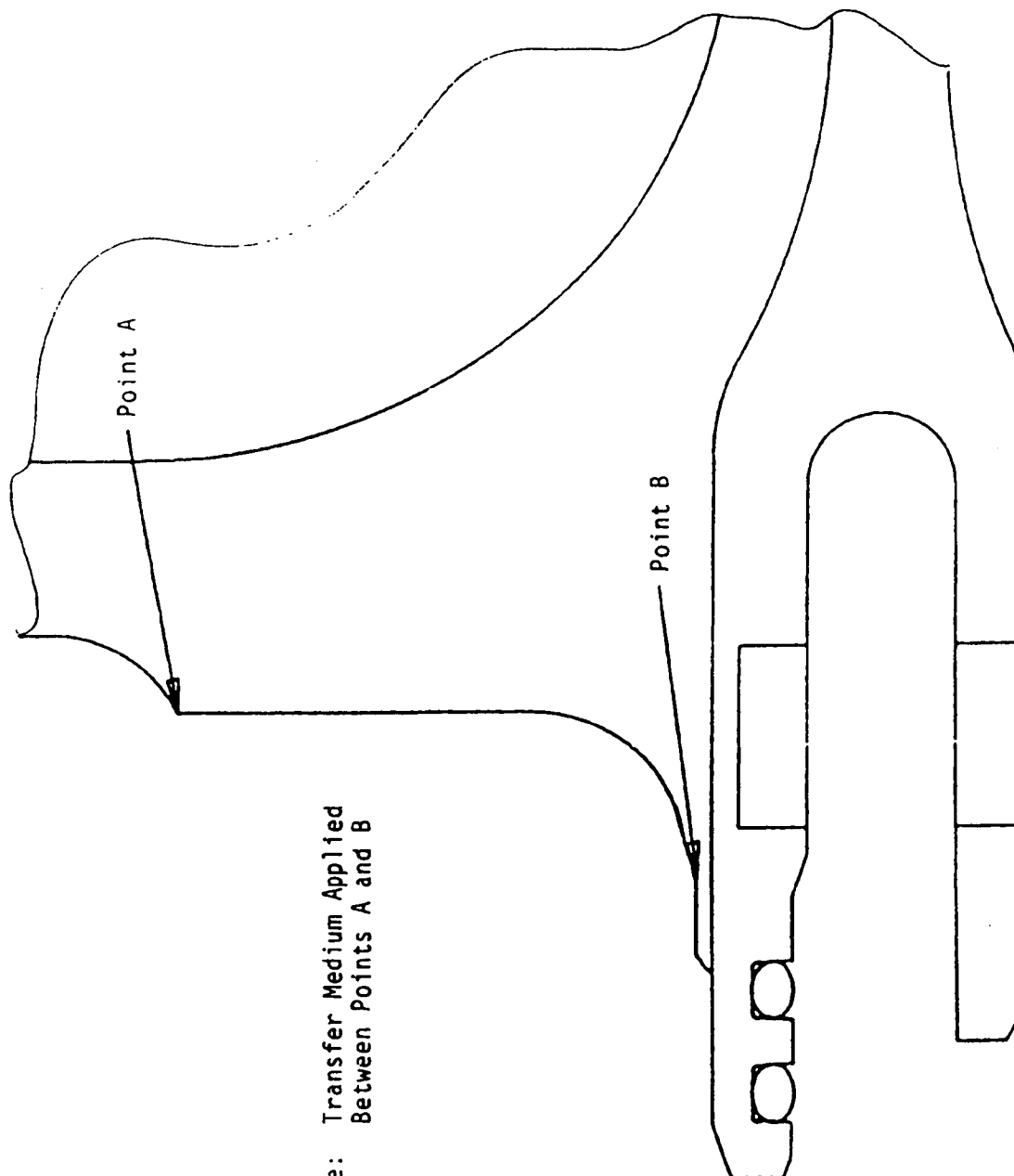
** - Other values not available.

2. Joint Transfer Inspection. Prior to assembly, a transfer medium was sprayed on the clevis joint surfaces in the areas shown in Figure 7.3-8. The joint was then assembled for a dry fit to verify joint contact at assembly. The ID tip of the J-insulation failed to show contact for the full circumference and the rest of the surface face indicated that joint contact was poor. Specific measurements are listed in Table 7.3-2. Joint contact was also measured in the radius region.

The transfer medium test showed that test Joint A appeared to make very poor contact during the dry mate, and there were several areas up to 12 deg in circumference which showed no contact at all. Additional bore inspections were done, which seemed to indicate that the J-insulation did not make full contact in several places.

b. Test Joint B

1. Joint Gaps. The aft cylinder-to-ETA joint, Joint B, is an unvented J-insulation configuration. The cured joint surfaces left larger than expected gaps in this joint as well. The gaps were evaluated in the same locations as Joint A. A summary of the gap analysis is given in Table 7.3-1. Results are compared to engineering design and data from a DM-8 cylinder-to-cylinder field joint. The average, maximum, and minimum joint gaps at Points A and B were within the engineering design tolerances. At Point C the design tolerances were exceeded; the minimum gap measurement was larger than the maximum gap specified by Engineering Design. At Point D the maximum engagement of the joint bondline was within specified tolerances; the average exceeded design limits. The J-insulation slot gaps for Joint B at Point E were all larger than the engineering design or the DM-8 gaps. None of the gap measurements at Point E were within the design tolerances, but again these values are not reliable.
2. Transfer Medium Inspection. Prior to assembly, a transfer medium was sprayed on the clevis joint surfaces, as was done for Joint A. The joint was then assembled for a dryfit and a minimum of eight



Note: Transfer Medium Applied
Between Points A and B

Figure 7.3-8. J-insulation Transfer Medium Application

Table 7.3-2. Joint A Transfer at J-insulation ID Tip

Location (deg)	Width of Transfer (in.)	Amount of Transfer
0-3	no transfer	none
3-4	0.01	very light dusting
4-10	no transfer	none
10-13	0.10	medium
13-16	no transfer	none
16-24	0.10	heavy
24-42	0.15	medium
42	dust	medium
43-46	0.15	heavy
47	dust	light
48-70	0.20	heavy
70-76	0.10	medium-light
76-78	dust	light
79-88	0.20	heavy
88-100	0.15	medium
100-110	0.10	medium
110-113	0.05	very light
113-118	no transfer	none
118-120	0.02	medium
120-124	no transfer	none
124-128	0.04	light
128-136	no transfer	none
136-140	0.02	medium
140-180	0.20	medium-heavy
180-192	0.15	medium-heavy
192-210	0.20	heavy
210-216	0.30	light
216-236	0.10	medium
236-240	0.10	light-medium
240-242	no transfer	none
242-270	0.20	heavy
270-285	0.15	medium
285-294	no transfer	none
294-302	0.20	medium
302-328	0.10	medium
328	0.10	dust
328-338	0.10	heavy
338-341	no transfer	none
341-348	0.05	light
348-353	0.10	medium
353-355	no transfer	none
355-357	0.05	medium
357-360	no transfer	none

pins installed prior to demating the joint and making an inspection. Contact was made around the entire circumference. Specific measurements are shown in Table 7.3-3. Contact was also made in the radius region. The contact was generally good, except for one area from 102 to 112 deg where only a light dust was transferred. The transfer medium test indicated that Joint B mated reasonably well.

c. Nozzle-to-Case Joint

1. Joint Gaps. Profile measurements for the nozzle-to-case joint are taken at 8 longitudinal locations along the joint interface shown in Figure 7.3-9. These measurements are spread out over 16 circumferential locations. They are taken with the flap gap in a closed position, referred to as being in a "restrained" state. Engineering design tolerances along with the TPTA gap dimensions are given in Table 7.3-4. This table shows that the joint is within tolerance at each location except for Points A and B. Point A has one point which is 0.003 in. below the minimum tolerance, which is not significant. The data also reveal that there is a maximum gap of 0.206 in. at Point B, which is 0.139 in. above the maximum tolerance. It is believed that the measurements at this location were taken from a wrong reference point in order to give such a large discrepancy consistently over the full circumference. The measuring techniques are subject to many types of errors making the values questionable. Post-test visual inspection confirmed the data to be in error.

Conclusions

Joint gap analysis is presented in this report to document pretest joint gaps. Post-test inspection will be made to all joints following each test and joint conditions will be documented. Nontest joints were not measured prior to testing and are not included in this analysis. Previous testing has shown the nontest joints to function adequately and the time spent analyzing nontest joints is no longer justified.

7.3.3.2 Test. The following define the test joints as they were configured for the TPTA 1.1 test.

Table 7.3-3. Joint B Transfer at J-insulation ID Tip

<u>Location (deg)</u>	<u>Width of Transfer (in.)</u>	<u>Amount of Transfer</u>
0-7	0.25	medium
7-10	0.25	medium
10-18	0.30	medium-light
18-28	0.35	medium dusting
28-34	0.35	heavy
34-38	0.35	medium dusting
38-42	0.30	heavy
42-46	0.40	light
46-58	0.40	medium
58-68	0.25	heavy
68-70	0.40	heavy dusting
70-90	0.50	heavy
90-100	0.55	heavy
100-112	0.35	heavy
112-120	0.45	heavy
120-136	0.35	heavy
136-180	0.40	heavy
180-246	0.35	heavy
246-260	0.60	heavy
260-300	0.80	heavy
300-314	0.40	heavy
314-360	0.10	medium

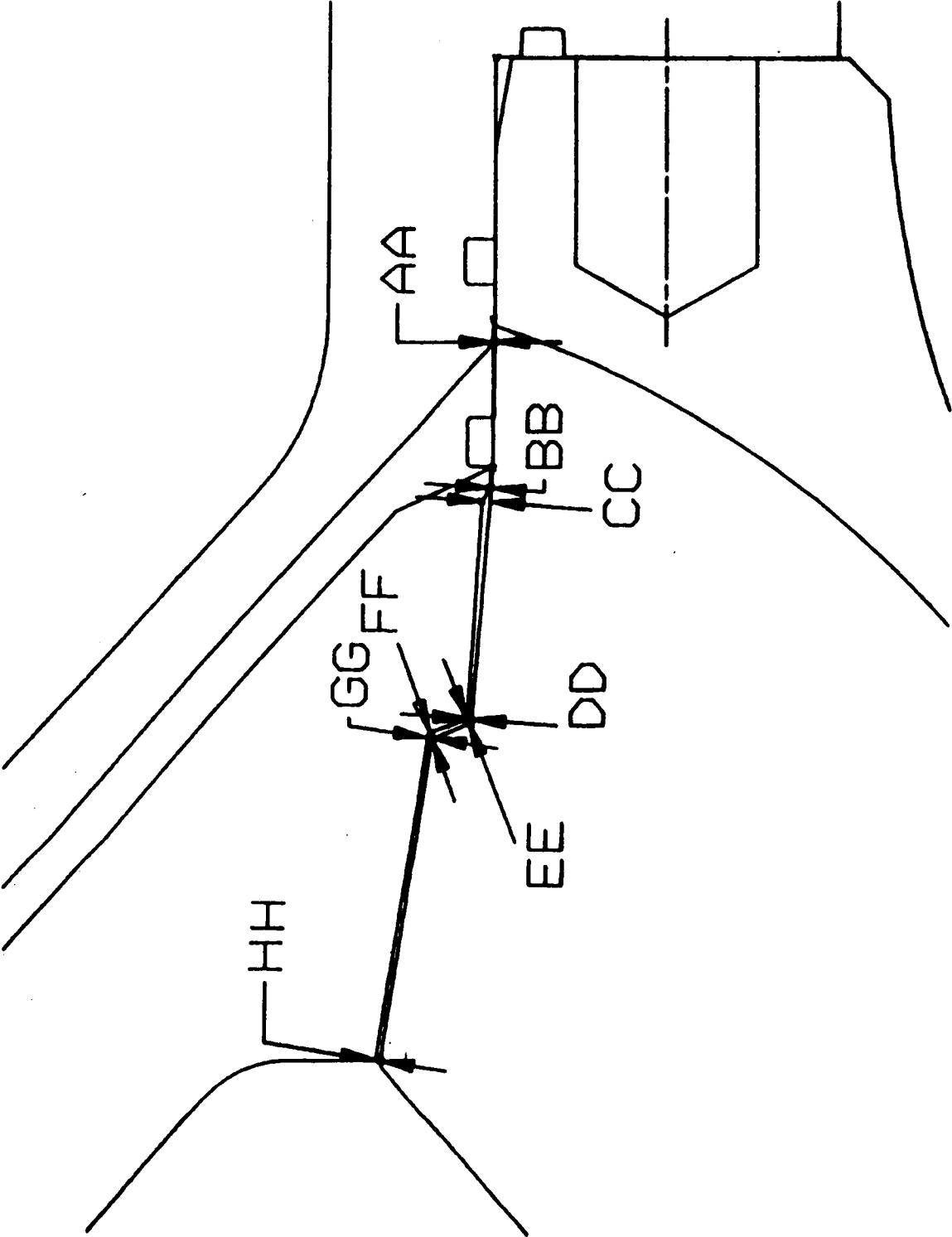


Figure 7.3-9. Gap Locations

Table 7.3-4. Nozzle-to-Case Gap Summary

	<u>Gap Location</u>							
	<u>AA</u>	<u>BB</u>	<u>CC</u>	<u>DD</u>	<u>EE</u>	<u>FF</u>	<u>GG</u>	<u>HH</u>
Engineering Design (75°F)								
Minimum	0.000	0.014	0.069	0.043	0.043	0.044	0.041	0.041
Maximum	0.040	0.067	0.124	0.132	0.142	0.144	0.135	0.136
Nominal	0.020	0.041	0.097	0.088	0.093	0.094	0.088	0.089
Nozzle/Case Joint (TPTA 1.1)								
Minimum	-0.003	0.178	0.090	0.037	0.041	0.026	0.041	0.050
Maximum	0.019	0.206	0.122	0.074	0.062	0.080	0.073	0.080
Average	0.007	0.190	0.100	0.051	0.051	0.058	0.053	0.064

Reference Figure 7.3-9

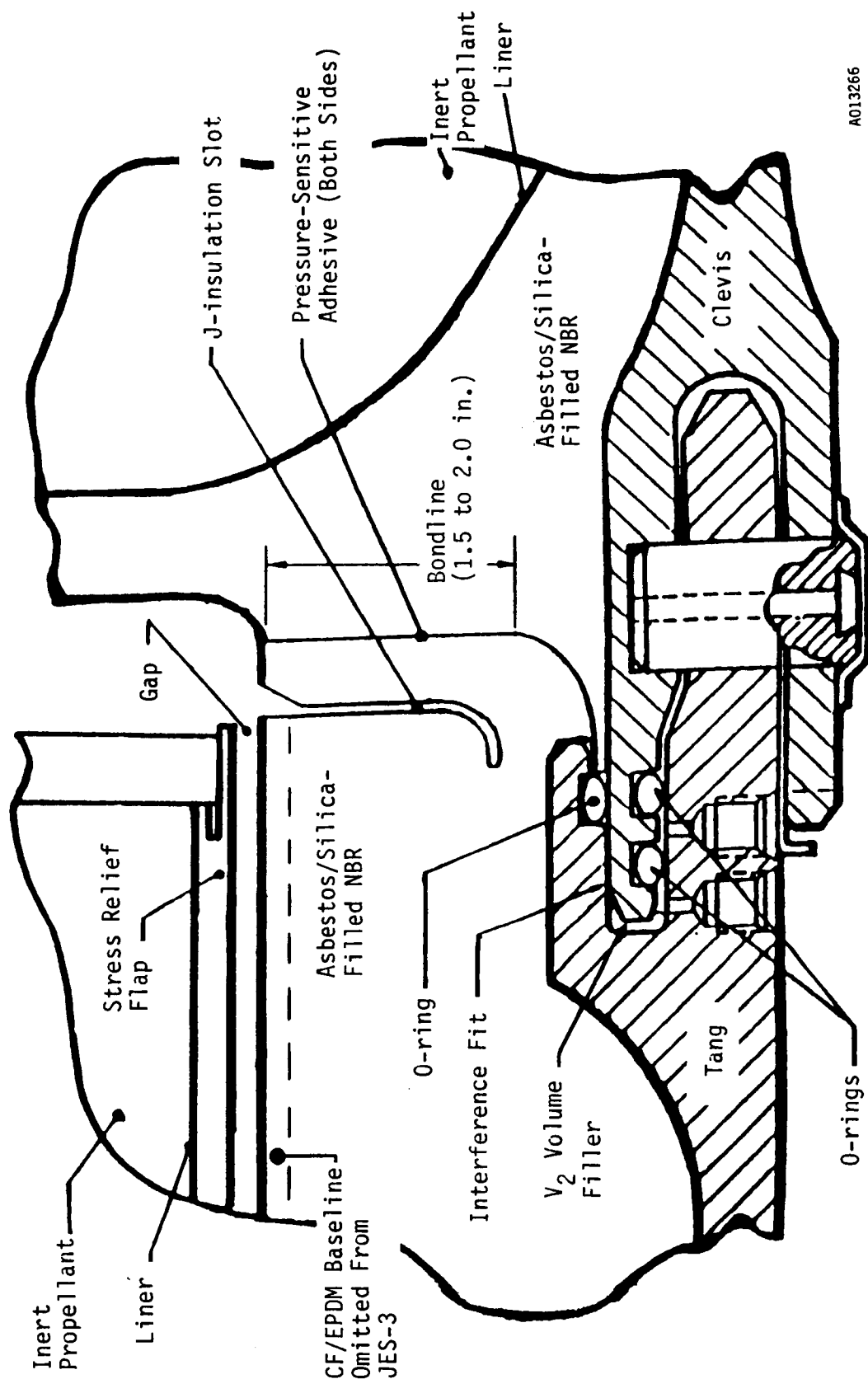
- a. Test Joint A. The unvented J-insulation configuration used in test Joint A, forward cylinder-to-aft cylinder, was a nominal joint with no defects present (Figure 7.3-10). The joint surfaces were lightly abraded and solvent cleaned prior to adhesive application in order to remove surface gloss and improve adhesion. The adhesive was thinned prior to application using two parts adhesive to one part methylchloroform by weight. Pressure-sensitive adhesive was applied 1.5 to 2.0 in. from the ID J-insulation tip outboard full circumference.

Instrumentation was installed in the joint areas to provide data prior to and during the test and at joint demate. Pressure transducers and thermocouples were placed in the slot, the joint bondline, and upstream of the CF O-ring. Stress gages were also placed in the joint bondline ID and outside diameter (OD) to provide joint engagement pressure during the test and joint separation loads at joint demate.

- b. Test Joint B. The aft cylinder-to-ETA was test Joint B and was of the same configuration as Joint A. Instrumentation was the same as Joint A and again there were no defects present.
- c. Nozzle-to-Case Joint. This joint has been identified as test Joint D and is the current RSRM baseline configuration. Wiper O-ring vent slots were cut into the aft dome NBR surface. These slots are used to vent air that would be trapped forward of the wiper O-ring as the fixed housing is mated with the aft dome. In this case, the vent slots were cut to former engineering design, but the design has been lengthened since then. This is to be incorporated on subsequent TPTA tests. A layer of polysulfide is also applied to this joint surface to act as a bonding agent and to fill joint gaps which prevent hot gases from reaching the O-rings.

7.3.3.3 Joint Instrumentation. This section describes locations of the instruments, readings of the instrumentation during the test, and the effects of the test on the instrument surfaces.

- a. Test Joint A. The instrumentation locations and summary are presented in Figure 7.3-11. Slot pressures P034, P035, and P036 were taken at 21,



A013266

Figure 7.3-10. Assembled DM-8 Baseline J-insulation Configuration

Pc = 910.23 psia max 0.61 sec
Pc = Chamber Pressure
*Fo follows Pc Plotted Geometry

Figure 7.3-11. Test Joint A Instrumentation Locations and Summary

147 and 261 deg, respectively. P002 was used for chamber pressure (P_c) comparison for all data. The data showed that the slot pressures followed the chamber pressure and all the gages peaked between 905.78 and 907.21 psia from 0.57 to 0.60 sec into the test. Chamber pressure peaked at 910.23 psia at 0.61 sec. The chamber pressure reached its peak between 0 and 1 sec and then began to drop off until it reached 450 psia. At this point the nozzle was plugged and the pressure was maintained at approximately 450 psia for 11 minutes before it was finally vented. Pressures in the slot tracked the chamber pressure very closely, with some short-term increases up to 75 psia over chamber pressure. The slightly higher pressure in the slot area was probably due to the slot propellant. The data from the slot pressure sensors indicated the joint was subject to full chamber pressure.

Thermocouples T205, T206, and T207 were placed at 21, 135, and 261 deg, respectively, in the joint inlet. T205 recorded a maximum temperature of 2,296°F at 0.15 sec, T206 showed 763°F at 0.19 sec and T207 recorded 2,593°F at 0.16 sec. T205 and T207 also both fell to approximately 200°F at 120 sec. These low readings have also been seen on the JES-3 test series and probably result from the placement and function of the thermocouple. These temperature readings are below the predicted values. The reason for the discrepancy is not well understood, and further investigation is being done in this area.

Stress gages were placed in the outboard and inboard surfaces of the joint bondline at 0, 120, and 240 deg to measure joint engagement pressures during the test. The stress gages were able to read positive and negative forces caused by gas or contact pressure. Joint engagement pressures on the inboard portion of the joint bondline were generally higher than pressures on the outboard portion of the joint. The inboard sensors, S178 at 0 deg, S179 at 120 deg and S180 at 240 deg all recorded their maximum pressures of 898.07 psia, 829.28 psia, and 853.53 psia, respectively, at 0.61 sec. Pressure rise rate for the inboard stress gages followed chamber pressure, peaked and then leveled off at an

average of 50 psia less than chamber pressure. The outboard stress gages S175, S176, and S177 recorded maximum pressure of 817.61 psia at 0.64 sec, 861.10 psia at 0.61 sec and 746.36 psia at 0.64 sec. None of the outboard gages recorded pressures greater than chamber pressure, but followed with the same rise rate. Joint pressure dropped at the same rate as chamber pressure, but remained an average 40 to 60 psia below. The pressures leveled out at about 400 psia due to the plugged nozzle. All plots for the stress gage readings showed that forces in the joint generally followed chamber pressure at a slightly lower level. Typical plots are given in Figures 7.3-12 and 7.3-13 for inboard sensor recordings and in Figures 7.3-14 and 7.3-15 for outboard sensor recordings.

Pressure gages P076, P077 and P078 were placed at 135, 235 and 341 deg, respectively, downstream of the joint radius and upstream of the capture feature. Because of their position in the joint, they basically read tang contact pressure. P076 (Figure 7.3-16) showed a maximum pressure of 875 psia at 0.5 sec. However, this was a temporary spike and had a subsequent maximum reading of 602.8 psia at 0.81 sec. The pressure then fell gradually to 200 psia, with two spikes down to 0 psia at 0.4 sec and 11 sec, which is probably due to a relaxation of the tang on the clevis radius. P076 was listed as a damaged sensor prior to the test. P077 and P078 were installed inoperable and no data were received from them. Thermocouples T162, T163, and T164 were also installed downstream of the joint radius at the same degree locations. They were also damaged and were not hooked up for the test.

Instrumentation data indicated that the joint sealed at ignition and allowed no pressure downstream of the joint bondline.

- b. Test Joint B. The instrumentation locations and summary are presented in Figure 7.3-17. Slot pressure gages P051 and P052 were located at 111 and 291 deg, respectively. The slot pressures followed the chamber pressure geometry and peaked at 910.02 to 910.79 psia at 0.58 sec.

Pressures downstream of the joint bondline were taken at 135, 235, and 341 deg by P079, P080, and P081, respectively. These gages read tang contact pressure. P081 was damaged and produced no usable data.

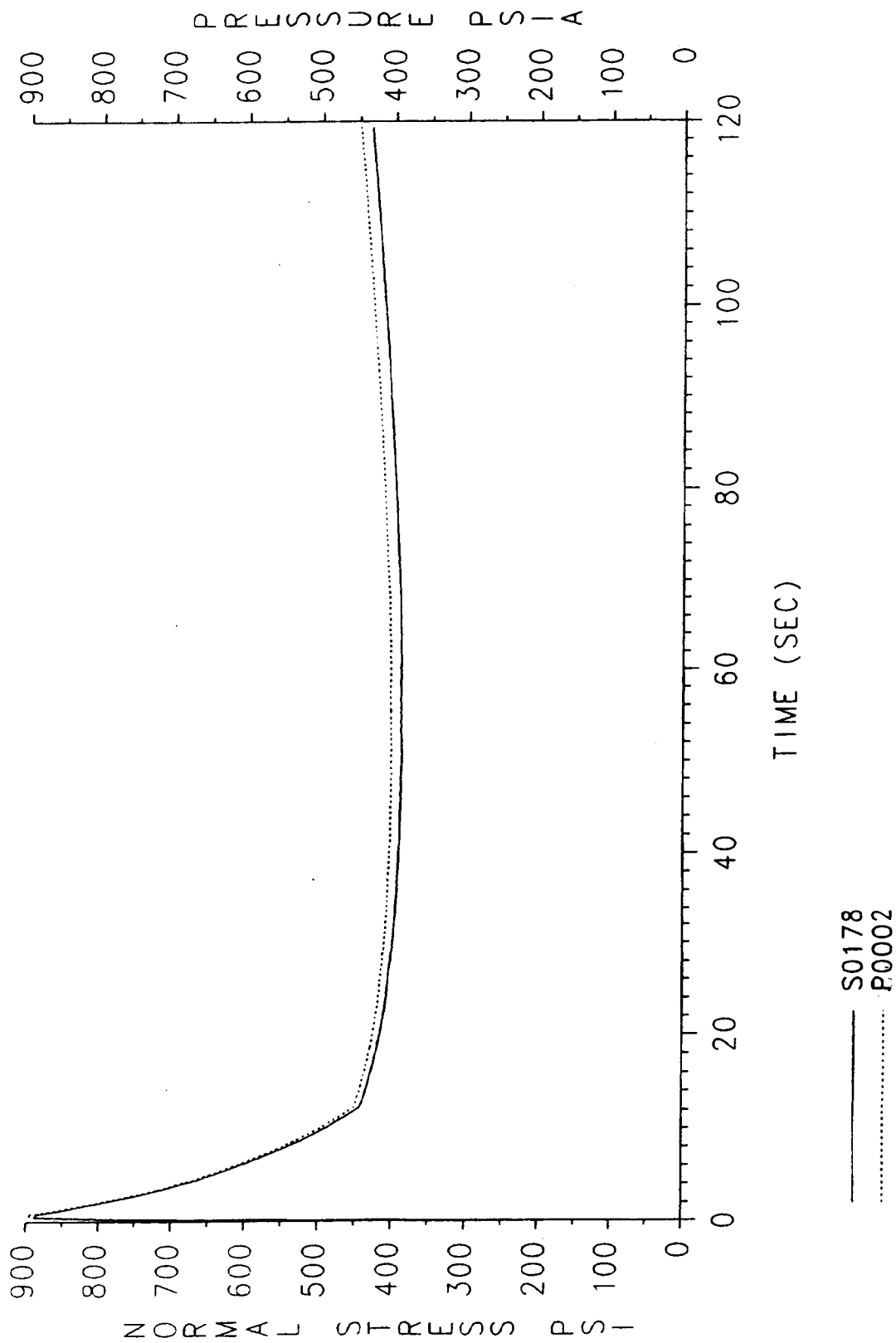


Figure 7.3-12. Joint A Bondline Normal Stress - Inboard 0 deg

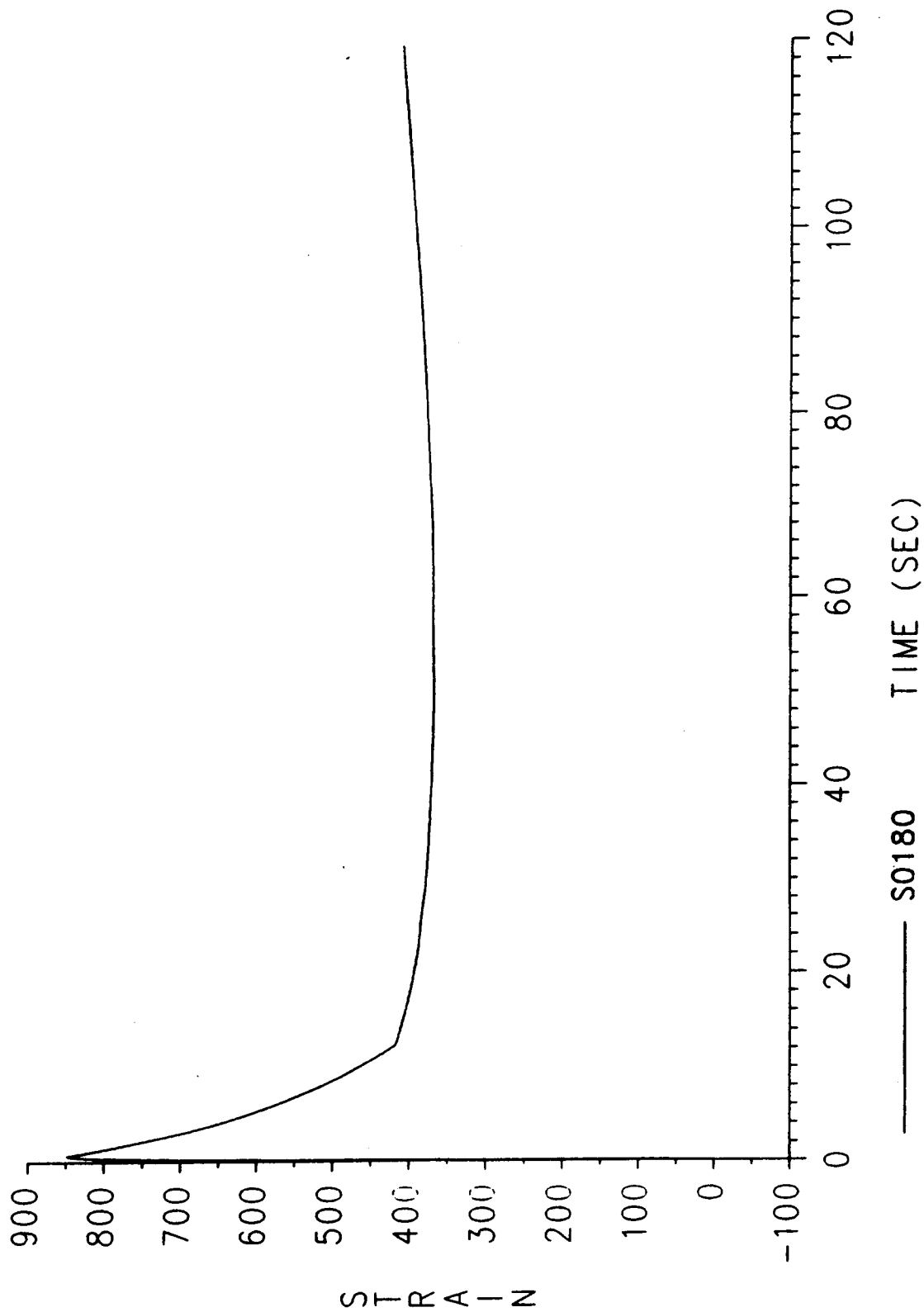


Figure 7.3-13. Joint A Bondline Normal Stress - Inboard 240 deg

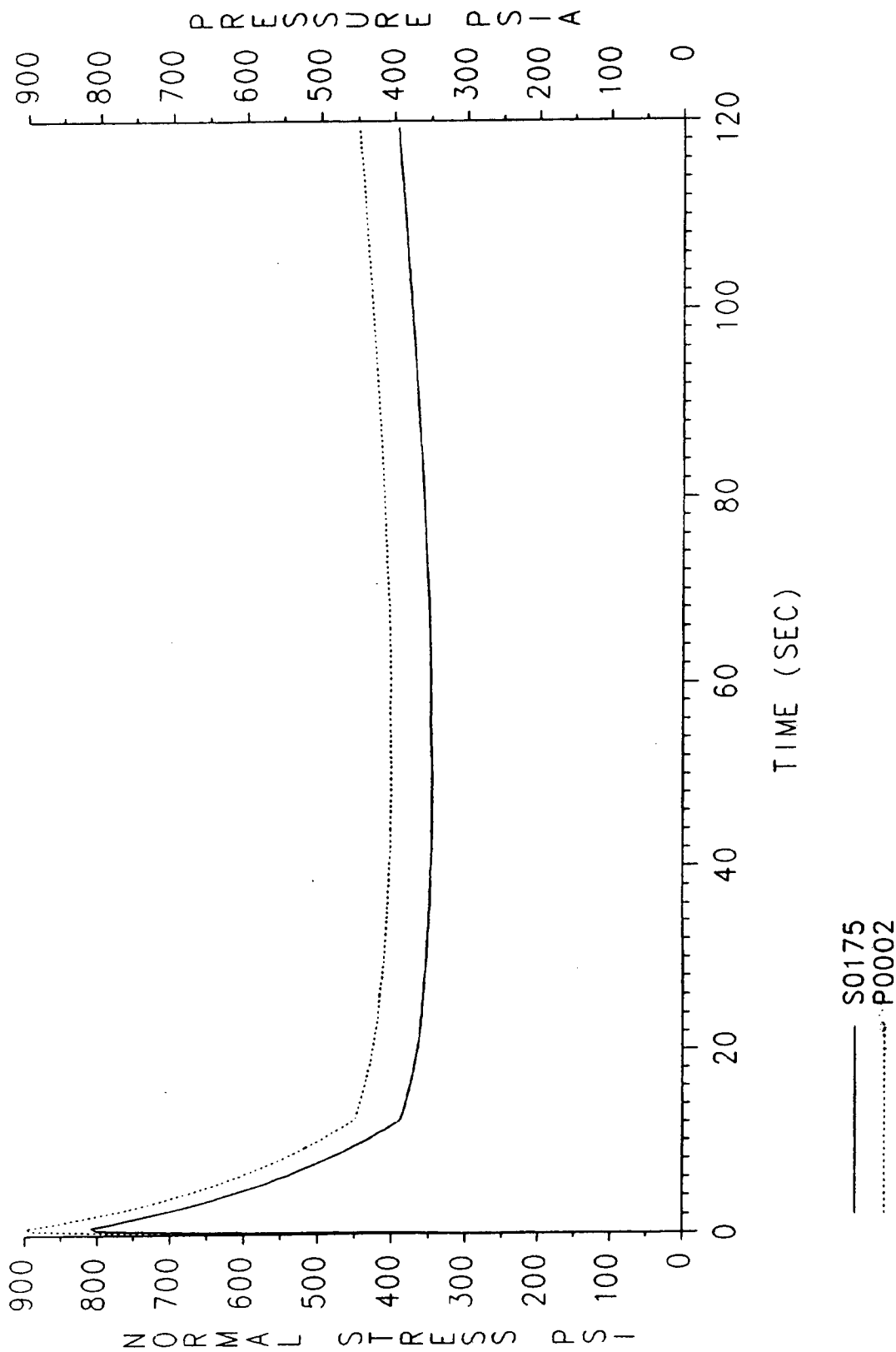


Figure 7.3-14. Joint A Normal Stress - Outboard 0 deg

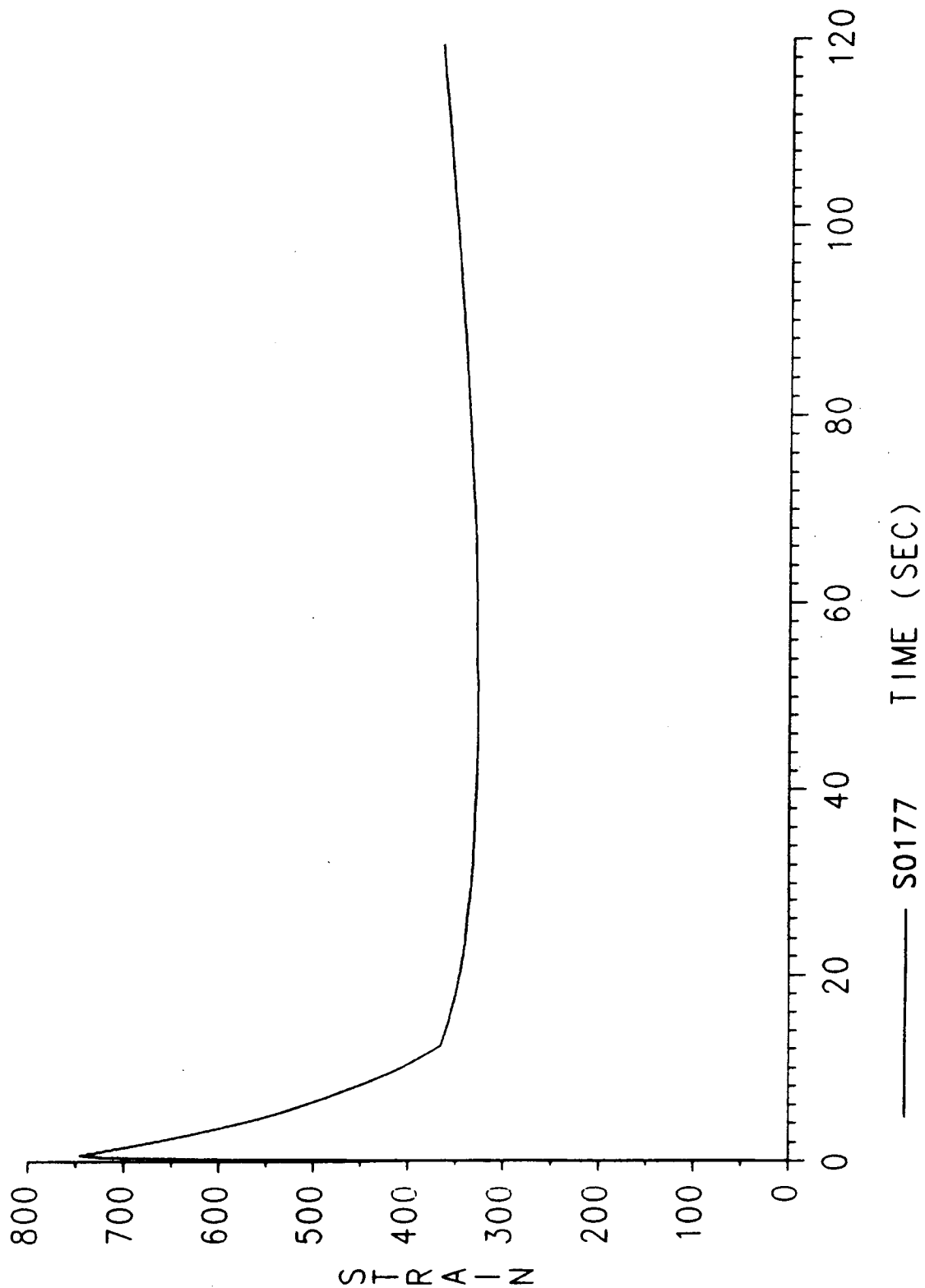


Figure 7.3-15. Joint A Normal Stress - Outboard 240 deg

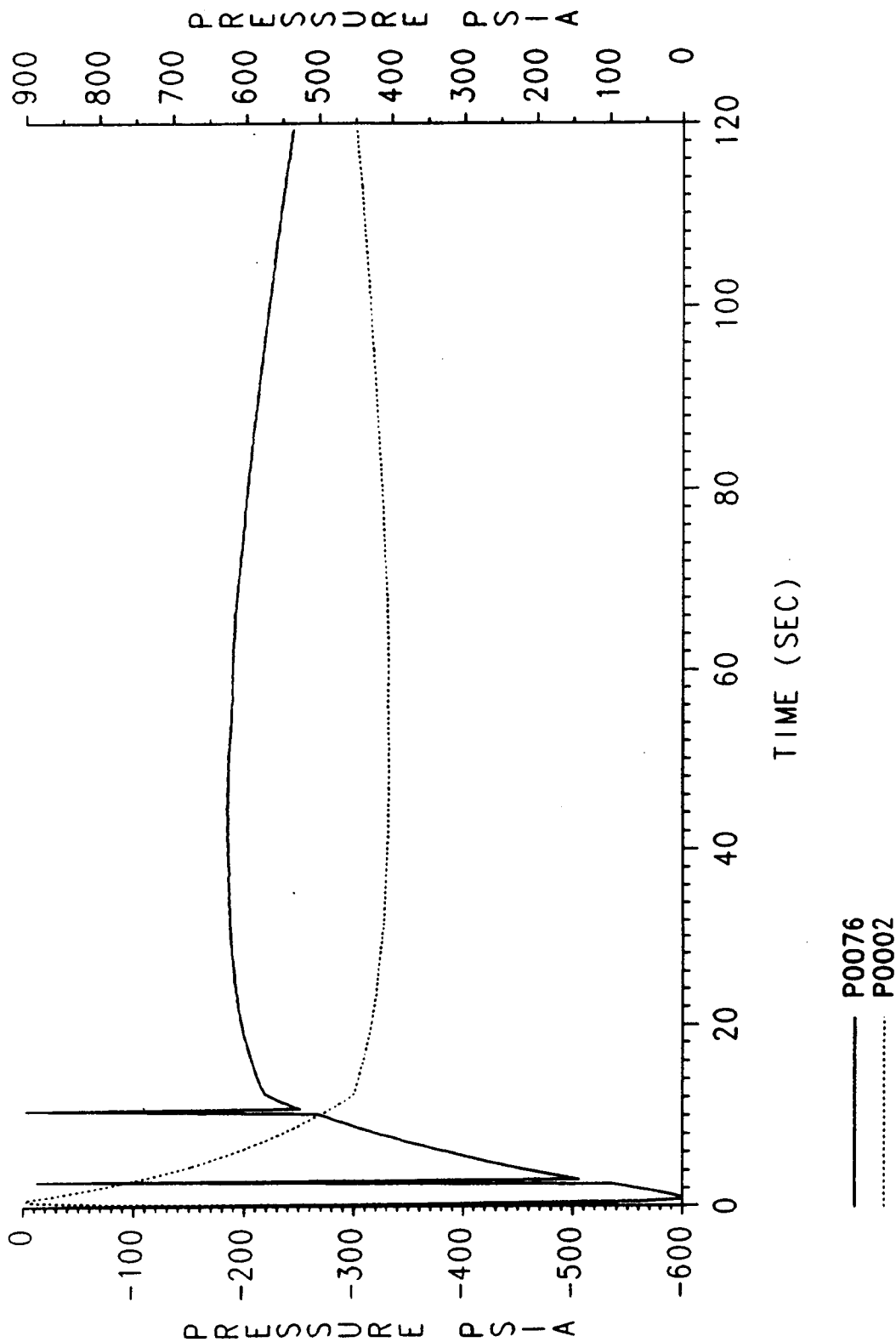
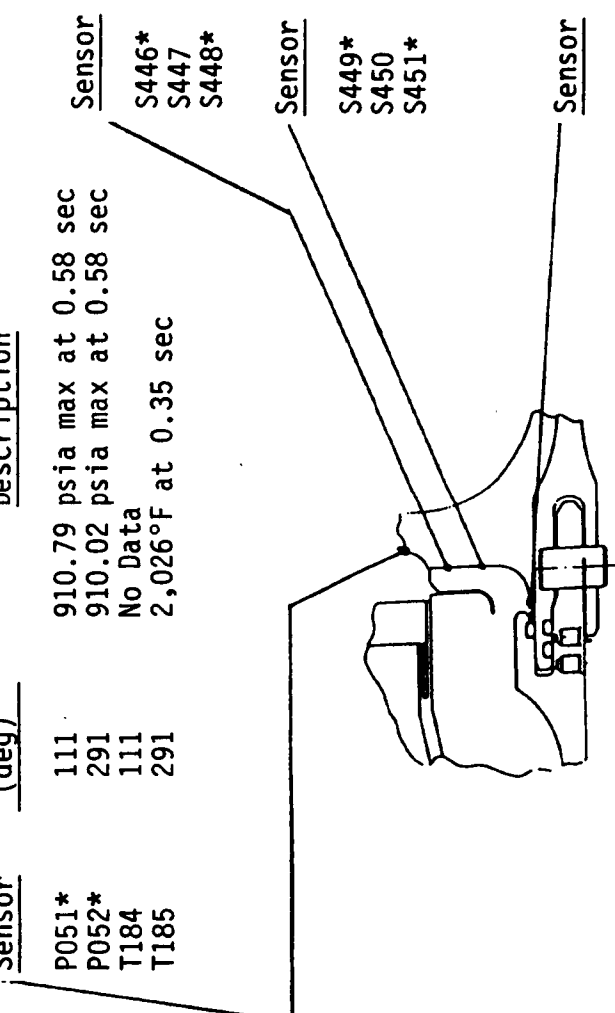
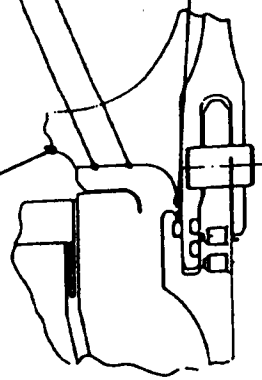


Figure 7.3-16. Joint A Capture Hook Seal Pressure - 135 deg

<u>Sensor</u>	<u>Location (deg)</u>	<u>Description</u>	<u>Sensor</u>	<u>Location (deg)</u>	<u>Description</u>
P051*	111	910.79 psia max at 0.58 sec	S446*	0	873.59 psia max 0.62 sec
P052*	291	910.02 psia max at 0.58 sec	S447	120	No Data
T184	111	No Data	S448*	240	809.10 psia max 0.66 sec
T185	291	2,026°F at 0.35 sec			
					
			<u>Sensor</u>	<u>Location (deg)</u>	<u>Description</u>
			S449*	0	901.72 psia max 0.63 sec
			S450	120	No Data
			S451*	240	904.67 psia max 0.63 sec
					
			<u>Sensor</u>	<u>Location (deg)</u>	<u>Description</u>
			P079*	135	924.70 psia max 0.62 sec
			P080*	235	798.82 psia max 0.62 sec
			P081	341	No Data
			T165	135	No Data
			T166	235	No Data
			T167	341	No Data

Pc = 910.23 psia max 0.61 sec

Pc = Chamber Pressure

*Follows Pc Plotted Geometry

Figure 7.3-17. Test Joint B Instrumentation Locations and Summary

P079 reached 924.70 psia at 0.62 sec and P080 reached 798.82 psia at 0.62 sec. P079 was slightly greater than chamber pressure until about 10 sec; then it follows chamber pressure as shown in Figure 7.3-18. Thermocouples T165, T166, and T167 were also installed downstream of the joint radius at the same degree locations. T167 was damaged and T165 and T166 were not hooked up. Thermocouples T184 and T185 were placed in the slot to read slot temperatures; only T185 produced usable data showing a maximum temperature of 2,026°F. However, both gages were considered damaged.

The stress gages in the bondline indicated the joint sealed along the entire circumference. Instrumentation indicated that the joint held pressure for the duration of the test.

7.3.3.4 Post-Test Insulation Condition. The segments of the TPTA 1.1 test article were visually inspected during destack operations. Due to an equipment malfunction the strut load was not applied to Joint B during the static hot-firing. Therefore, all postfire results do not show the effects of strut loads during ignition. The post-test condition of the segments and joints from the demate inspection are described in the following paragraphs. Any anomalies discovered during refurbishment are also documented below.

- a. Forward Dome-to-Forward Cylinder Joint. The tang joint surfaces showed some heat effects in the inner face surface. No gas paths or anomalous damage was noted. The forward cylinder joint surfaces had some pitting at 236 deg and from 338 to 342 deg along the forward corner of the 0.5-in. restrictor piece. Other than this, no anomalous conditions were found on the forward cylinder.
- b. Test Joint A. The forward cylinder tang-to-aft cylinder clevis joint showed no evidence of joint leakage or gas paths. The J-insulation slot contained soot and the joint ID had soot and heat effects which ended at the sealing point of the NBR joint. There were small areas of heavy sooting and slag past the tip of the J-insulation at 124 and 320 deg. The areas extended a maximum of 0.50 and 0.20 in., respectively, past the inboard tip of the J-insulation. The areas were a maximum of 1.5 in. in circumferential width (Figure 7.3-19). It is believed that this

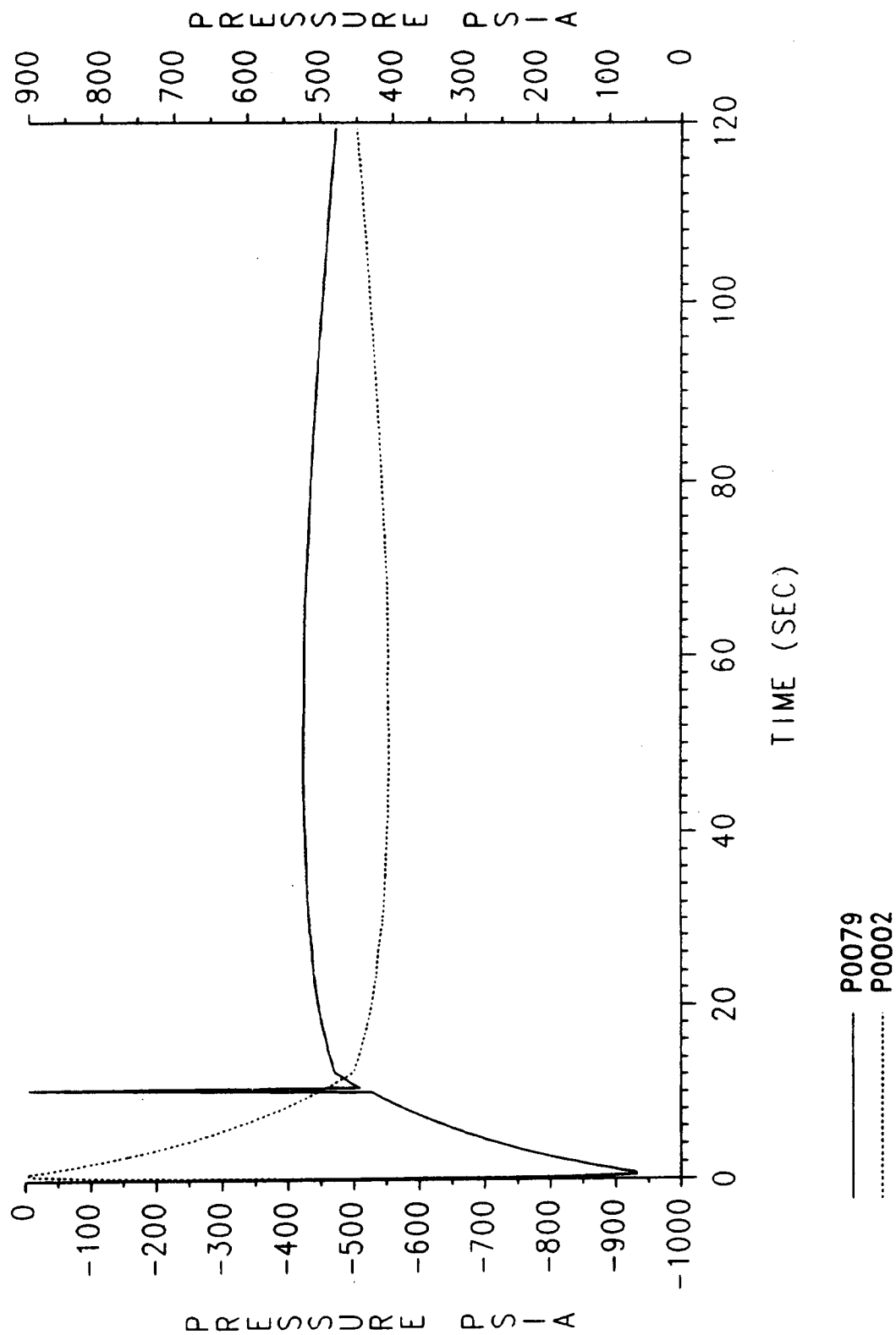


Figure 7.3-18. Joint B Capture Hook Seal Pressure - 135 deg

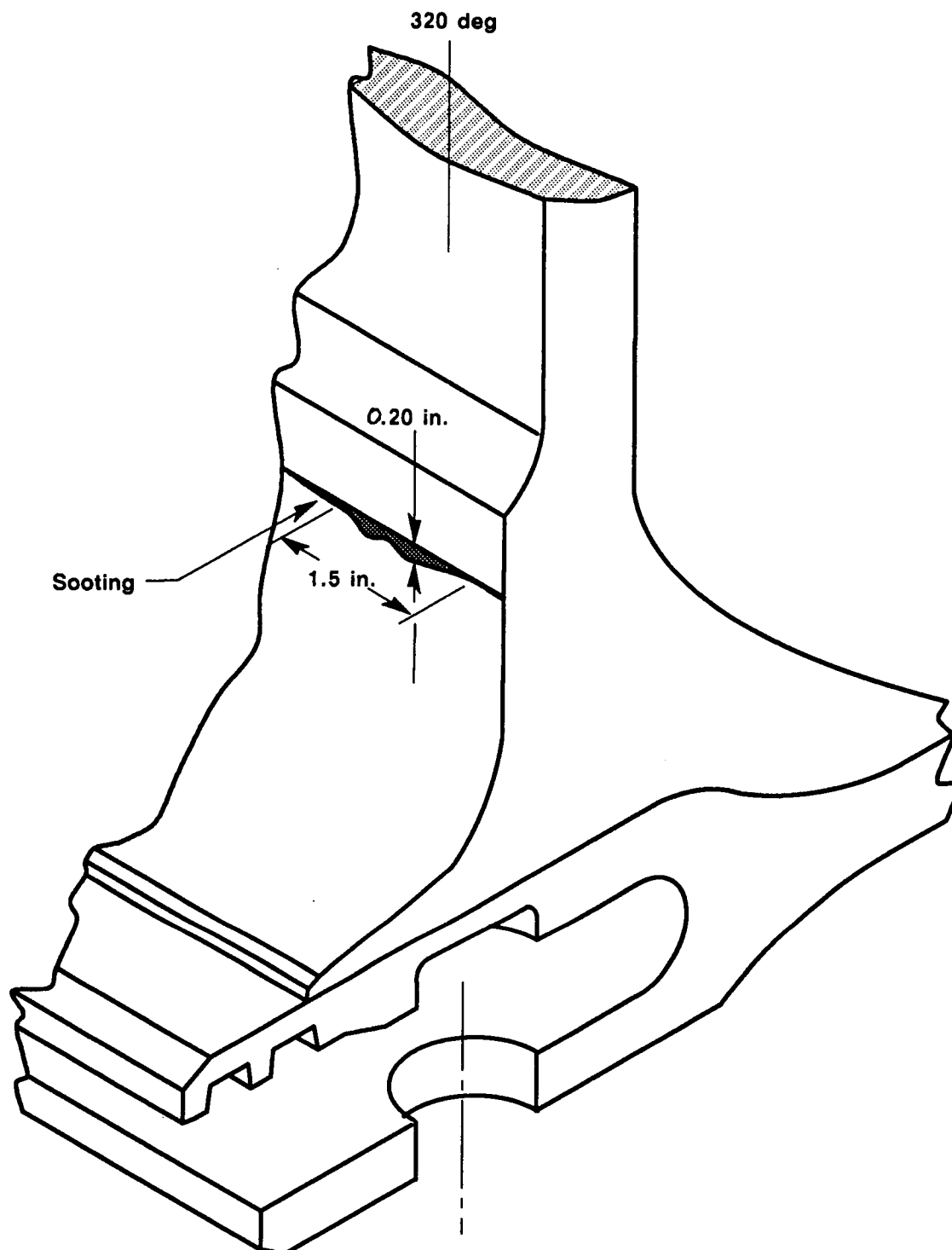


Figure 7.3-19. Typical J-Insulation Clevis Bondline Heat Effects

REVISION _____

DOC NO. TWR-17927
SEC _____

A012715a
VOL _____
PAGE _____
202

area was exposed to heat for the entire duration of the test. There was another location at 47 deg where soot had blown into the sealing surface area to a depth of 0.35 in. (Figure 7.3-20). In this area there was no erosion or slag, suggesting that the joint had sealed shortly after ignition. The joint transfer test had shown poor contact at 47 and 124 deg; however, the area at 320 deg had shown medium transfer. Of these three soot intrusions into the bondline, none progressed far enough to cause any damage to the CF O-ring as the joint sealed as designed.

The pressure-sensitive adhesive showed adhesive failure at the joint contact region, which was caused at disassembly. There was a small transition region of cohesive failure, after which there was adhesive failure between the tang and clevis which extended for most of the remainder of the bondline. Areas of the joint that were not in contact at assembly had adhesive that was still glossy. This was largely in the radius (Figure 7.3-21). The table following lists the approximate radial dimensions from the clevis bond surface ID to the joint contact position. The measurements taken are shown in Figure 7.3-22. These measurements were taken every 45 deg, but are representative for the full 360-deg circumference. The radial distance of joint engagement as shown by adhesive failure of the joint adhesive is also noted.

Engagement Distance and Joint Contact

<u>Location (deg)</u>	<u>Engagement Distance (in.)</u>	<u>Joint Contact (in.)</u>
0	0.45	0.90
45	0.40	0.70
90	0.45	1.10
135	0.40	1.00
180	0.45	0.90
225	0.40	1.00
270	0.60	0.95
315	0.40	1.00

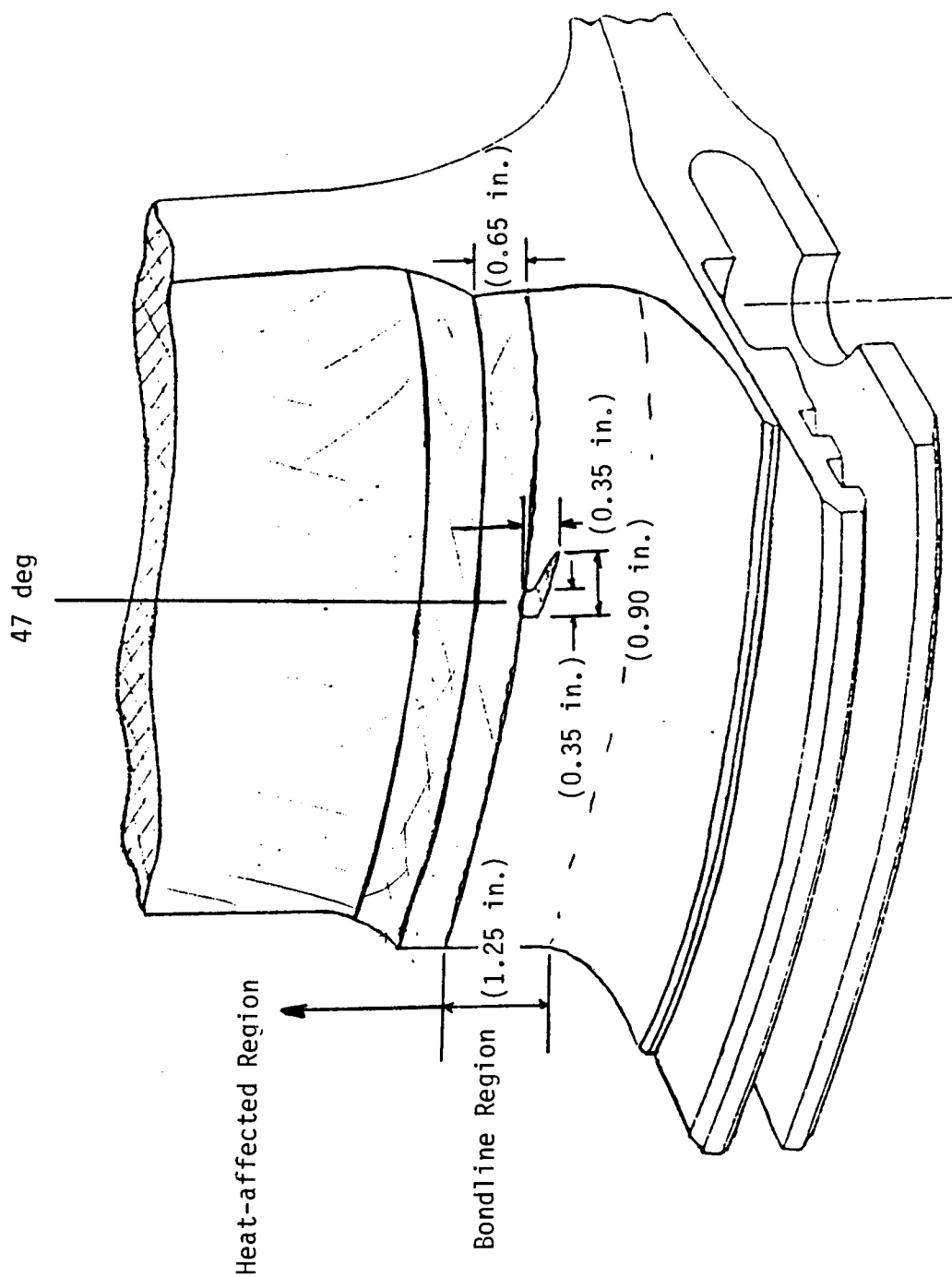


Figure 7.3-20. Joint A J-insulation Bondline Heat Effects

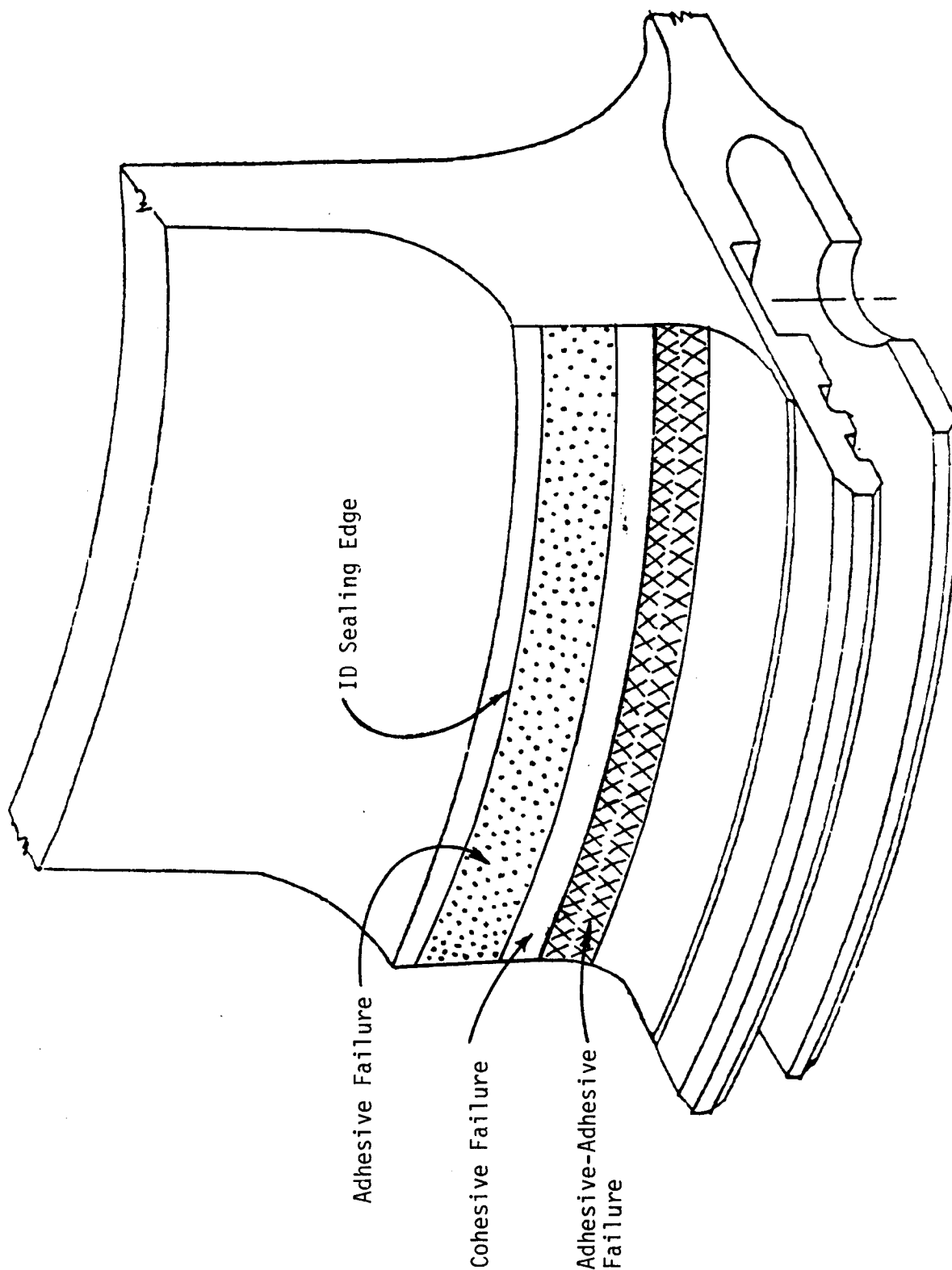


Figure 7.3-21. Pressure-Sensitive Adhesive Failure Locations

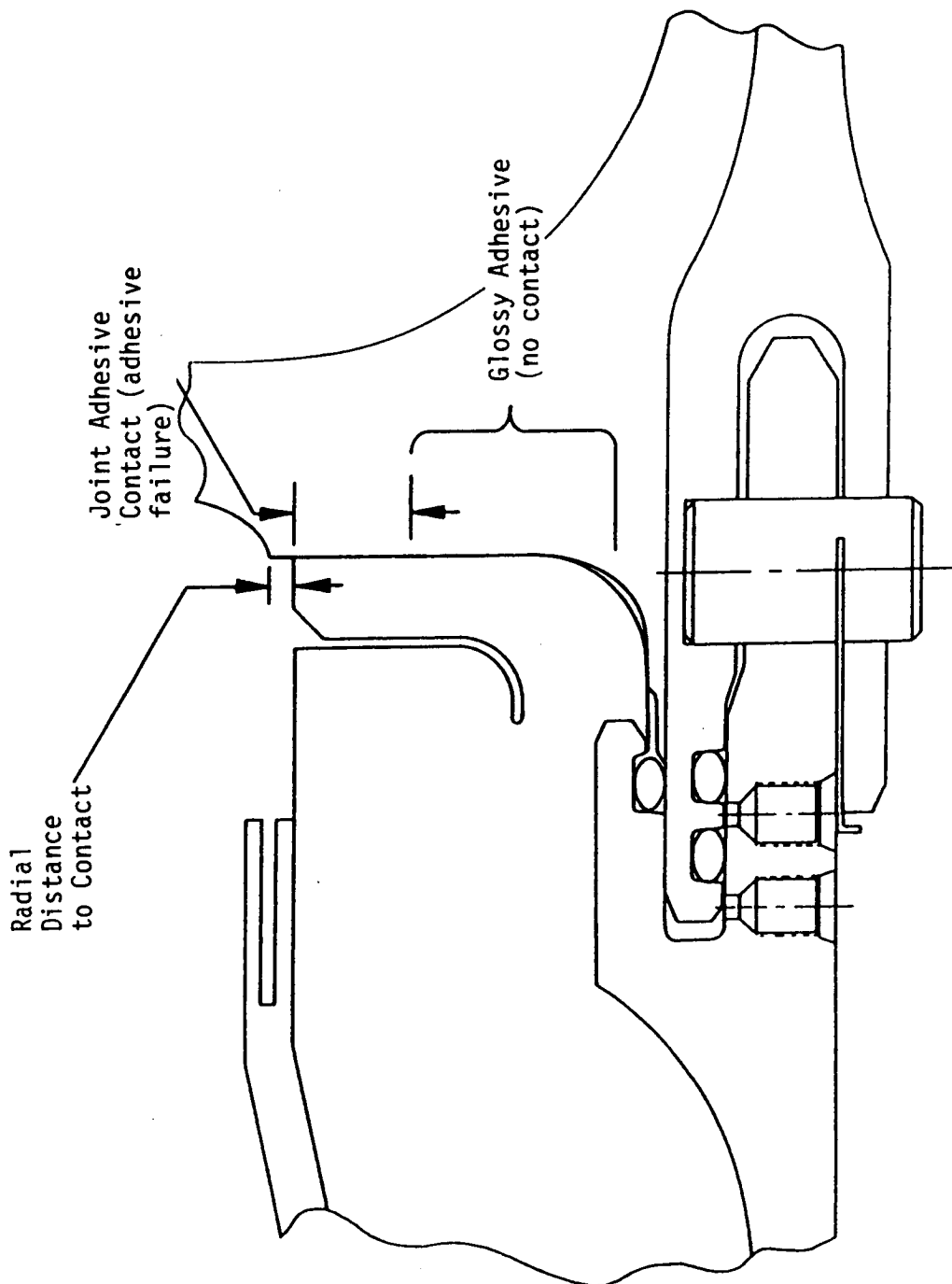


Figure 7.3-22. Joint Bondline Summary

The instrumentation appeared to be in as good condition after the test as prior to it. The following insulation-to-case unbonds were noted in the aft cylinder clevis insulation.

<u>Location</u> (deg)	<u>Description (in.)</u> (circumference x depth)
204*	0.30 x 0.10
244	0.70 x 0.15
255	1.0 x 1.5
258	0.50 x 0.25
258-260	0.70 x 1.5

All of the unbonds noted above, except those marked with an asterisk (*), coincide with the unflow areas which were restructured with asbestos-filled epoxy.

The final condition of the joint was very good. Even though TPTA 1.1 was an unintentional closed vessel, no major defects or gas paths were created and it appeared as if major refurbishment in the joint area would not be required.

- c. Test Joint B. The aft cylinder-to-ETA stiffener joint showed no evidence of joint leakage or hot gas paths, except in two isolated cases which will be discussed later. The J-insulation slot was full of soot, as is normally the case. No case unbonds were noted in this joint. The clevis joint was heat affected around the entire circumference from the edge of the inhibitor outboard 0.4 to 0.5 in. to the sealing point of the joint as in Joint A. The tang was heat affected at the tip of the J-insulation approximately 0.1 in. outboard and 360 deg circumferentially. There were areas of heat-affected rubber at 0 and 248 deg, which were 0.2 in. outboard from the sealing point and 1.2 to 1.4 in. circumferential. This was similar to what was seen on Joint A.

There was also evidence of soot and heat effects past the sealing point on the clevis side of the joint at 120 deg. It was 0.8 in. wide at the ID tip of the seal area, narrowing to 0.2 in. at the point farthest outboard. The soot reached in 1.5 in. from the tip of the

J-insulation (Figure 7.3-23). The soot paths were located near the normal bondline transducers. These transducers were slightly above the surface of the insulation, and it is evident that the transducers created enough gap to allow the hot gas from the motor to intrude in the joint bondline. During refurbishment of the postfire hardware, this area will be brought back to a smooth surface. Another similar area, but not as severe, was seen near the 240-deg bondline transducers. It measured approximately 1.5 in. circumferentially and extended into the bondline only 0.6 in. maximum (Figure 7.3-24). Both areas (120 and 240 deg) appeared to have been exposed to the motor environment for the full duration of the test; yet the remainder of the J-insulation functioned as designed, allowing no circumferential sooting or further intrusion into the bondline surface.

As noted for Joint A, the tang J-insulation contacted the clevis sealing surface further outboard than was depicted on the joint assembly drawings. This was also seen on the JES-3 motors. The distances shown are in the table following. The radial distance of joint contact, as shown by adhesive failure of the joint adhesive, is also noted. Both are shown in Figure 7.3-22.

Engagement Distance and Joint Contact

<u>Location (deg)</u>	<u>Engagement Distance (in.)</u>	<u>Joint Contact (in.)</u>
0	0.40	1.4
45	0.40	1.4
90	0.45	0.6
135	0.40	0.8
180	0.45	1.6
225	0.40	0.5
270	0.40	1.0
315	0.40	1.7

These measurements taken every 45 deg are representative of the full circumference, except at 216 to 220 deg. At this location the adhesive

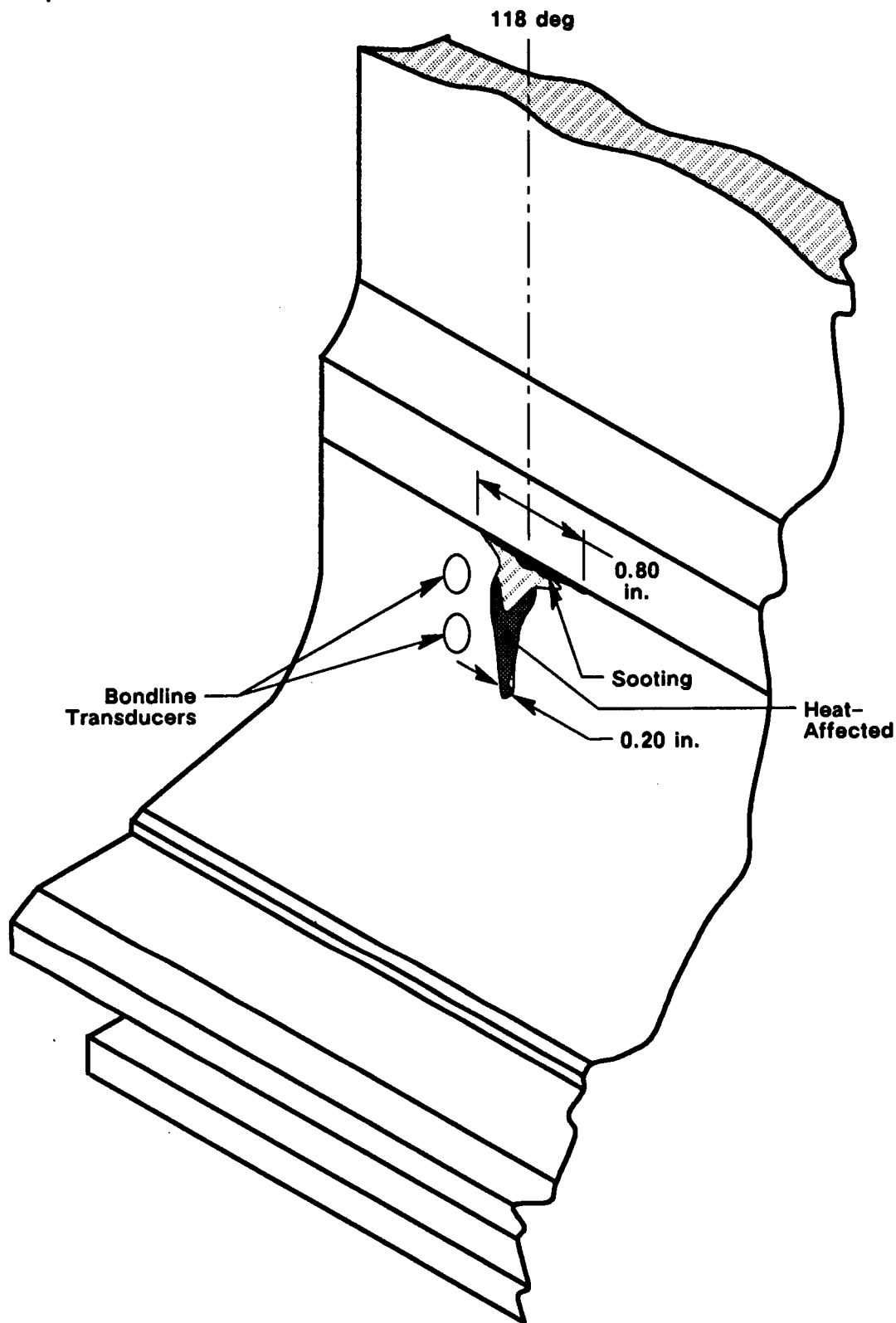


Figure 7.3-23. Joint B J-Insulation Clevis Soot Path

A012716a

REVISION _____

DOC NO. TWR-17927
SEC _____

VOL _____
PAGE _____
209

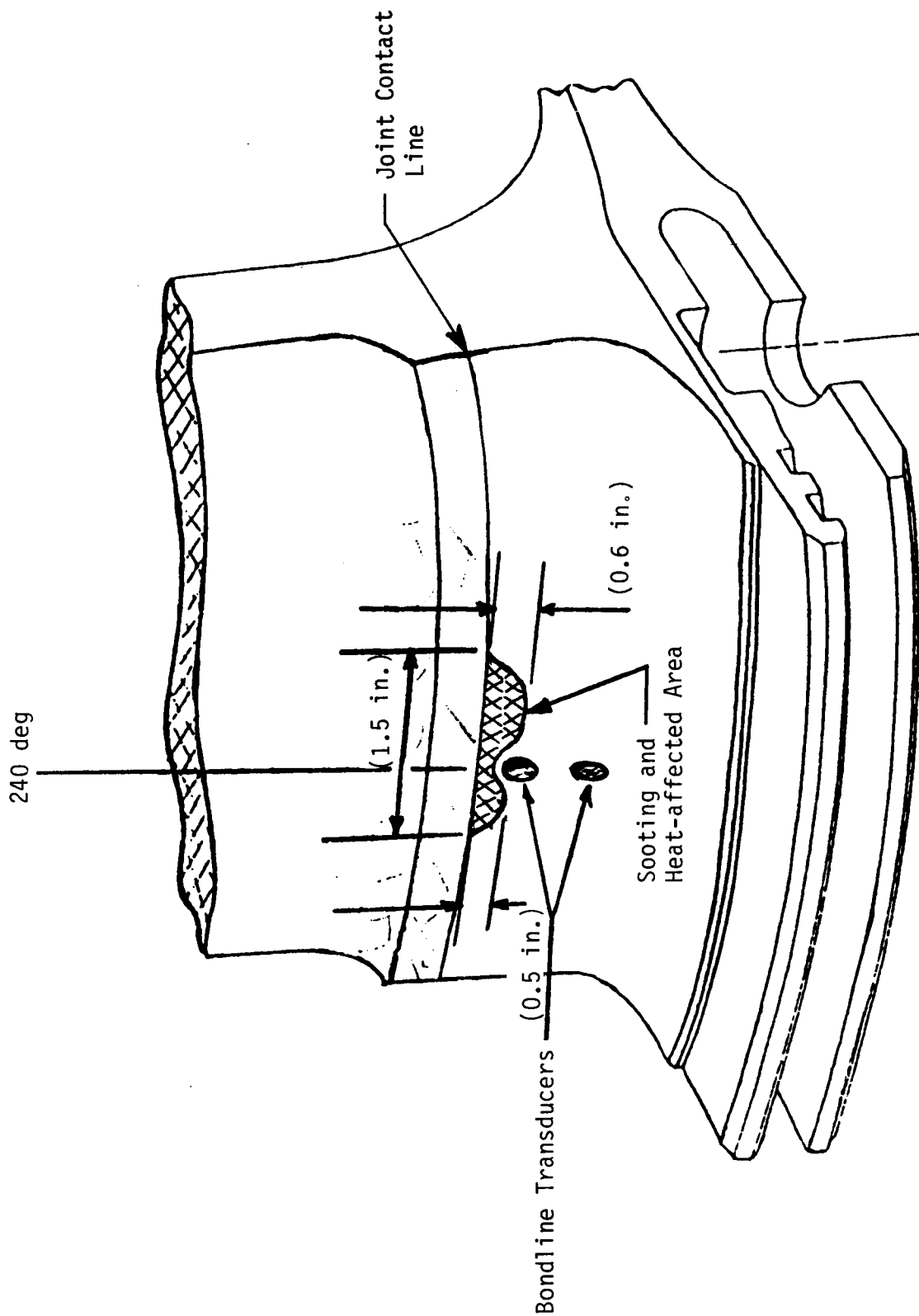


Figure 7.3-24. Joint B J-insulation Clevis Soot Path

failed adhesively for the full radial length of the bondline for a 6-in. circumference. The P8 strut load, which was applied at 223 deg, may have been a possible contributor to this, but nothing was observed which could prove this conclusively. Subsequent TPTA test hardware will be inspected in this area for similar anomalies.

Insulation separations in the clevis joint, which were noted and inspected prior to test, did not appear to have propagated, but may have opened up slightly in the "C" dimension (Figure 7.3-25). The instrumentation appears to be in as good condition after the test as it was prior to the firing. The joint in general appeared to have come through the test in reasonably good condition. No major refurbishment seems necessary at this time.

- d. ETA/Aft Dome Joint. The nontest joint was similar to the forward dome joint and to previous aft dome joints in the JES tests. No gas jetting or other anomalous conditions were noted from the test. No unbonds were noted on the joint surface.
- e. Nozzle-to-Case Joint. The joint performance of test Joint D (nozzle-to-case) appeared nominal and comparable to previous tests on NJES. A gas path was noted at 188 deg, which extended from the entrance of the joint to the wiper O-ring. The gas path ranged from 0.280 in. wide at the entrance, to 0.160 in. at the step in the phenolic, to 0.180 in. forward of the wiper O-ring (Figure 7.3-26). The gas path was filled with a dark viscous material, which was identified as heat-affected and decomposed polysulfide adhesive. This differed from the NJES-2B test where the intentional defect had been filled with soot. The decomposed polysulfide penetrated into the wiper O-ring groove approximately 8 to 10 deg in either direction from the defect. The material, however, did not get past the O-ring; nor was any damage to the wiper O-ring evident. Several other voids were also noted in the polysulfide material. Some of the voids at the wiper O-ring were colored dark. This indicates that there was hot gas flow to almost the full circumference just forward of the wiper O-ring.

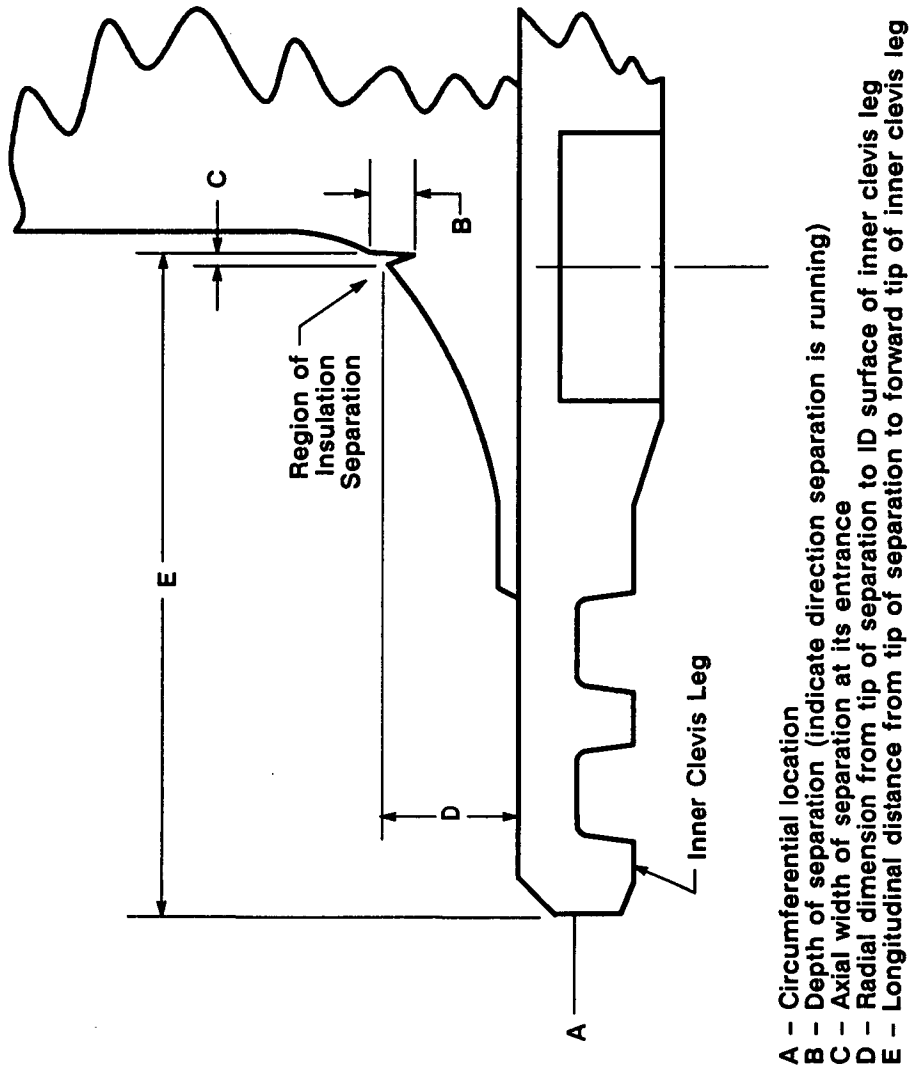


Figure 7.3-25. Test Joint Clevis Unbond Inspection Locations

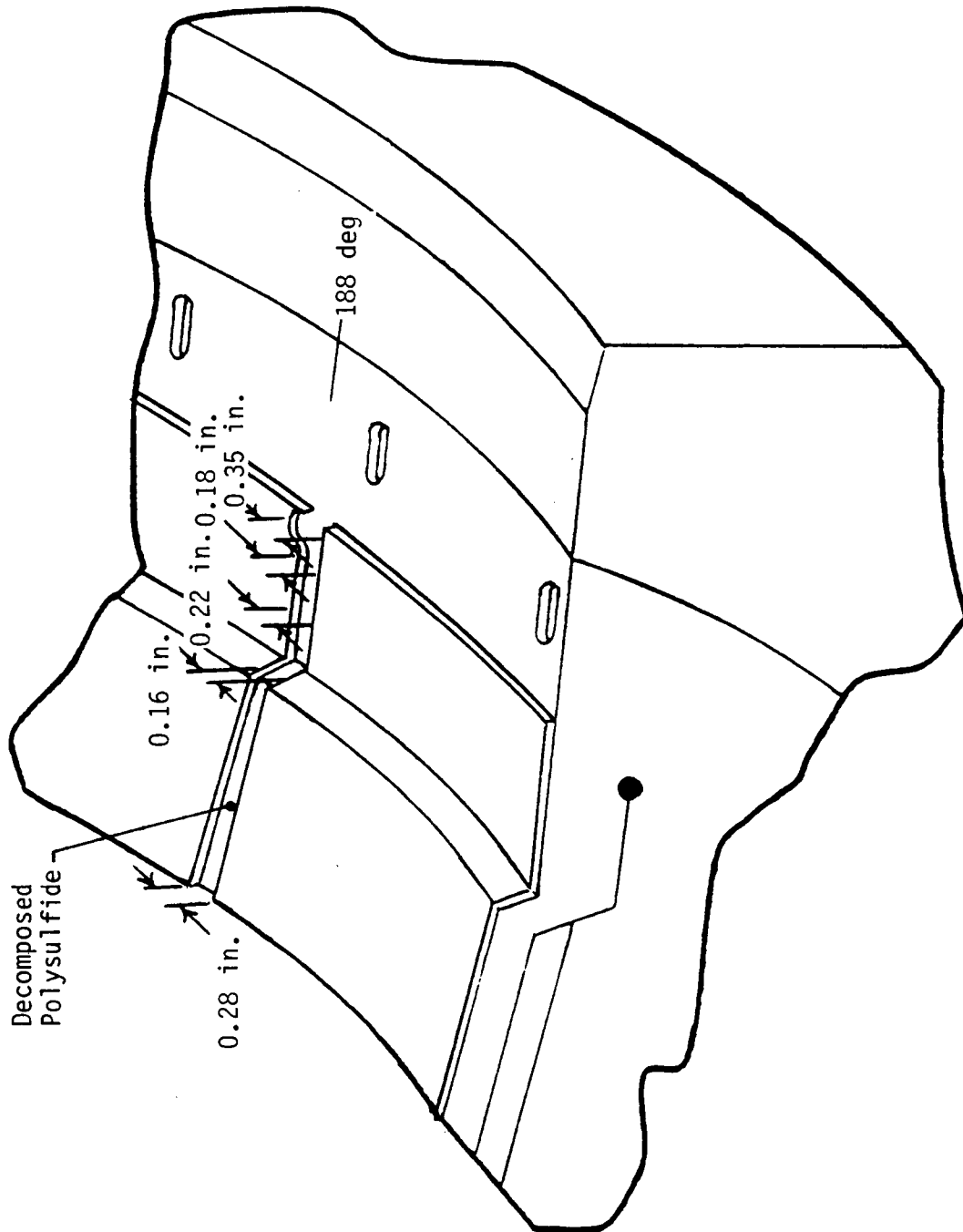


Figure 7.3-26. Nozzle-to-Case Joint (Joint D) Gas Path to Wiper O-ring

There was no polysulfide adhesive squeezeout in any of the wiper O-ring vent slots. The polysulfide failure mode was 100 percent adhesive at the phenolic interface at the step region and aft of the step, 30 percent adhesive at the phenolic interface, 60 percent adhesive at the NBR interface, and 10 percent cohesive within the polysulfide forward of the step. There was porosity noted in the polysulfide at the bondline step region, as previously seen in NJAD, NJES-2A, NJES-2B, DM-8 and laboratory test specimens. The bondline area was heat affected to a maximum depth of approximately 0.5 inch.

The increased number of polysulfide voids and the occurrence of the gas path are probably due to the short wiper vent slots used in the test. These slots were designed to the initial configuration length of 0.42 in. to 0.52 in., which was shorter than the current RSRM baseline length of 0.54 to 0.64 inch. The actual slots were even shorter than the design length, so they were much shorter than the RSRM baseline. The short slots did not allow air to be vented aft of the wiper O-ring during nozzle installation. The trapped air caused voids to occur in the polysulfide. The slots in future TPTA tests will be lengthened to match the RSRM baseline. The Insulation Design team was satisfied with the performance of the nozzle-to-case joint. Although there was a gas path through the bondline, no gas reached the primary O-ring and none of the joint components were damaged, including the wiper O-ring. This verifies that the redesigned joint can withstand such damage without compromising the joint performance.

- f. NBR Acreage Areas. The acreage areas of all segments were insulated with the thicker insulation used on the JES-3 tests. All segments were newly manufactured and insulated for this test and had 1.0 in. minimum NBR on all exposed areas and 0.200-in. thick corner patterns. The segments came through the test in reasonably good condition with no major damage.
- g. Joint Separation Loads. The stress gages in test Joint A and B were used to provide joint separation loads at demate. Data from the gages recorded loads from demate at values less than the gage accuracy. Test

data showed the demate load for the pressure-sensitive joint adhesive should be 8 to 10 pli. The joint at the bond is roughly 375 in. circumferential. At 10 pli, 3,750 lb total force would be needed to separate the joint insulation bondline.

7.4 GLOBAL FINITE ELEMENT ANALYSIS

7.4.1 Introduction

A global static analysis of the TPTA test configuration was conducted to study the basic structural response to internal pressure and strut loads of the case structure and aft field joint. "Global" refers to the modeling of the entire structure; no axisymmetric assumptions were made. The analysis was conducted using a NASTRAN finite element model. Predictions of case strain and joint gap opening were made and presented at the TPTA 1.1 test readiness review. Data from the ignition test, TPTA 1.1, were used to correlate predictions of structural response due to internal pressure. Data from the high Q test, TPTA 1.1A, were used to correlate predictions of the structural response due to strut loads.

7.4.2 Model Description

The TPTA model contains roughly 200,000 degrees of freedom (DOF) and represents one of the largest NASTRAN models ever built. The model was divided into superelements (substructures) for efficiency. A picture of the model is shown in Figure 7.4-1. The model is made up of 60 circumferential elements that evolve into 180 circumferential elements in the aft field joint (test Joint B) and ETA ring regions. Case structures are primarily modeled with plate (CQUAD4) elements. Propellant is primarily modeled with solid (CHEXA) elements.

The computer resources required to handle this model dictate that several linearizing assumptions be made, including small displacement theory, linear material properties (no yielding of steel parts, nonviscoelastic propellant), and constant load paths (contact surfaces) in the joints. The configuration was modeled with nominal geometry. For D6AC steel, an elastic modulus of 29,600 ksi and a Poisson's ratio of 0.3 were used. For propellant, an elastic modulus of 5,000 psi and a Poisson's ratio of 0.499 were used.

The 360-deg ETA ring model was built and successfully correlated to a more detailed model built by USBI (reference L225:FY88:210). A close-up picture of a section of the ETA ring is shown in Figure 7.4-2. For the

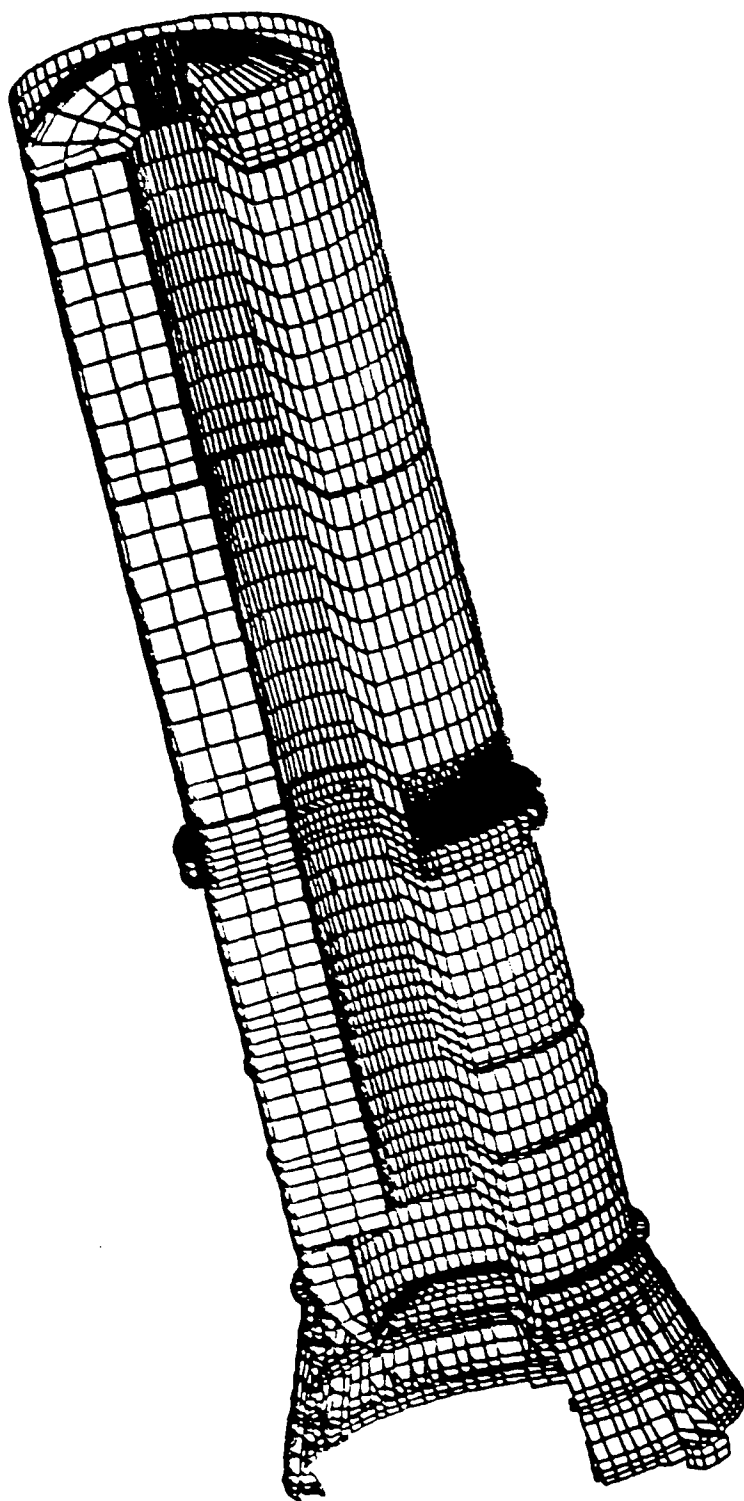


Figure 7.4-1. TPTA Finite Element Model

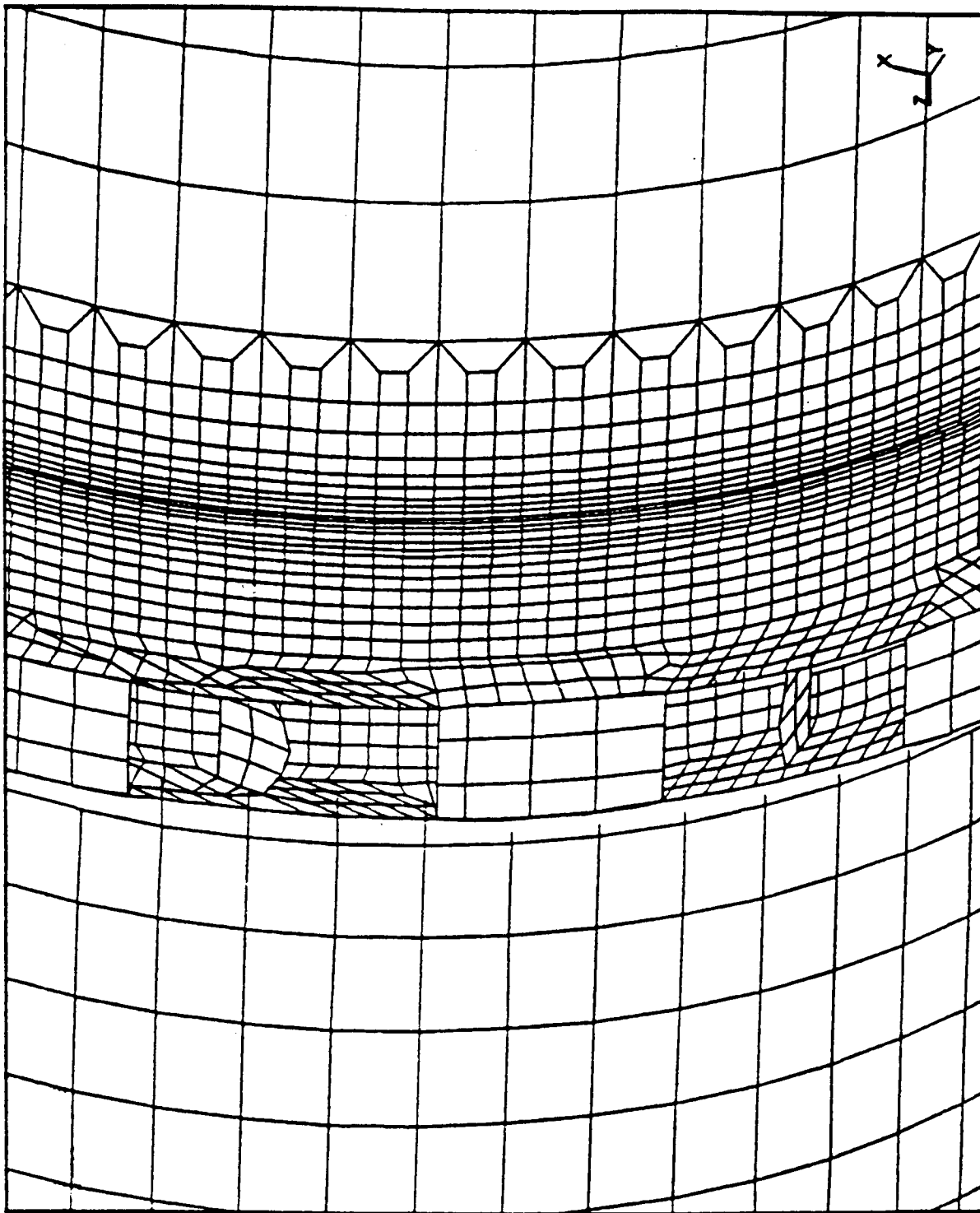


Figure 7.4-2. ETA Ring Model

TPTA configuration, this is a right-hand ETA ring. The aft skirt is a modified Lockheed model. Preliminary correlation to a detailed USBI model of the aft skirt shows reasonable agreement. The aft field joint has been modeled in some detail to enable prediction of gap response to internal pressure and strut loads. A picture of the joint model's cross section is shown in Figure 7.4-3. This joint model has been reasonably correlated to Referee Test No. 3 data (not yet documented) and JES-3A test data (reference L225:FY88:261). All other field and factory joints are modeled as continuous steel with bar elements to characterize increases in thickness.

7.4.3 Correlation of Predictions With Test Data

7.4.3.1 Strain Due to Static Hot-firing Test (TPTA 1.1). Several axial locations (stations) along the motor length were chosen to study case strain due the effects of internal pressure, strut loads, and the nonsymmetries of the aft skirt. These axial stations are shown in Figure 7.4-4.

Pretest predictions were made for an ignition test with strut loads. However, due to the failure of the strut load delivery system, no strut loads were applied during the static hot-firing test. Although unfortunate, this provided an opportunity to study case response to internal pressure, similar to a JES test. Since no pretest predictions of such a test were made, predictions for response to internal pressure had to be made after the fact. But no changes in the model were made to produce the predictions since they are as good as the original pretest prediction.

A time trace of the pressure build-up during the ignition transient of TPTA 1.1 is shown in Figure 7.4-5. Strain data at $T = 1.0$ sec was used to study the effects of internal pressure on case strain. This time period was chosen as a near maximum internal pressure (876 psig) where acoustic oscillations have dampened out.

Figure 7.4-6 is a plot of predicted versus measured hoop strain at Station 1511.0, the ETA ring midpoint. This plot shows the predictions to be within 5 percent of the measured strain values. The instrumentation is located in a manner to measure the magnitude of the predicted strain

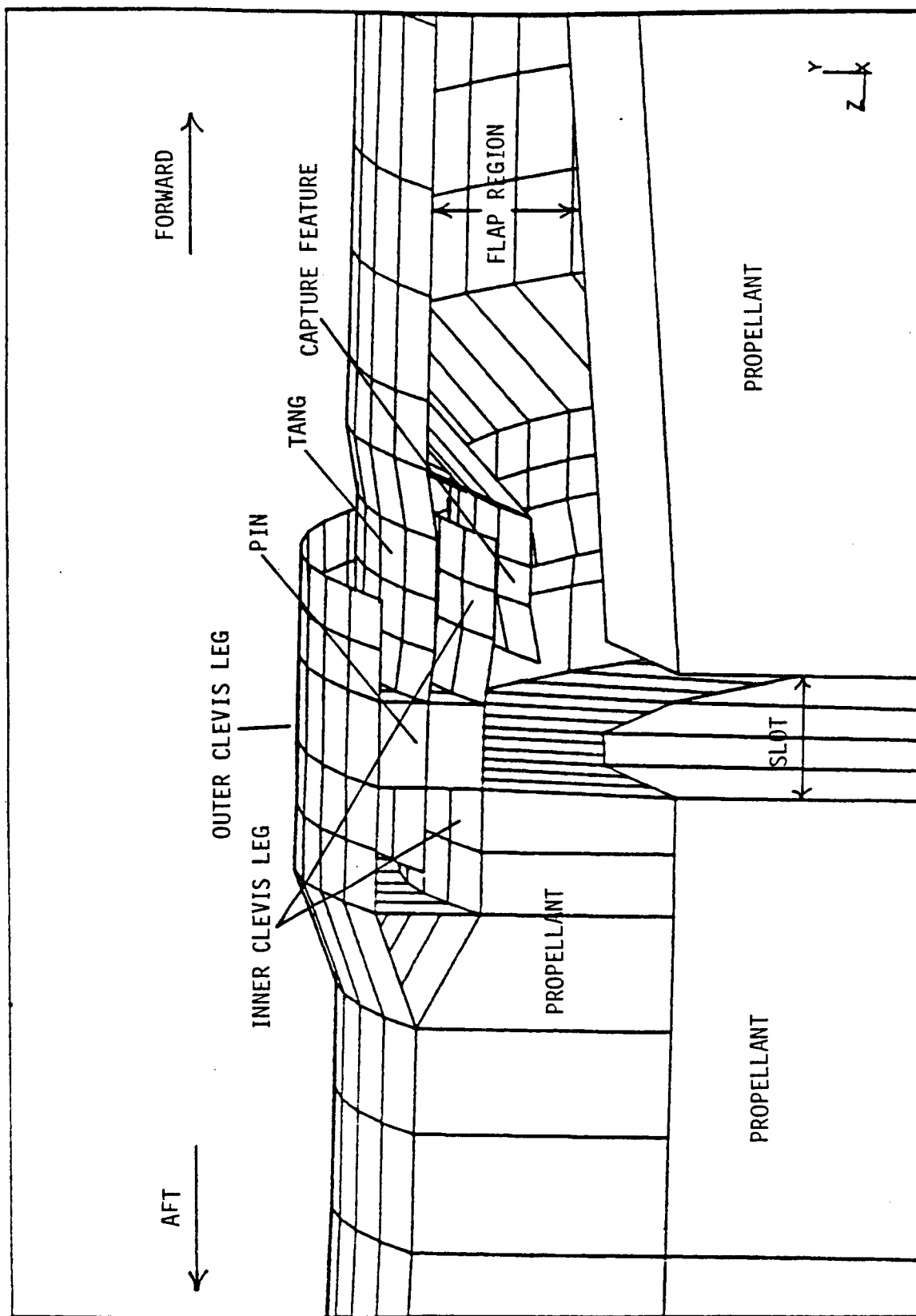


Figure 7.4-3. TPTA Field Joint Model

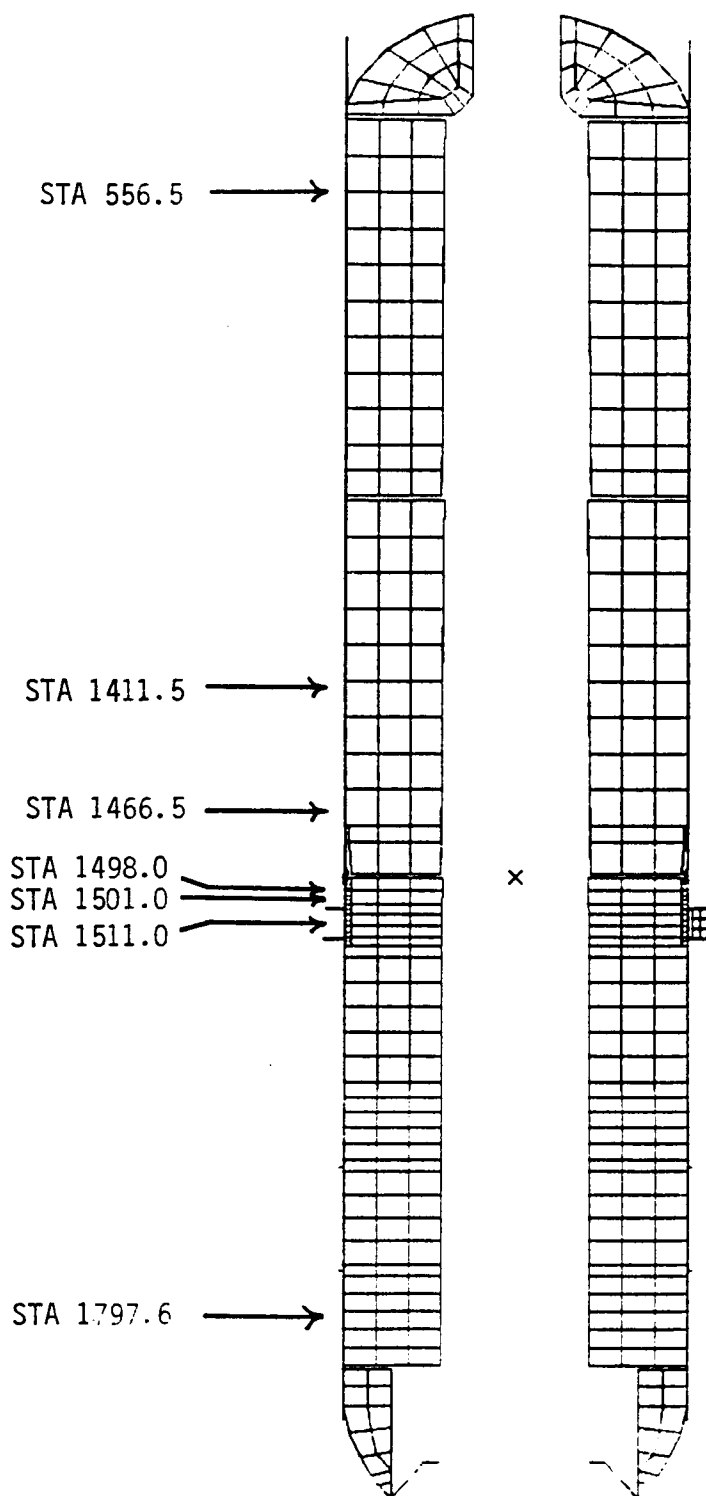


Figure 7.4-4. Axial Stations of Predicted Strain Gages

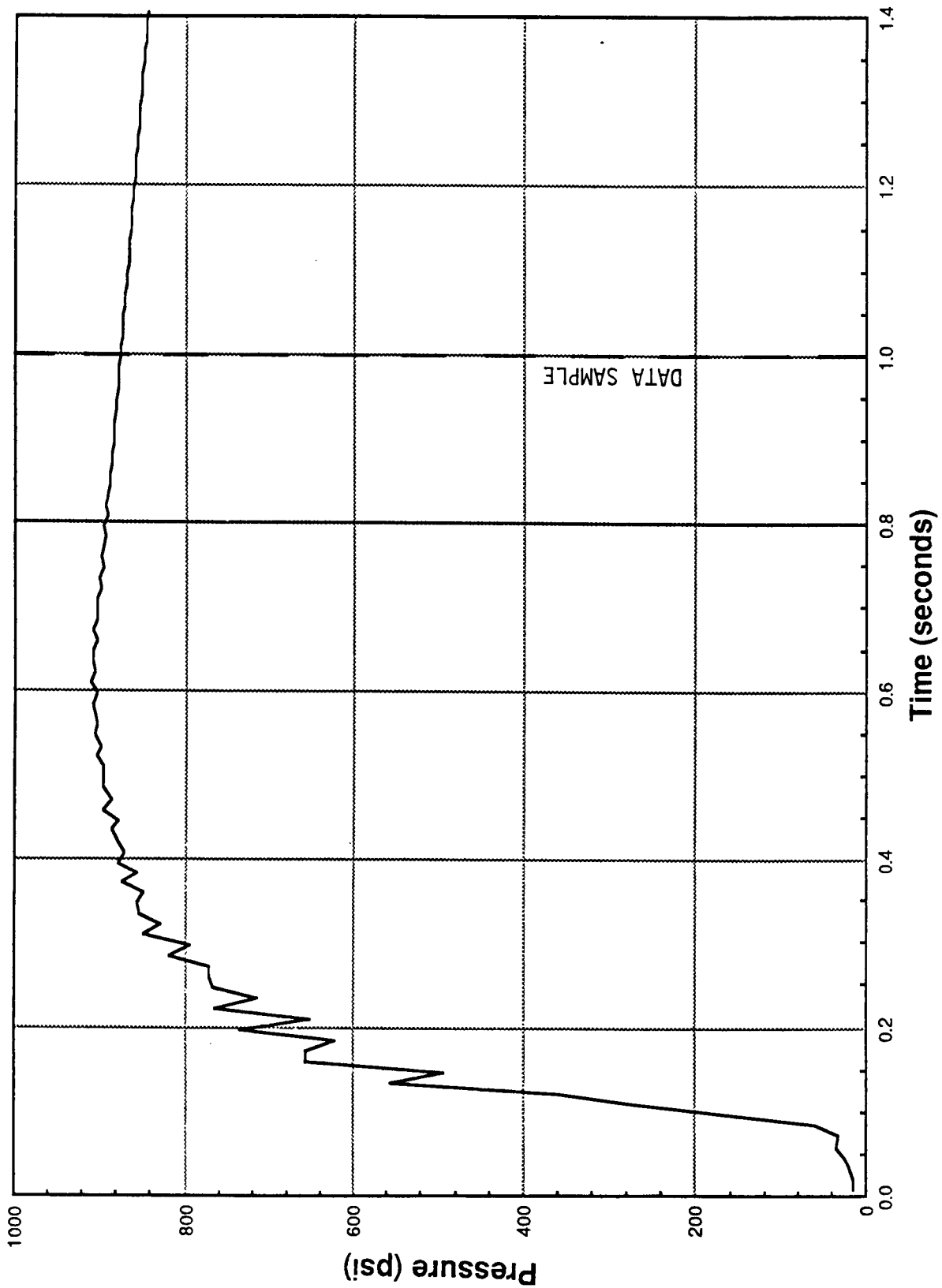


Figure 7.4-5. TPTA 1.1 Ignition Pressure Time Trace

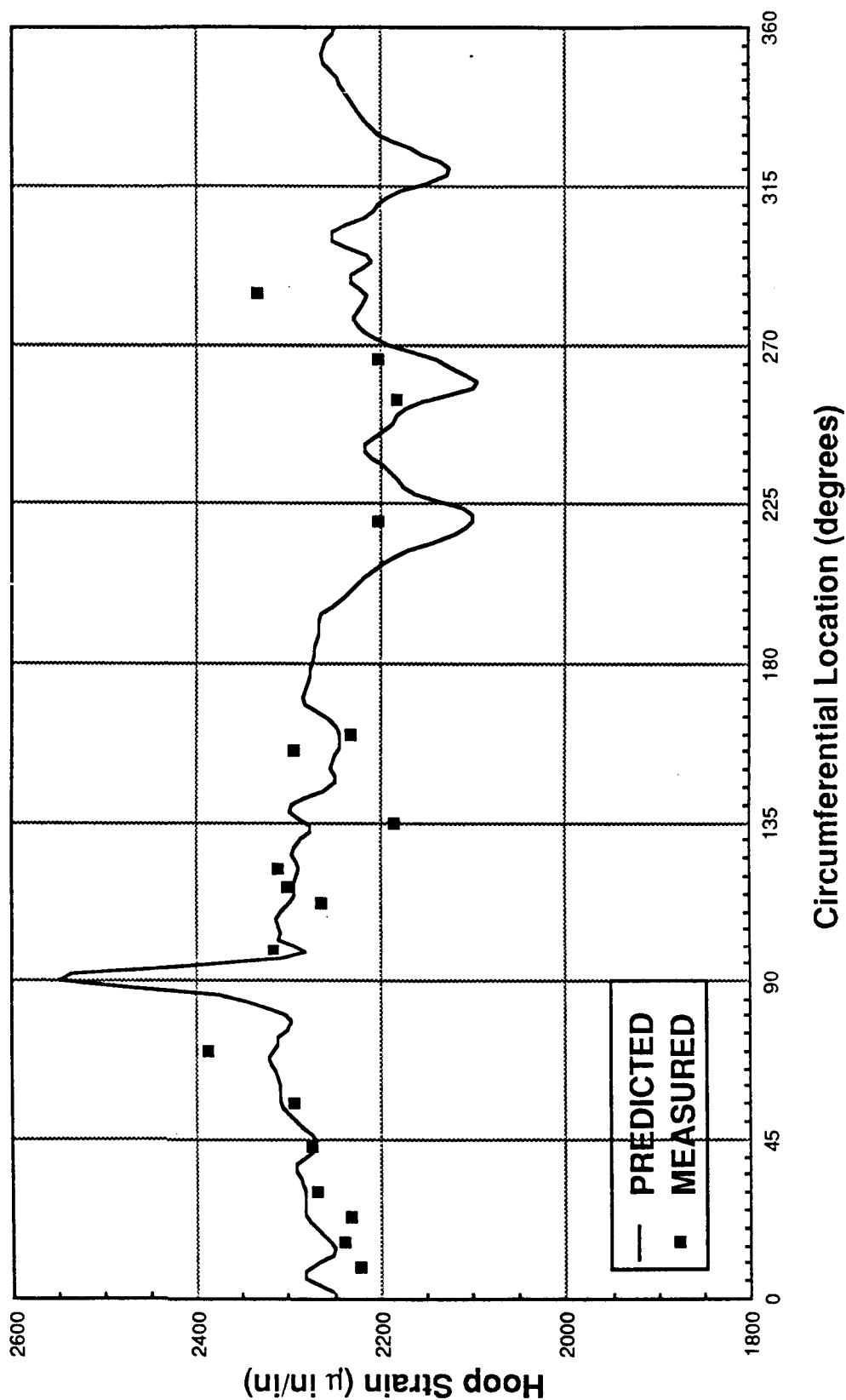


Figure 7.4-6. TPTA Post-Test Correlation, Predicted Versus Measured Hoop Strain at Sta 1511.0 Due to Maximum Ignition Pressure (876 psig)

peak at 90 deg because of the stiffness discontinuity at the ETA ring/systems tunnel interface. Figure 7.4-7 is a plot of the axial strain correlation at the same location. Although the prediction tends to be high, it correlates within 10 percent of the measured values.

Figure 7.4-8 through 7.4-11 are plots of hoop and axial strain correlations at two stations (1498.0 and 1501.0) that lie between the aft field joint and the ETA ring. These plots show agreement between the predicted and measured data within 1 to 10 percent. This agreement is very good for this region since it is an area with large strain gradients caused by the varying thickness of the case. The gradient is especially noticeable in the axial strains of the two stations. Though these stations are only 3 in. apart, the predicted strain varies from 1,900 $\mu\text{in./in.}$ at Station 1498.0 (Figure 7.4-8) to 1,100 $\mu\text{in./in.}$ at Station 1501.0 (Figure 7.4-11). This is a change in strain of more than 20 percent over only a 3-in. region. The measured data suggests that the gradient might even be larger. Lack of fidelity in the model would likely underpredict this gradient. The existence of the gradient also suggests that if the strain gages are only a fraction of an inch out of place, the readings would change drastically. Considering this, the correlation of the predicted-to-measured strain data to within 10 percent at these locations is very good.

Figures 7.4-12 and 7.4-13 are plots of hoop and axial strain correlations, respectively, at Station 1797.6, which is located in the stiffener segment several inches above the aft skirt. The hoop strain is predicted within 10 percent. The axial strain prediction, though off by a larger percentage, is still within 100 $\mu\text{in./in.}$, which is reasonable considering the coarseness with which the aft skirt/aft dome interface is modeled. The nonsymmetries of the aft skirt holddown posts can be seen in the axial strain prediction (Figure 7.4-13). The doublehumped curve is representative of the two planes of symmetry created by this configuration. The measured data suggest that this out-of-roundness is even more severe than predicted. Since the hoop correlation suggests that the case membrane region modeled is too flexible in the case region, it is likely that the model is too stiff at the aft skirt. More data would be necessary to confirm this.

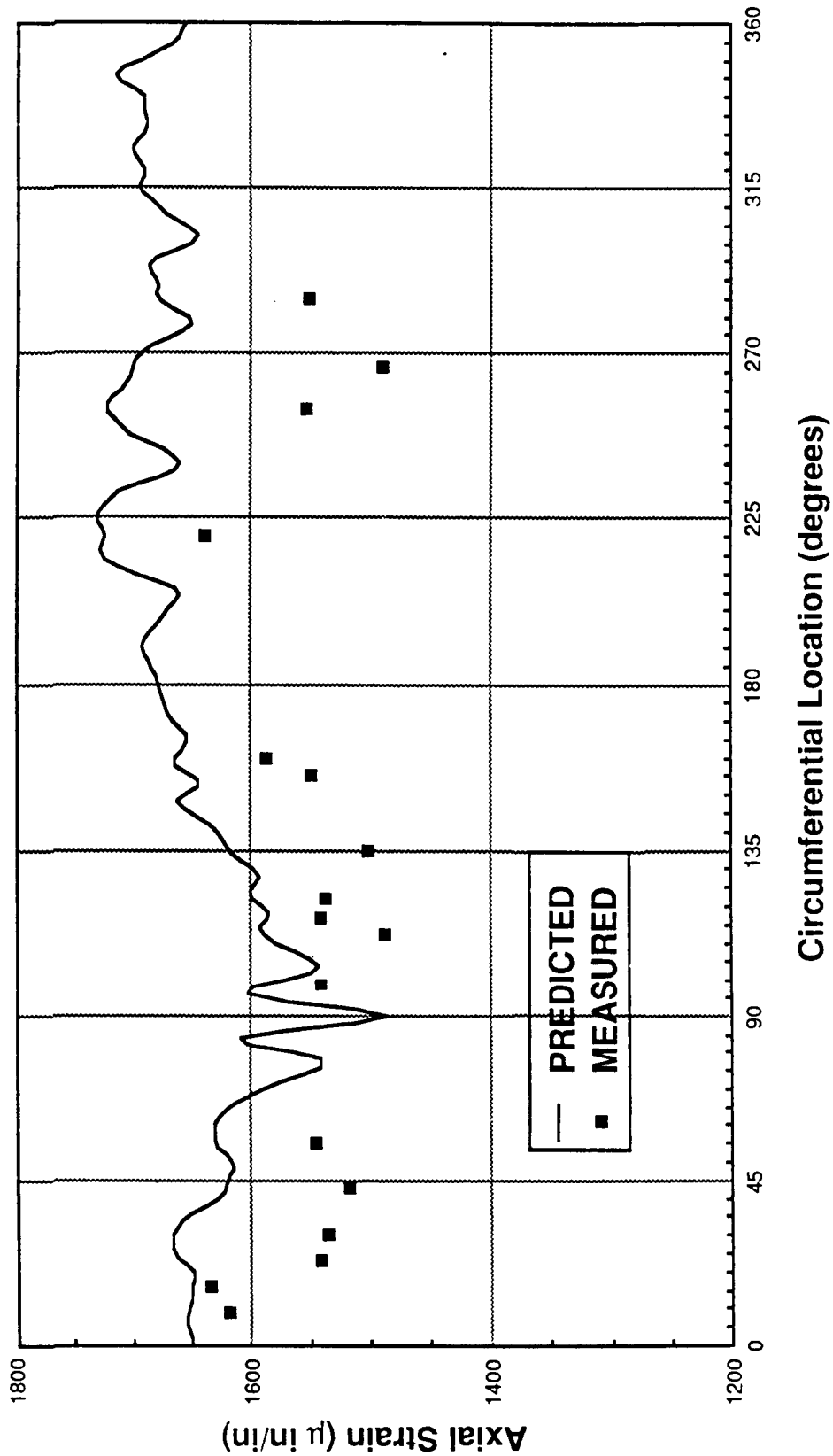


Figure 7.4-7. TPTA Post-Test Correlation, Predicted Versus Measured Axial Strain at STA 1511.0 Due to Maximum Ignition Pressure (876 psig)

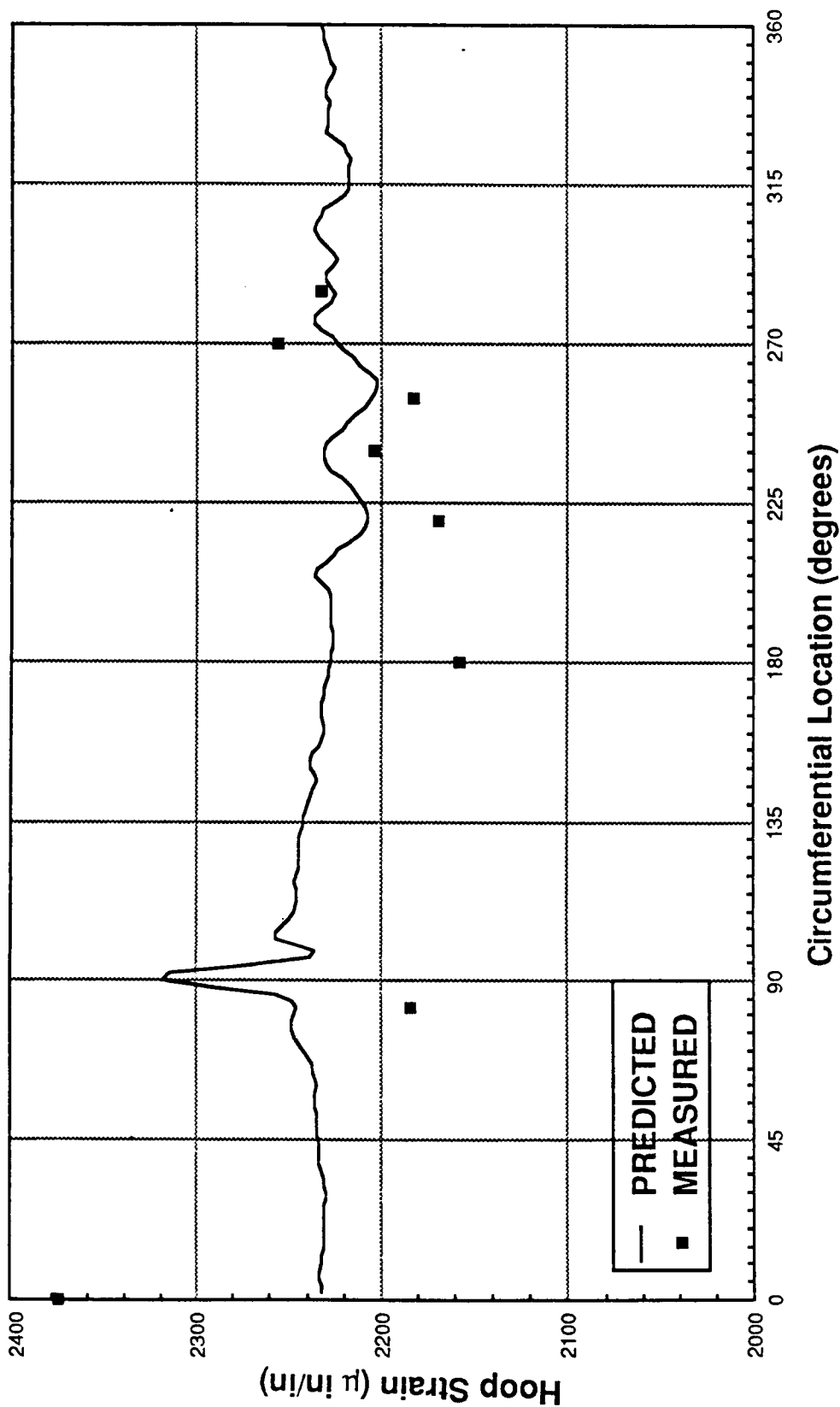


Figure 7.4-8. TPTA Post-Test Correlation, Predicted Versus Measured Hoop Strain at Sta 1498.0 Due to Maximum Ignition Pressure (876 psig)

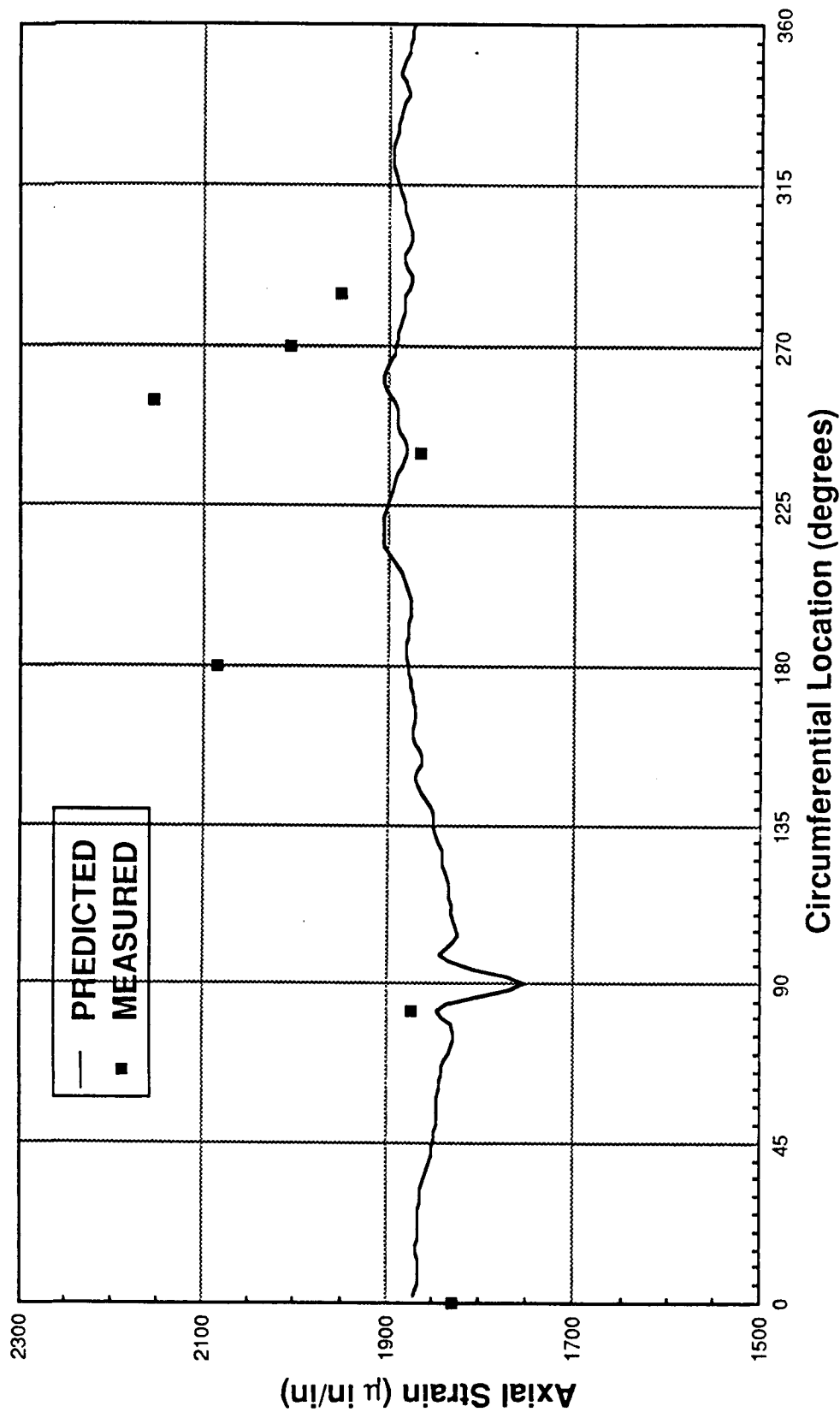


Figure 7.4-9. TPTA Post-Test Correlation, Predicted Versus Measured Axial Strain at Sta 1498.0 Due to Maximum Ignition Pressure (876 psig)

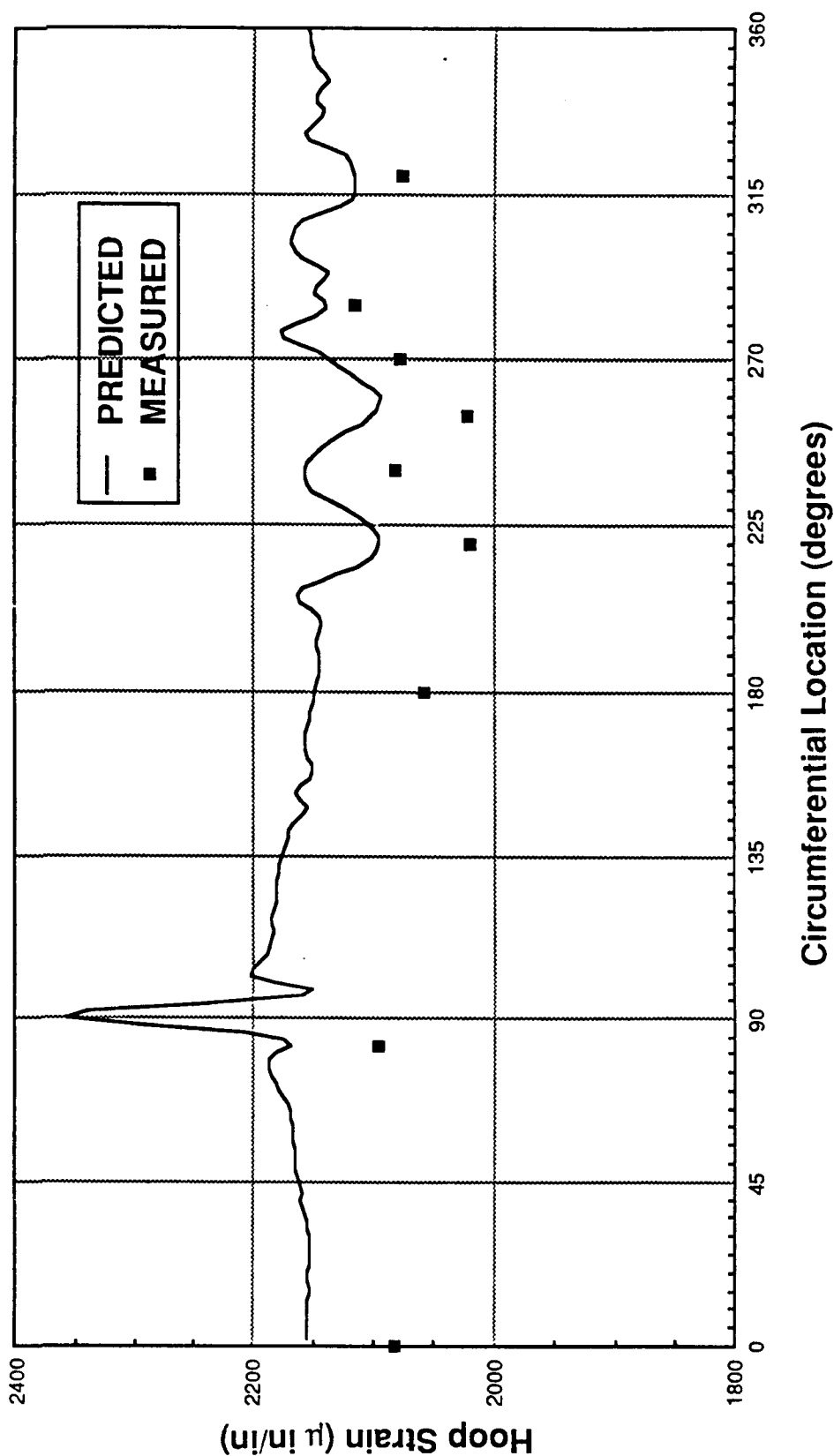


Figure 7.4-10. TPTA Post-Test Correlation, Predicted Versus Measured Hoop Strain at Sta 1501.0 Due to Maximum Ignition Pressure (876 psig)

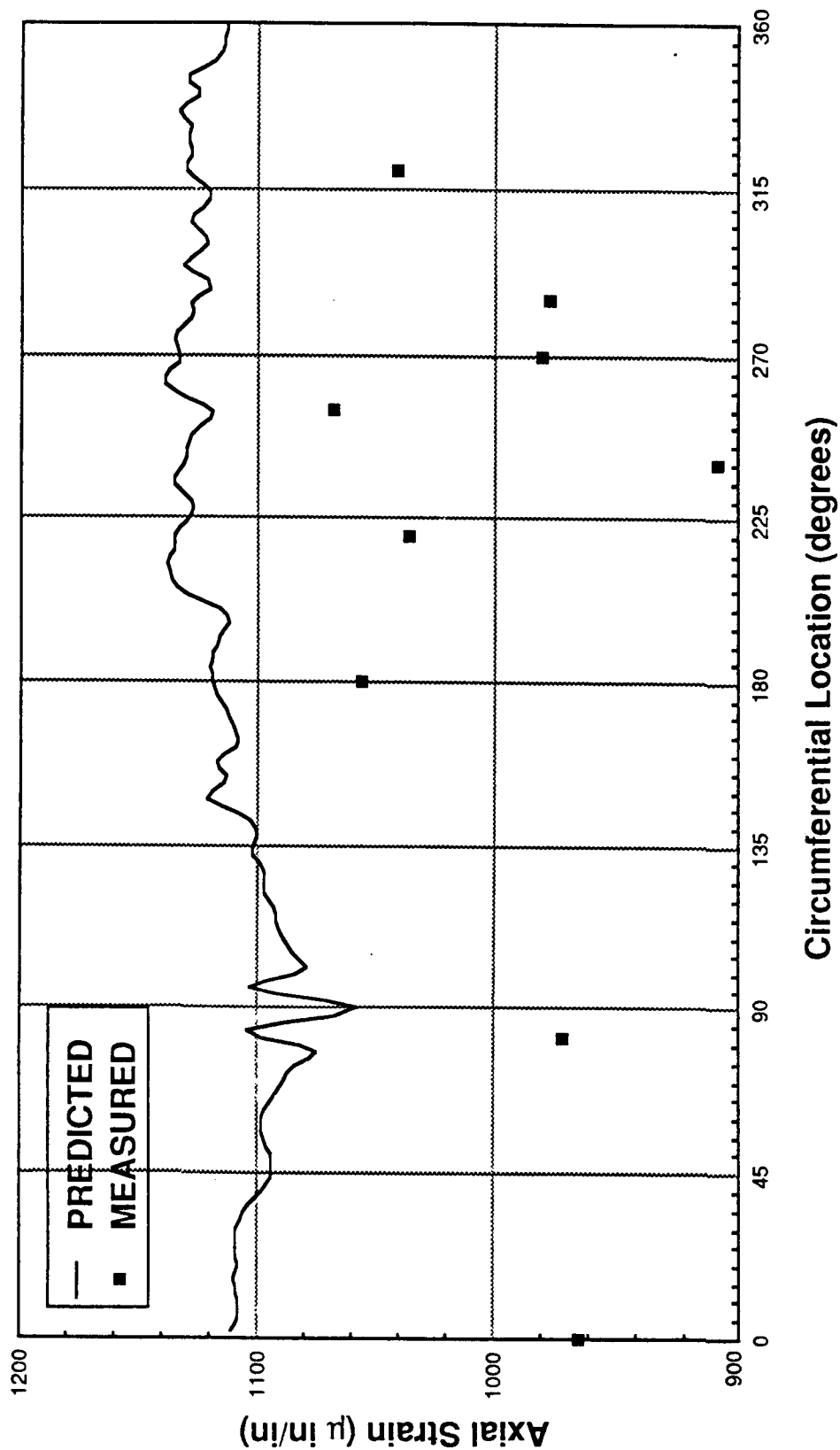


Figure 7.4-11. TPTA Post-Test Correlation, Predicted Versus Measured Axial Strain at Sta 1501.0 Due to Maximum Ignition Pressure (876 psig)

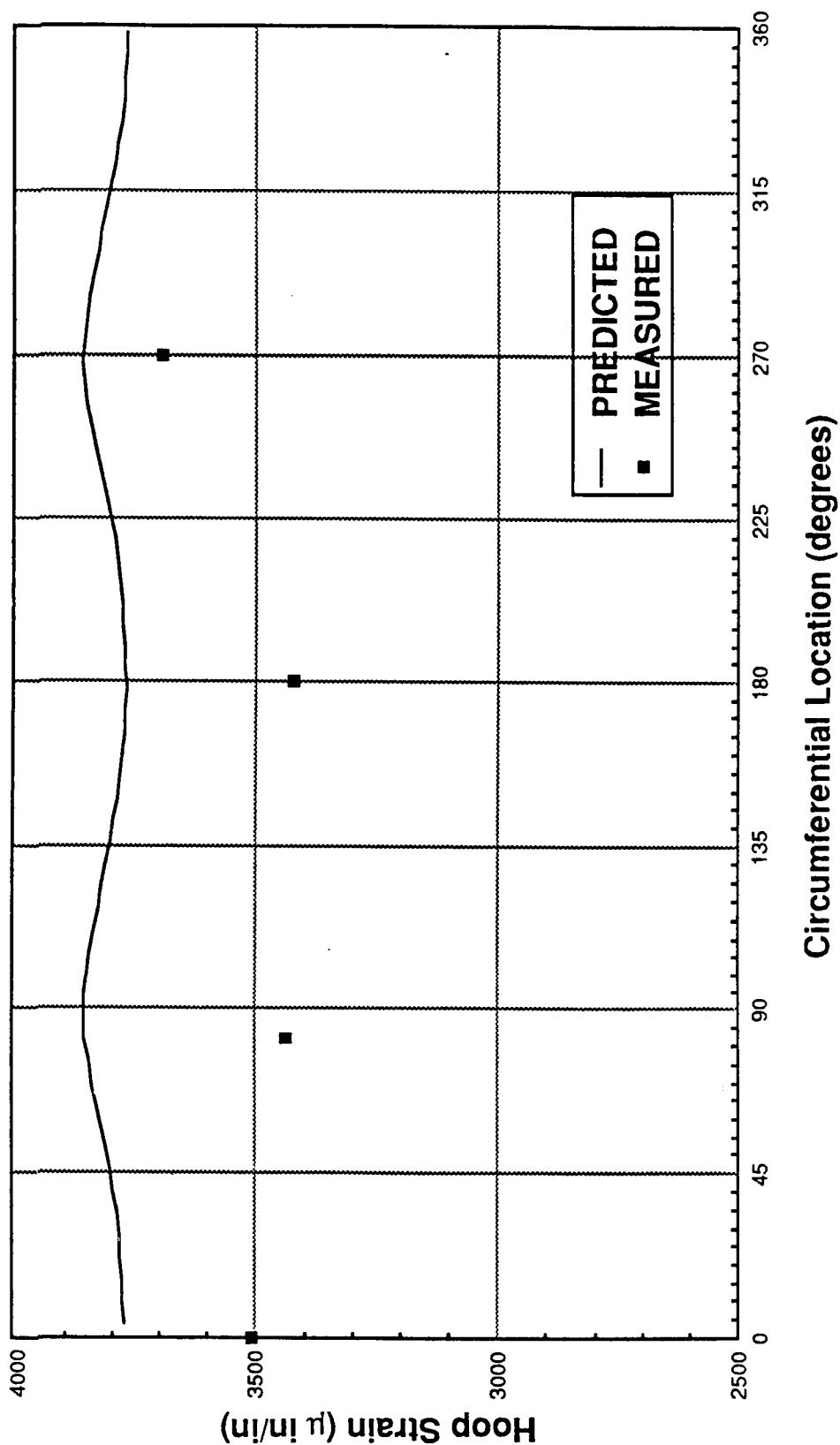


Figure 7.4-12. TPTA Post-Test Correlation, Predicted Versus Measured Hoop Strain at Sta 1797.6 Due to Maximum Ignition Pressure (876 psig)

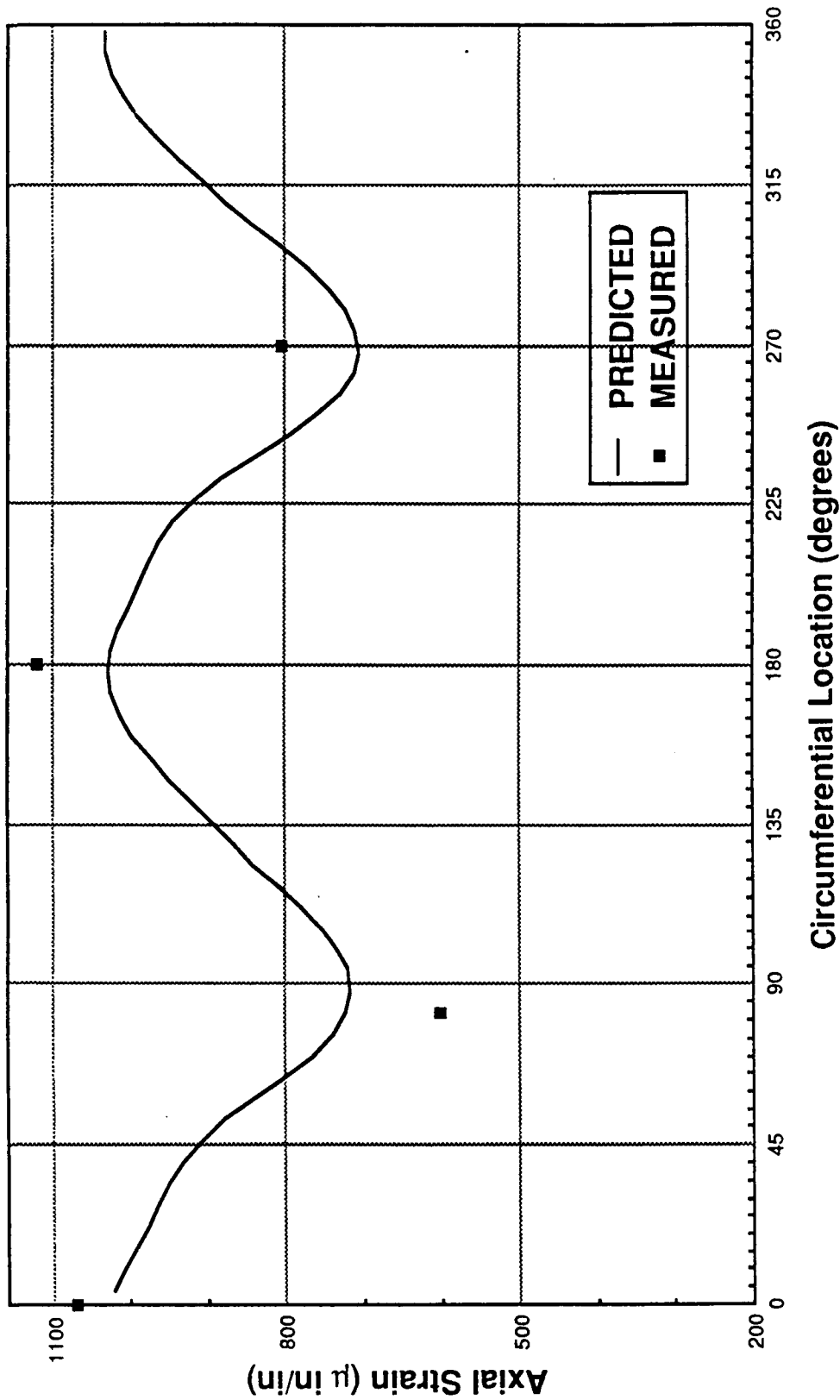


Figure 7.4-13. TPTA Post-Test Correlation, Predicted Versus Measured Axial Strain at Sta 1797.6 Due to Maximum Ignition Pressure (876 psig)

7.4.3.2 Strain Due to Strut Loads During the Cold Gas High Q Test (TPTA 1.1A). High Q loads applied in TPTA 1.1A were used to study case strain response to strut loads. For this loading condition, the internal pressure was brought up to 610 psig (using GN_2) and then the high Q strut loads were applied. Figure 7.4-14 is a plot of the strut time histories. Data sampled at $T = 9$ sec measure response from 610 psi internal pressure. Data sampled at $T = 12.4$ sec measures response from the strut loads and the internal pressure. By using the difference between these two time slices, the response of the case from only the strut loads is measured. At $T = 12.4$ sec, the strut loads are $P8 = -157.3$ kips, $P9 = 241.5$ kips, and $P10 = 245.7$ kips, where a positive force denotes tension. Since this strut load combination differs from the combination used for the pretest prediction, the predictions were redone at the actual applied load levels. Again, no changes were made in the model when generating the load-updated predictions; they are as valid as the original set.

Figures 7.4-15 through 7.4-28 are plots of predicted versus measured hoop and axial strain data at the seven axial stations shown in Figure 7.4-4. In the correlation of strain due to internal pressure, the best tool for judging the agreement between predicted and measured values was percentage difference. This was true because all the values were at a high strain level and fairly consistent circumferentially. However, there are many ways to judge the quality of a correlation. One can look at percentage differences, absolute differences, trends, slopes, or other factors for judgment. Choosing the appropriate tool with which to measure agreement between predicted and measured values will enable the observer to best judge the quality of a correlation. In the case of studying response to strut loads, percentage difference is not the appropriate tool because the strain levels are very low and are generally not uniform circumferentially.

For example, at low amplitude strains, as in the hoop strain at Station 556.5 (Figure 7.4-15), it is more appropriate to observe absolute differences rather than percentage difference. A difference of $5 \mu\text{in./in.}$ at 88° , with respect to the $7,000 \mu\text{in./in.}$ range of the gages, is a very good correlation, regardless of the percentage difference it represents.

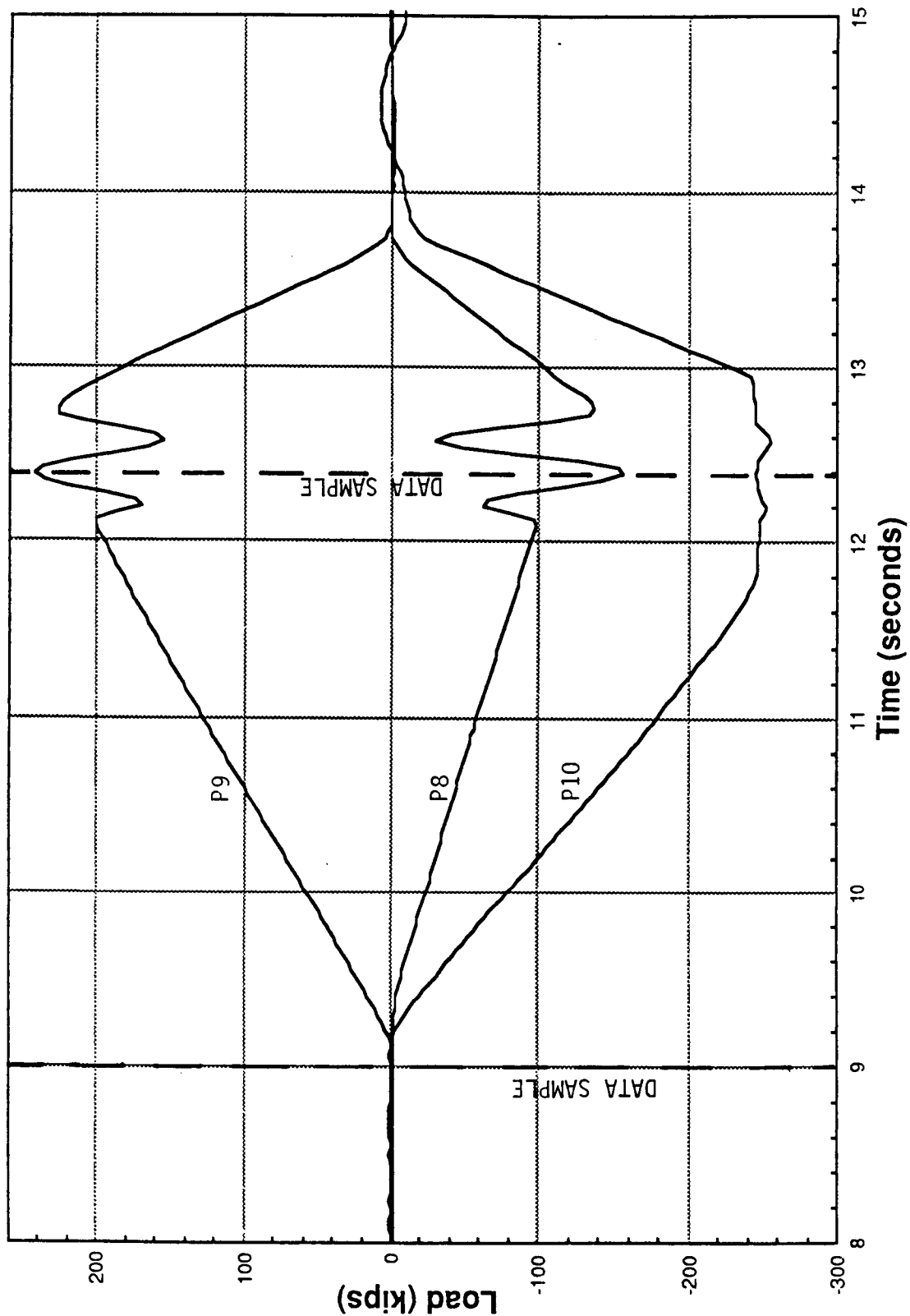


Figure 7.4-14. TPTA 1.1A Applied Max Q Strut Loads

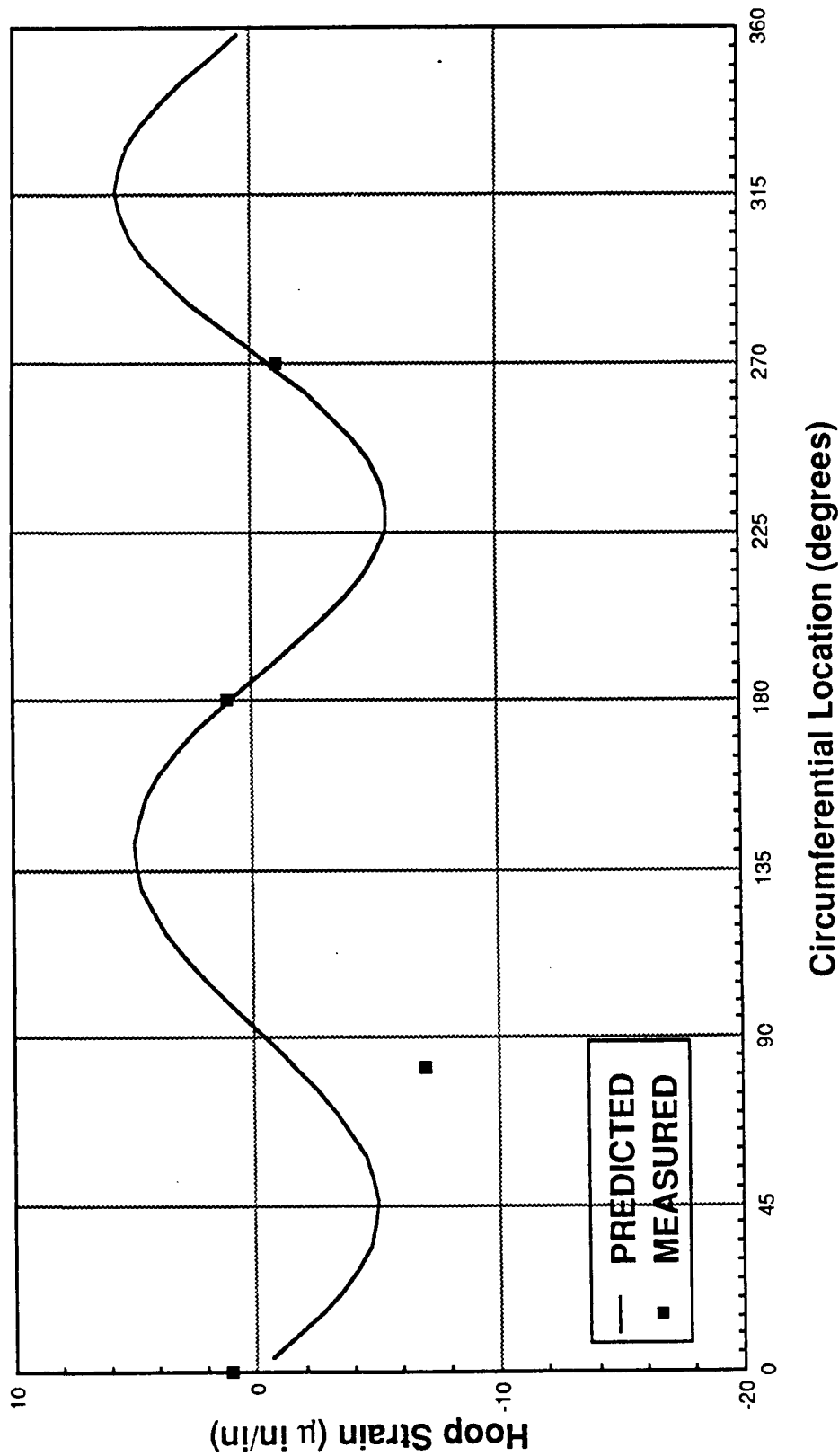


Figure 7.4-15. TPTA Post-Test Correlation, Predicted Versus Measured Hoop Strain at Sta 556.5 Due to Max Q Strut Loads (No Pressure)

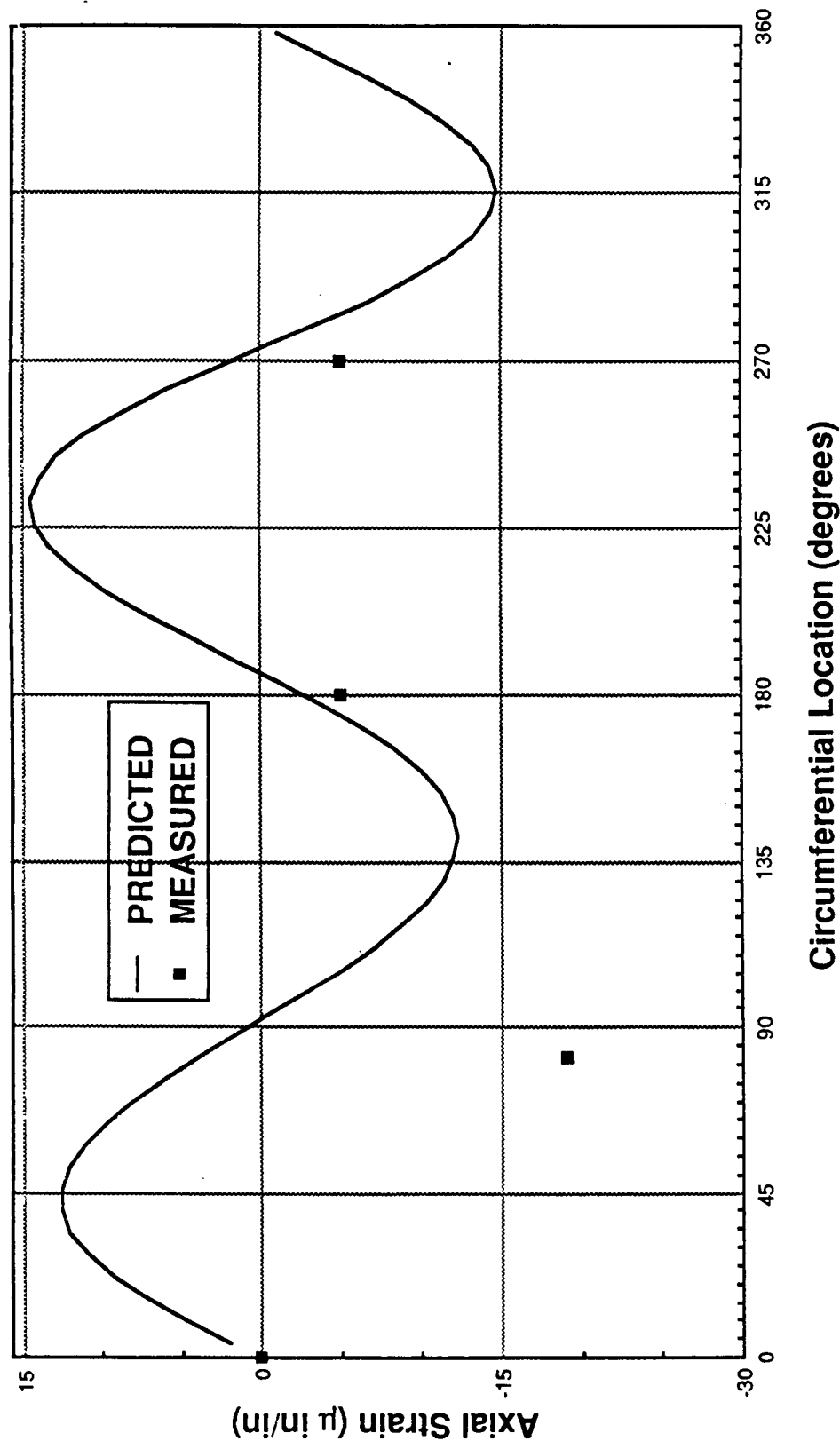


Figure 7.4-16. TPTA Post-Test Correlation, Predicted Versus Measured Axial Strain at Sta 556.5 Due to Max Q Strut Loads (No Pressure)

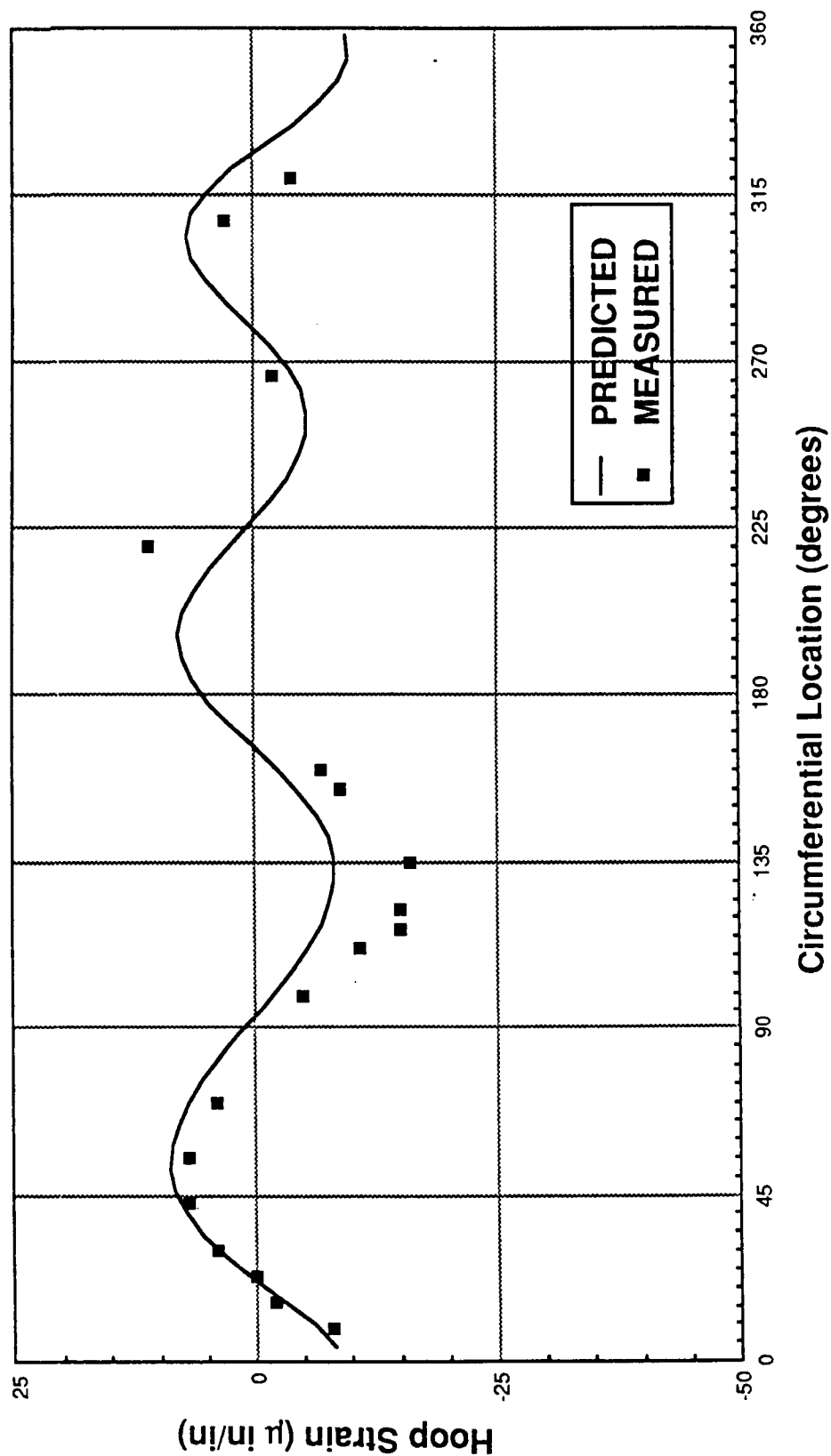


Figure 7.4-17. TPTA Post-Test Correlation, Predicted Versus Measured Hoop Strain at Sta 1411.5 Due to Max Q Strut Loads (No Pressure)

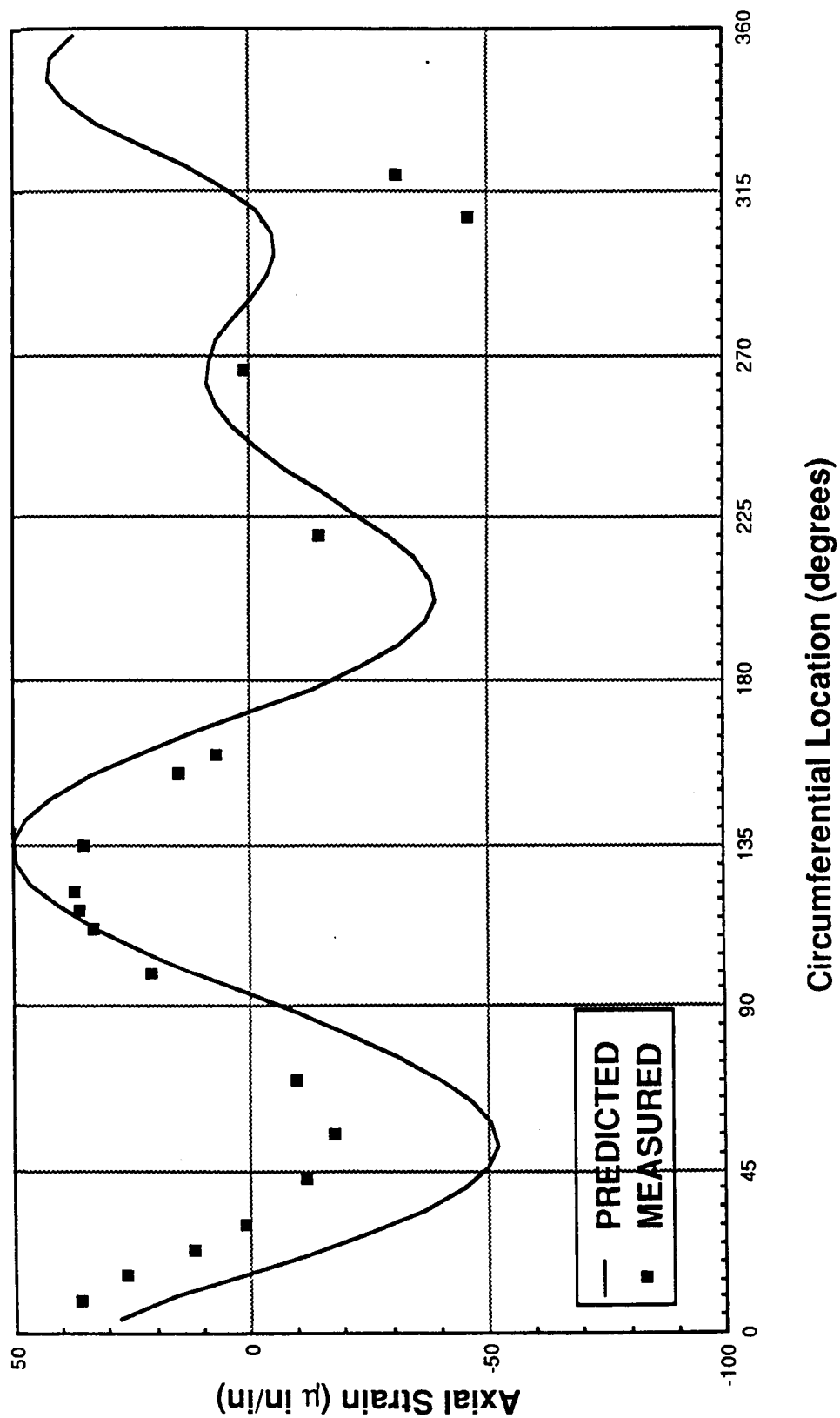


Figure 7.4-18. TPTA Post-Test Correlation, Predicted Versus Measured Axial Strain at Sta 1411.5 Due to Max Q Strut Loads (No Pressure)

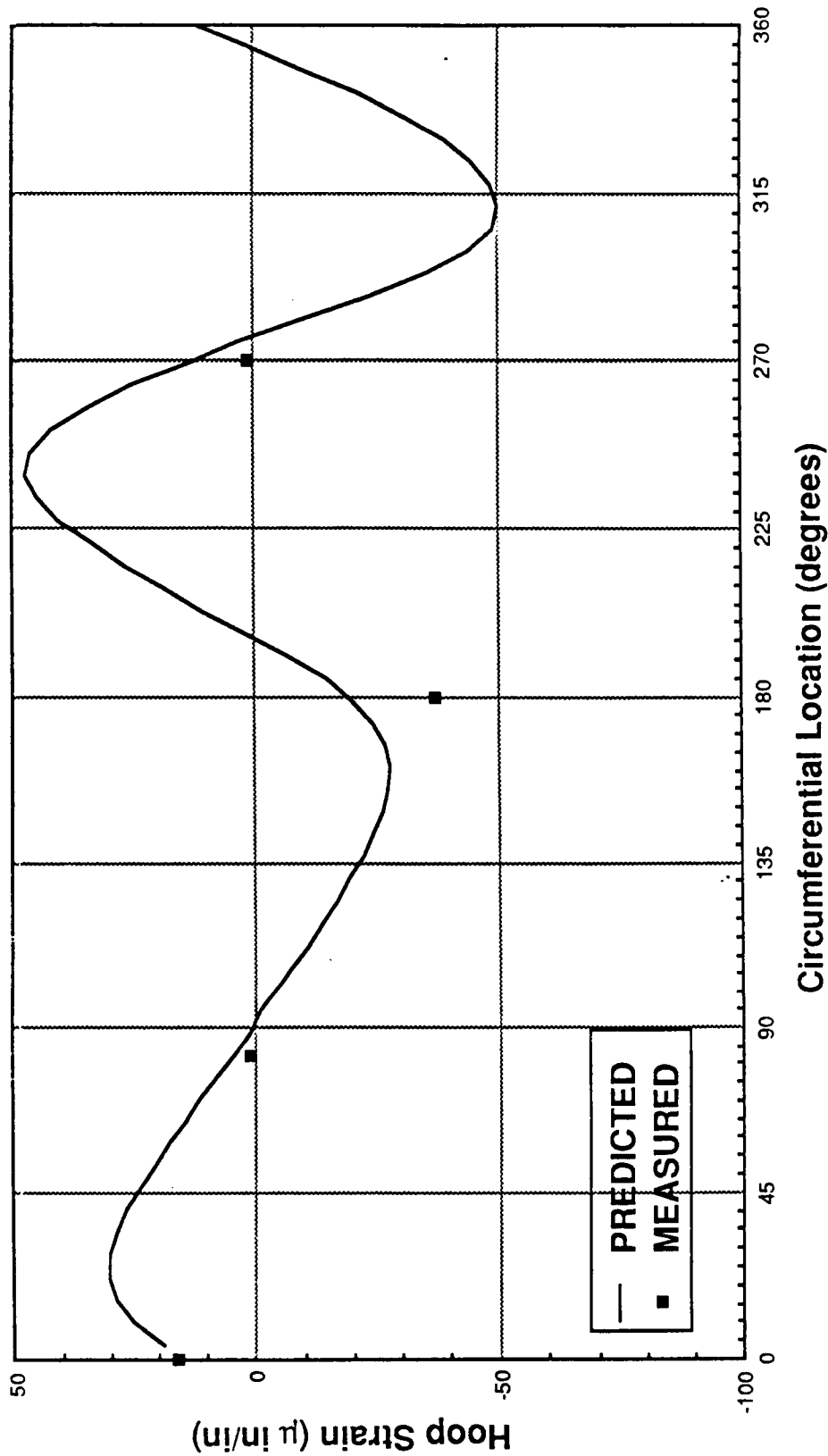


Figure 7.4-19. TPTA Post-Test Correlation, Predicted Versus Measured Hoop Strain at Sta 1466.5 Due to Max Q Strut Loads (No Pressure)

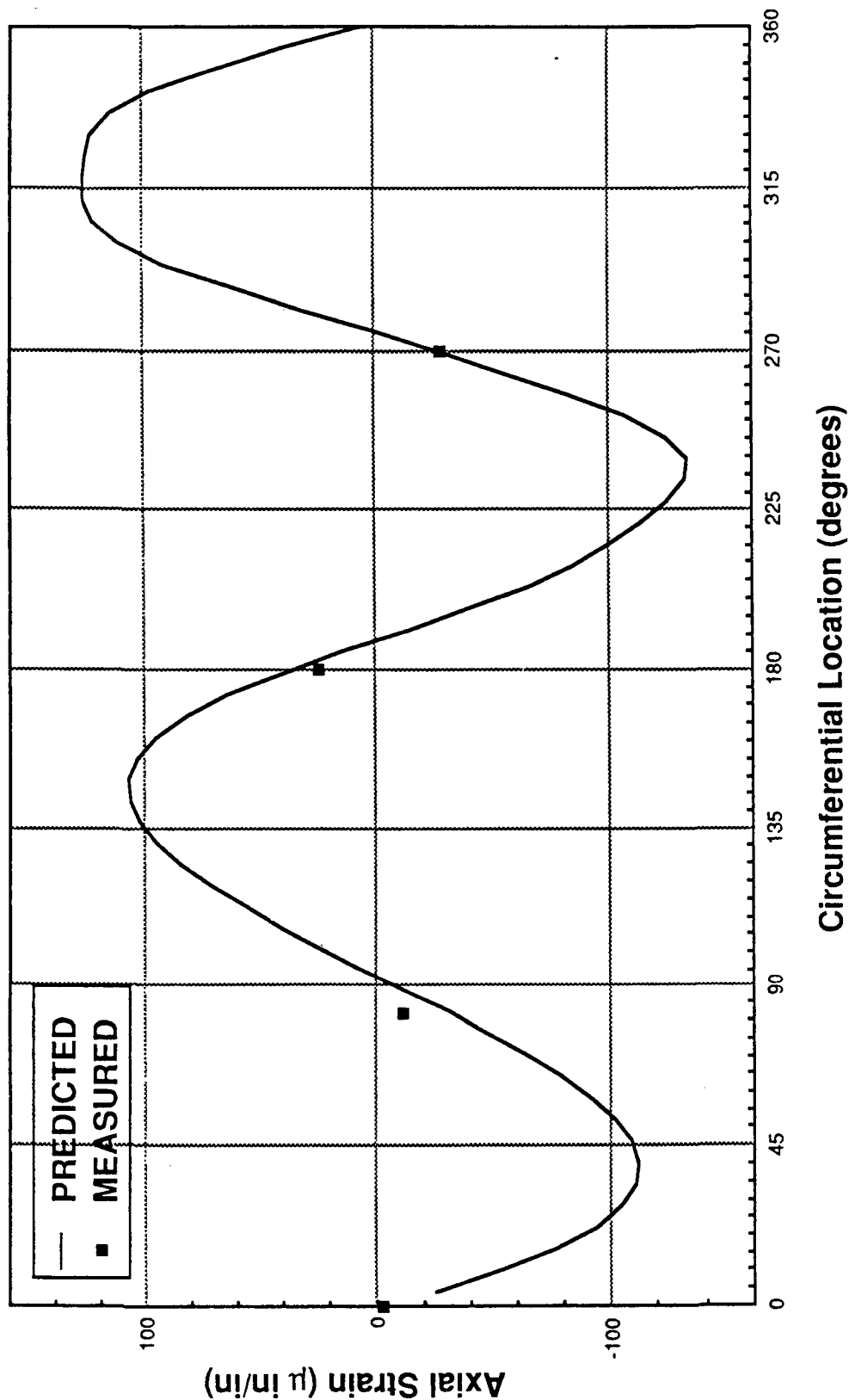


Figure 7.4-20. TPTA Post-Test Correlation, Predicted Versus Measured Axial Strain at Sta 1466.5 Due to Max Q Strut Loads (No Pressure)

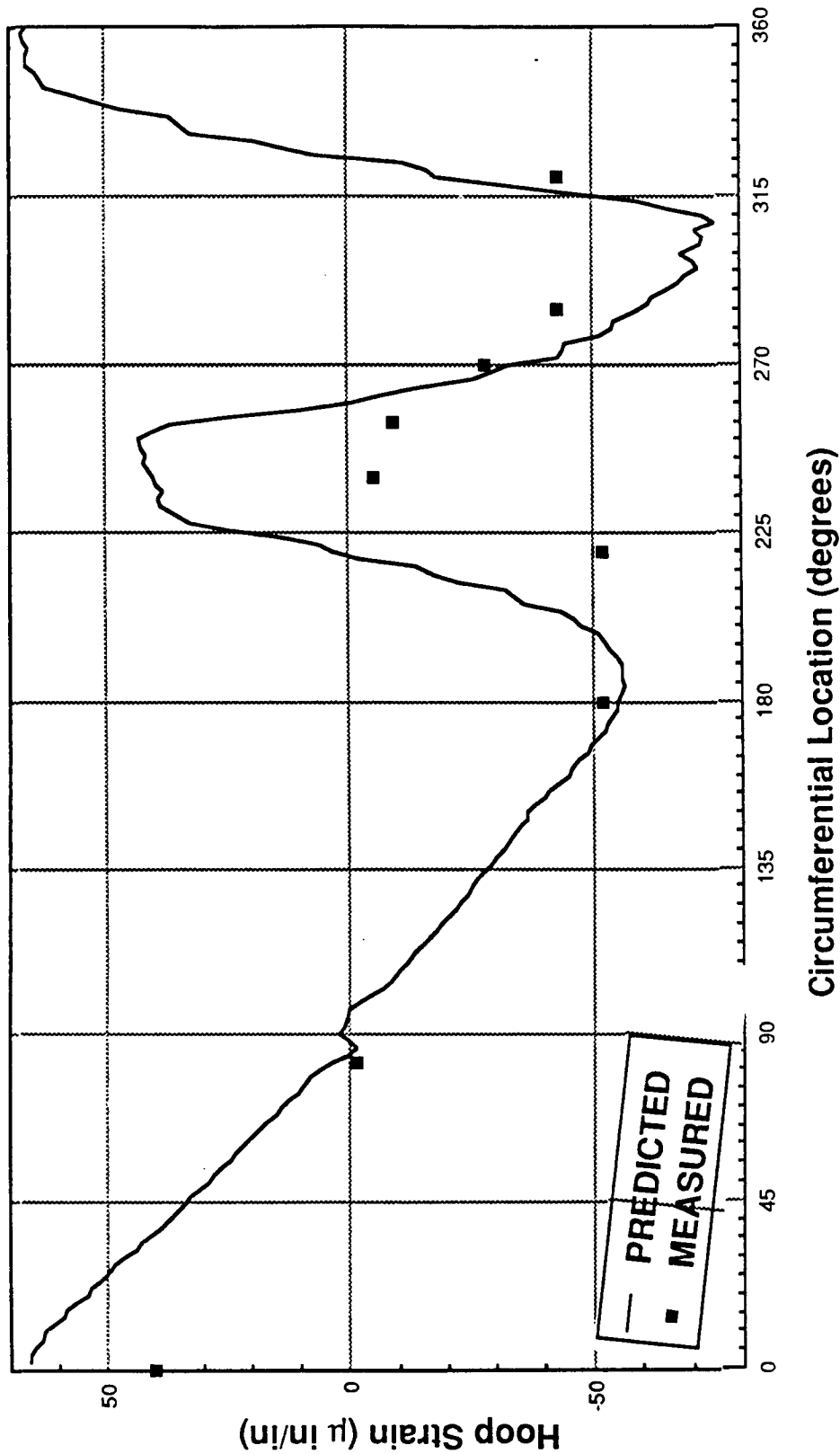


Figure 7.4-21. TPTA Post-Test Correlation, Predicted Versus Measured Hoop Strain at Sta 1498.0 Due to Max Q Strut Loads (No Pressure)

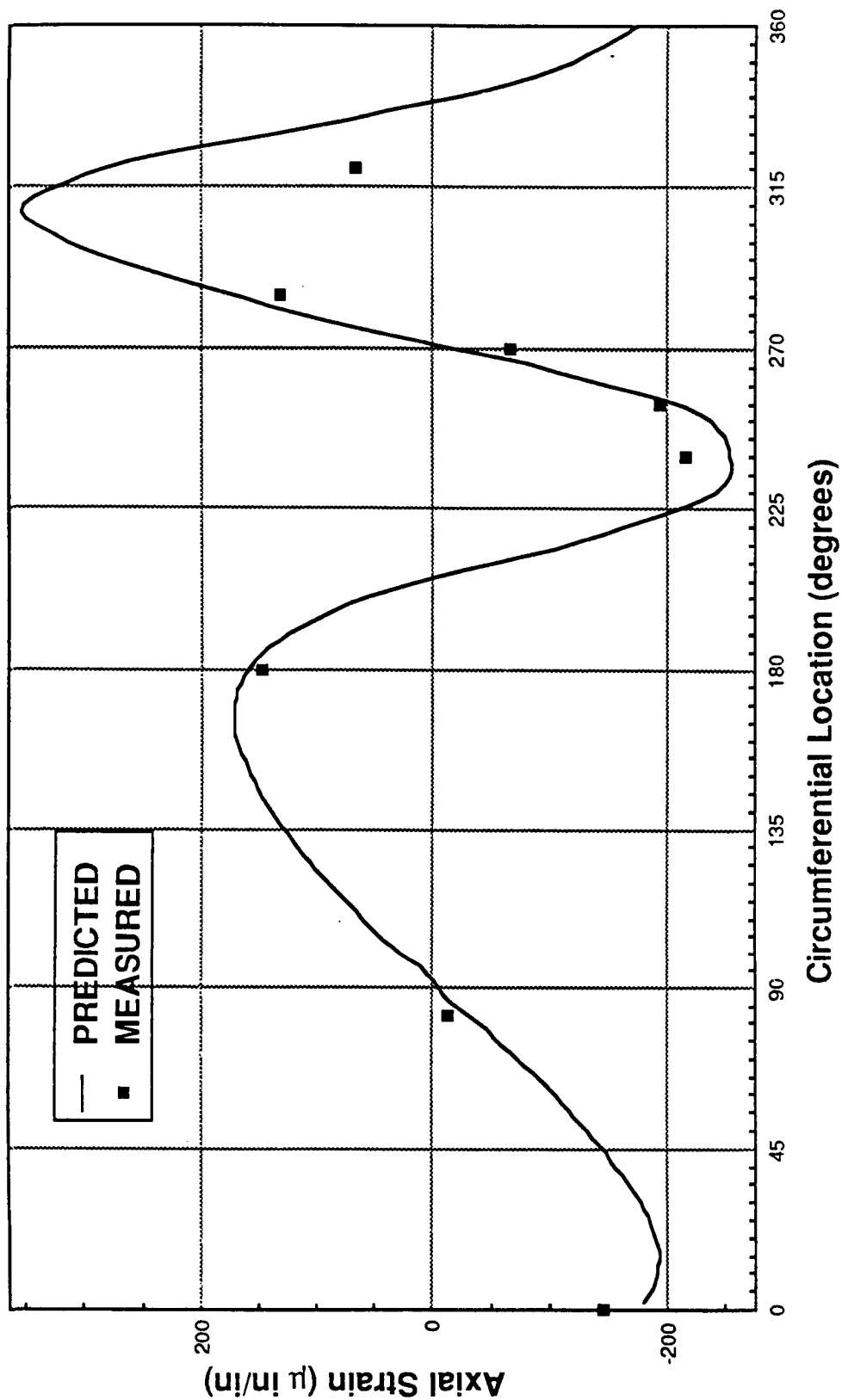


Figure 7.4-22. TPTA Post-Test Correlation, Predicted Versus Measured Axial Strain at Sta 1498.0 Due to Max Q Strut Loads (No Pressure)

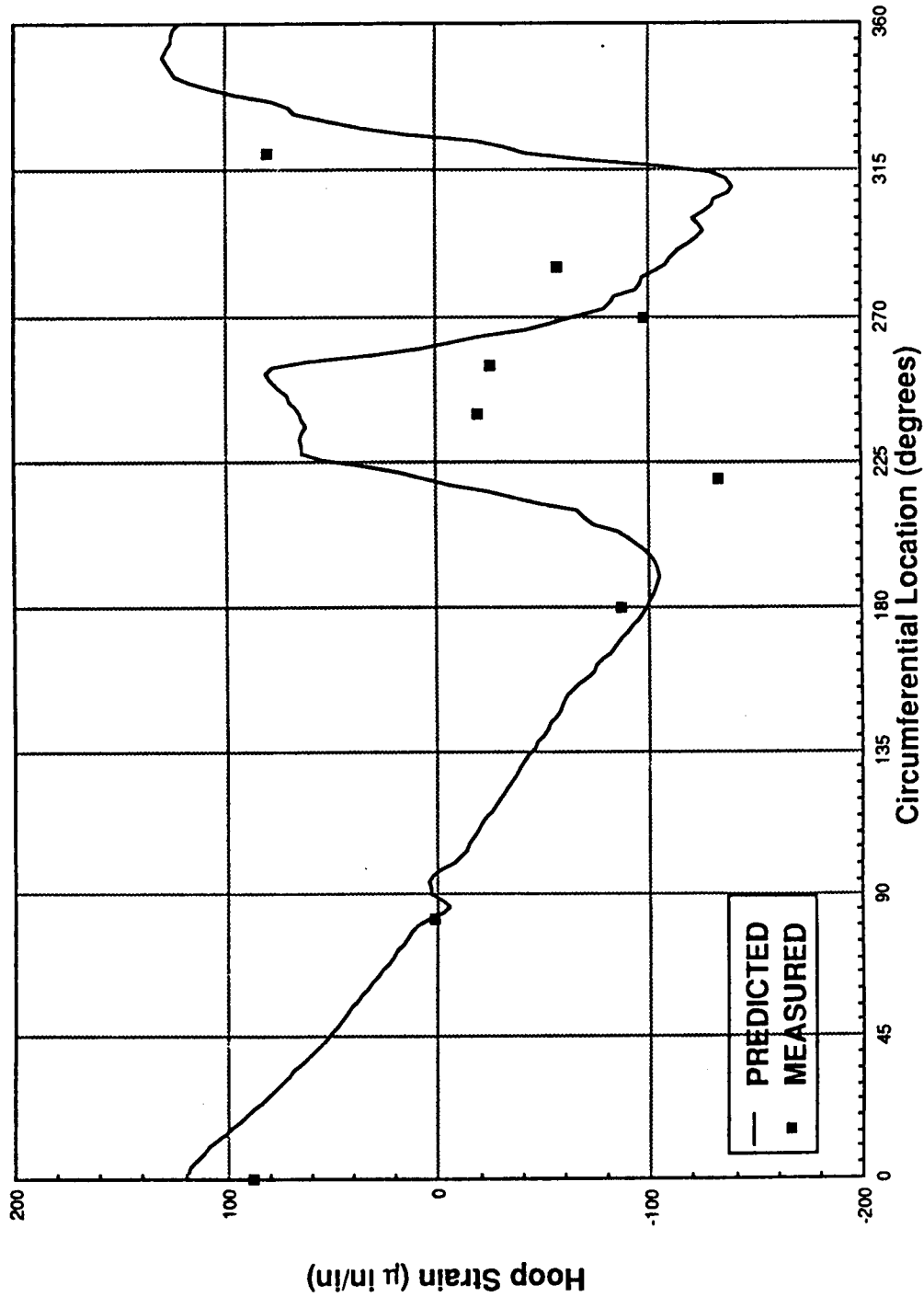


Figure 7.4-23. TPTA Post-Test Correlation, Predicted Versus Measured Hoop Strain at Sta 1501.0 Due to Max Q Strut Loads (No Pressure)

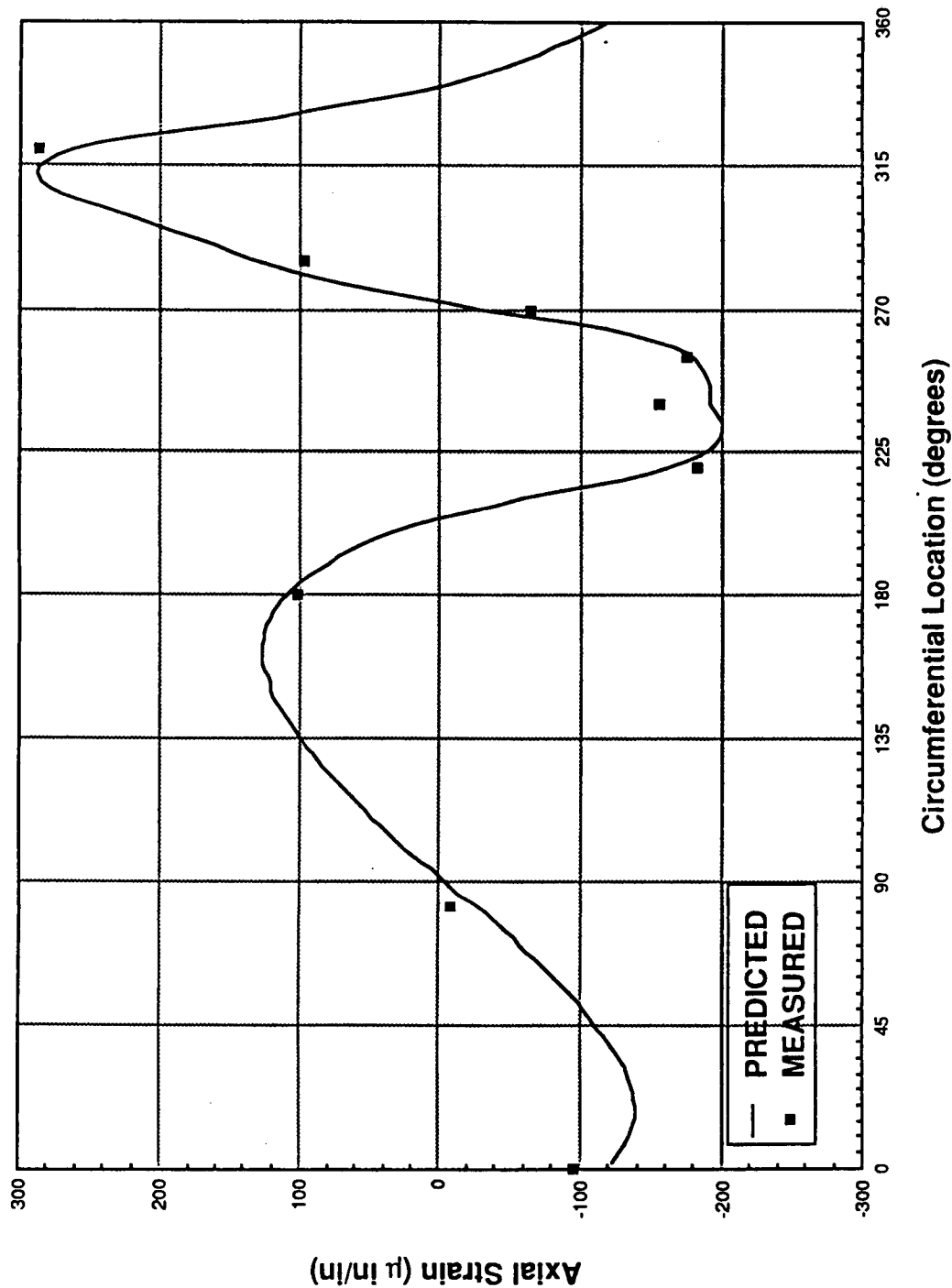


Figure 7.4-24. TPTA Post-Test Correlation, Predicted Versus Measured Axial Strain at Sta 1501.0 Due to Max Q Strut Loads (No Pressure)

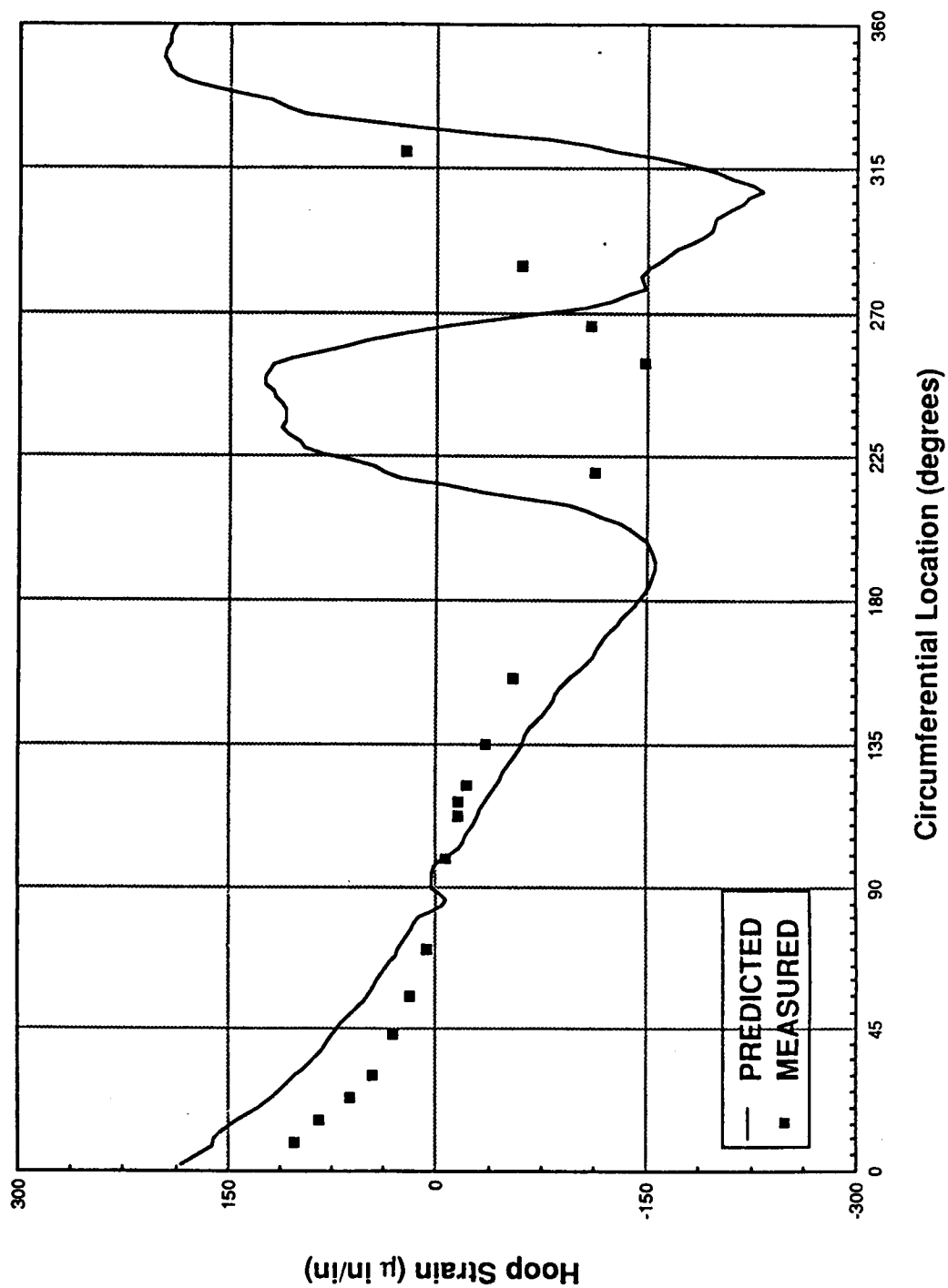


Figure 7.4-25. TPTA Post-Test Correlation, Predicted Versus Measured Hoop Strain at Sta 1511.0 Due to Max Q Strut Loads (No Pressure)

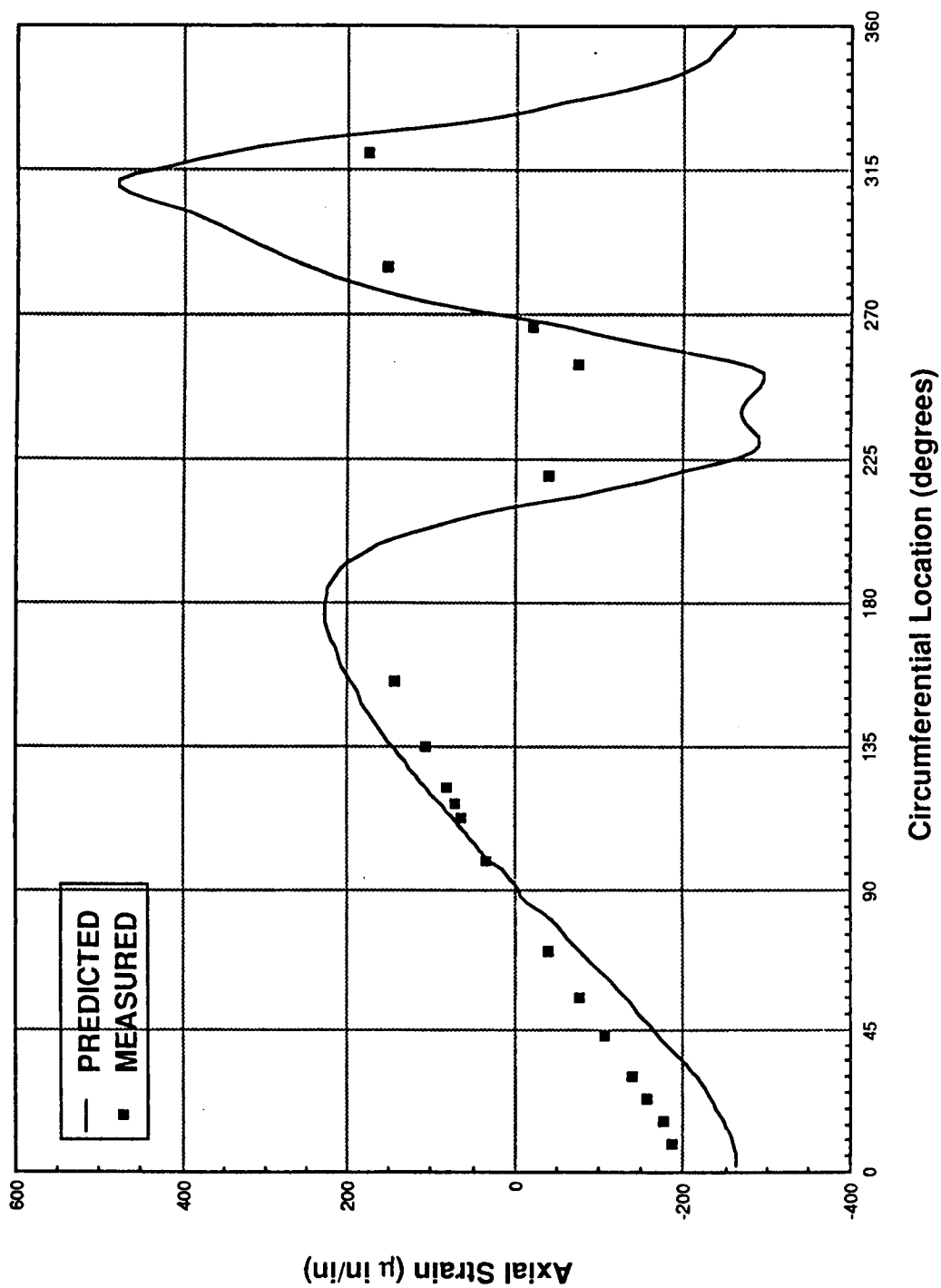


Figure 7.4-26. TPTA Post-Test Correlation, Predicted Versus Measured Axial Strain at Sta 1511.0 Due to Max Q Strut Loads (No Pressure)

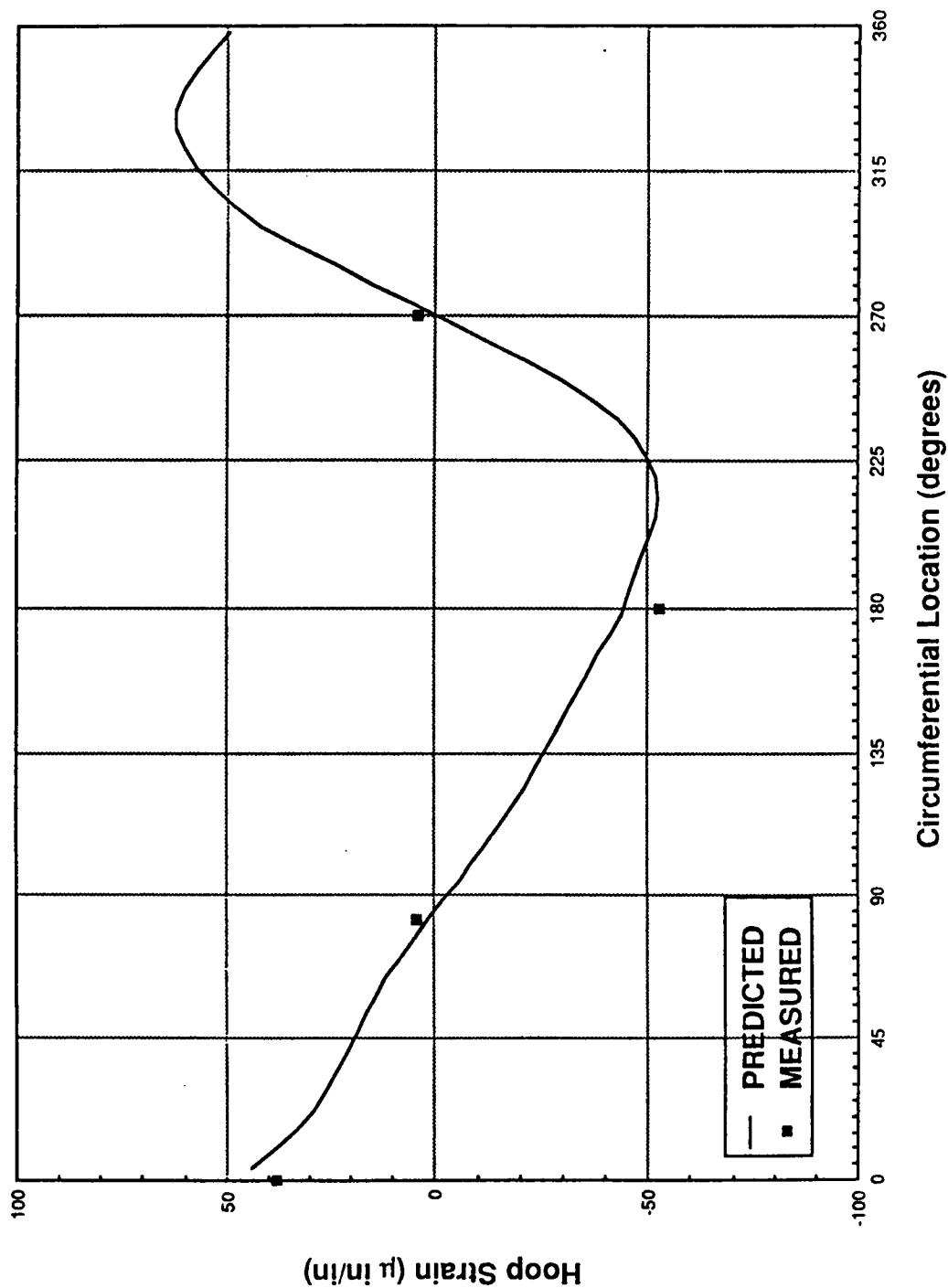


Figure 7.4-27. TPIA Post-Test Correlation, Predicted Versus Measured Hoop Strain at Sta 1797.6 Due to Max Q Strut Loads (No Pressure)

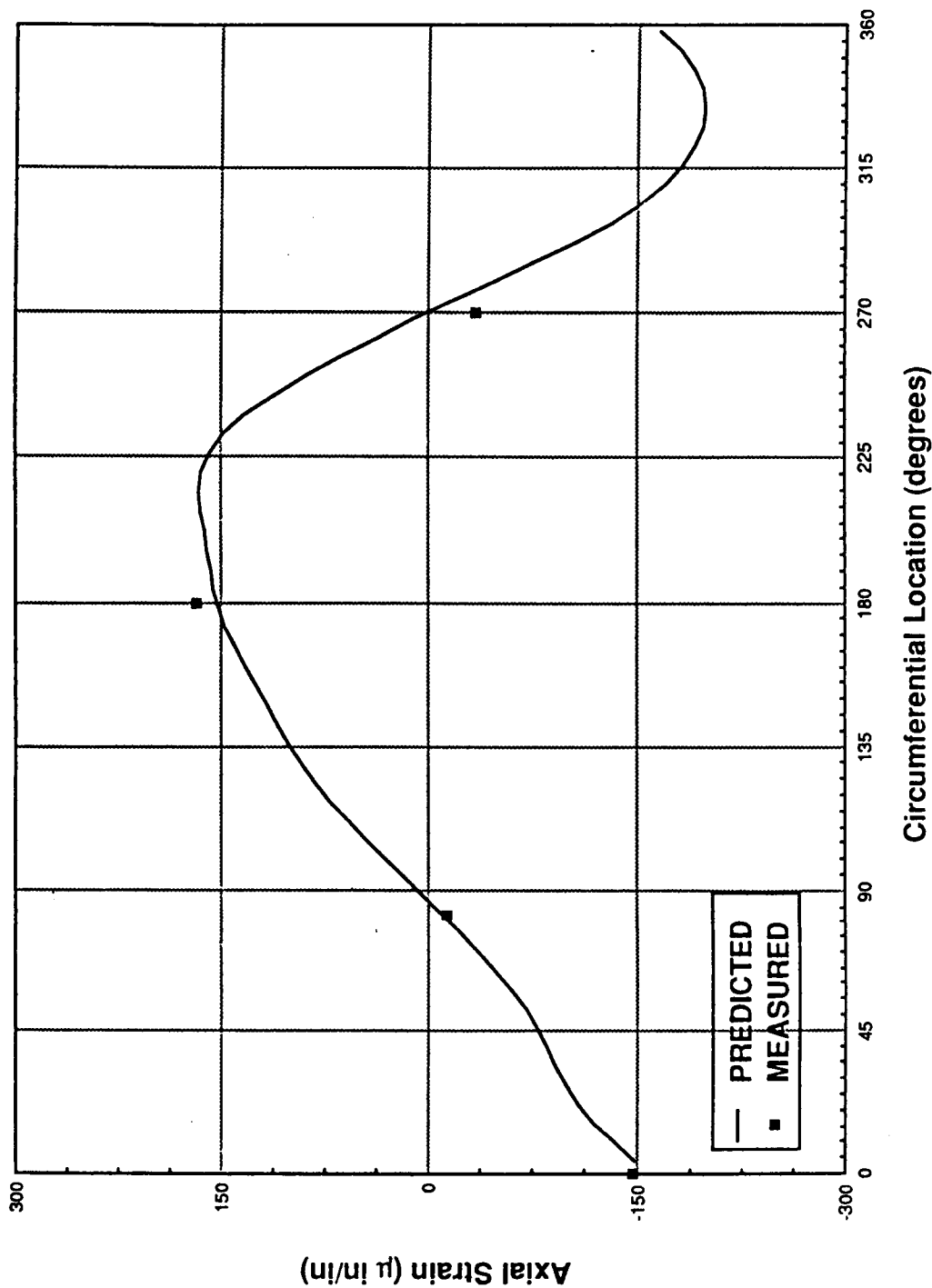


Figure 7.4-28. TPTA Post-Test Correlation, Predicted Versus Measured Axial Strain at Sta 1797.6 Due to Max Q Strut Loads (No Pressure)

In some cases it is best to observe distribution as a criteria for judging correlation. This is especially true when steep strain gradients (slopes) exist circumferentially (Figure 7.4-26, Station 1511.0). Here the measured data between 180 and 360 deg are not close to the predicted in terms of both absolute values and percentage difference, but the steepness of the slopes of the predicted data suggests that the load path need only be a few degrees off circumferentially to create a large difference. Considering the lack of fidelity in the ETA ring model, this is easily possible. The predicted data here correlate with the actual phenomena.

Some correlations are excellent regardless of the judgment tool. Most notable are the predictions of axial strain at the stations that lie between the aft field joint and the ETA ring (Figures 7.4-22 and 7.4-26). The agreement between predicted and measured values of axial strain at these stations is very good considering the variation of strain circumferentially and the overall low magnitude of strain when compared to the measuring range. Hoop strains as shown in Figures 7.4-22 and 7.4-24 correlated well with the predictions. The hoop strains in Figures 7.4-21 and 7.4-23 did not correlate well with the predictions at this station and cannot be explained. Any simple explanation for the hoop strain prediction inaccuracies, such as improper material properties or misplaced gages, cannot be considered without affecting the good correlation of the axial strain. The answers might lie in the host of nonlinearities not taken into account in this analysis.

Taken as a group, the predictions of case strain response to strut loads agree very well with the measured values. Considering the magnitude of the measurements being made, the large circumferential variations, and the large strain gradients axially, the correlation is satisfactory. The conclusion of the predictions that strut loads do not introduce significant strain levels to the case is supported by the measured data.

7.4.3.3. Gap Opening. Gap opening has always been difficult to predict and measure due to the extremely low magnitude of the movement and the large influence of nonlinearities. Nonlinearities include joint slope, changing load paths, interference by grease, gage movement, etc. The changing of

load paths, in terms of contact surfaces and the pressure profile, change radically during initial pressurization, making the prediction of gap response due to ignition difficult. Historically through the recovery program testing, measurements show that joint gaps close (decrease) initially upon internal pressurization, then open. This initial closing due to the nonlinearities cannot be taken into account with a linear model. Therefore, it is expected that a linear model should over-predict that magnitude of gap opening due to pressurization.

Gap opening predictions were made only in the aft field joint. This was the only joint modeled in enough detail to make predictions. A schematic of the field joint model showing the locations of gap opening predictions is shown in Figure 7.4-29. The high Q test pressure (610 psi), measured at $T = 9$ sec in Figure 7.4-14, was used to correlate gap opening due to internal pressure. Figure 7.4-30 is the comparison of predicted and measured gap opening at the inner clevis leg midland. The gap opening at the midland is over-predicted, as expected. The scatter of measured data is representative of the nonlinearities in the joint and how they vary circumferentially. In terms of magnitudes, the linear predictions are still 0.001 in. off from the measured average.

Prediction of gap opening at the inner clevis leg tip represents another non-linearity that cannot be taken into account in the prediction. A chamfer (sloped edge) exists at the tip of the leg, which lies near the LVDT making the measurement. As the joint grows axially due to the line load created by internal pressure, the chamfer moves under the gage enabling it to slide down its slope, thus throwing off the measurement. Since it is not known exactly when and how much the chamfer affects the LVDT slip, it is difficult to take the chamfer into account, even as a post-prediction correction factor. Figure 7.4-31 shows the comparison of predicted and measured gap opening at the inner clevis leg tip. The predicted gap opening lies near the average of the scatter of the measured data. Considering all the nonlinearities, the magnitude of the measurement, and the chamfer, this is excellent correlation.

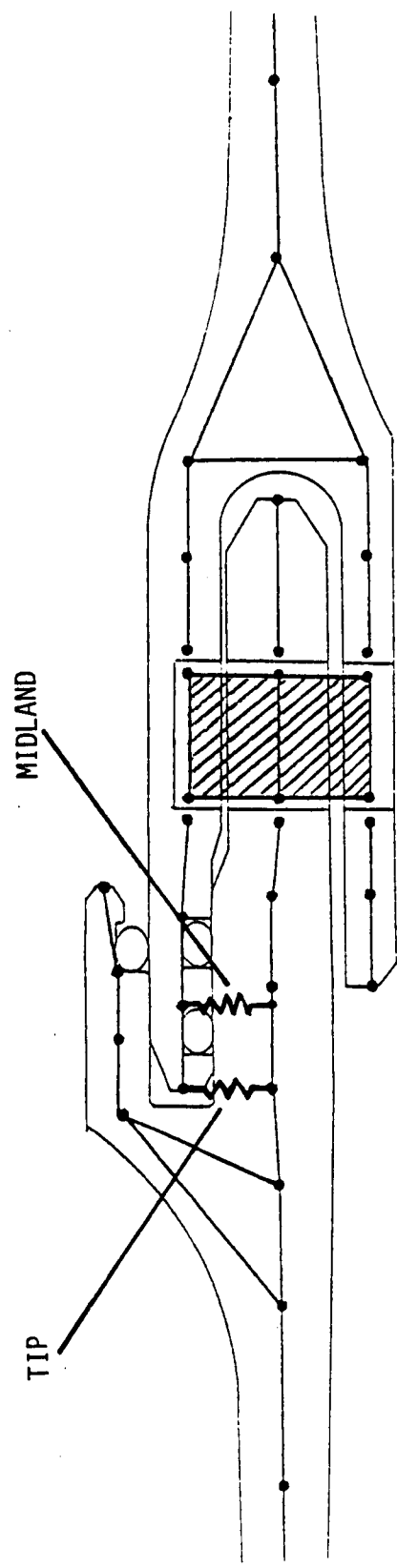


Figure 7.4-29. Joint B Gap Opening Prediction Locations

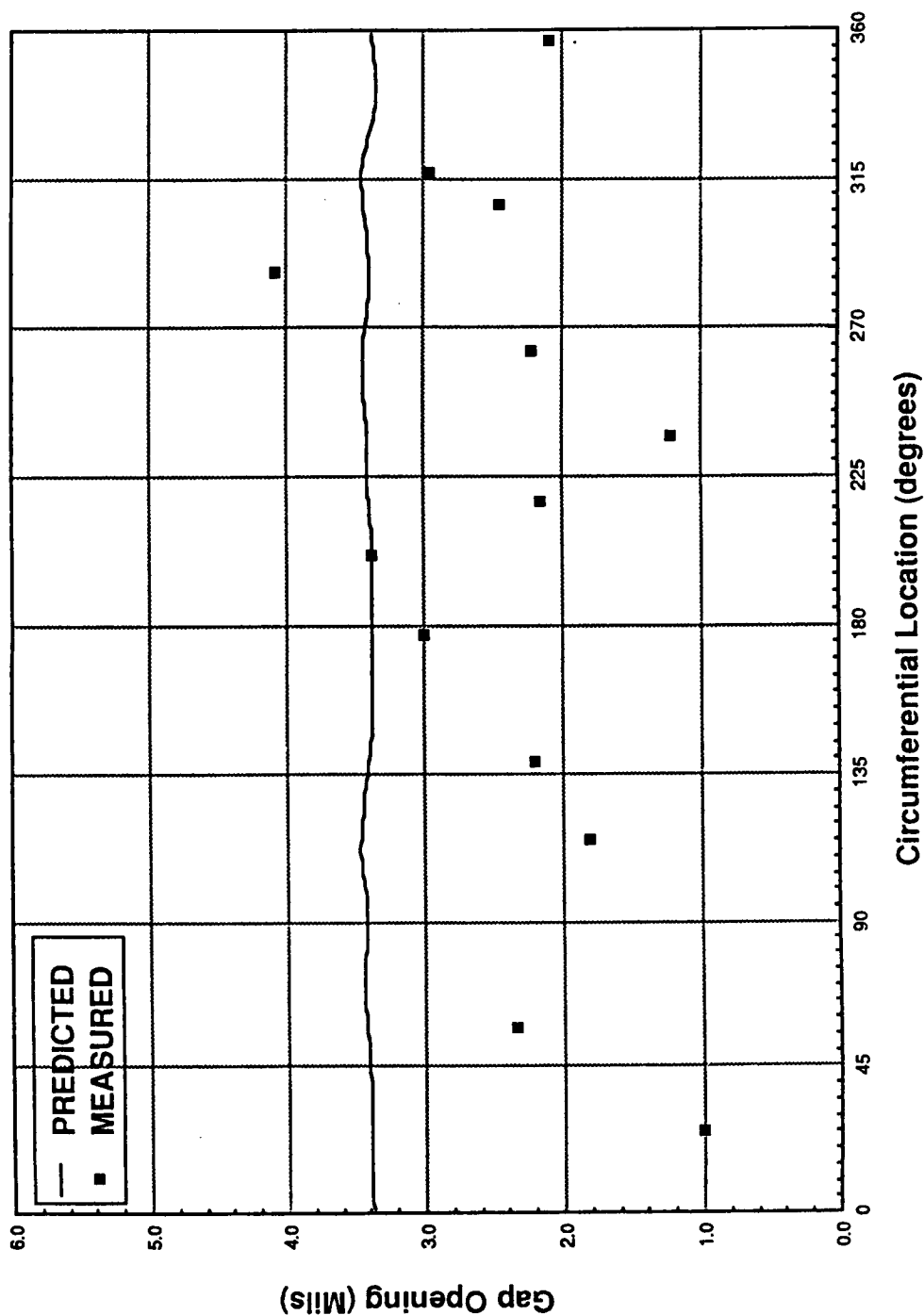


Figure 7.4-30. TPTA Post-Test Correlation, Predicted Versus Measured Gap Opening at Aft Field Joint Inner Clevis Leg Midland Due to Max Q Pressure (610 psig)

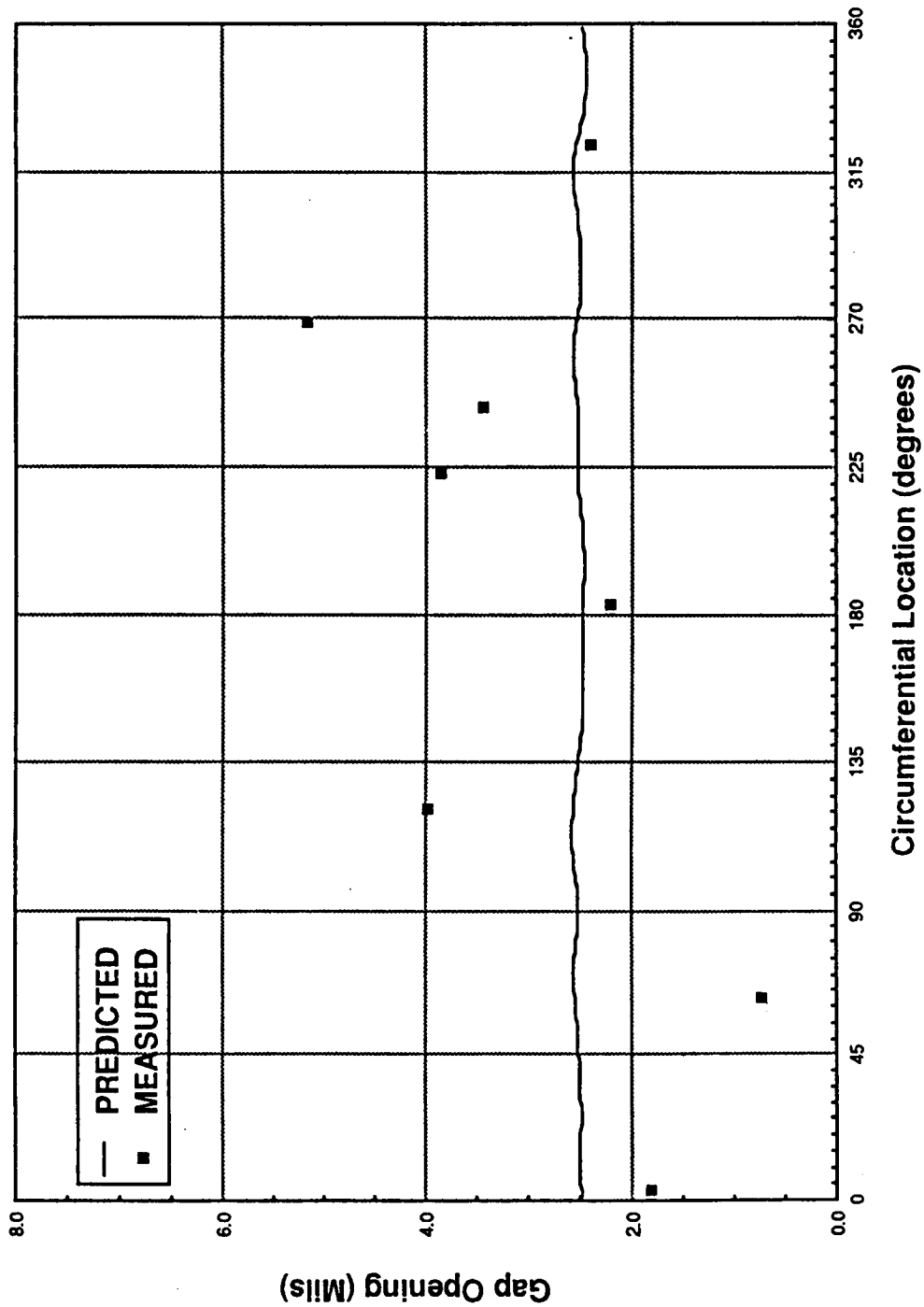


Figure 7.4-31. TPTA Post-Test Correlation, Predicted Versus Measured
Gap Opening at Aft Field Joint Inner Clevis Leg Tip
Due to Max Q Pressure (610 psig)

The same procedure used to study strain response to strut loads--taking the difference of the time slices at $T = 12.4$ and $T = 9$ sec--was employed to study gap opening due to the strut loads. Figures 7.4-32 and 7.4-33 are comparisons of predicted and measured gap openings due to strut loads at the inner clevis leg midland and tip, respectively. These plots show very good correlation to within 0.0001 in. (on the average). This excellent correlation occurs because the high and constant internal pressure (though factored out) takes out most of the nonlinearities discussed in the previous sections. The chamfer on the leg tip is not a factor either, since the joint does not grow axially due to the strut loads. The measured data support the conclusion drawn from the prediction that strut loads do not significantly affect gap openings.

7.4.4 Conclusions

In general, the correlation of predicted-to-measured strains and gap opening were very good. Predictions of the structural response of the case walls and the aft field joint due to strut loads were generally better than predictions due to internal pressure. This is because most of the nonlinearities that make linear predictions difficult disappear when the pressure is held at a high, uniform level, as was done during the application of high Q strut loads.

Pressure is the primary driver for case strain, stress, and gap motion. The pretest prediction conclusion that strut loads do not introduce significant strain levels or significantly affect gap opening was strongly supported by the measured data.

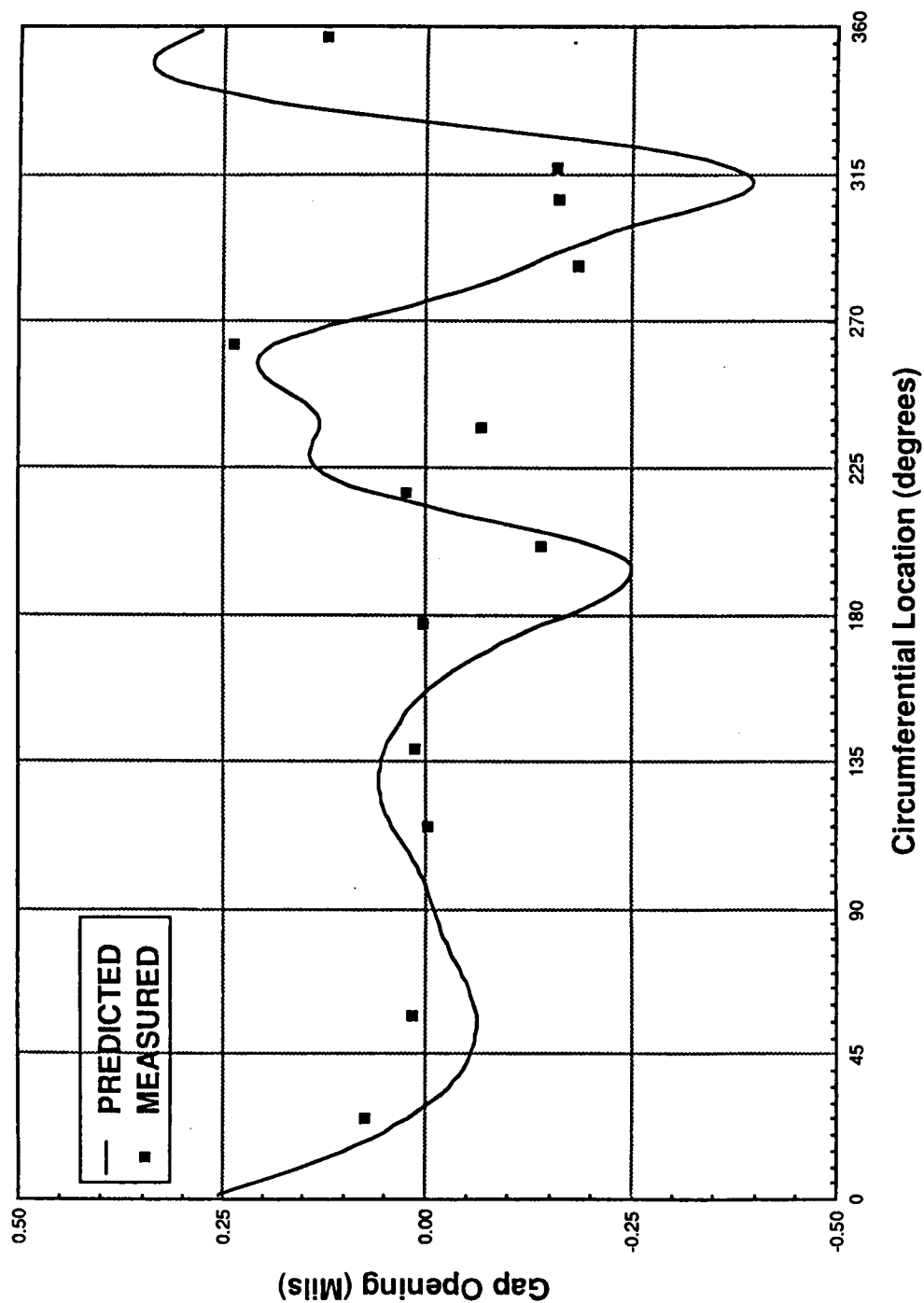


Figure 7.4-32. TPTA Post-Test Correlation, Predicted Versus Measured
Gap Opening at Aft Field Joint Inner Clevis Leg Midland
Due to Max Q Strut Loads (No Pressure)

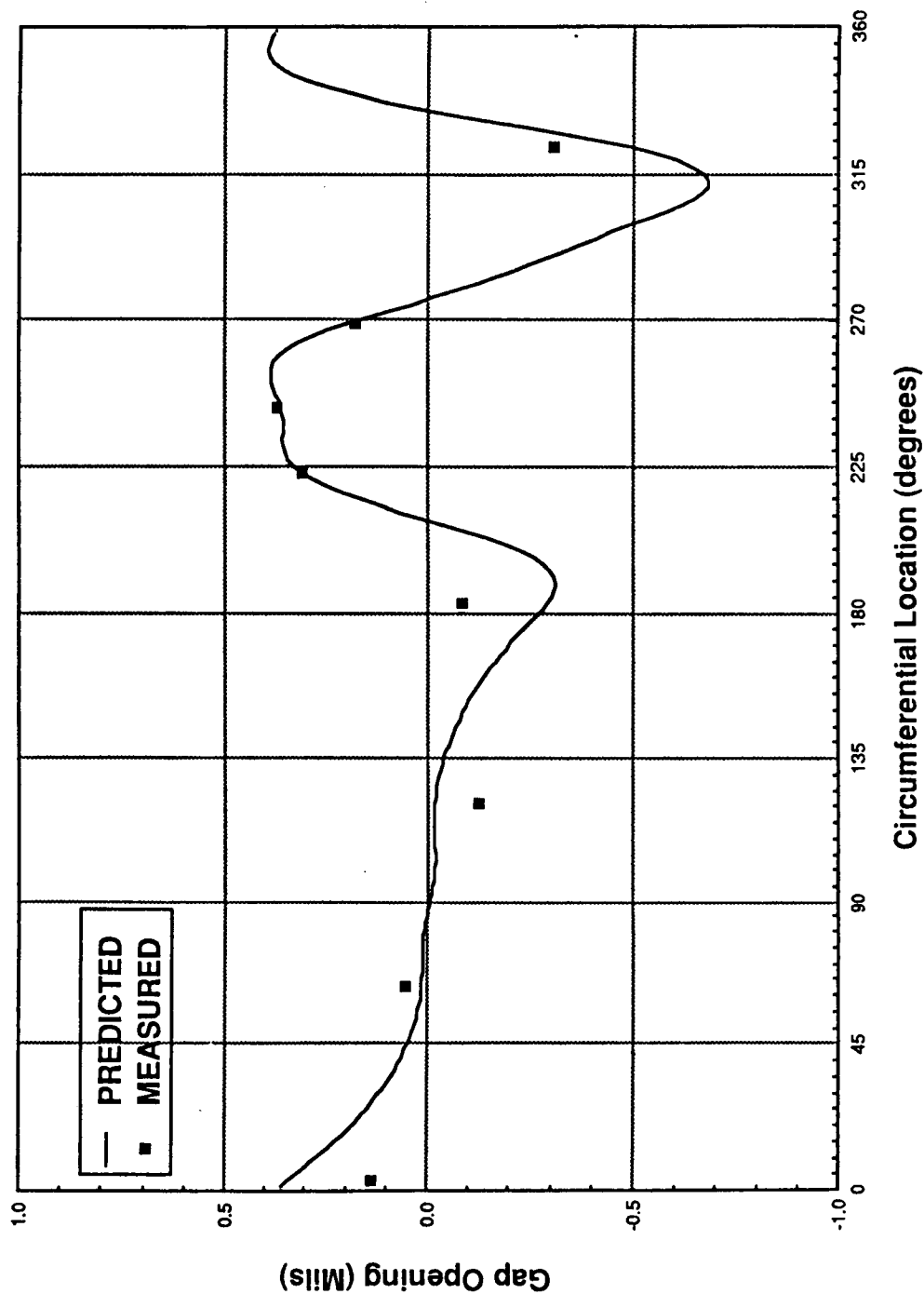


Figure 7.4-33. TPTA Post-Test Correlation, Predicted Versus Measured
Gap Opening at Aft Field Joint Inner Clevis Leg Tip
Due to Max Q Strut Loads (No Pressure)

7.5 GRAIN STRUCTURES

7.5.1 Introduction

Stress gages were placed in the A and B field joint regions and the aft dome insulation. Two types of gages were used, measuring either normal or shear stress. The gages were placed at the insulation/case and insulation/propellant interfaces, and at the J-insulation bond.

7.5.2 Objectives

The stress gage data will show induced stresses during firing, storage, and field joint demate. The gages should also verify structural analysis of the propellant liner insulation.

7.5.3 Results/Discussion

The peak shear stresses which occurred during the TPTA 1.1 firing are shown in Table 7.5-1. Comparisons with previous tests (JES-3A, NJES-2A and -2B) and finite element analysis are also shown in Table 7.5-1. Some data are missing, probably due to damaged, deleted, or malfunctioning gages. As expected, normal stress gages were highly compressive during firing, in the 750 to 900 psi range.

Tensile stress gages at the J-insulation bond indicated very low values during joint disassembly. One gage showed a sudden peak to 48 psi; the others were much lower. Data from TPTA 1 storage conditions (zero offset voltages) have been obtained, but not processed.

7.5.4 Conclusions/Recommendations

Considering a 515 psi shear stress allowable (TWR-17039, Table 6.10), the induced shear stresses are relatively low and verify a safety factor greater than 2.0. Considering a 390-psi stress allowable, all the disassembly-induced loads were low enough to maintain a 2.0 safety factor. Previous tests and structural analysis support these conclusions.

Table 7.5-1. TPTA 1.1 Firing, Insulation Shear Stress
Gages - Comparison and Analysis

Field Joint

<u>Gage Location</u>	<u>Gage No. (Joint A/Joint B)</u>	<u>TPTA 1.1 Joint A</u>	<u>TPTA 1.1 Joint B</u>	<u>JES-3A Joint A</u>	<u>Finite Element Analysis</u>
Insulation-to-Capture Feature	S166/S443	10	20	30	4
	S167/S444	26	41	16	
	S168/S445	15	23	25	
Insulation-to-Clevis	S169/S458	--	--	15	24
	S170/S459	--	--	26	
	S171/S460	--	13	31	
Insulation-to-Propellant	S184/S455	12	--	114*	2
	S185/S456	6	19	10	
	S186/S457	2	8	13	

Aft Dome Insulation

<u>Gage Location</u>	<u>Gage No.</u>	<u>TPTA 1.1</u>	<u>NJES-2A</u>	<u>NJES-2B</u>	<u>Finite Element Analysis</u>
1 in. from Nozzle-to-Case Joint	S402	7	39	7	27
	S404	--	46	30	
	S406	10	28	12	
3 in. from Nozzle-to-Case Joint	S408	15	--	157*	12
	S410	140*	--	21	
	S412	26	--	2	

*Possibly bad gage.

Note: Peak shear stresses in psi

Considering the high ranges of the shear stress gages (up to 600 psi), their variation at low stress levels is acceptable. Verification of analytical predictions may not be satisfactory, and the finite element analysis should be reviewed to see if accuracy can be improved. Storage stress data still need to be reported.

7.6 SEAL LEAK CHECK

Seal leak checks were done in accordance with STW7-3447 and STW7-3448. All test requirements were met with no anomalies. Tables 7.6-1 and 7.6-2 summarize the test results for test Joints A and B. Table 7.6-3 summarizes the test results for test Joint D.

Table 7.6-1. Joint A Leak Check Results

<u>Primary to Secondary O-ring</u>		<u>Allowable</u>	<u>Time (hr)</u>
<u>1,000 psig</u>			
Decay Test Volume = 25.46 in. ³	Decay Leak Rate = 2.7×10^{-3} sccs	3.2×10^{-1} sccs	3.01
Rise Test Volume = 24.01 in. ³	Rise Leak Rate = 6.39×10^{-4} sccs		
<u>30 psig</u>			
Decay Test Volume = 35 in. ^{3*}	Decay Leak Rate = 5.89×10^{-3} sccs	8.2×10^{-3} sccs	1.75
Rise Test Volume = 17 in. ³	Rise Leak Rate = 3.78×10^{-3} sccs		
<u>Primary to CF O-ring</u>			
<u>100 psig</u>			
Decay Test Volume = 34.08 in. ³	Decay Leak Rate = 5.98×10^{-3} sccs	1.0 sccs	1.02
Rise Test Volume = 22.72 in. ³	Rise Leak Rate = 5.50×10^{-3} sccs	5.1×10^{-2} sccs	
<u>30 psig</u>			
Decay Test Volume = 30.71 in. ³	Decay Leak Rate = 9.92×10^{-4} sccs	3.0×10^{-1} sccs	1.00
Rise Test Volume = 30.14 in. ³	Rise Leak Rate = 5.24×10^{-4} sccs	8.2×10^{-3} sccs	

*Volumes for the 30 psig primary/secondary leak check (decay and rise) could not be determined because of a procedural error in the operation of the equipment. Due to this anomaly, respective Joint B volumes with an added 20 percent safety factor were utilized to determine conservative leak rates for both decay and rise.

Table 7.6-2. Joint B Leak Check Results

Primary to Secondary O-ring1,000 psig

OPN 010 Step 055, Substeps 13, 16

Decay Test Volume = 22.04 in.³Rise Test Volume = 24.29 in.³Decay Leak Rate = 3.58×10^{-3} sccsRise Leak Rate = 3.40×10^{-4} sccs30 psig

OPN 010 Step 055, Substeps 25, 28

Decay Test Volume = 13.66 in.³Rise Test Volume = 28.05 in.³Decay Leak Rate = 3.24×10^{-4} sccsRise Leak Rate = 4.77×10^{-4} sccsPrimary to CF O-ring100 psig

OPN 010 Step 060, Substeps 13, 16

Decay Test Volume = 30.87 in.³Rise Test Volume = 23.07 in.³Decay Leak Rate = 2.76×10^{-2} sccsRise Leak Rate = 1.06×10^{-3} sccs30 psig

OPN 010 Step 060, Substeps 27, 31

Decay Test Volume = 27.17 in.³Rise Test Volume = 24.35 in.³Decay Leak Rate = 1.30×10^{-3} sccsRise Leak Rate = 5.04×10^{-4} sccs

Note: sccs = standard cubic centimeters per sec

Table 7.6-3. Joint D Leak Check Results

Primary to Secondary pretorque)

920 psig Decay leak rate 0.154 sccs (required less than 0.29 sccs)

30 psig Decay leak rate 0.000 sccs (required less than 0.0082 sccs)

Primary to Secondary (post-torque)

920 psig Decay leak rate 0.032 sccs (required less than 0.29 sccs)

Primary to Wiper (post-torque)

20 psig Decay leak rate 0.0049 sccs (required less than 0.0082 sccs)

Note: sccs = standard cubic centimeters per sec
Leak check performed with Klughe system.

DISTRIBUTION

<u>Recipient</u>	<u>Copies</u>	<u>Mail Stop</u>
J. McCluskey	1	E12
M. Hopkins	1	E12
L. Bailey	1	E12
J. Sutton	1	L10
B. McQuivey	1	L10
M. Allison	1	L10
J. Kapp	1	L20
D. Ketner	1	L21
A. Neilson	1	L21
M. Lee	1	L21
G. Anderson	1	L22
S. Stein	1	L22D
J. Burn	1	L22D
M. Nejatifar	1	L22D
J. Robinson	1	MSFC
J. Morgan	1	L22D
K. Eckhardt	1	L21
K. Albrechtsen	1	L23B
D. Blevins	1	MSFC
P. Zielke	1	L36
R. Jensen	1	L36
V. Steineck	1	L36
T. Hoffman	1	L22
L. Abrahamson	1	L22
D. Mason	1	L22
A. Freed	1	L22
H. Gittins	1	851
K. Sanofsky	1	851B
C. Johnson	1	L36
D. Cox	1	L36
D. Sauvageau	1	L36
M. Williams	1	L36
C. Rebello	1	L36
J. McKellar	1	E11
J. Ralston	1	K68A
C. Vibbart	1	MSFC
E. West	1	LMSC
F. Call	80	E05
Data Management	7	L23E
Print Crib	5	K23B